UNIVERSITY OF NOTTINGHAM

DEPARTMENT OF CIVIL ENGINEERING

DEFORMATION CHARACTERISTICS OF DENSE BITUMEN MACADAM SUBJECTED TO DYNAMIC LOADING

by

Martin Somerville Snaith, M.A., B.A.I., M.Sc.

Thesis submitted to the University of Nottingham
for the degree of Doctor of Philosophy

May 1973

CONTENTS

ACKNOWLEDGEMENTS

The author wishes to express his thanks to Professor R.C. Coates for making available the facilities of the Department of Civil Engineering.

The author is also deeply indebted to Professor P.S. Pell and Dr. S.F. Brown who have throughout given advice, help and support so generously.

Thanks are also due to Mr. J.G. Redfern and to the assistance, given so willingly, of Mr. R.H. Collins and Mr. F. Brookes in the production and maintenance of the testing equipment.

The financial sponsorship of the Transport and Road Research Laboratory is gratefully acknowledged.

Last, but by no means least, Miss J.L. Clerbaut is thanked both for her patience and for her typing ability.

ABSTRACT

The purpose of the investigation was to determine the resilient and permanent deformation characteristics of dense bitumen macadam under dynamic loading conditions. To effect this, various techniques for the testing of bituminous bound materials have been devised and used. These have necessitated the development of suitable measuring and recording systems which have allowed the accurate determination of the deformation behaviour of cylindrical specimens of a dense bitumen macadam subjected to both static and dynamic triaxial loading. The loading regimes were chosen to simulate as closely as possible in situ road pavement conditions. The effect of changes in the magnitude of vertical loading, confining pressure, temperature and frequency of loading together with variations in the binder content of the material were investigated. Attention was also paid to the effect of rest periods between individual vertical loading pulses.

The resilient deformation behaviour of the material gained from these experiments provided accurate values of resilient modulus and Poisson's ratio for the elastic analysis of pavement systems.

A method is suggested for the calculation of the permanent deformation contribution of the bound layers of a road pavement to the overall rut depth. The method is suitable for use with existing "structural design" procedures for flexible pavements.

CHAPTER ONE

INTRODUCTION

The function of the road designer is to produce a pavement with a safe and comfortable riding surface that is economical both in construction and in maintenance. This is proving to be an increasingly difficult task as the volume of commercial traffic had, in ten years, by 1970 risen to the 1980 prediction level (1). Furthermore, the weight of these vehicles has tended to increase, and may be expected to increase again with the entry of the United Kingdom (U.K.) into the European Economic Community. The cost of providing roads to meet the increasing volume and size of traffic has risen also. In the period 1960 to 1970, the annual expenditure on new roads increased fourfold to a level of £400 M (1,2).

It is plain from these figures that a method of road design that is able to produce a satisfactory pavement more economically than at present will result in a large saving of public money and for this reason the money and effort spent on research represents a good investment for the future.

The procedures, recommended by the Ministry of Transport, for the design of new roads in the U.K. are contained in Road Note No. 29 (1) which when used with the Ministry of Transport's "Specification for Road and Bridge Works" (3) gives the basis for the selection of both the thickness and composition of the pavement layers above the subgrade. These procedures are typical of the "subgrade protection" methods of design

used since before the war. They attempt to provide an adequate thickness of pavement material to protect the subgrade from excessive stress that might lead to shearing, or excessive permanent deformation, of the subgrade.

The method proposed in Road Note No. 29 is based on a development of the California Bearing Ratio (C.B.R.) method. The C.B.R. of the subgrade is measured and taking into account the traffic flow and required design life the necessary thicknesses of the pavement layers are read from the charts provided. Whilst this method has yielded a road system in the U.K. that is comparatively free from pavement failures, it is founded mainly on empirical information. The great disadvantage of such systems is stated in the "Shell 1963 Design Charts for Flexible Pavements" (4):

"Existing design procedures, including the C.B.R. method, were all largely empirical and rested essentially on extensive full-life experience of conventional constructions. These could not therefore cater for "new materials". Only a design system based on theory is capable of application outside current experience, i.e. able to predict life under traffic of constructions which have not been built before."

The Shell design charts were an attempt to make design recommendations for flexible constructions based on theory. They depend on an understanding of the properties of paving materials as known at the time of their publication and are intended to be capable of being updated as more information on material properties becomes available.

Brown and Pell (5) have more recently presented a

structural design procedure for the design of flexible pavements. This is similar to the Shell charts in that the tensile strain in the bottom of the bituminous layer, and the compressive strain on the top of the subgrade are regarded as critical design factors. In their procedure a pavement design is selected using engineering judgement, bearing in mind the predicted traffic during the design life and the properties of the available materials. This pavement structure is then analysed to make sure that the critical stresses and strains are within the allowable limits. The limit for the tensile strain in the bottom of the bound material is derived from the results of extensive laboratory fatigue tests, whilst the limiting value of compressive strain on the subgrade is that presented by the Shell investigators in 1965 from their analysis of the AASHO road test results (6). In addition to these values the tensile stress at the bottom of the sub-base is limited to a value depending on the overall vertical stress at this point (7).

The above procedure should produce a road pavement that will resist fatigue failure in the bound layers and excessive permanent deformation in the subgrade.

Whilst in the U.S.A. it is mainly the elastic deformation of a pavement under passing wheel loads that has led to pavement failure (8), the opposite situation exists in the U.K. where Croney (9) has found that:

"With the base and surfacing materials in common use in Britain, permanent deformation was accepted by engineers as the principal indication of failure."

He found that remedial work was usually undertaken when the deformation in the path of the nearside wheel had reached a level of 20 mm (measured with a 1.8 m straight edge) which usually meant a total deformation from the original pavement level of 25 mm. The small amount of cracking of the pavement that did occur was confined to longitudinal hair cracks in the wheel paths, at rut depths of between 10 mm and 20 mm, rather than the extensive cracking known as "alligator" cracking, which is associated with large elastic deformations and a fatigue type of failure (10).

The formation of a rut results from permanent deformation accruing in the various layers of a pavement. Lister (11) has shown that over 40% of the total pavement deformation visible at the surface of a full scale test section had occurred in the bituminous layers. Hofstra and Klomp (12) making observations in a laboratory wheel tracking machine, state that all the permanent deformation apparent at the surface had occurred in the bituminous layers in those sections where these layers exceeded 100 mm in thickness. It is therefore important to know the permanent deformation behaviour of the bituminous layers of a pavement if the limiting rut depth is to be taken as a failure criterion.

The present knowledge of in situ behaviour in this field is limited to that inferred from full scale experimental sections, such as those already quoted in this chapter. Relevant results from laboratory testing had been reported

from only two centres of research at the commencement of this work (13,14). During the last three years a greater research effort has been directed towards this problem both in Europe and the U.S.A. This should lead to an increased knowledge of the factors that affect the plastic behaviour of bituminous materials which contributes to the permanent deformation that occurs in road pavements.

In order to predict the plastic strain that will occur in the bituminous layers of a pavement, a method similar to that of Barksdale (15) and Romain (16) is proposed. The stresses accruing beneath a wheel load are computed from an elastic analysis of the pavement and from this it is possible to make a prediction of the permanent strain that may occur in the bound layers of a flexible pavement structure.

The object of the investigation reported in this thesis has been to obtain sufficient laboratory data on the *permanent as well as the *resilient deformation behaviour of a dense bitumen macadam, in order to allow the development of a subsystem for a structural design procedure that considers the level of permanent deformation in the pavement.

To this end, laboratory facilities were designed and constructed to test cylindrical specimens of bituminous bound road base materials under both static and dynamic triaxial loading conditions. Attention was given to specimen preparation and to the conditions of testing to ensure that the laboratory test would simulate as closely as possible

---

* A full definition of these two terms is given in Chapter 2.

the in situ conditions of the material undergoing traffic loading.

A considerable amount of information is presented herein on both the resilient and permanent deformation characteristics of dense bitumen macadam as determined from these triaxial testing facilities.

The information thus gained on the permanent deformation behaviour of this material has allowed an approximate preliminary method for the prediction of permanent deformation in the bituminous layers of a pavement to be formulated. This has resulted in the ability to add a further sub-system to the structural design procedure for flexible pavements, advocated by Brown and Pell (5), that can check the rutting potential of a road pavement.

CHAPTER TWO

METHOD OF TESTING

2.1 INTRODUCTION

"An important part of the development of a structural design approach to the design of flexible pavements is adequate characterisation of the constituent materials in the context of the part they play in the pavement structure" (17).

As stated in Chapter 1, the object of this thesis has been to obtain the above characterisation of a dense bitumen macadam. The deformation characteristics of this material may be divided into two types, permanent and resilient. The boundary between these two is indistinct as the response of the material to a change in stress contains a viscous as well as elastic and plastic components. In order to obtain strain (or deformation) parameters that take this into account when a specimen is subjected to cyclic loading, the resilient strain is defined as the peak to peak fluctuating strain component, and the permanent strain is defined as the non-recovered component of strain with time. The two may be seen in a diagrammatic representation in Fig. 2.1.

This investigation was carried out in a laboratory as it is impractical to hold in situ trials for all materials and conditions. Full-scale trials should be reserved for verifying the results of laboratory work. At present it is not possible to reproduce in the laboratory the exact

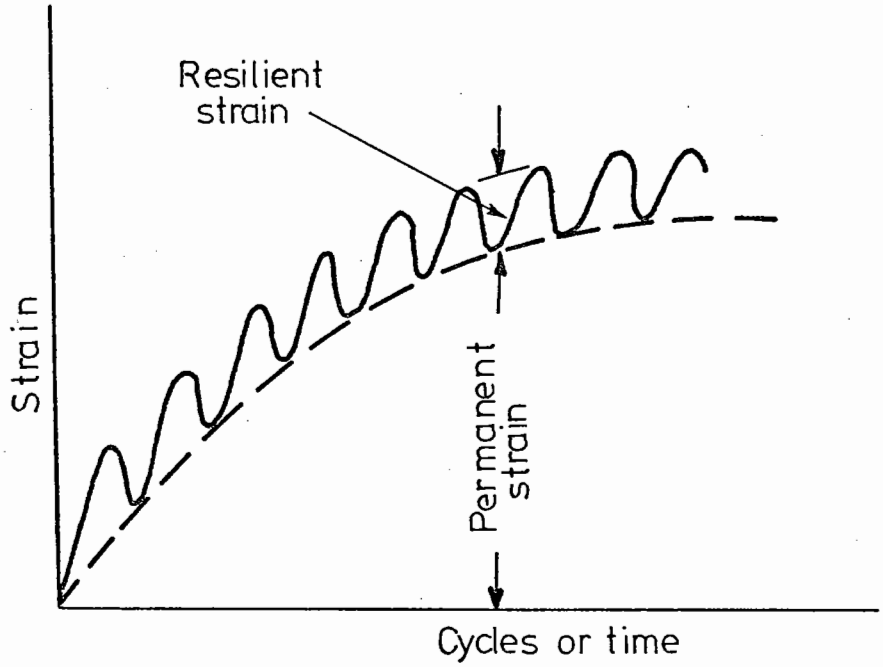

IDEALISED STRAIN PATTERN SHOWING THE RESILIENT AND PERMANENT COMPONENTS OF STRAIN.

Fig. 2.1

stress patterns occurring beneath a rolling wheel load. It was considered that a dynamic type of triaxial test, already used widely for soils (18,19,20), probably gives the best approximation to pavement conditions. The three reasons picked out by Chomton and Valayer (21) for using this type of test are listed below.

(1) Tests, and particularly fatigue tests, give much better accuracy when they are performed with homogeneous stressing than with for instance, flexural stressing.

(2) The variety of stresses available is higher together with the possibility of using a lateral pressure.

(3) Although the stresses that are applied to the cylindrical sample do not follow the same "path" as in the road when a vehicle passes on the surface, it is "no worse" than any other kind of simulation which does not exactly reproduce the in situ stress patterns.

In view of these the servo-hydraulic techniques developed for the dynamic triaxial testing of soils at Nottingham University (18) have been adopted and developed for the dynamic triaxial testing of bituminous bound materials. The methods of applying the stresses to cylindrical specimens are set out in Chapter 3 whilst the manner in which the specimens are manufactured to simulate in situ material is set out in Chapter 4. This chapter is concerned with the mode of application of stresses, and

the choice of testing conditions for the simulation of in situ pavement conditions, as it is only by approaching realistic loading conditions in the laboratory that useful results can be produced.

2.2 STRESS OR STRAIN CONTROL

Dynamic triaxial testing may be carried out by applying either dynamic stress or dynamic strain at a constant amplitude. It is well known that a material undergoing a fatigue test under constant stress conditions will exhibit a shorter life than under constant strain conditions (22). It is therefore important to use the type of test applicable to the simulated in situ position of the specimen. There have been generalisations that full depth pavements require constant stress testing (23), but the approach of Monismith and Deacon (24) is seen as the most rational. They proposed a "mode factor" which recognised that during the life of a pavement the stiffness of the bituminous layer will decrease and cause changes in the stress and strain distribution in a pavement. At any level in the pavement, it is the value of stress or strain that changes least for a given stiffness change that should be regarded as the constant amplitude parameter for testing.

In the case of the author's work it was decided at an early stage that constant stress testing was the more applicable with the in situ vertical stress being simulated by an axial stress to the specimen. When test results became available for the stiffness decrease in dense bitumen

macadam a check was made on this decision. Four road systems were selected to cover the extremes of temperature and subgrade conditions.

Table 2.1 - Systems used in elastic analysis

System No.	Layer 1				Layer 2			Layer 3		Subgrade CBR - %	Temperature Condition
	Thickness (m)	Initial Stiffness (MN/m^2)	Final Stiffness (MN/m^2)	Poisson's ratio	Thickness (m)	Stiffness (MN/m^2)	Poisson's ratio	Stiffness (MN/m^2)	Poisson's ratio		
I	.3	1400	1200	.5	.5	60	.3	20	.4	2	HOT
II	.3	7000	4300	.4	.5	60	.3	20	.4	2	COLD
III	.3	1400	1200	.5	.15	300	.3	100	.3	10	HOT
IV	.3	7000	4300	.4	.15	300	.3	100	.3	10	COLD

(All systems loaded with 40 kN load of .30 m diameter)

These systems were analysed using the BISTRO computer programme. The analysis consisted of assigning stiffness values to the bituminous bound layer from the laboratory results. The initial and final resilient modulus values yielded from the laboratory tests were used to predict the magnitudes of vertical stress and strain at the beginning and end of the life of a pavement. The initial and final stresses and strains of the four systems were compared in a graphical manner (Fig. 2.2), rather than by using the full "mode factor" technique of Monismith and Deacon (24). The percentage change in vertical stress and strain over the pavement life is plotted against depth in the bound layer. Only at the bottom of system III is the percentage change in

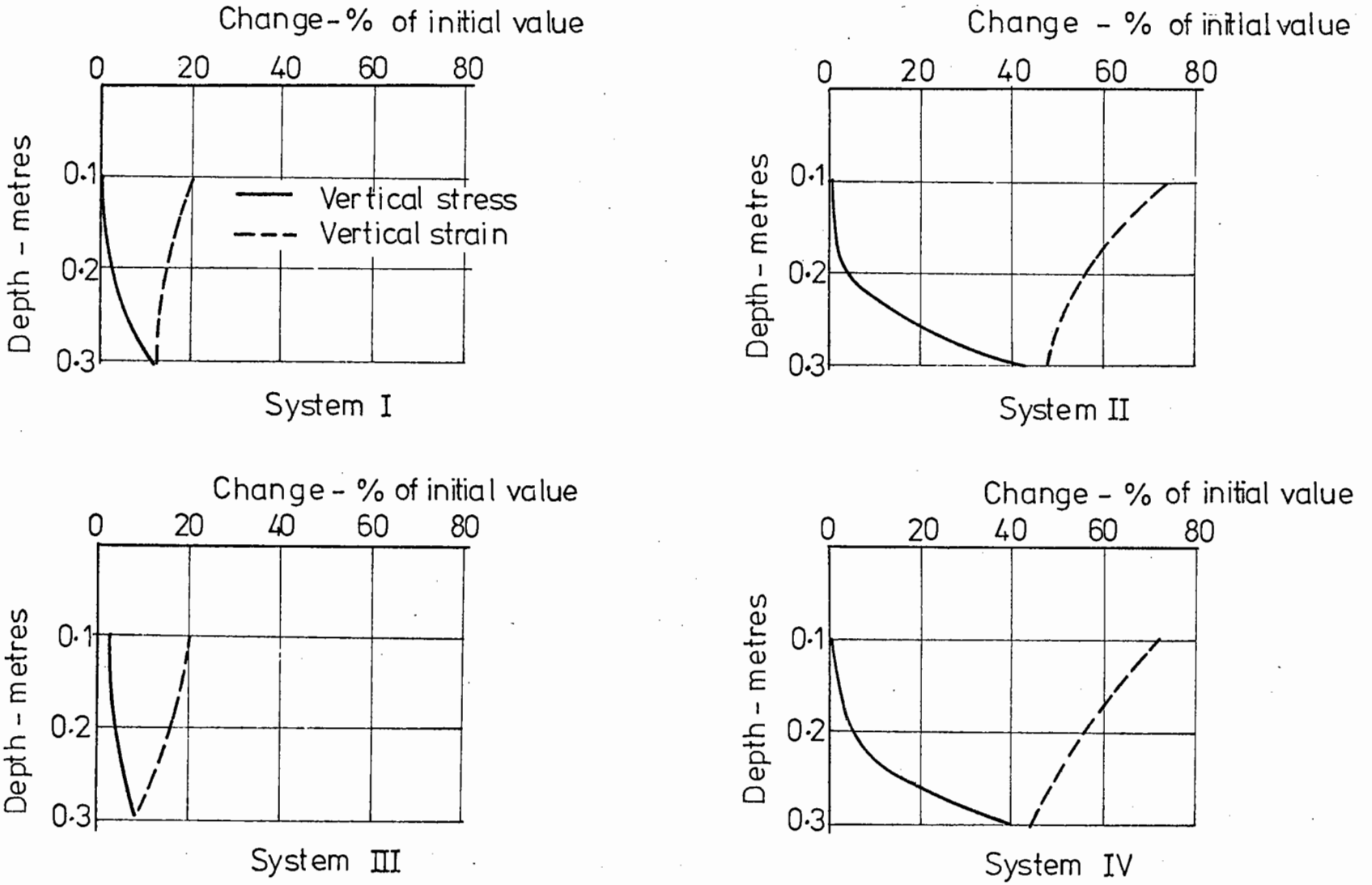

Fig. 2.2

ELASTIC ANALYSIS OF THREE LAYER SYSTEM SHOWING HOW VERTICAL STRESS AND STRAIN VARY THROUGH THE LIFE OF A PAVEMENT. (Systems defined in Table 2:1)

strain less than the percentage change in stress. This would indicate that whilst not ideal the constant stress test is the more applicable when considering the behaviour of the roadbase in a bituminous bound roadbase structure.

2.3 SHAPE OF APPLIED STRESSES

Various stress pulses have been applied to bituminous materials in laboratory investigations. For example, Hanson (25) applied a triangular wave, Cragg and Pell (26) a sinusoidal wave, Dehlen a rectangular pulse (27), whilst van Dijk et al (28) have applied a modified sinusoidal wave. Barksdale (29) carried out a theoretical investigation into the stress patterns at various depths in a pavement, and concluded that in the upper portion of a deep lift pavement, a sinusoidal stress pulse was appropriate, but that in the lower layers triangular shaped stress pulses approximated more closely to reality. The author has investigated, using the BISTRO programme, a number of vertical stress pulse shapes at different depths in different pavement systems and has concluded that a sinusoidal vertical stress pulse is close to the predicted in situ shape. Barksdale has also stated that:

"More complicated stress pulse forms are not, at the present time, considered necessary because of the many uncertainties associated with the use of layered theory."

With the triaxial test there is also the ability of applying a confining pressure to a specimen. The simple case of a constant confining pressure has been investigated

by a number of workers (30,31,32) but the more difficult pulsing of the confining pressure had only been reported by Dehlen (27). Although it was decided that a sinusoidal wave was the most appropriate form for a pulsed confining pressure, the majority of tests would be carried out at a static level. Thrower et al (33) have reported longitudinal strain pulse times that are as much as ten times the duration of the vertical strain pulse at the same depth in the pavement surfacing.

In order to investigate the effect, if any, of the two stress components acting for different times, provision was made to simulate this phenomenon in the laboratory triaxial test with the confining pressure pulse lasting for a longer time than the vertical stress pulse.

2.4 MAGNITUDE OF APPLIED STRESSES

In order that the laboratory specimens could be subjected to realistic vertical stresses and confining pressures, it was necessary to estimate the values of the in situ vertical and horizontal stresses occurring beneath a rolling wheel load on a road base. The four systems used in section 2.2 were analysed by Snaith, Brown and Pell (34) to give the likely in situ stresses. In all cases, a 200 mm base was considered with a 100 mm surfacing layer (considered together as one layer in the analysis). Two subgrades were chosen with C.B.R.'s of 2% and 10% representing the practical extremes. For the weak subgrade a 500 mm sub-base was used and for the other a 150 mm sub-base. To represent the extremes of

temperature the stiffness of the bituminous layers was taken as 7000 MN/m^2 and 1400 MN/m^2 on each structure. The stresses induced at the top and bottom of the 200 mm base by a standard wheel load were recorded. Figs. 2.3 and 2.4 show the range of vertical and horizontal stresses plotted against radial distance from the loads. It was noted that the difference between the two horizontal stresses, radial and tangential, was sufficiently small to justify the axially symmetrical test conditions imposed by the use of triaxial testing. Unfortunately, no in situ measurements of stresses in bound base layers are available to check these theoretical results. Measurements in subgrade soils have indicated that theoretical values of radial stress are generally lower than those in situ. If this is also true for the base layer, then the high negative values predicted in Fig. 2.4 may not be realistic.

The transient stresses resulting from a passing wheel load are superimposed on an overburden stress for the structure, which at the centre of a thick bituminous layer would be about 3 kN/m^2 (or 6 kN/m^2 at the bottom).

From this theoretical study, it may be seen that transient vertical stresses of up to 450 kN/m^2 and compressive horizontal stresses of up to 250 kN/m^2 may occur in the road base, together with an overburden pressure of up to 6 kN/m^2. These values allowed test programmes to be formulated that would reflect the in situ stresses in the values of vertical (or deviator) stress and confining pressure applied to the specimen.

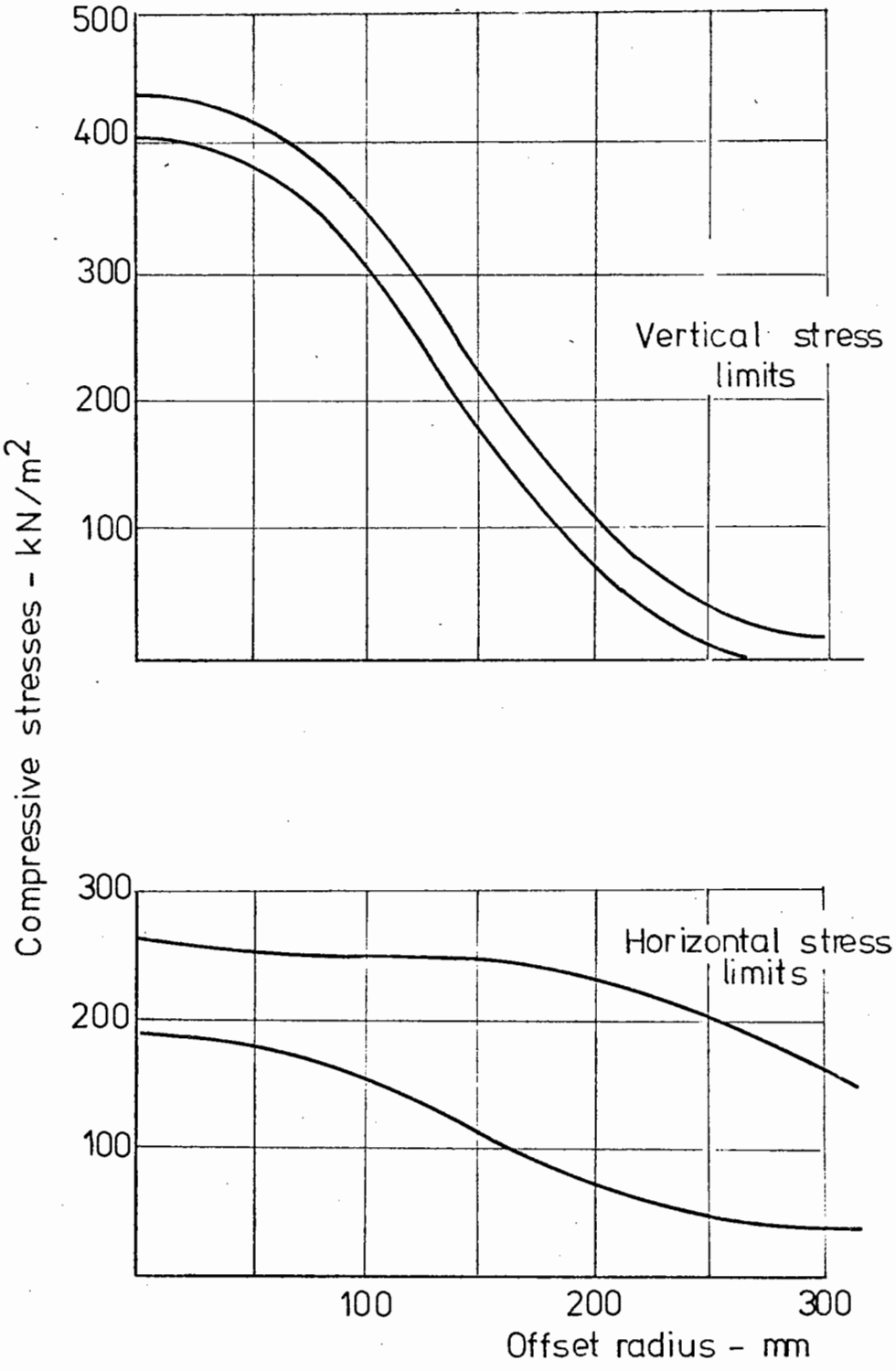

RANGE OF STRESSES IN THE TOP OF THE ROADBASE

Fig. 2.3

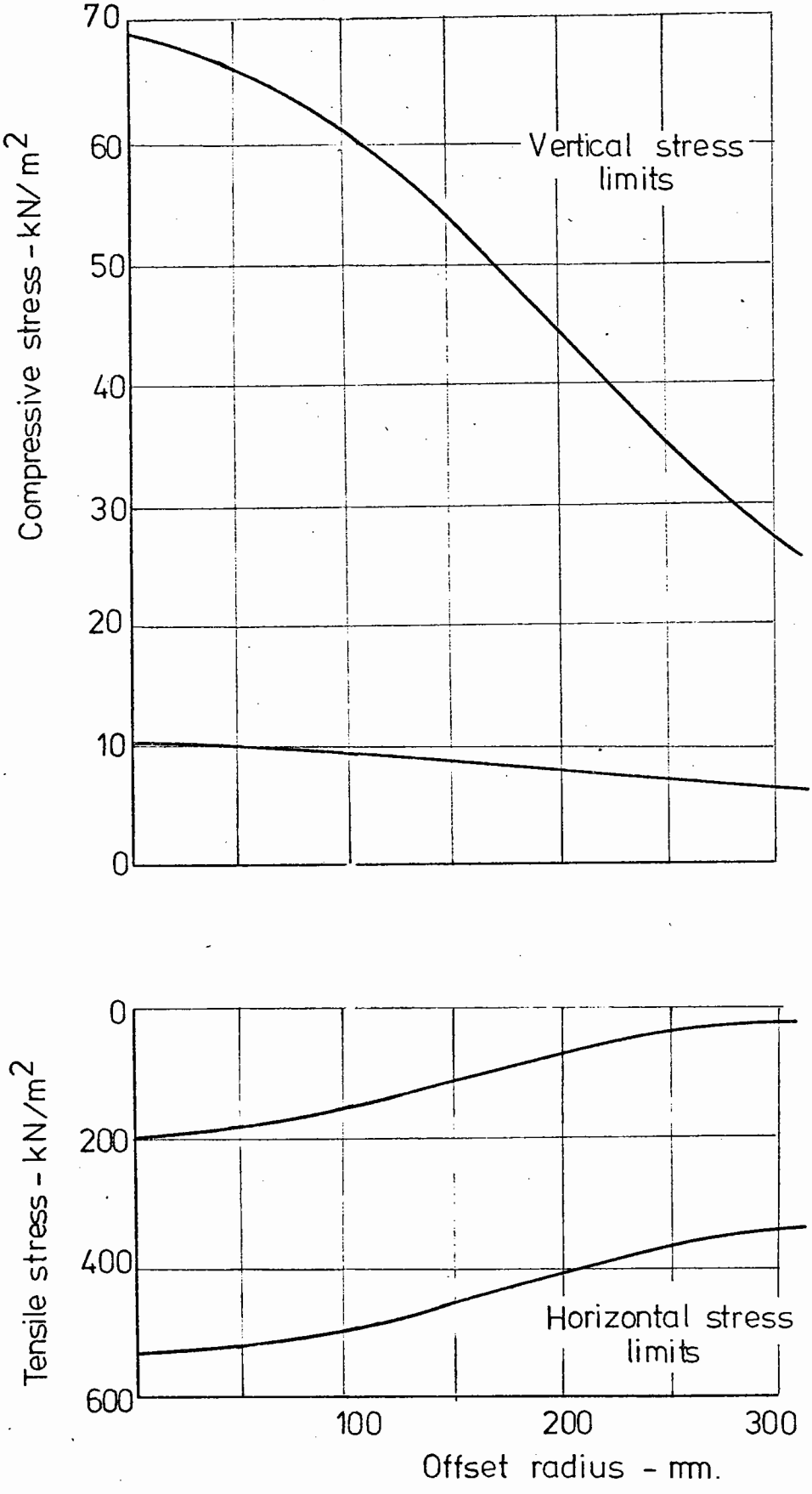

RANGE OF STRESSES IN THE BOTTOM OF THE ROADBASE.

Fig. 2.4

2.5 FREQUENCY OF LOADING

Bitumen is a viscoelastic material and hence its behaviour in a bituminous mixture will depend on the frequency of load application. The constant stress testing machine adequately models a stationary vehicle (see Section 3.3), but in the dynamic tests, the frequency of the deviator stress pulse has to be chosen to simulate the frequency of the vertical stress wave in the road base due to a moving load. This will depend on the speed of the vehicle and the apparent wavelength of the stress pulse at a particular depth.

When a wheel load passes over a position in the roadbase, the vertical stress will start to rise before the wheel is vertically over that position, and similarly, the stress decays as the wheel moves away. If the stress pattern was, say, trapezoidal, it would be easy to assign a wavelength to this stress. It has been indicated in Section 2.3 that a sinusoidal wave shape is appropriate, but as noted by Brown (35) it is difficult to assess where such a wave starts or finishes. There are three ways of defining these points. Firstly, on the assumption that the stress wave has passed when the stress level has dropped to a chosen percentage of the applied stress, secondly to assume that it has passed when the stress level has reached a chosen percentage of the maximum stress existing at that particular depth, or thirdly, to fit a standard curve to the stress pulse (29,35). The first is easy to operate, especially when analysing field results; the third has been used in the prediction of vertical and principal stress pulse times in pavements by

Barksdale (29). However, at the time of this investigation, the second method was felt to be the most appropriate of the three.

The difference in stress wavelength with depth for the two non-curve fitting methods is shown in Fig. 2.5. It may be seen from this simple layered system, analysed using the BISTRO programme, that by employing the second definition, the wavelength-depth relationship is linear with the equation:

$$\lambda = kd + a$$

where λ is the wavelength

d is the depth

k and a are constants.

Using this relationship, a value of vehicle speed may be taken and used to give the frequency of testing applicable for any depth in the pavement.

$$\text{Frequency (Hz)} = \frac{277 \times \text{vehicle speed (km/h)}}{(kd + a)}$$

where d is in mm and only the top layer of any system is included, as the shape constant "k" changes for each layer.

The work of Klomp and Niesman (36) would appear to rely on the first definition as they do not obtain the linear increase in wavelength with depth, but rather the curved shape shown in Fig. 2.5. Their figures were obtained from in situ measurements with strain gauges placed longitudinally at layer interfaces, and the "loading time" was inferred from their outputs.

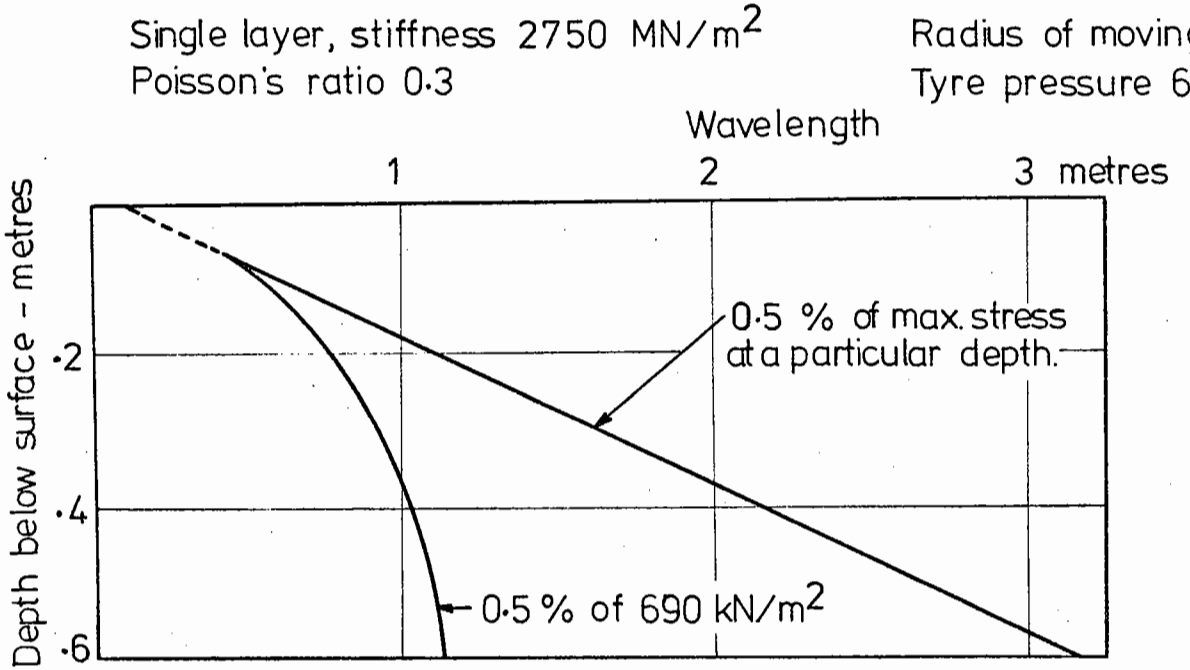

Fig. 2.5

WAVELENGTH OF VERTICAL STRESS PULSE WITH DEPTH (BISTRO ANALYSIS)

Barksdale (29) has more recently carried out the same type of analysis of pulse times using the curve fitting technique and has shown that the length of the vertical stress pulse does increase markedly with depth. Barksdale also compared his results from an elastic analysis with in situ results from the AASHO Road Test and found reasonable agreement, though he did point out that the elastic analysis did not take account of inertia forces and viscous effects.

In order to obtain a range of frequencies suitable for a laboratory testing programme the linear wavelength-depth relationship was derived for the four systems (Section 2.2) covering extremes of subgrade type and bituminous layer stiffness. Fig. 2.6 shows the four systems analysed and also shows the frequency appropriate for simulating the conditions of a specimen from any depth in the bound layer with any vehicle speed. The small changes in all but the top of the layer due to variations in subgrade and temperature should be noted, and this also was reported by Barksdale (29).

2.6 REST PERIODS

The ability of a bituminous bound material to "heal" the damage sustained under loading if suitable conditions are available has been reported by a number of research workers (28,37,38).

Furthermore, in situ pulses due to moving vehicles will not be continuous, and so, although most of the testing was of a continuous nature it was decided to investigate the possibility of a beneficial effect being felt by a specimen if a rest period was present between load applications.

System No.	LAYER 1			LAYER 2			LAYER 3			Subgrade	Temp.
	Thickness (m)	E (MN/m^2)	ν	Thickness (m)	E (MN/m^2)	ν	Thickness (m)	E (MN/m^2)	ν	CBR - %	Condition
I	·3	1400	·5	·5	60	·3	∞	20	·4	2	HOT
II	·3	7000	·4	·5	60	·3	∞	20	·4	2	COLD
III	·3	1400	·5	·15	300	·3	∞	100	·3	10	HOT
IV	·3	7000	·4	·15	300	·3	∞	100	·3	10	COLD

(All systems loaded with 40 kN load of ·30 m. diameter)

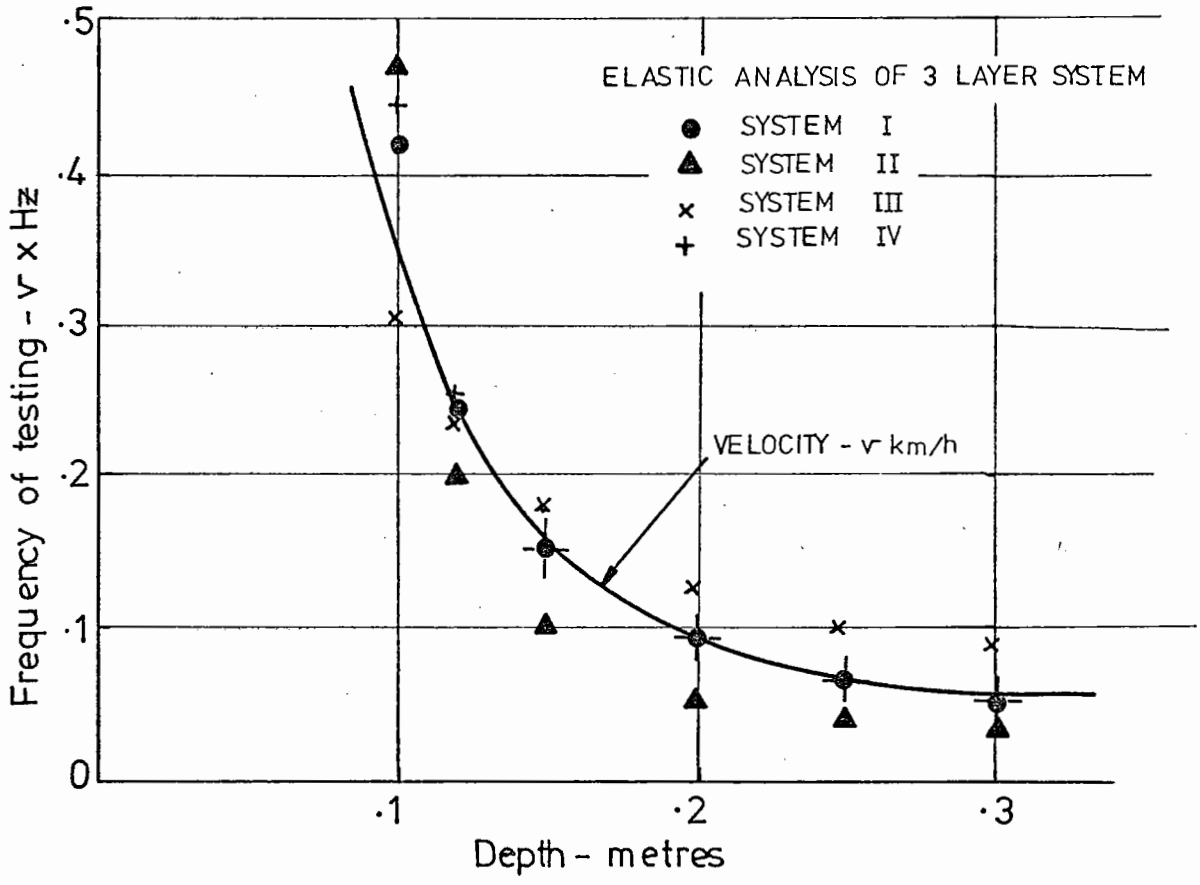

NOMOGRAPH TO OBTAIN APPROPRIATE FREQUENCY OF VERTICAL LOAD APPLICATION CONSIDERING SPEED OF PASSING LOAD AND SAMPLE DEPTH.

Fig. 2.6

CHAPTER THREE

LABORATORY TESTING EQUIPMENT

3.1 INTRODUCTION

The previous chapter has outlined the form of the dynamic triaxial test necessary to investigate permanent deformation phenomena in roadbase materials. In order to design a machine capable of performing the test on a specimen satisfactorily, two things must be known - the loading conditions that are to be simulated, and the approximate behaviour of the specimen. The first was obtained from the methods of analysis shown in Chapter 2 and from consultation with the Transport and Road Research Laboratory (T.R.R.L.). The specification of the loading conditions is summarised in Table 3.1. As investigators have not studied simultaneously resilient and permanent deformation characteristics to failure, the second can only be found to a sufficient accuracy by the use of pilot tests.

3.2 INSTRON TESTING MACHINE

The Instron testing machine described by Hanson (25) was further modified to permit a pilot programme of dynamic triaxial tests on 100 mm diameter (4 in.*) specimens. Hanson had already modified the loading frame so that a constant frequency of testing of up to 50 cycles per minute could be obtained despite any change in stiffness of a

---

* In the case of S.I. figures derived from Imperial units, the approximate S.I. figure is written with the exact Imperial unit in brackets following.

specimen. The loading frame was further modified to carry a standard Farnell triaxial cell (for soil samples 100 mm (4 in.) diameter by 200 mm (8 in.) long). This system was capable of applying a longitudinal load of 44 kN and a maximum constant confining pressure of 550 kN/m^2 to 100 mm (4 in.) diameter specimens.

Provision was made for electrical cables to pass through the base of the cell in order that electronic methods of measuring specimen deformations inside the triaxial cell, during a test, could be investigated (see Section 3.6).

The loading frame was inside a temperature controlled room with the control and monitoring systems placed outside this environment. Hanson's method of measuring the apparent load applied to the specimen was employed. The axial deformation of a specimen was translated into an electrical impulse employing LVDT's* (Section 3.6). This resulted in a system for recording, in which both load and deformation were available on a 3-channel pen recorder, for future analysis.

3.3 CONSTANT STRESS TESTING MACHINE

The purpose of this testing facility was to apply a constant longitudinal stress to cylindrical specimens of roadbase material. A soil consolidometer was modified to apply stresses, through a second order lever system, of up to 1000 kN/m^2 to specimens 150 mm (6 in.) long by 100 mm (4 in.) diameter. A photograph of the apparatus with a

---

* Linear Variable Differential Transformers

specimen under test, may be seen in Fig. 3.1 in position inside the temperature controlled room.

3.4 ELECTRO-HYDRAULIC SERVO-CONTROLLED TESTING MACHINE*

It has been noted in this chapter that to design a dynamic testing facility, the loading conditions and approximate specimen behaviour must be known. When those two areas had been investigated, design and fabrication could proceed.

The control system developed was based on similar equipment used for soils testing at Nottingham University (18). It was designed to operate on cylindrical specimens 225 mm long by 150 mm in diameter, which allowed aggregate sizes of up to 35 mm to be included in a specimen. The basic requirements for the system were as follows:

(1) Application of a sinusoidally varying vertical stress with rise times varying between 5 minutes and 0.025 seconds.

(2) Application of a sinusoidally varying confining pressure either in or out of phase with the vertical stress with rise times varying between 5 minutes and 0.05 seconds.

(3) Provision of rest periods between one or more stress pulses.

(4) Measurement of the above stresses.

---

*The electro-hydraulic servo-controlled testing machine will in the narrative be known as the servo-hydraulic machine.

(5) Measurement of recoverable (resilient) and irrecoverable (permanent) deformations in the vertical and lateral directions.

(6) Provision for recording the various measurements.

(7) The use of triangular waveforms in addition to the sinusoidal ones was also required in order to provide continuity with the work using the Instron testing machine.

(8) A temperature controlled environment for the specimens during testing. This was achieved by placing the complete loading frame inside a temperature controlled room with variations of temperature around the specimen restricted to plus or minus a quarter of a degree Celsius.

Quantitative details of the above are given in Table 3.1 and a description of the various parts of the equipment is contained in the following paragraphs.

Table 3.1 - Overall system specification

Variable	Details
Temperature	-10^{o} to 40^{o}C
Vertical stress	0 to 1400 kN/m^2
Confining stress	0 to 1000 kN/m^2
Frequency of vertical stress pluse	0 to 20 Hz
Frequency of confining stress pulse	0 to 10 Hz
Rest periods between pulse trains	0 to 40 minutes
No. of pulses in train	1, 2, 4, 8
Shape of pulse	Triangular or sinusoidal

Stress Application System

The vertical stress was applied to the specimen by an hydraulic actuator fitted to the top of the load frame as shown in Fig. 3.2. This actuator was capable of exerting a maximum compressive force of 25 kN.

The confining stress cycling system was operated by a smaller actuator driving a piston on a cylinder which was connected, through the confining medium, to the cell pressure system. The arrangement, shown in Figs. 3.2 and 3.3, was capable of raising the confining pressure to 1000 kN/m^2. The triaxial cell had an aluminium, instead of the usual perspex, shell to reduce the compliance of the confining pressure system so that pressures of the above order of magnitude could be pulsed at up to 10 Hz without undue liquid flow (compliance of system: 0.28 $ml/kN/m^2$).

These two actuators were independently controlled by closed servo loops operating a servo valve on each of the actuators. A block diagram of these control loops is given in Fig. 3.3.

The reference signals for both systems were provided by a modified function generator with two outputs whose phase difference was adjustable. The comparative signals were obtained from a load transducer and pressure transducer for the vertical and confining pressure systems respectively.

The vertical load transducer was situated inside the triaxial cell beneath the test specimen. This ensured that friction due to the ram passing through the cell top was not included in the measurement. The transducer took

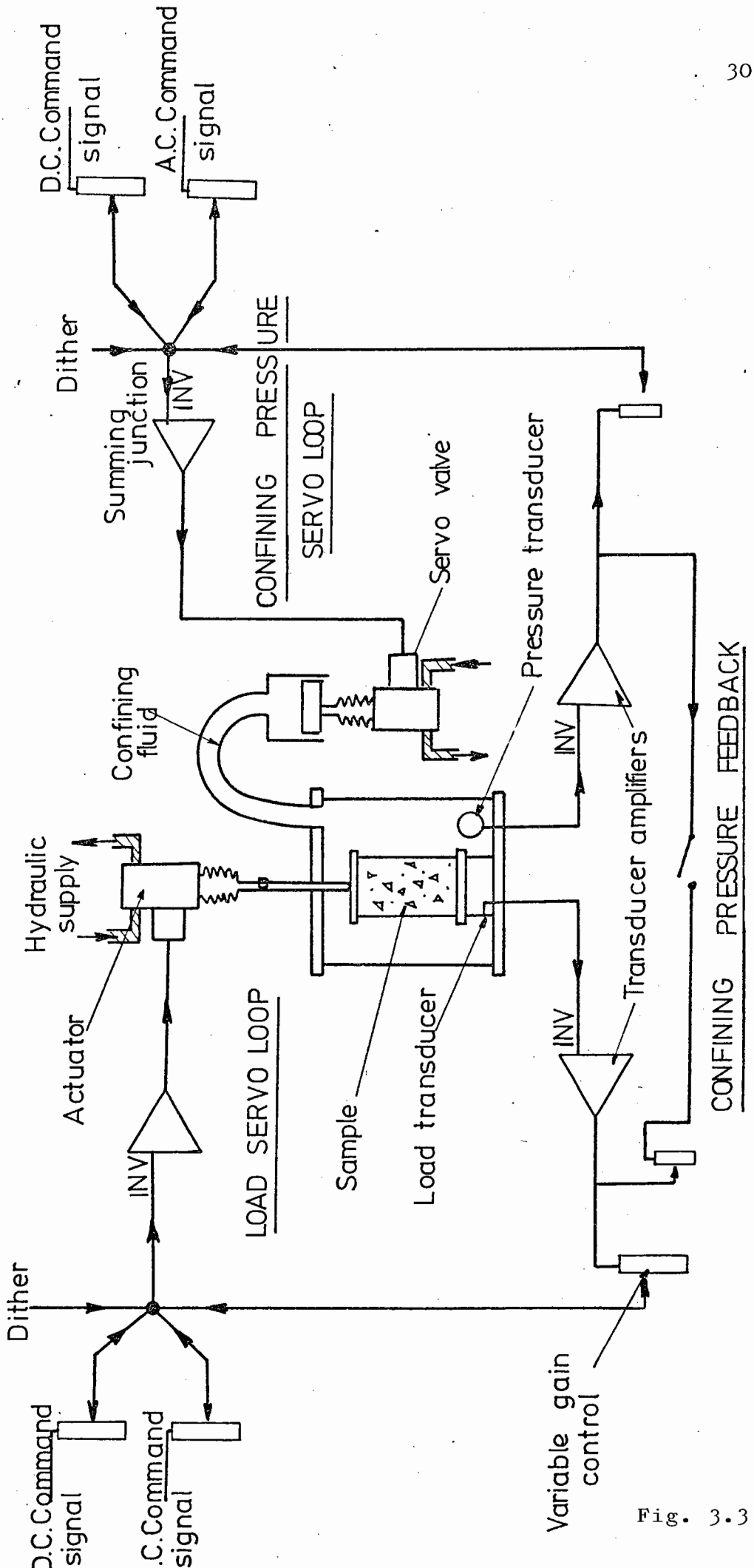

SCHEMATIC OF THE TWO SERVO LOOPS USED FOR THE TRIAXIAL TESTING OF BITUMINOUS MATERIALS.

Fig. 3.3

the form of a thin walled aluminium cylinder which constituted the pedestal of the triaxial cell. The walls were strain gauged to provide an electrical signal. Small holes were located in the cylinder walls so that the confining medium pressure was able to act on both the inside and outside of the load transducer, thus avoiding cross-sensitivity of the transducer to confining pressure. A diaphragm type pressure cell was suspended in the confining fluid to monitor pressure. The transducer element was a strain gauge bridge cemented to the diaphragm.

The vertical load system normally operated on controlled deviator stress ($\sigma_1-\sigma_3$), where σ_1 is the vertical stress in the specimen and σ_3 is the confining pressure. However, it was also possible to operate under controlled vertical stress (σ_1) or, with modification, controlled vertical strain.

The type of servo system used is susceptible to drift and electronic interference. The problem of drift was overcome by placing the control system amplifiers inside the temperature controlled environment used for testing the bituminous materials. Only essential controls and non-temperature sensitive parts of the circuit were located outside this environment.

Interference was minimised by arranging for the transducer signals to be of large magnitude thus ensuring a high signal to noise ratio. This also had the effect of reducing the influence of drift.

Both servo loops were controlled in the same way. A constant static load was applied by setting the D.C. level

of the reference signal at an appropriate value. This "dead load" was introduced to represent the effect of overburden pressure in an actual road. The dynamic load, in either the sinusoidal or triangular mode, was superimposed on this dead load by selecting the required amplitude and frequency of the reference signal from the function generator. This represented the effect of wheel loads on the pavement and is known as the "live load". The dead and live loads could be varied independently.

The provision of rest periods between trains of one or more pulses (see Table 3.1) was achieved by an external control to the function generator. This external control introduced a pause of varying length (up to forty minutes) between the commands triggering the function generator. The length of the pause was controlled by a binary counter operating off the 50 Hz mains supply.

In practice, the vertical and horizontal pulses due to a passing wheel load may not be of the same length (Section 2.3). The vertical pulse may be of large amplitude and short length, and the horizontal pulse, lower and longer. The peaks will coincide. This could be achieved in the equipment by the use of an additional module whose effect was to give short vertical pulses, with rest periods, whose peaks coincided with those of the continuously cycled confining pressure.

To explain the mode of operation it is simplest to consider the reference signal coming to the module as a continuous pulse train of triangular waves. The bottom of

the triangular wave train is then truncated, leaving triangular pulses of diminished amplitude with rest periods in between. The amplitude of the triangular signals is then increased to the normal level of input to the servo-loop. In the case of the sinusoidal reference signal, conditioning of the signal was performed at this stage to obtain a full sinusoidal wave shape after the truncation. (An example of continuous stress variation and the above regime of loading is given in Figs. 3.4 and 3.5).

The only trouble encountered has been with the hydraulic power supply. It has been found that the design of the inlet manifold to the pump from the oil reservoir is such as to cause an unnecessarily high vacuum in this region. This led to air being sucked into the oil and finding its way into the hydraulic actuators, resulting in a sluggish response. The level of the vacuum and hence the air entrapment was kept to a minimum by constant attention to the suction filters attached to the manifold.

The servo-hydraulic machine was moved into the temperature controlled room previously occupied by the Instron testing machine, care being taken to position the main part of it on the vibration free platform built into the room. Although adjacent to the constant stress testing machine (Section 3.3) the operation of the two was completely independent.

3.5 LOADING PLATENS

The triaxial test has for a considerable time been a

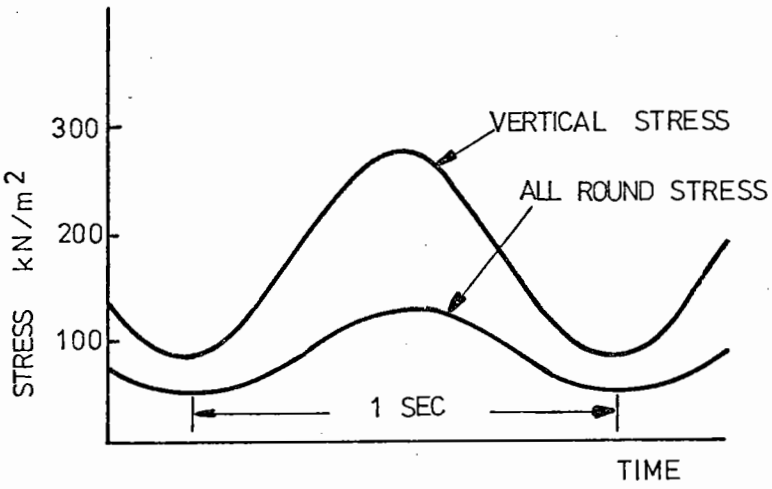

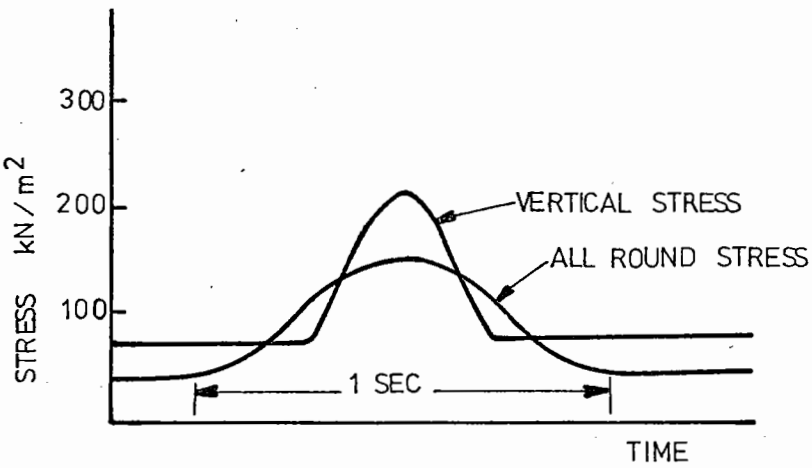

EXAMPLES OF IMPOSED STRESS PATTERNS

(TRACED DIRECT FROM U.V. RECORDER OUTPUT)

Fig. 3.4

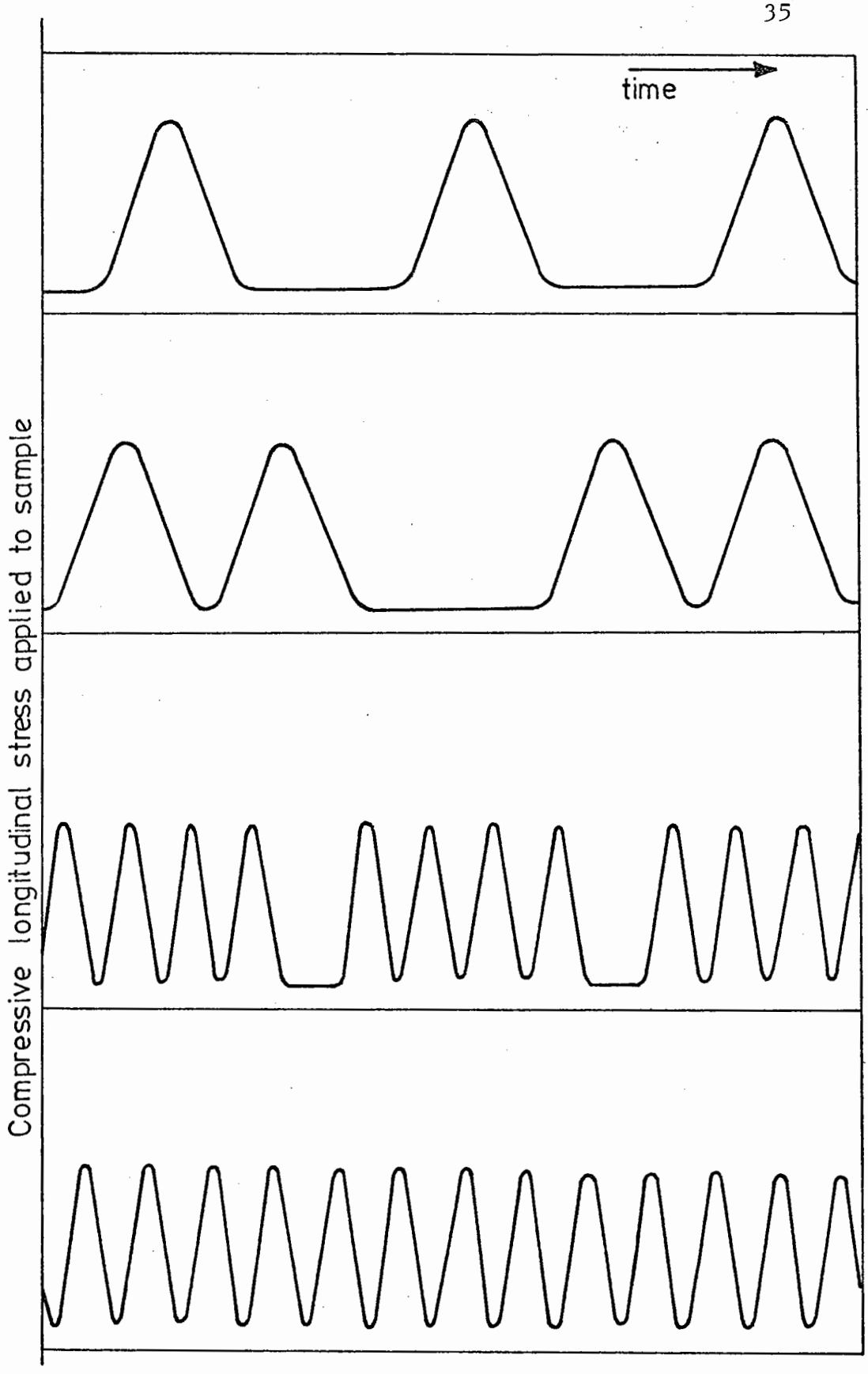

TYPICAL VERTICAL STRESS PATTERNS

Fig. 3.5

standard test for soils. In soil mechanics the specimen has a 2:1 length to diameter ratio so that end platen restraint does not have a large influence on failure stresses. Rowe and Barden (39) showed that the use of "frictionless" end platens allowed specimens to deform as right cylinders with uniform stress conditions throughout the length of the specimen. These special end platens consisted of polished steel covered with a layer of silicone grease and a rubber membrane.

In general, previous work on bituminous specimens has looked either at initial resilient behaviour or permanent deformation behaviour but not at the two combined. In direct compression testing there is no necessity to glue the loading plates to the specimen and hence "frictionless" platens may be used. Taylor (40) using a finite element technique has studied the stress and strain distribution in a bituminous specimen with varying degrees of end restraint. He concluded that the measured elastic properties would only be changed by 7% by high friction platens but also showed that there is a conical "zone of constraint" at both ends of a specimen so loaded. In repeated load tests Taylor predicted that this would lead to the following result:

"All work would have been done (or all shear deformation occurred) away from the conical regions of all round compression and have led to a local failure in the specimen rather than an overall breakdown."

Employing the Instron testing machine with non-lubricated platens a bituminous specimen was dynamically tested and the

observation made by Taylor was found to be true (Fig. 3.6). Bulging occurred at mid-height, probably causing a premature failure. It became evident both from laboratory and theoretical work that, if sensible deformation measurements of specimen behaviour throughout a test were to be taken, then this bulging had to be eliminated.

In order to establish what loading conditions would be acceptable, various values of the coefficient of friction between platen and specimen were fed into Taylor's finite element programme. These values were obtained by experimentation. Employing a modified shear box (Fig. 3.7) platens of five materials were tested. Of these, the platen of polished chrome on case hardened steel gave the best results. The coefficient of friction of this test material in direct contact with a bituminous specimen was measured at 0.1, which was further reduced to 0.003 by separating the two by a sandwich of thin rubber membranes and silicone grease. With this low value of the coefficient of friction, Taylor predicted that a uniform stress field would result, and that failure would occur uniformly throughout the specimen. The first of these findings was corroborated by the author experimentally using a photoelastic technique (described below) and the second by testing a specimen in the servo-hydraulic machine as may be seen in Fig. 3.8.

The photoelastic experiment was a simple one with a two dimensional model of a triaxial specimen being loaded as shown, Fig. 3.9. The top of the specimen was in contact with the loading platen through a rubber-silicone grease-rubber

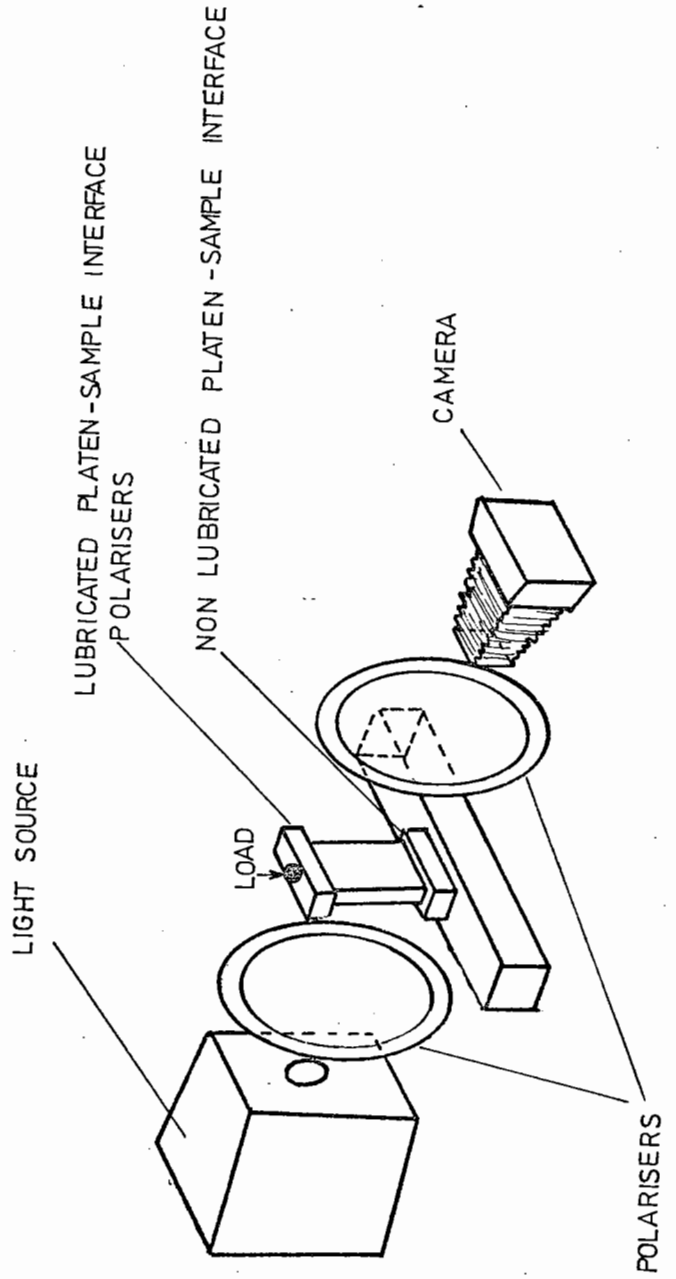

APPARATUS FOR QUALITATIVE PHOTOELASTIC INVESTIGATION OF END FIXITY CONDITIONS IN THE TRIAXIAL TEST

Fig. 3.9

"sandwich" whilst the bottom of the specimen made direct contact with the loading platen. It is evident from Fig. 3.10 that considerable shear strain resulted when there was no lubrication.

Ko, Masson and Nymoen (41), using a three dimensional model, with a frozen strain technique, came to the same conclusion about the release of shear by "sandwich" lubrication. They further stated that it was probable that the sandwich layer between specimen and loading platen effectively screened out the effects of the rigidity of the loading platen on the uniform stress distribution.

Taylor (40), again using the finite element technique, also showed that the top platen provided would bend sufficiently to cause non-uniform stresses in the specimen. The thickness of the top platen was, therefore, increased to minimise this effect.

The configuration of the platens used in all test machines resulting from the above work may be summarised as follows.

Both ends of the prepared specimen (see Chapter 4) were loaded through rigid platens with a shear break. This arrangement required some mechanism to prevent lateral slipping of the specimen. This was provided by a small spigot set into the lower platen locating into a hole in the bottom of the specimen. The bottom platen fitted onto the aluminium pedestal cum load transducer. With the shear break between the top platen and the specimen it was found advisable to locate the loading plunger of the triaxial cell

positively onto the top platen to prevent lateral movement. In order to give uniform stress distribution in the specimen, the platen should be free to accommodate any small deviation from the horizontal that may be present in the top of the specimen, hence the hemispherical end of the plunger was located in a conical hole in the top of the platen. When these platens were in use specimens of up to 225 mm in length could be tested in the servo-hydraulic machine, or 150 mm (6 in.) in the Instron and constant stress testing machines.

3.6 DEFORMATION MEASUREMENT SYSTEMS

Longitudinal deformation of specimens tested in the servo-hydraulic machine was measured over two 150 mm diametrically opposed gauge lengths about the mid-height of the specimen. The measurements were thus free of specimen end effects and errors which could be introduced by the use of an arbitrary datum such as the cell base or the cell lid.

Four locating targets were glued to the specimen at each end of the two gauge lengths. The relative deformation of each pair of targets was measured by using a pair of L.V.D.T.'s. The two parts of the L.V.D.T. were held in contact with the targets by a pair of perspex collars. Each collar was split to allow for the lateral permanent strain developing during a test. The two halves were hinged at one end and connected by a spring at the other. The action of the spring kept two pointers, one on each half of the collar, located in the targets. Small pieces of rubber were placed between the collars and the specimen to prevent

tilting. The arrangement is shown in Fig. 3.11 and also diagrammatically in Fig. 3.12. In Fig. 3.11, the two collars discussed here are the top and bottom ones.

The two L.V.D.T. signals were summed to eliminate any error introduced due to the specimen buckling and to provide a measure of the average deformation over the central portion of the specimen. This measuring system was a development of the one used by Dehlen (27) to measure resilient deformations.

The output from each of the L.V.D.T.'s, making the longitudinal deformation measurements, consisted of a steadily increasing permanent component with the resilient deformation superimposed. The different magnitudes of these two components presented a problem if accurate measurements were to be made. Fig. 3.13 illustrates how the signal for the permanent deformation was separated from the resilient signal, and led directly to the U.V. recorder. The resilient signal was of the order of 0.01 volts while the permanent deformation change during a test might be from -1.8 volts to +1.8 volts.

If the smaller signal was amplified for accurate determination, it would quickly drift due to the influence of the permanent deformation signal. This problem was overcome by the use of an "auto-offset generator" which electronically kept the drifting signal close to zero. The resulting signal could then be amplified by up to 800 times using switched gain amplifiers. This signal had a poor signal to noise ratio and to eliminate electronic noise of 50 Hz and above, an active filter was introduced. This component eliminated

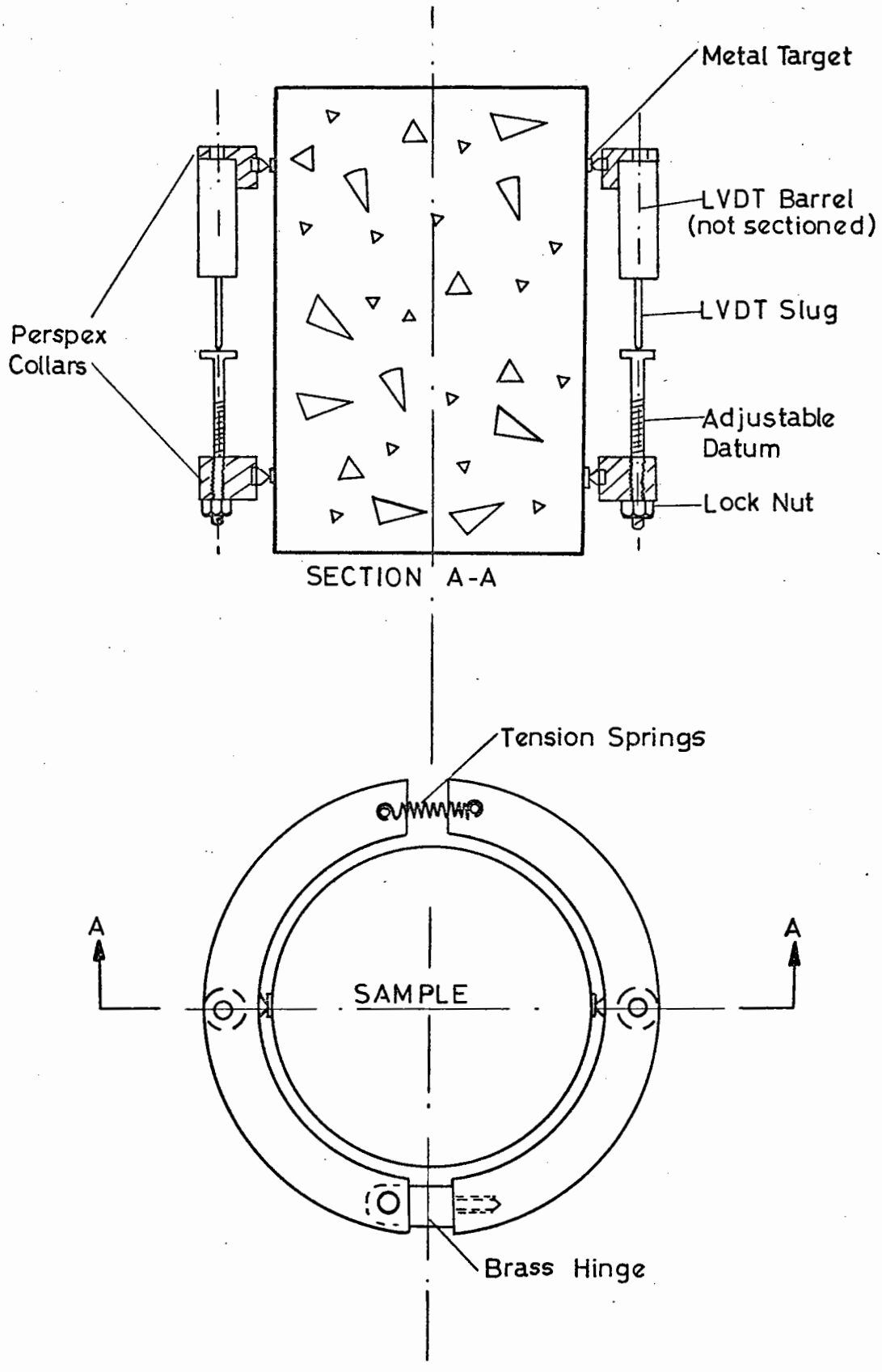

LONGITUDINAL STRAIN COLLARS FOR USE WITH BITUMINOUS BOUND MATERIALS.

Fig. 3.12

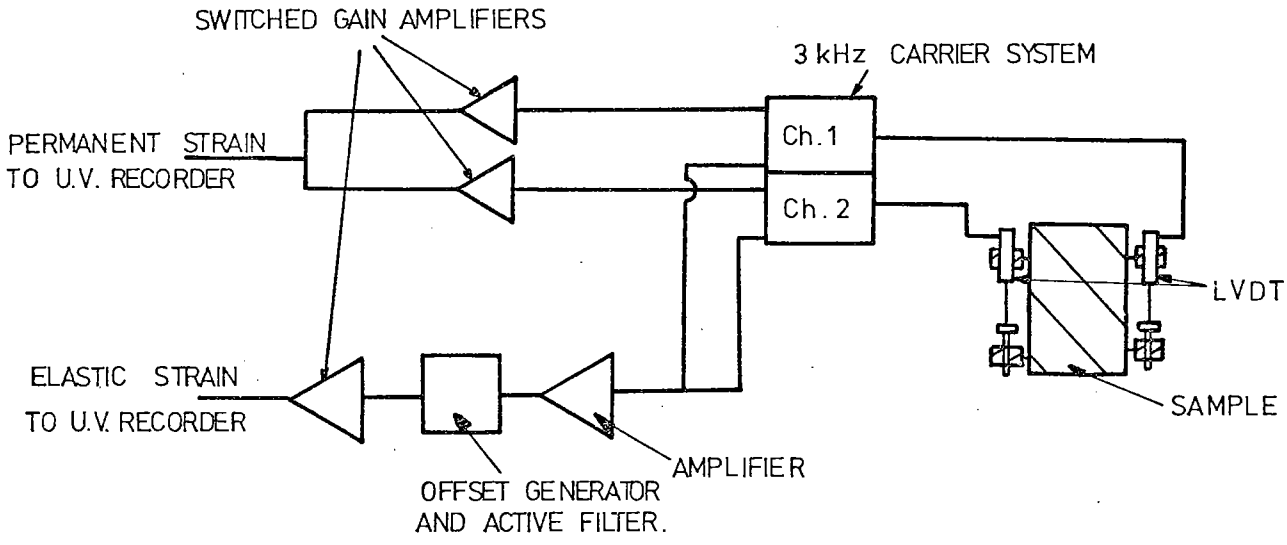

SCHEMATIC REPRESENTATION OF THE STRAIN MEASUREMENT CIRCUIT.

Fig. 3.13

all noise above 30 Hz and the resulting signal enabled resilient strains down to 1.5×10^{-6} mm/mm to be seen.

The strain collars described above were developed during the pilot dynamic triaxial testing programme, employing the Instron testing machine. The 100 mm (4 in.) diameter specimens used in this machine were also used in the constant stress testing machine. The collars used in the pilot tests were re-employed in the static tests. The output from the collars in this type of test consisted only of the steadily increasing permanent deformation and so a digital voltmeter was adequate for recording the change in voltage induced by the movement of the L.V.D.T.'s.

Radial deformation was also measured directly on the specimen in the servo-hydraulic machine. The central collar shown in Fig. 3.11 was similar to the type described by Bishop and Henkel (42) for radial deformation measurement. It was a hinged collar locating onto two diametrically opposed targets at the centre of the specimen. As the specimen expanded laterally, the gap between the free ends of the collar changed and this change was measured by an L.V.D.T.

The permanent and resilient components of the signal were determined in the same way as for vertical deformation. The L.V.D.T. arrangements for vertical deformation passed through holes in the lateral strain collar (see Fig. 3.11).

While the lateral strain collar was convenient to use it had the disadvantage that the measurement obtained was a "point value" of deformation rather than an average for all diameters.

The above internal methods of strain measurement necessitated the use of a non-conducting, non-corrosive confining medium. After various trials a transformer oil, Lorco B.29, was selected. This oil, however, attacked both bitumen and latex, and consequently, when in use, neoprene membranes were placed around the specimens (and targets). The collars were attached in the normal way to the targets, necessitating the perforation of the neoprene. This perforation was then sealed with a viscous compound.

3.7 CALIBRATION TESTS

The accuracy of the two servo-control transducers, the vertical load transducer and the confining pressure transducer, was checked against a proving ring and Bourdon gauge respectively. They were both found to give linear outputs with increasing stresses.

It was desirable that all the measuring instruments should have a flat frequency response over the range of operation of the apparatus. Tests employing unamplified signals, in series with the normal amplified signals, indicated that this was true for the strain gauge bridges in both the load and confining pressure transducers, but because of their novelty and greater complexity fuller calibration tests were thought necessary for the deformation measurement devices.

A dummy specimen consisting of a thin walled steel cylinder was set up in the load frame. It was designed to have an apparent stiffness similar to that expected for a

bituminous specimen. The strain collars were attached to this dummy specimen and the output from the L.V.D.T.'s was compared with that from strain gauges bonded to the dummy specimen for calibration purposes.

The results indicated that there was no frequency effect up to 25 Hz at which level the active filter used for the resilient deformation signals began to cut down the output. These tests also revealed that the error in strain measurement using the collars was less than 1.5×10^{-6} mm/mm.

During the course of these tests it became apparent that there was a time lag of about 0.03 seconds between the signals to the actuators and their response. It was reported by Snaith and Brown (43) that this lag was equal for both actuators. However, it has been found that the compliance of a specimen undergoing dynamic confining pressure tests leads to a "sponginess" in the confining pressure servo-loop. This sponginess was reduced to manageable proportions with the application of a small constant confining pressure (25 kN/m^2) but a definite phase difference appeared between the deviator load and the confining pressure. This was easily overcome by adjusting the relative positions of the two reference signals until the deviator load and the confining pressure were synchronised.

The signals from both the load and pressure transducers did not suffer from any time lag during amplification. However, the high amplification and active filtration of the resilient deformation signals did cause a lag, reaching 180^{o} out of phase at high frequencies.

3.8 DATA ACQUISITION

Two factors were considered of prime importance in designing a data acquisition system for this project. Firstly, all parameters had to be monitored simultaneously since they were to be interrelated subsequently. Secondly, the process had to be largely automatic as rapid changes in the measured quantities occurred at the beginning and end of a test. In addition, as some tests proceeded for several days, automatic recording at preselected intervals was desirable.

In the absence of an established computer controlled analogue to digital processor, and because of financial limitations, a semi-automatic system was designed around an ultra violet light recorder (U.V. recorder). A good quality machine with grid lines and trace identification facilities was selected. After each reading of all channels simultaneously, the paper was fed onto a take-up unit for storage and subsequent processing. The recorder could be remotely controlled and could be switched in at preselected time intervals ranging up to 12 hours. To facilitate processing at a later date one channel of the recorder indicated the number of pulse trains which had been applied at any given time of recording.

Data from the recording paper was taken off manually and processed by computer. This manual operation was the only time consuming part of the operation, but it did afford an opportunity for the traces to be inspected for errors or anomalies.

(A view of the control and recording systems is given in Fig. 3.14.)

CHAPTER FOUR

THE TEST SPECIMEN

4.1 INTRODUCTION

The specimens of bituminous road base material to be studied were produced in the cylindrical form appropriate to triaxial testing. The Ministry of Transport's specification for road base materials (3) includes aggregate up to that passing a 38 mm ($1\frac{1}{2}$ in.) sieve. As Hanson (25) has suggested that the minimum ratio of the specimen diameter to maximum aggregate size is four to one, the diameter of the specimen was fixed at 150 mm for the servo-hydraulic machine. In fact, all the laboratory manufactured specimens contained only aggregate passing 25 mm (1 in.) sieves and so it was permissible to continue using 100 mm (4 in.) diameter specimens for the Instron testing machine, and also for the static tests in the constant stress testing machine.

In soil mechanics, length to diameter ratios vary from 2:1 to 1:1 and so it was decided that the servo-hydraulic machine should be able to accept specimens up to 300 mm in length. However, as stated in Section 4.3, lubricated end platens enabled the length to diameter ratio to be cut to $1\frac{1}{2}$:1. Hence the final specimen size, after preparation, was fixed at 225 mm for the 150 mm diameter specimens and 150 mm (6 in.) for the 100 mm (4 in.) diameter specimens.

4.2 COMPACTION

A specimen of dense bitumen macadam for a laboratory test should resemble as closely as possible the material manufactured by a road construction process (44). One method to obtain such a specimen is by coring specimens from a carpet of the material laid by road paving machinery. In the case of the 150 mm diameter specimens, carpets of material of sufficient thickness are not readily available for coring. It was, therefore, decided to use a laboratory compacted specimen. Specimens for programme FS were cored from an experimental slab, but were of insufficient length to permit lateral deformation measurements to be used.

Nevitt (45) has noted that road compaction utilises low intensity forces with alternating horizontal components which lead to effective compaction and considerable particle orientation. This particle orientation is usually seen in a sample of road material sawn from a pavement. Compression methods of compaction used in laboratory preparation may lead to excessive degradation of the aggregate and, as there is no horizontal component of stress, negligible particle orientation. Impact methods of compaction, having high stress intensities, can cause localised shattering of the aggregate at the particle contacts. They do, however, have the benefit of providing some lateral stress as the point of impact moves about over the face of the specimen, resulting in a particle orientation similar to that found in a road pavement.

Following a number of trials to evaluate different

methods of compaction, it was decided that the procedure of Hanson (25) for 100 mm (4 in.) diameter by 200 mm (8 in.) long specimens contained the desirable features of the above methods and lent itself to adaption to the production of the larger 150 mm diameter specimens. Briefly, the method consisted of placing the mixed bituminous material in a steel mould (both heated to 150°C) in three layers and hand tamping each layer until a random distribution of aggregate was achieved. Then, a fixed number of blows with a modified AASHO hammer was applied to both ends in succession (25 blows for 100 mm (4 in.) diameter specimens, 65 blows for 150 mm diameter specimens). The specimen was left for 24 hours and then removed from the mould. Hanson's method was by extrusion, but this was avoided with the larger specimens by employing a split mould, which prevented possible specimen damage during the extrusion process due to the material sticking to the mould.

The large specimens had a lower void content than the small ones. This was due to two factors. When the 150 mm diameter specimens were made, the Farnell automatic compactor, which had been used for the 100 mm (4 in.) specimen, could not be used due to the size of the mould andspecimen. This necessitated hand compaction using a modified AASHO hammer. It was found that the 65 blows per end necessary for the larger specimens could be delivered with this in 45 seconds whereas the 25 blows per end required for the 100 mm (4 in.) diameter specimens took 80 seconds in the automatic compactor. This, together with the greater

heat retention of the larger specimens due to their mass, resulted in a reduction in the void content of the larger specimens of over $1\frac{1}{2}\%$ from the 100 mm (4 in.) diameter specimens.

Both sizes of specimen produced in the above manner showed a drop in density at the layer interfaces. Fig. 4.1 shows the drop in density in this area, but by careful hand tamping, which appeared to be the vital factor, this drop in density could be minimised to obtain an even distribution of the aggregate.

The overall density of both specimen sizes has been tested using a straightforward weighing method on horizontal slices of the specimen, and the gamma-ray apparatus at the Transport and Road Research Laboratory. Comparative results may be seen in Fig. 4.1.

It will be seen that while the same pattern emerges, the density indicated by the gamma-ray machine is lower than that yielded by the method of slices. The reason for this is that the former does not make allowance for the surface voids of the specimen. However, the figure shows that the method of slices does tend to minimise the variation in specific gravity through a specimen, as found by Shackel (46).

The orientation of particles resulting from impact compaction was investigated by cutting cubes from specimens and testing them in direct compression tests (47). From a number of such tests it was found that the strength of the material along the radial axis was 21% lower than along the longitudinal axis for the smaller specimens. This

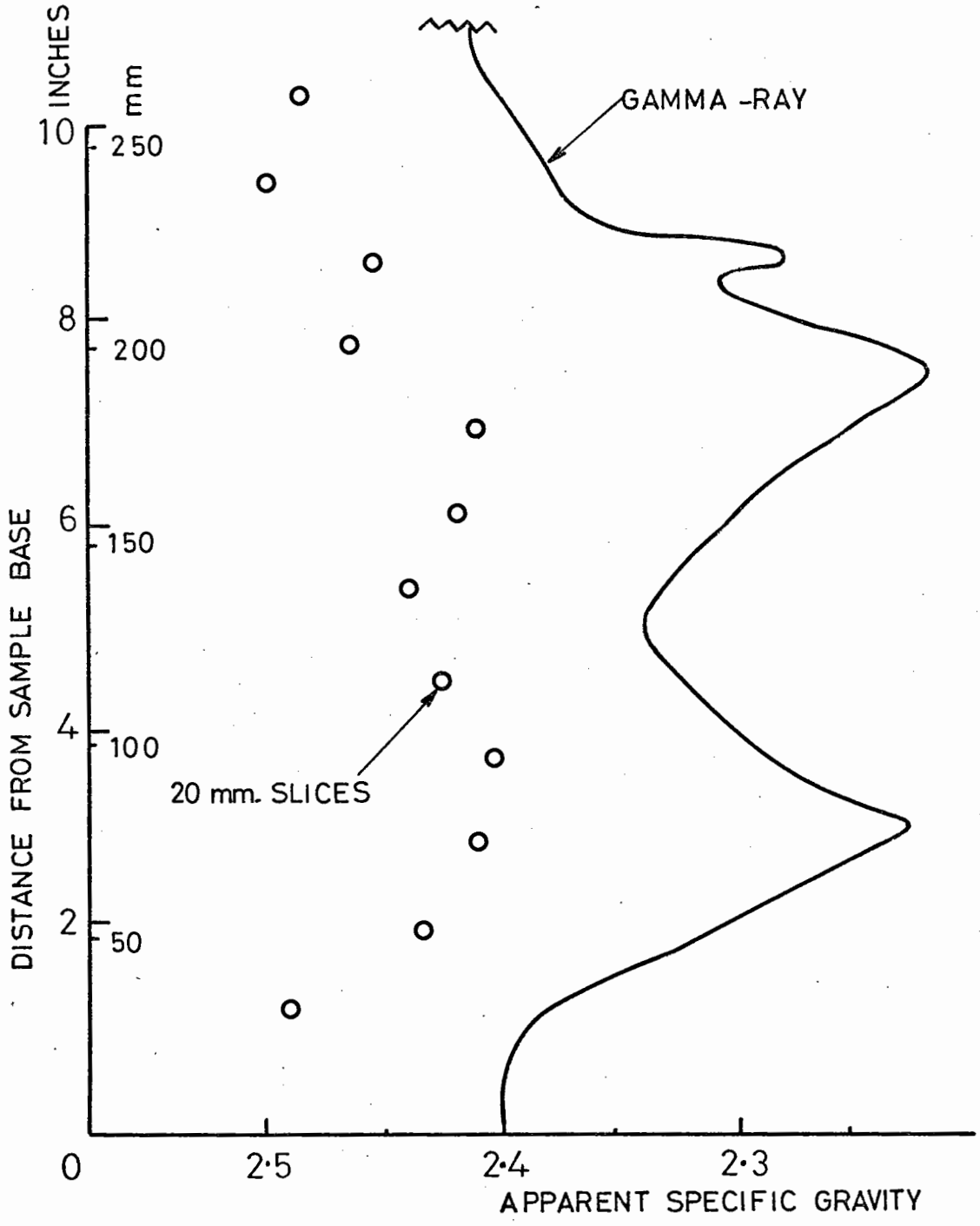

SPECIFIC GRAVITY OF A SAMPLE OF DENSE BITUMEN MACADAM BY GAMMA-RAY TECHNIQUE AND BY WEIGHING SLICES OF THE MATERIAL IN AIR AND WATER.

Fig. 4.1

indicated that there was some horizontal orientation of the particles due to the method of compaction. In the larger specimens, as might be expected, this anisotropy, though still present, was not so marked.

A typical specimen of dense bitumen macadam may be seen in Fig. 4.2. A section of the specimen has been cut away to show the distribution of the aggregate.

4.3 SPECIMEN LENGTH

As stated in Section 3.5, the traditional ratio of length to diameter for the triaxial test was 2:1. Employing the techniques of Rowe and Barden (39) the end fixity condition is removed and for soil testing a ratio of unity is allowable. If these techniques are not adopted for bituminous materials, the effectsof end restraint for various length to diameter ratios have to be carefully studied and calibrated as done by Pagen (47). If, on the other hand, they are employed, then only two contradictory requirements for the length to diameter ratio remain to be satisfied. Firstly, the gauge length should be as long as possible to give the maximum deformation to be measured by the recording instruments, and secondly, to keep the length to diameter ratio down to avoid buckling.

Dynamic triaxial compression trials were performed on specimens of dense bitumen macadam during the pilot programme in the Instron testing machine. 100 mm (4 in.) diameter specimens of various lengths were tested under various end fixity conditions.

Employing the loading techniques described in Section 3.5, it was found that a length to diameter ratio of $1\frac{1}{2}:1$ would not lead to buckling at $30^{o}C$, and hence this ratio was adopted for both specimen sizes.

4.4 CUTTING SPECIMENS TO LENGTH

In order to take full advantage of the "frictionless" end platens and to distribute the normal stress to the specimen evenly, the ends of the specimen should be smooth and perpendicular to the longitudinal axis of the specimen. In the testing of concrete, Hughes and Bahramiam (48) have suggested that the ends should be perpendicular to the axis to within $\frac{1}{2}^{o}$. In order to obtain this accuracy, and also to obtain the required length to diameter ratio, the specimens were placed in specially constructed jigs for cutting. In the case of the small specimen, the cutting was done by mounting a carborundum blade on a milling machine, together with the jig to hold the specimen to the bed, giving support to both sides of the cut area. As the action of the carborundum blade was abrasive, it was thought that a considerable amount of heat might be generated in the specimen which could change its properties. It was, however, noted that Valayer (49) had ground down the centres of his specimens with apparently no ill effects. In order to check that there was not an excessive rise in temperature, a thermocouple was inserted 6 mm behind the proposed cutting line of the blade, on the longitudinal axis of the specimen. The thermocouple was placed by drilling a small hole,

entering the thermocouple and then filling the hole with bitumen. If no coolant was used on the blade, the temperature rose to 65°C, that is, 45°C above ambient, but when using a coolant the temperature at this point was only 36°, that is, 16°C above ambient, which was considered satisfactory. The ends of the small specimens prepared in this way were considered adequate for the pilot Instron tests. In the case of the larger 150 mm diameter specimens, it was found that the whip present in the carborundum blade resulted in an unacceptable degree of misalignment. It was decided, therefore, to use a diamond blade. Trials were done in conjunction with the manufacturers, "Clippers", and the Clipper diamond blade No. MD459ST was found to give an adequate alignment and finish to the ends. As a result of this, all 150 mm diameter specimens were trimmed to length in the jig mounted on a Clipper sawbench using a diamond blade.

4.5 SPECIMENS CORED FROM A TEST SLAB

A few specimens were tested that were not manufactured as described in this chapter. The Transport and Road Research Laboratory laid a test slab of dense bitumen macadam to investigate the effects of binder content and compactive effort on the density and subsequent laboratory behaviour of specimens cut from it. Eighteen 150 mm (6 in.) diameter cores from this slab were sent to the University for dynamic testing in the servo-hydraulic machine. Nine different specimen states were represented (three binder contents, three levels of compactive effort).

After preparation of the ends in the normal way, the specimens were found to vary between 125 mm and 150 mm in length as the thickness of the bituminous layer in the slab was only in the order of 150 mm. Furthermore, the coring operation had not produced specimens of a constant cross-sectional area. Therefore, to select one specimen for testing from each pair, those with the most regular cored surface were chosen.

The aggregate grading curve for these specimens is shown in Fig. 4.3.

4.6 SPECIMEN CONSTITUENTS

All specimens manufactured in the laboratory were made to the same aggregate grading curve (Fig. 4.3), which conforms to the M.O.T. specifications (3) for a dense bitumen macadam roadbase. The aggregate is a crushed porphyry from Barden Hill quarries with a specific gravity of 2.82. The binder (which was all taken from the same barrel) is a nominal 90/110 penetration bitumen with the following properties:

Ring and Ball Softening Point	46.5°C
Penetration at 25°C	98

The majority of tests were performed on specimens containing 4% binder content by weight, but some tests in Programme BS were carried out on specimens with 3% and 5% binder content as well as with 4% (see Table 5.1).

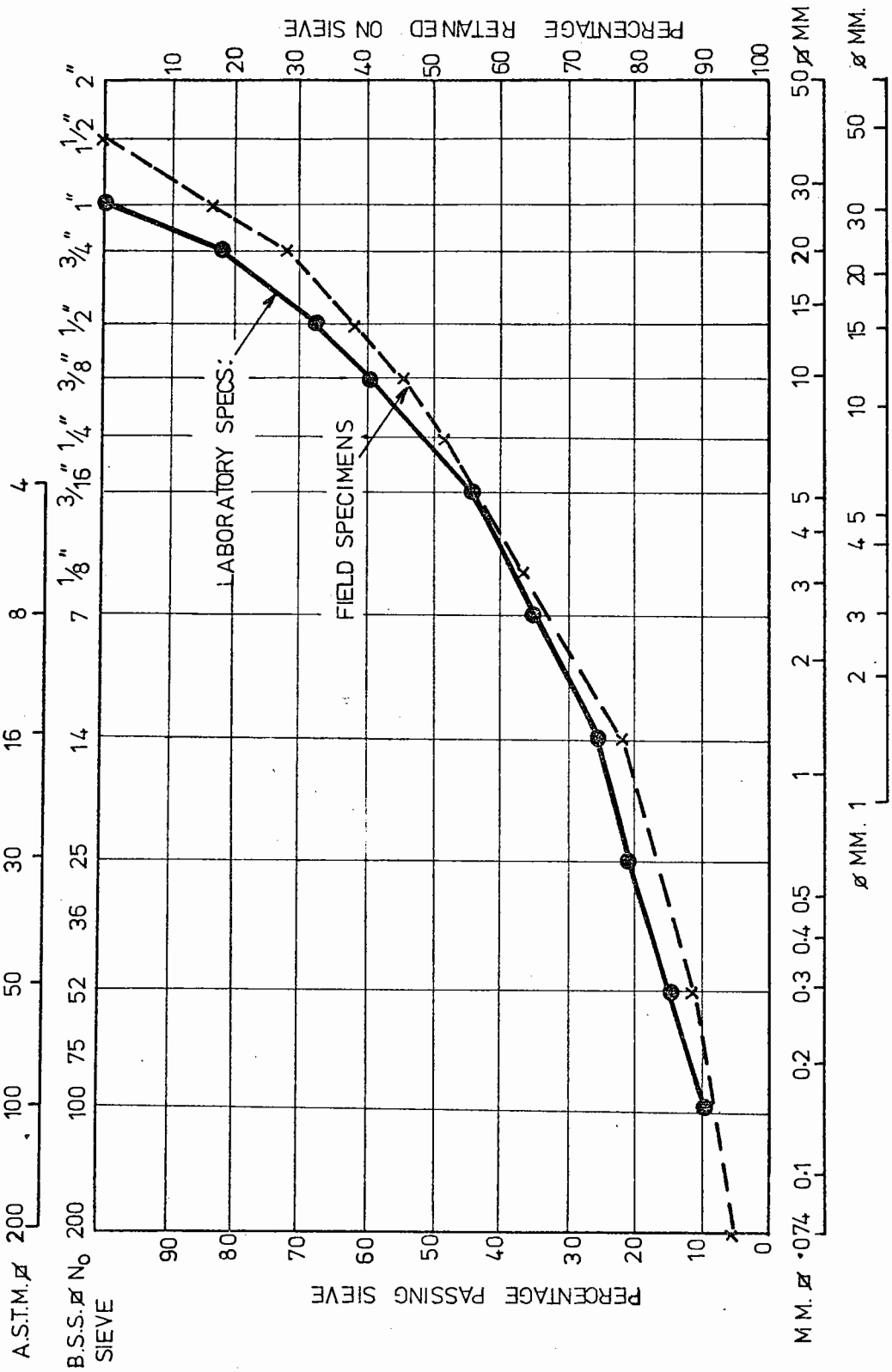

COMBINED AGGREGATE GRADING CURVE FOR LABORATORY AND FIELD COMPACTED SPECIMENS.

Fig. 4.3

CHAPTER FIVE

THE TESTING PROGRAMME

5.1 INTRODUCTION

The purpose of the tests carried out in the three testing machines was to determine the permanent and resilient deformation characteristics of a dense bitumen macadam road-base material subjected to various conditions of static and dynamic loading. The tests in the Instron testing machine were formulated to give an indication of the material properties so as to facilitate the design of the servo-hydraulic machine. The latter machine was constructed in the light of this knowledge and was subsequently used in the testing of 149 specimens during this investigation. Whilst the servo-hydraulic machine was being used for dynamic testing, the constant stress testing machine was able to perform static creep tests independently with a view to correlating the static and dynamic behaviour of the material.

All tests in the Instron testing machine and constant stress testing machine were on cylindrical specimens 100 mm (4 in.) diameter and 150 mm (6 in.) long, whilst those in the servo-hydraulic machine (except programme FS) were on cylindrical specimens 150 mm diameter and 225 mm long. Details of the specimens are given in Chapter 4.

The following sections of this chapter outline the tests that were undertaken with the three testing machines. As these tests consider different variables investigated in the various machines, Table 5.1 is presented for reference purposes.

Table 5.1 Summary of investigations carried out

Machine	Test programme	Variable	Range investigated (or comment)
Instron	Instron	Vertical stress	275 kN/m^2 - 900 kN/m^2
"	"	Temperature	0°C - 30°C
"	"	Confining pressure	Not reported in thesis
"	"	Frequency of load application	Not reported in thesis
"	Constant rate of strain	-	c and φ investigation
Servo-hyd.	Transition	Size of specimen and shape of vertical stress wave	100 mm and 150 mm dia. triangular and sinusoidal
"	AS	Vertical stress	150 kN/m^2 - 900 kN/m^2
"	"	Temperature	10°C - 30°C
"	"	Confining pressure	0 - 600 kN/m^2
"	"	Frequency	0.1 - 10 Hz
"	"	Rest periods	0 - 8 secs
"	BS	Binder content and temperature	3%, 4%, 5% 10°C, 20°C, 30°C
"	"	Binder content at high temperature	3%, 4%, 5% 40°C
"	CS	Confining pressure	0 - 200 kN/m^2
"	CS	Confining pressure wave	Various
"	DS	Rest period	Supplementary to AS
"	ES	Frequency	Supplementary to AS
"	FS	Binder content and compaction	Cores from experimental slab
Constant stress	Creep test	Temperature	10° - 30°C
"	"	Vertical stress	150 kN/m^2 - 900 kN/m^2

5.2 INSTRON TESTING MACHINE PROGRAMME

The testing machine of Hanson (25) when modified (Section 3.2) proved to be adequate to obtain a guide to the deformation characteristics of the material, and also for trying out various methods of deformation measurement. An attempt was made to investigate the influence of the following loading conditions on the materials:

Magnitude of vertical stress pulse

Temperature

Confining pressure

Frequency of the applied stress pulse

It was stated in Section 2.4 that a constant vertical stress level of up to 6 kN/m^2 would be a realistic figure for the simulation of overburden pressure. It was found to be impossible to control the machine at this value and the minimum obtainable value of constant vertical stress was found to be 34 kN/m^2 (5 lbf/in^2).

It will be seen from Tables 5.1 and 7.1 that the values of dynamic vertical stress and temperature are of the same order as those suggested in Chapter 2. Unfortunately, the machine was only capable of applying a triangular stress pulse at up to 50 cycles per minute, rather than the suggested sinusoidal pulse at higher rates of loading (Chapter 2).

As the Instron testing machine is ideal for the constant rate of strain type of test, a short series of these were performed to give values of the cohesion (c) and the angle of shearing resistance (φ) of the material.

5.3 DYNAMIC TESTING PROGRAMMES

The dynamic tests performed in the servo-hydraulic machine may be divided into four categories:

(a) Transition from testing in the Instron machine to the servo-hydraulic machine.

(b) Main investigation of material properties.

(c) Supplementary investigations

(d) Tests on cored specimens supplied by the T.R.R.L.

All specimens (unless otherwise stated) were subjected to a constant vertical stress of 30 kN/m^2 to simulate the overburden pressure. This was considered high (Section 2.4), but it did give continuity with the Instron testing machine programme. The specimens, except for those in the transition tests, were all subjected to a sinusoidal vertical (or deviator) stress pulse. When a dynamic confining pressure was applied, the pulse shape was also sinusoidal.

(a) Transition tests

The purpose of the transition tests was to ascertain the compatability of the results from the dynamic tests in the Instron machine with those from the servo-hydraulic machine. There were two major differences to be considered.

The Instron results were obtained by testing 100 mm (4 in.) diameter specimens whereas 150 mm diameter specimens were used in the servo-hydraulic machine. Three tests were carried out on 150 mm diameter specimens under the same conditions of loading as existed for a set of results from the Instron testing machine. The results from these and the Instron tests were then compared.

As already stated, the Instron testing machine was only capable of applying a triangular vertical loading pattern, whereas the tests in the servo-hydraulic machine were to be carried out with a sinusoidal one. Again, three tests were performed on 150 mm diameter specimens under the same conditions except for the waveshape, which was sinusoidal. Hence, a comparison of the results of the application of sinusoidal and triangular vertical waveforms could be made.

(b) Main investigation of material properties

The purpose of this investigation was to obtain the deformation behaviour of the material up to failure. This necessitated recording both the resilient and permanent components of deformation, both longitudinal and radial, at intervals throughout every test. The programmes AS, BS and CS were formulated to illustrate the effect of the following variables on the material:

Dynamic vertical stress
Temperature
Static confining pressure
Frequency of dynamic vertical stress pulse
Rest periods between single stress pulses
Binder content
Effect of pulsing the confining pressure

The ranges of these variables, which were chosen to simulate in situ values (Chapter 2), may be seen in Table 5.1.

The details of each set of three tests with their particular set of testing conditions may be seen listed in Tables 7.3 to 7.5.

(c) Supplementary investigations

These tests were carried out in programmes DS and ES. Both arose from the analysis of the results of programme AS and were required to clarify certain points. It will be noted in Table 7.7 that DS specimens have no constant vertical stress applied to them during a test, apart from that resulting from the weight of the top platen. It was felt that if specimens were to show an increase in life due to "healing" in a rest period between pulses, then the constant stress should be removed so as not to mask any effect of the rest period.

The ES specimens were tested at 25°C over a range of frequencies from 1 Hz to 15 Hz (Table 7.8). The information obtained from these tests would supplement that derived from programme AS which was concerned with the effects of frequency on permanent deformation behaviour.

(d) Cored specimens

The cored specimens were obtained from a test slab laid at the T.R.R.L. and prepared for testing as described in Section 4.5. The object of programme FS was to test one of the two specimens available for each of the nine combinations of binder contents and compactive efforts provided. Each specimen was tested to failure at 25°C in an unconfined state under a

dynamic vertical stress of 650 kN/m^2, at a frequency of 1 Hz, superimposed on a constant vertical stress of 30 kN/m^2.

As stated in Section 4.5, the specimens were not of the standard length. After preparation, they were less than 150 mm long which necessitated shortening the gauge length for longitudinal measurement to 100 mm. This in its turn precluded any measurement of radial deformation.

5.4 STATIC CREEP TESTING PROGRAMME

During the course of the investigation into the material properties under dynamic loading it was decided to investigate the creep behaviour of dense bitumen macadam subjected to a static vertical stress level, with no superimposed dynamic loading. The tests were carried out in the constant stress testing machine (Section 3.3) using the same ranges of stress level and temperature as in programme AS, i.e. at stress levels of 900, 650, 400, 150 kN/m^2 at 20^{o}C and 650 kN/m^2 at temperatures of 10^o, 20^o and 30^{o}C (Table 5.1). The test specimens were 100 mm (4 in.) diameter and were manufactured in the same manner as those for the Instron tests.

It was found that the loading yoke and top platen exerted a vertical load on the specimen equivalent to 30 kN/m^2, the constant stress applied to all tests in the servo-hydraulic machine. The vertical stress value given in the results (Chapter 7) is the stress applied in addition to this load, so that direct comparison may be made between the effect of the superimposed dynamic and the superimposed static stress levels. As with the dynamic tests, three specimens were tested at each loading condition.

CHAPTER SIX

TEST PROCEDURE

6.1 INTRODUCTION

Three testing facilities have been used in this investigation - the Instron testing machine, the servo-hydraulic machine and the constant stress testing machine. The first two were capable of subjecting cylindrical specimens, both to a uniaxial compressive load and to a confining pressure. The constant stress testing machine could apply a uniaxial compressive load only.

The pilot programme in the Instron testing machine enabled the subsequent programmes in the servo-hydraulic machine to operate successfully. Therefore, the dynamic testing procedure finally adopted for the servo-hydraulic machine will be described to cover the two, and Section 6.5 describes the test procedure for the static creep tests in the constant stress testing machine.

Hanson's (25) practice of testing three specimens at any set of conditions was continued. Whilst three will not yield a sufficient number of results to use statistical analysis, this is not important provided that the scatter obtained is sufficiently small. By using three specimens in a test batch, a test result that is inconsistent will be obvious and thus apparent anomalies at a later stage will be avoided (Section 6.4).

6.2 SETTING UP A SPECIMEN FOR DYNAMIC TESTING

The specimen was weighed in air and in water to determine its specific gravity and hence the void content.

A perspex jig was then clamped to the cylindrical surface of the specimen which facilitated the sticking of the six measuring targets to the specimen in the appropriate position (Section 3.6). The jig was left in place for at least six hours to ensure that the targets were not disturbed during the curing period of the adhesive.

The specimen was then placed in the temperature controlled room for sufficient time to allow it to assume the temperature of the environment. Fig. 6.1a shows the temperature at the centre of a specimen changing with time. A thermocouple was sealed into the centre of a specimen and the temperature at this point studied. The specimen was moved from an ambient temperature of 20°C into the temperature controlled room at 10°C. The figure shows the temperature dropping exponentially with time. It may be seen from the figure that a specimen will assume the temperature of its surroundings in about six hours. In fact, all specimens were allowed at least 15 hours in the testing environment before a test was commenced. In the case of tests at 30°C, the specimens were laterally supported in the target-sticking jigs for this time to minimise the possibility of flow under self weight.

The positioning of the specimen and measuring equipment in the triaxial cell was facilitated by having a trolley that

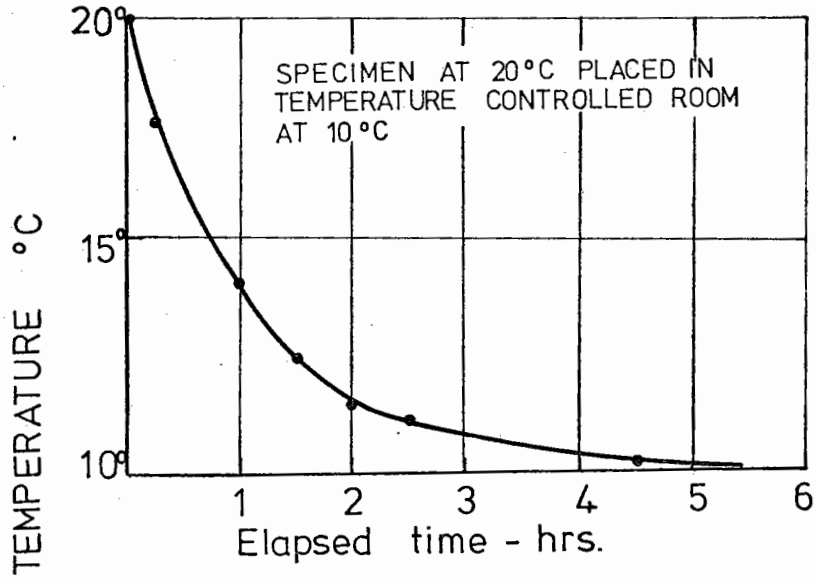

(a) COOLING TIME FOR 150mm. DIAMETER D.B.M. SPECIMEN

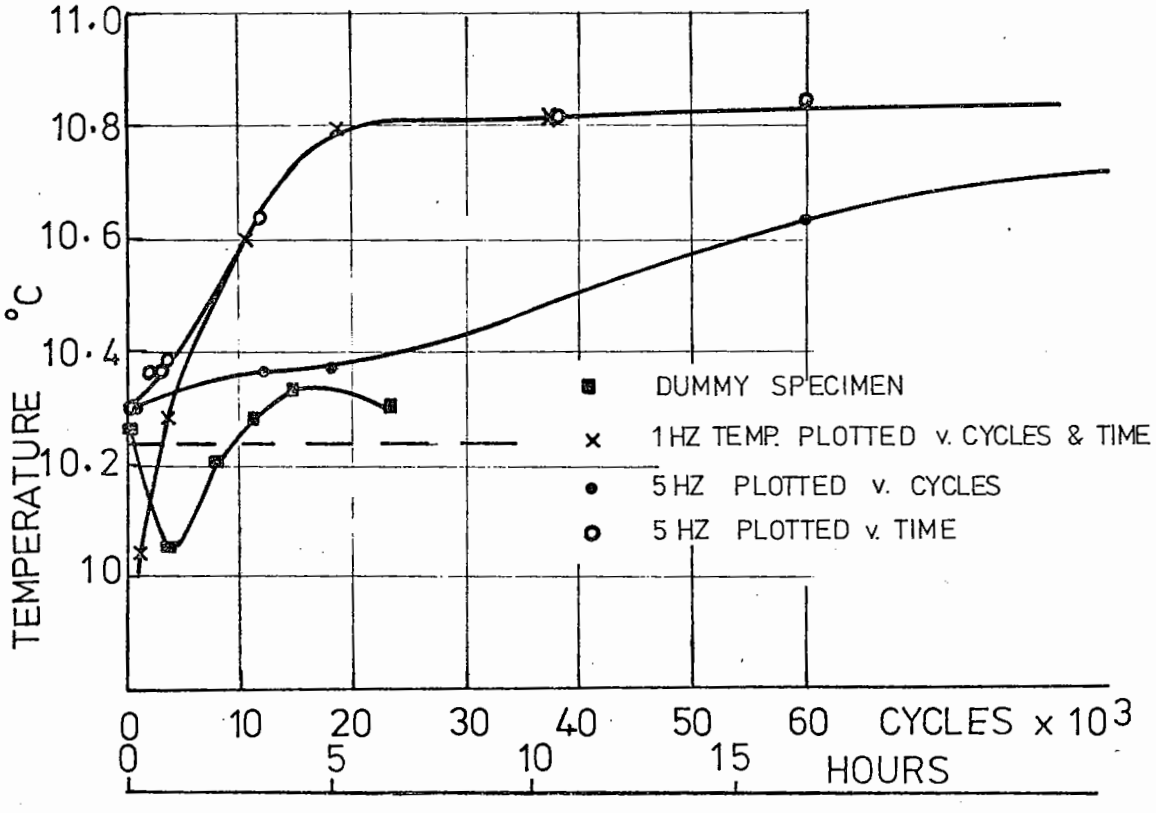

(b) TEMPERATURE VARIATION INSIDE A SPECIMEN DURING A TEST.

Fig. 6.1

carried the triaxial cell, along guide rails, clear of the loading frame to a position allowing all round access. The cell itself could be stripped down to minimise difficulty in setting up the specimens on the cell base.

The specimen was located onto a spigot set into the top of the triaxial cell plinth, but separated from the latter by the shear break membranes (Section 3.5). If a confining pressure was to be applied, a neoprene membrane would already have been placed over the specimen with holes cut to allow access to the centre of the targets. The neoprene was stuck to the target with a Bostik compound (No. 1755) to prevent ingress of the confining medium. The membrane was attached to the bottom platen with O-rings to prevent ingress of fluid.

The collars holding the L.V.D.T.'s measuring the relative movement of the targets were placed in position (see Section 3.6). When in place, the area of contact was surrounded with the Bostik compound to further inhibit fluid ingress. The cores of the L.V.D.T.'s were positioned in their respective barrels to be at one end of their linear range of output, so that during the test, as permanent deformation occurred, the full linear range of the transducers was used. The positioning was done by taking the transducer outputs singly and passing them through a galvanometer in the temperature controlled room. The position of each core was physically adjusted until the output shown by the galvanometer indicated that the core was in the correct position.

The top platen was placed in position on the specimen,

separated from it by shear break membranes. The top platen was accurately centred before the neoprene membrane was fastened to it with O-rings. The triaxial cell wall, lid and plunger were then added to the base and the whole cell and specimen wheeled into position above a manual jack which lifted the triaxial cell from the trolley into the required testing position. If a confining pressure was to be used, the nylon tubes from the transformer oil reservoir and the pulsing device were connected and the cell filled with oil.

6.3 TESTING A SPECIMEN UNDER DYNAMIC LOADING

It was necessary to set all control and recording equipment before the commencement of a test, as from the start the overall behaviour needed monitoring by the operator.

The following parameters could be monitored simultaneously by the U.V. recorder:

Vertical (or deviator) load

Confining pressure

Permanent longitudinal strain

Permanent radial strain

Resilient longitudinal strain alternating with resilient radial strain

During the major part of a test, changes occurred slowly in specimen behaviour, and therefore this part of the test lent itself to automatic recording. It was possible to set the U.V. recorder to take readings of all measured parameters at pre-determined time intervals.

It was important that the temperature of a specimen remained close to the nominal test temperature throughout. As dense bitumen macadam is a viscoelastic material, it is reasonable to suppose that the heat absorbed by a specimen under test may not be dissipated fast enough to maintain the ambient temperature throughout the specimen (50,51). In order to investigate this possibility, thermocouples were sealed at the centres of two specimens. One specimen, the dummy, was placed in the temperature controlled room, the other subjected to two tests.

The response of the dummy to ambient temperature indicated that the total change of temperature expected in a sample due to ambient fluctuations was less than $0.4^{o}C$ (Fig. 6.1b). It should be noted that this specimen was not enclosed in the triaxial cell and consequently, the measured temperature changes were greater than for a specimen undergoing a test.

The specimen in the triaxial cell was tested at two rates of loading, 1 Hz and 5 Hz. In both cases, there was an increase in temperature at the centre of the sample. The magnitude of this was $0.5^{o}C$ before an equilibrium state was attained. Fig. 6.1b also shows that the heating effect is a time dependent phenomenon. However, the conclusion was that the above variations in specimen temperature could be ignored.

Failure in the context of this investigation is not the point at which all load bearing capacity has departed from a specimen. In the classic creep deformation against time

plot for a material, the rate of increase of deformation declines until failure is approached, at which point it increases and continues to increase until rupture occurs. Similar behaviour was observed in the Instron pilot programme, and it was therefore decided to define the point of increase in the rate of deformation as the point of failure under both dynamic and static loading. Fig. 6.2 shows a typical plot of the deformation rate, against number of cycles, indicating the point of failure of the specimen.

After the completion of a test the triaxial cell was drained of the confining medium, run clear of the loading frame and stripped down.

6.4 PROCESSING OF RESULTS

At the completion of a test, the data on the behaviour of the specimen was in the form of a number of traces on U.V. light sensitive photographic paper. The position of each trace on the paper at particular numbers of cycles was noted down on a data sheet. This information was then put onto punch tape for analysis by a small computer (Wang 720 B). The programme written by the author to turn the information on the photographic paper into useful engineering terms was quite long, but due to problems in the Cripps Computing Centre at the time, it was decided to use the small computer rather than the large University facility. Including the input of calibration factors and the final print out, the average time for one test to be processed was in the order of four minutes (see Appendix).

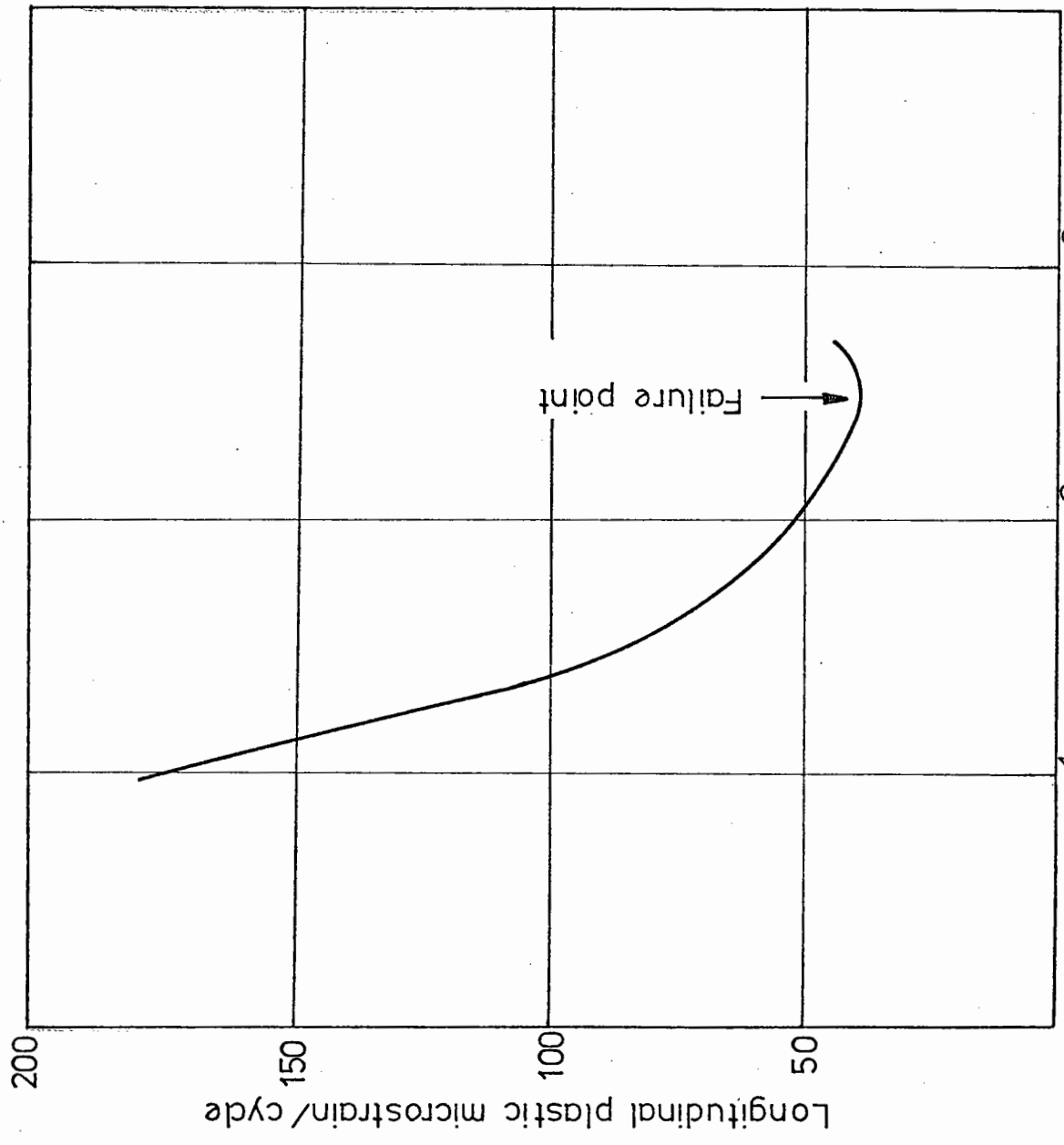

TYPICAL FAILURE POINT AS DEFINED BY THE RATE OF INCREASE OF PERMANENT DEFORMATION

Fig. 6.2

The trace readings for deviator load, confining pressure and the longitudinal and radial deformations were fed into the computer and, after processing, a labelled print out giving the following items was given:

The cycle number, and its logarithm

The permanent longitudinal strain, and its logarithm

The increase in permanent strain per load application

The resilient longitudinal strain

The resilient modulus

The permanent radial strain

Poisson's ratio

Plastic strain ratio*

The bulk modulus)
) If required
The shear modulus)

From this information, it was possible to draw up the tables and graphs shown in the succeeding chapters. As stated in the introduction to this chapter, three specimens were tested at each set of conditions. This is not a sufficient number to use statistical techniques that require a Gaussian distribution of results (52) and so simple averaging is used to produce the values shown in the tables and figures.

The scatter on the various resilient parameters may be seen in Chapter 7, where the value from each individual test result is plotted on Figs. 7.15 to 7.19 and 7.21 or in

---

* Radial permanent strain divided by longitudinal permanent strain.

Fig. 6.3 where the values for the resilient modulus from a typical set of three tests are shown. A similar technique is used to indicate the scatter on the permanent strain plots. Fig. 6.4 shows a typical set of permanent strain curves. It may be seen that the scatter of the permanent strain in the three tests, expressed as a percentage of the mean, remains fairly constant throughout. The worst scatter measured, from all sets of tests, was 60% on the mean and the average scatter was found to be 24% on the mean. The scatter may be seen plotted in Figs. 7.4 to 7.10, 7.12 to 7.14, 7.23 to 7.25 and Figs. 8.11 and 8.12.

6.5 PROCEDURE FOR STATIC LOADING TESTS

The specimens for the constant stress testing machine were 100 mm (4 in.) diameter by 150 mm (6 in.) long. They were placed onto the bottom platen of the loading frame with a shear break between the specimen and the platen, necessitating a spigot to prevent the possibility of sideways movement. The collars (for the longitudinal measurement of deformation only) were put onto the specimen, locating into the four targets, previously fixed to the surface.

The outputs from the transducers on the collar were fed directly into a digital voltmeter (D.V.M.). The physical position of the cores in the barrels of the transducers were adjusted as for the servo-hydraulic machine.

The top platen (and shear break) was placed onto the specimen. A spigot located this platen to prevent sideways movement. The loading yoke was then suspended from the top

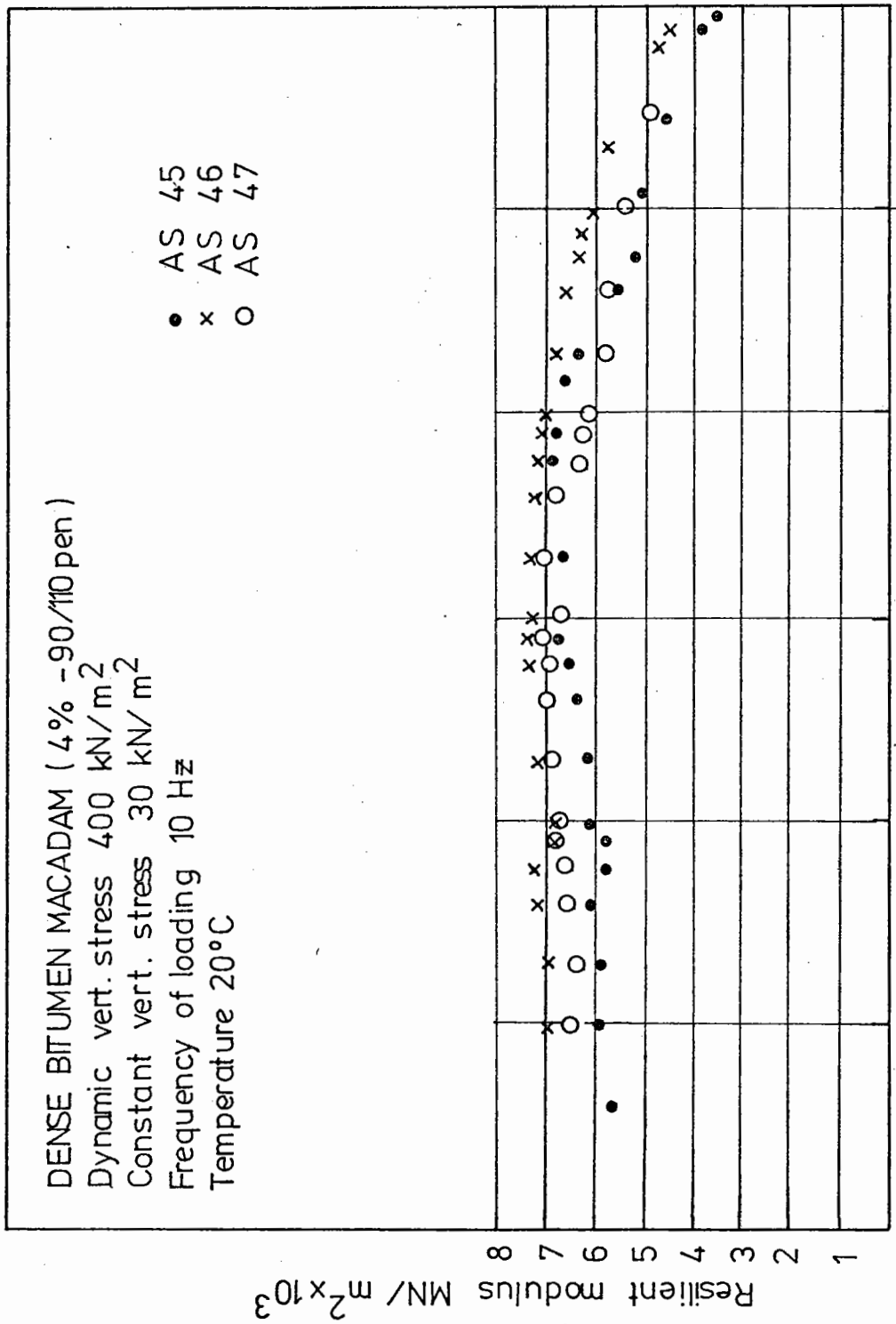

TYPICAL VARIATION OF RESILIENT MODULUS OF THREE SPECIMENS THROUGH A TEST.

Fig. 6.3

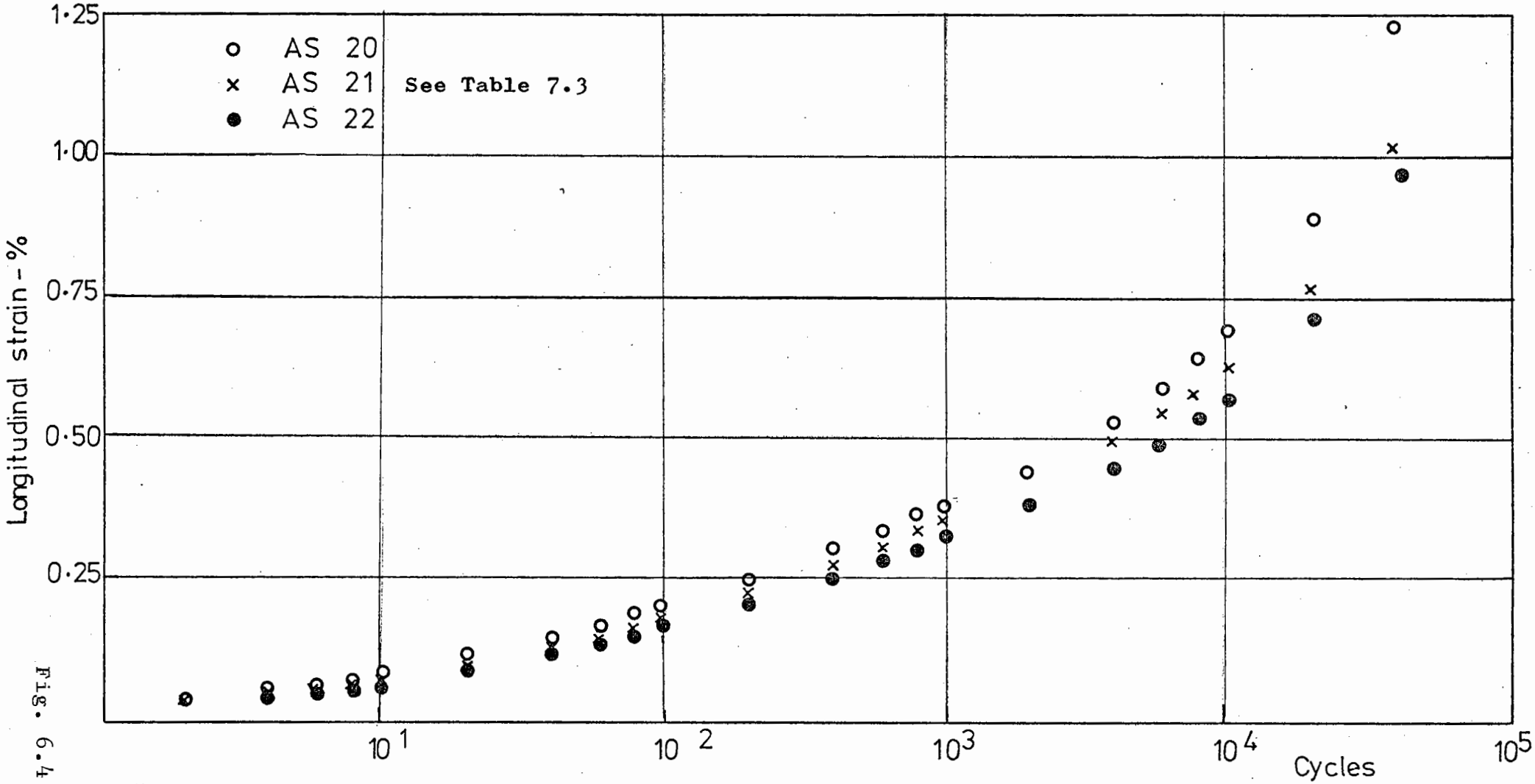

Fig. 6.4

A TYPICAL PERMANENT LONGITUDINAL STRAIN vs. CYCLES PLOT FOR A SET OF THREE TESTS

platen without the loading arm being brought into contact with the yoke.

After the deformation, due to this small loading, had decreased, the main load was applied through the loading arm and readings of the L.V.D.T. outputs were taken from the D.V.M. at appropriate intervals of time. The end of the static tests was defined as for the dynamic tests in the servo-hydraulic machine. The readings from the D.V.M. were then reduced to longitudinal strains with time by using a simpler version of the computer programme devised for the analysis of the tests in the servo-hydraulic machine.

CHAPTER SEVEN

PRESENTATION OF RESULTS

7.1 INTRODUCTION

In this chapter, the basic results of the test programmes are presented with no discussion. (This may be found in Chapter 8). The results of the tests in the servo-hydraulic machine are presented in tabular and in graph form. The tables include the conditions of loading and note the particular variable being investigated. In the tables, the "Initial" and "Final" resilient moduli refer to the resilient modulus of the material measured after about ten cycles of loading, and at the time of failure respectively. The "cycles to failure" is the number of load pulses applied to the specimen at the time of failure and the "permanent longitudinal strain at failure" is self-explanatory. The "initial elastic Poisson's ratio" is the ratio of the radial to the longitudinal resilient strain measured after about ten cycles.

The results of the Instron tests concerning confining pressure and frequency effects are not included in this thesis. Although serving as an indication of material behaviour they were not sufficiently accurate and were superseded by the results of programme AS.

The results of the static creep tests are not tabulated.

In addition to the tables, the permanent longitudinal deformation behaviour is plotted on a strain versus log cycles graph. (The Instron tests are omitted from these plots.) The resilient properties of modulus and initial Poisson's

ratio are plotted to show their variation with the various loading conditions.

It was found that a discontinuity in material behaviour appeared to occur between test programme BS and test programme CS so that comparison of results before and after this point might be misleading. An example of this may be seen in Fig. 7.1 which shows the permanent longitudinal strain plotted against the number of load applications for a set of tests in the BS and CS programmes. It may be seen that the rate of deformation and the number of load applications to failure of the two sets of tests are different. An investigation into the cause of this difference was carried out, and it was found that the average void content of the AS and BS programme specimens containing 4% binder was 4.78% (with a standard deviation of 0.38) whereas subsequent specimens in programmes CS, DS and ES had an average void content of 5.11% (with a standard deviation of 0.24). The reason for this change in void content was not established. The recovered properties of the binder of specimens before and after the void content change were investigated with no conclusive results. The specific gravity of the aggregate was also tested, as it was suspected that it may have come from another seam at the quarry, again with no result.

7.2 RESULTS OF THE INSTRON TEST PROGRAMME

Table 7.1 gives the results of the tests investigating the effect of dynamic vertical stress magnitude and the temperature of testing on specimen behaviour. The last two

DENSE BITUMEN MACADAM (90/110 pen)
(225 mm by 150 mm dia. spec.)
Dynamic vertical stress 650 kN/m^2
Constant vertical stress 30 kN/m^2
Unconfined
Frequency of vertical stress pulse 1 Hz
Mean no. of cycles to failure *

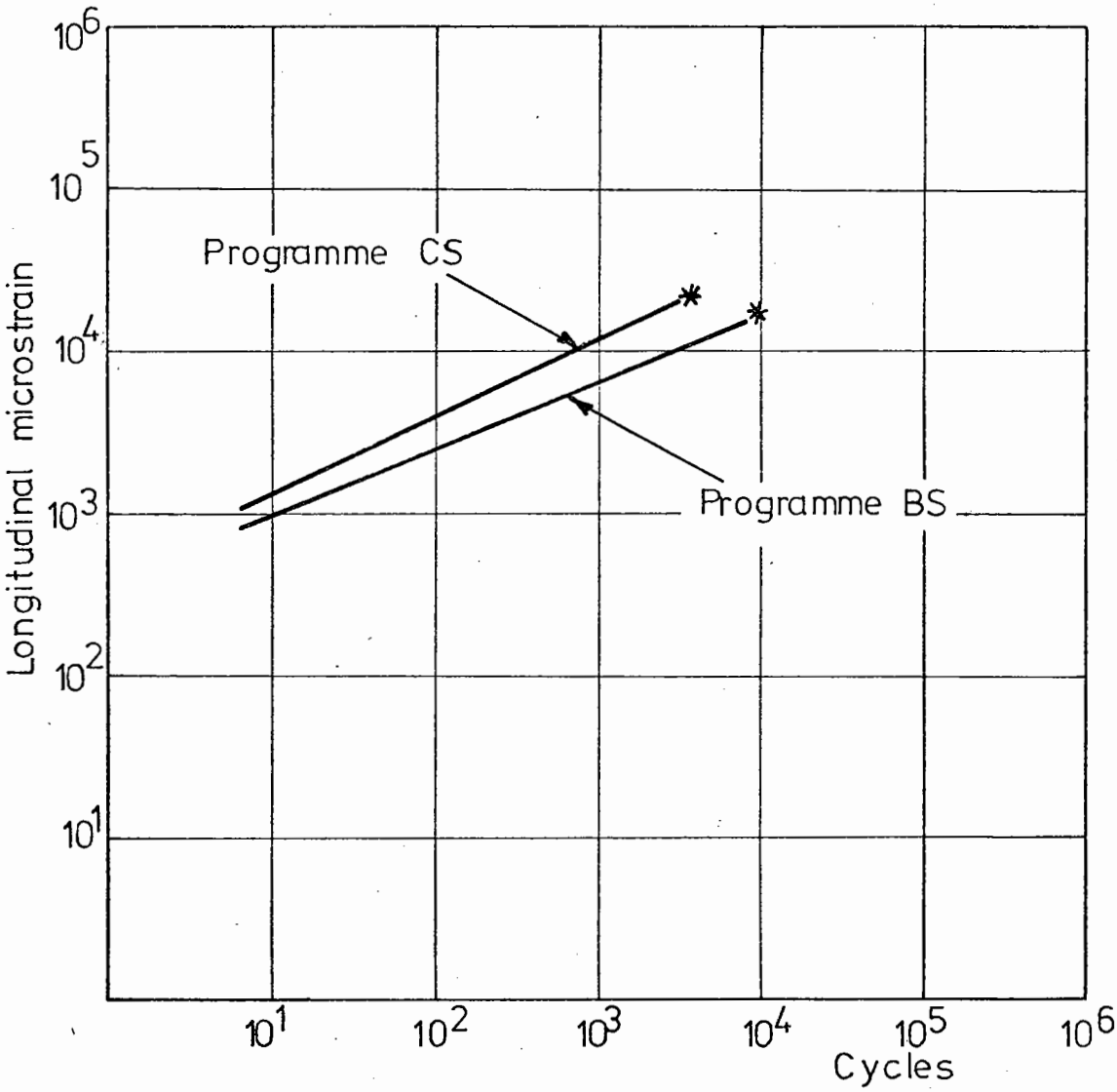

AN EXAMPLE OF THE CHANGE IN MATERIAL BEHAVIOUR THAT OCCURRED AFTER PROGRAMME BS

Fig. 7.1

Table 7.1 Results of Instron Test Programme
(Stress and temperature results only)

Test No.	Nominal dynamic vertical stress - kN/m^2	Confining pressure kN/m^2	Temperature - ^oC	Frequency of applied stress pulse - Hz	Voids - %	Resilient Modulus MN/m^2		Cycles to failure	Permanent longitudinal strain at failure - %	Initial $\frac{\text{elastic } \epsilon/\text{cycle}}{\text{plastic } \epsilon/\text{cycle}}$	Final $\frac{\text{elastic } \epsilon/\text{cycle}}{\text{plastic } \epsilon/\text{cycle}}$
						Initial	Final				
VARYING STRESS											
40,41,42	276	0	10	0.5	6.49	5,580	-	-	-	5.51	2090
37,38,39	483	0	10	0.5	6.84	7,440	-	-	-	5.9	1770
34,35,36	690	0	10	0.5	6.85	10,820	-	-	-	6.56	2010
$1,2,4_A$	895	0	10	0.5	6.76	7,960	-	-	-	3.3	1000
VARYING TEMPERATURE											
14,15,16 17	895	0	0	0.5	6.68	10,700	-	-	-	8.5	2470
$1,2,4_A$	895	0	10	0.5	6.76	7,960	-	-	-	3.3	1000
18,19,20	895	0	20	0.5	7.09	3,380	2,470	2,330	2.15	1.1	50
31,32,33	895	0	30	0.5	6.73	2,070	1,500	290	2.26	2.7	8

columns in the table show the relative size of the resilient and permanent deformation at the start and end of a test. This facilitated the design of the amplifiers for deformation measurement in the tests in the servo-hydraulic machine.

It should also be noted that the tests at 0°C and 10°C were not carried through to failure as this had not occurred after a day's testing and it was considered unsafe to operate the machine unattended through the night.

The constant rate of strain triaxial tests were carried out at two rates of loading and three temperatures on specimens of two levels of void content. The Mohr envelopes obtained may be seen in Figs. 7.2 and 7.3. In the figures, "low voids" indicate the range of void content 6 - 6.4% and "high voids" the range of void content 7.2 - 7.9% in the specimens tested.

7.3 RESULTS FROM THE DYNAMIC TESTING PROGRAMMES

As stated in Chapter 5, the dynamic tests performed in the servo-hydraulic machine may be divided into four groups, and the results are presented in these four groups.

(a) Transition tests

These tests were to investigate the change in the deformation behaviour of a dense bitumen macadam if the size of the specimen or the shape of the applied vertical stress pulse was changed.

Three sets of tests were carried out at 10°C and at a frequency of 0.5 Hz. The resilient modulus varied as shown in Table 7.2.

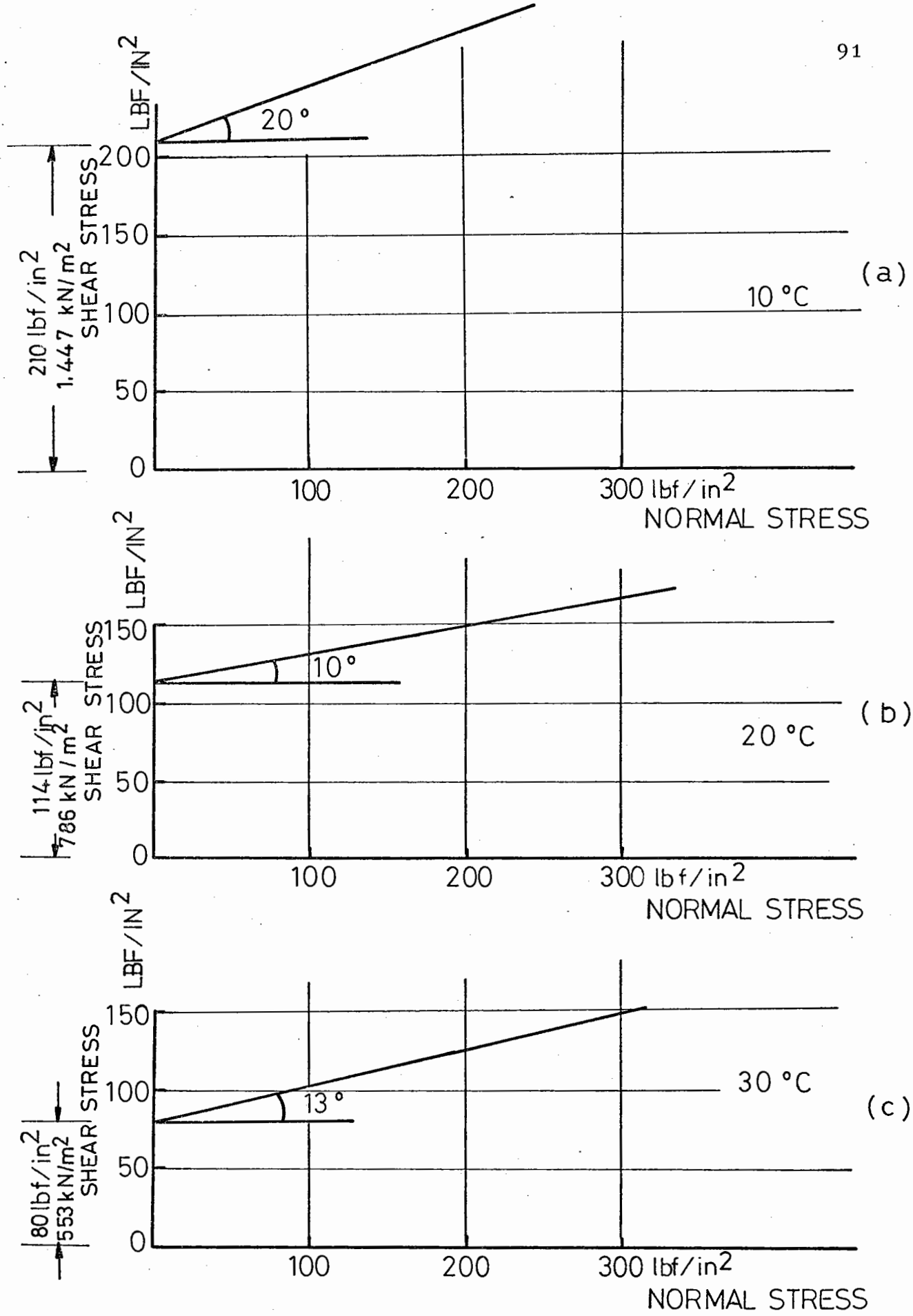

MOHR ENVELOPES FOR LOW VOID, DENSE BITUMEN MACADAM (90/110 pen, 100 mm. (4 inch) dia specimen - rate of strain 0·05 in/minute)

Fig. 7.2

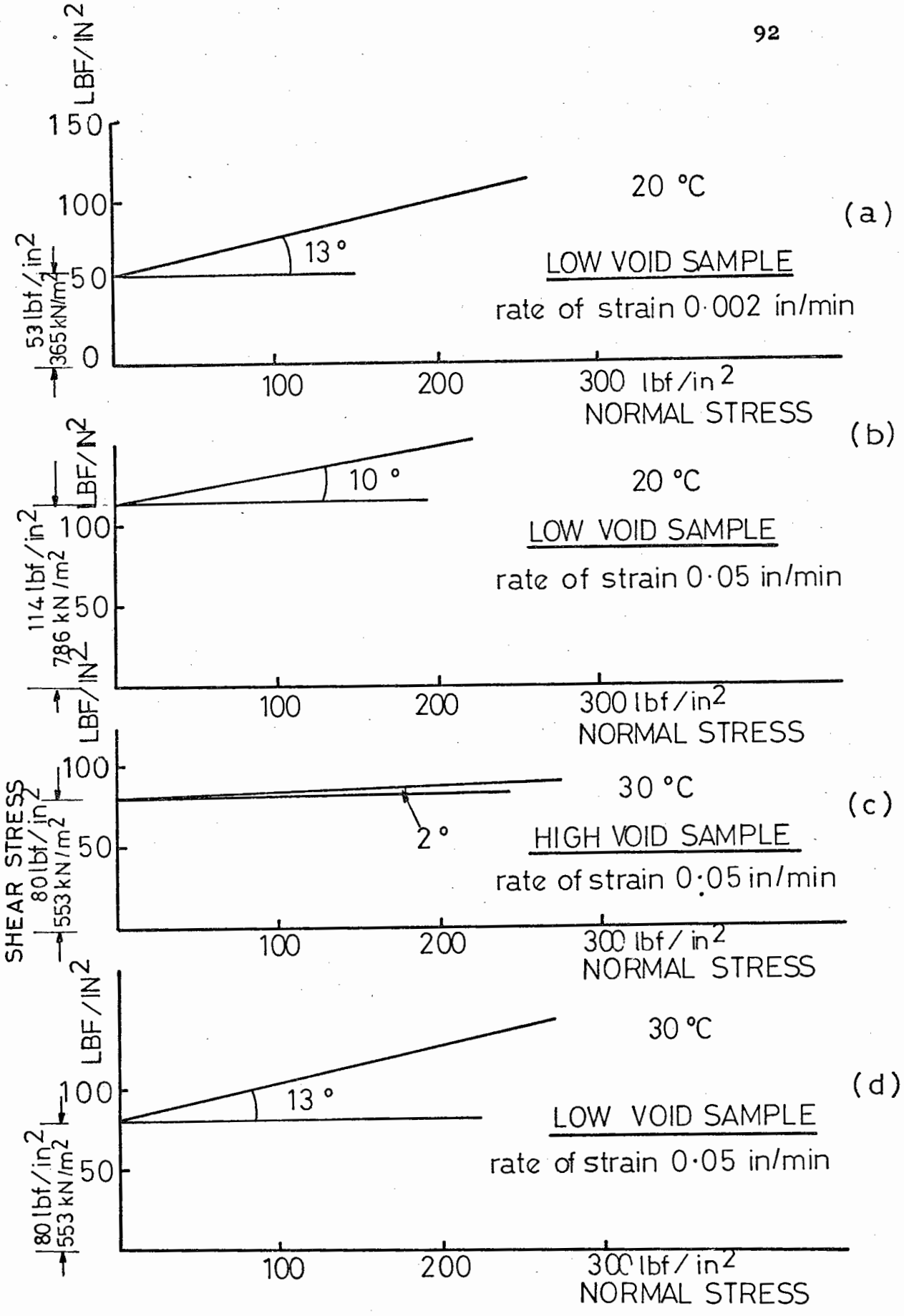

MOHR ENVELOPES FOR DENSE BITUMEN MACADAM (90/110 Pen, 100 mm (4 inch) dia. specimen.)

Fig. 7.3

Table 7.2 - Resilient modulus variations in the transition tests

Specimen diameter mm	Shape of stress pulse	Resilient modulus MN/m^2
100 (4 in.)	Triangular	7960
150	Triangular	8500
150	Sinusoidal	6790

The manner in which the permanent deformation behaviour was affected by the size of the specimen and the shape of the stress pulse may be seen in Fig. 7.4.

(b) Main investigation of material properties

Tables 7.3 to 7.5 show how the various loading conditions affect the resilient and permanent deformation characteristics and the number of cycles to failure. The variables studied in each testing programme are listed in Table 7.6, together with the appropriate figure number that shows the effect of the variation of the loading condition.

In the CS programme the term "deviator stress" is used to describe the dynamic longitudinal stress pulse applied by the vertical actuator to the specimen. This is in addition to the vertical stress pulse applied to the top of the specimen due to the action of the varying confining pressure.

(c) Supplementary investigations

As stated in Section 5.3, programme DS was to ascertain if a retarding effect on the rate of permanent deformation was obtained with rest periods between individual stress pulses.

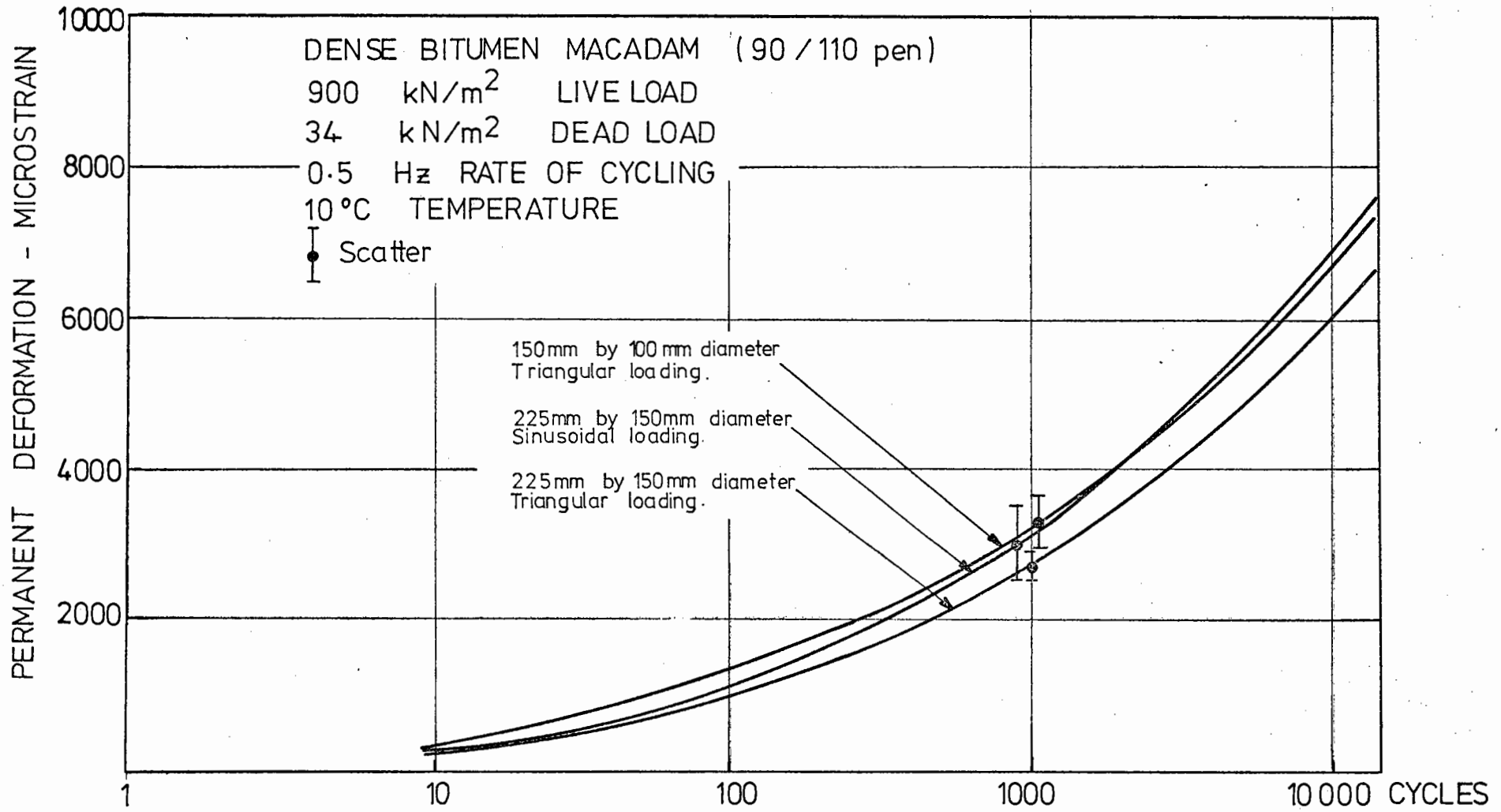

Fig. 7.4

THE EFFECT OF SPECIMEN SIZE AND VERTICAL LOAD WAVEFORM ON PERMANENT DEFORMATION.

Table 7.3 Results of Test Programme AS

Test No.	Dynamic vertical stress - kN/m²	Confining pressure kN/m²	Temperature - °C	Frequency of applied stress pulse - Hz	Rest period - seconds	Voids - %	Resilient Modulus MN/m²		Cycles to failure	Permanent longitudinal strain at failure - %	Initial elastic Poisson's ratio
							Initial	Final			
VARYING STRESS											
12,13	900	-	20	1	-	4.27	3620	2820	3,000	1.955	.366
17,18,19	650	-	20	1	-	4.66	3720	2440	10,000	1.821	.336
20,21,22	400	-	20	1	-	4.48	3610	2270	70,000	1.420	.326
48,49,70	150	-	20	1	-	5.04	2930	2010	480,000	0.772	.369
VARYING TEMPERATURE											
67,68,69	650	-	10	1	-	4.94	7070	4340	290,000	1.565	.324
17,18,19	650	-	20	1	-	4.66	3720	2440	10,000	1.821	.336
60,61,62	650	-	30	1	-	5.56	1440	1210	400	2.598	.416
VARYING CONFINING PRESSURE (No membranes)											
33,37,38	400	0	20	5	-	4.38	5230	3550	290,000	1.161	.289
32,39,42	400	200	20	5	-	4.84	4980	3810	144,000	0.899	.297
34,35,41	400	400	20	5	-	4.83	4390	3060	296,000	1.139	.287
36,43,44	400	600	20	5	-	4.84	4660	3140	345,000	1.273	.278

/contd.

Table 7.3 contd.

Test No.	Dynamic vertical stress - kN/m²	Confining pressure kN/m²	Temperature - °C	Frequency of applied stress pulse - Hz	Rest period - seconds	Voids - %	Resilient Modulus MN/m²		Cycles to failure	Permanent longitudinal strain at failure - %	Initial elastic Poisson's ratio
							Initial	Final			
VARYING FREQUENCY											
53,54,55	400	-	20	0.1	-	5.22	1500	1210	1,900	2.080	.377
57,58	400	-	20	0.5	-	5.39	2420	1600	13,400	2.030	.360
20,21,22	400	-	20	1.0	-	4.48	3610	2270	70,000	1.420	.326
33,37,38	400	-	20	5.0	-	4.38	5230	3550	290,000	1.161	.289
45,46,47	400	-	20	10.0	-	4.51	6470	3810	774,000	1.330	.285
REST PERIODS											
17,18,19	650	-	20	1	0	4.66	3720	2440	10,000	1.821	.336
23,24,25	650	-	20	1	$\frac{1}{4}$	4.64	3060	2240	8,000	1.596	.369
26,27,28	650	-	20	1	$\frac{1}{2}$	4.67	2840	1870	9,300	1.983	.333
29,30,31	650	-	20	1	2	4.54	2260	1620	4,500	2.328	.384
50,51,52	650	-	20	1	8	5.09	1670	1410	3,000	2.270	.377
53,54,55	400	-	20	0.1	0	5.22	1500	1210	1,900	2.080	.377
64,65,66	400	-	20	0.1	2	5.02	1320	1000	2,400	2.085	.431

Table 7.4 Results of Test Programme BS

Test No.	Dynamic vertical stress - kN/m²	Confining pressure kN/m²	Temperature - °C	Frequency of applied stress pulse - Hz	Rest period - seconds	Voids - %	Resilient Modulus MN/m²		Cycles to failure	Permanent longitudinal strain at failure - %	Initial elastic Poisson's ratio
							Initial	Final			
3% BINDER											
77,78,79	650	-	10	1	-	8.29	5390	2730	101,000	1.414	.289
71,72,73	650	-	20	1	-	8.29	2650	1880	1,200	1.283	.359
83,84,85	650	-	30	1	-	8.07	1300	1110	90	1.439	.435
4% BINDER											
67,68,69	650	-	10	1	-	4.94	7070	4340	290,000	1.565	.324
17,18,19	650	-	20	1	-	4.66	3720	2440	10,000	1.821	.336
60,61,62	650	-	30	1	-	5.56	1440	1210	400	2.598	.416
5% BINDER											
80,81,82	650	-	10	1	-	4.11	6050	4990	94,600	1.695	.280
74,75,76	650	-	20	1	-	4.20	2500	2130	2,530	2.711	.390
86,87,88	650	-	30	1	-	4.11	1240	1180	200	2.554	.468
VARYING BINDER CONTENT AT HIGH TEMPERATURE											
3% BINDER											
119,120 121	650	100	40	1	-	8.18	910	890	8,000	4.508	.562
4% BINDER											
116,117, 118	650	100	40	1	-	5.20	830	900	2,670	4.695	.487
5% BINDER											
113, 114, 115	650	100	40	1	-	3.94	770	910	1,170	4.021	.482

Table 7.5 Results of Test Programme CS

Test No.	Dynamic deviator stress - kN/m²	Confining pressure kN/m²	Temperature - °C	Frequency of applied deviator stress pulse Hz	Rest period of deviator stress - secs	Voids - %	Resilient Modulus MN/m²		Cycles to failure	Permanent longitudinal strain at failure - %	Initial elastic Poisson's ratio
							Initial	Final			
VARYING STATIC CONFINING PRESSURE (with membranes)											
89,90,91	650	200	20	1	-	5.19	2860	2160	231,000	1.344	.282
92,93,94	650	100	20	1	-	5.41	2710	1940	102,000	2.111	.427
99,101,102	650	0	20	1	-	5.30	2440	1860	3,300	2.654	.467
VARYING MODES OF APPLICATION OF CONFINING PRESSURE											
95,96,97	650	a	20	1	1	4.92	1730	1360	3,200	2.664	.449
110,111,112	650	b	20	1	1	5.23	1600	1200	61,400	3.250	.318
105,106	650	c	20	1	1	5.04	2310	1190	116,750	3.664	.346
98,103	650	d	20	1	1	5.12	1940	1440	127,250	2.197	.454

	Confining pressure kN/m² Constant	Confining pressure kN/m² Dynamic	Hz Frequency
a	0	0	-
b	25	75	0.5
c	25	75	1 and 1 sec rest
d	100	0	-

Table 7.6 - Index of test results in programmes AS, BS, CS

Loading variable	Test Programme	Figure Nos.		
		Permanent Deformation	Resilient Modulus	Elastic Poisson's Ratio
Magnitude of dynamic vertical stress	AS	7.5	7.15b	7.19
Temperature	AS	7.6	7.15a	7.19
Magnitude of constant confining pressure (with no protective membranes)	AS	7.7	-	-
Frequency	AS	7.8	7.16a	7.19
Rest periods	AS	7.9, 7.10	7.16b	-
Binder content and temperature	BS	7.11	7.17	7.20
Binder content (at 40°C and a confining pressure)	BS	7.12	-	-
Magnitude of constant confining pressure (with protective membranes)	CS	7.13	7.18	7.21
Mode of application of confining pressure	CS	7.14	-	-

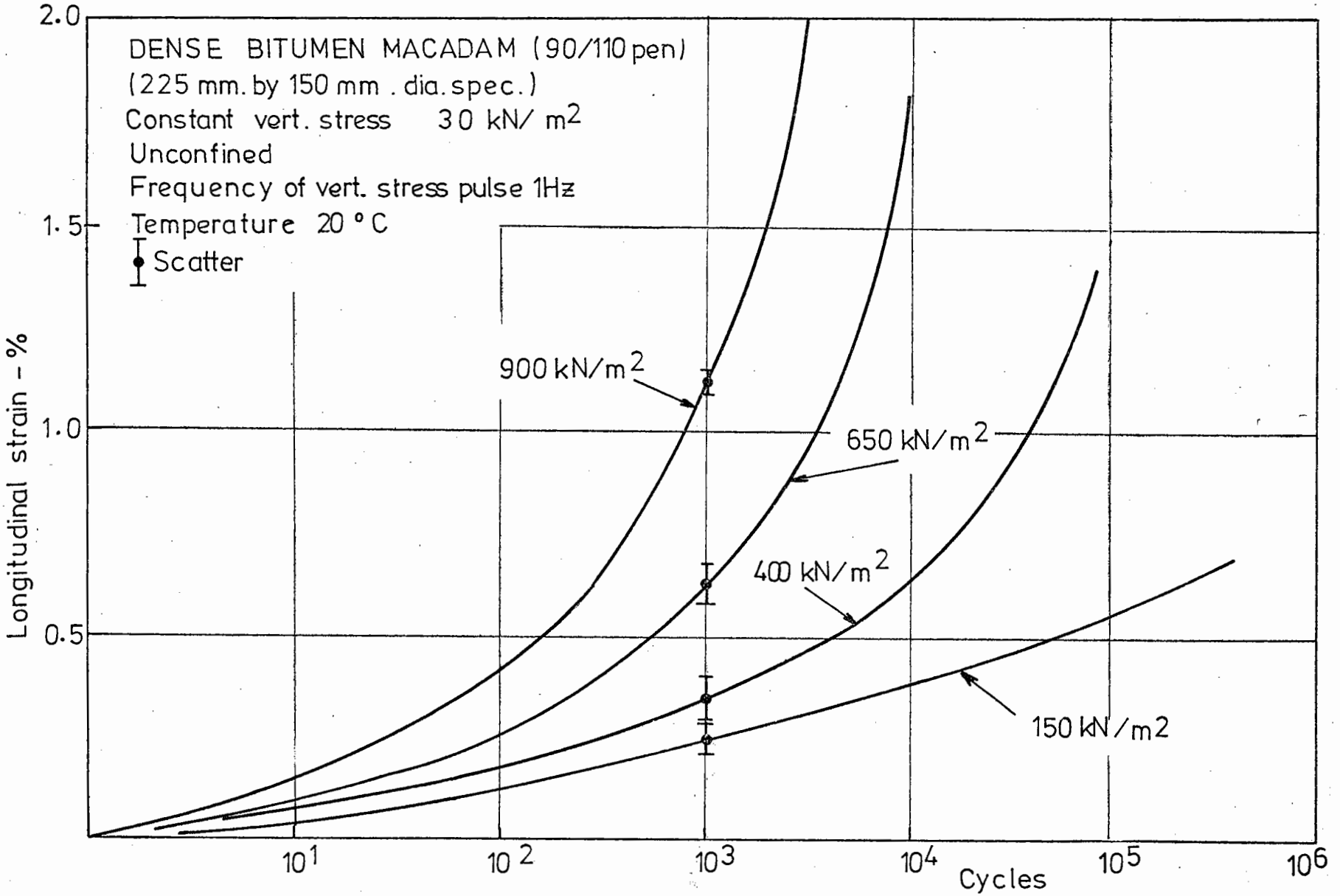

Fig. 7.5

THE INFLUENCE OF THE MAGNITUDE OF THE VERTICAL STRESS PULSE ON PERMANENT LONGITUDINAL STRAIN.

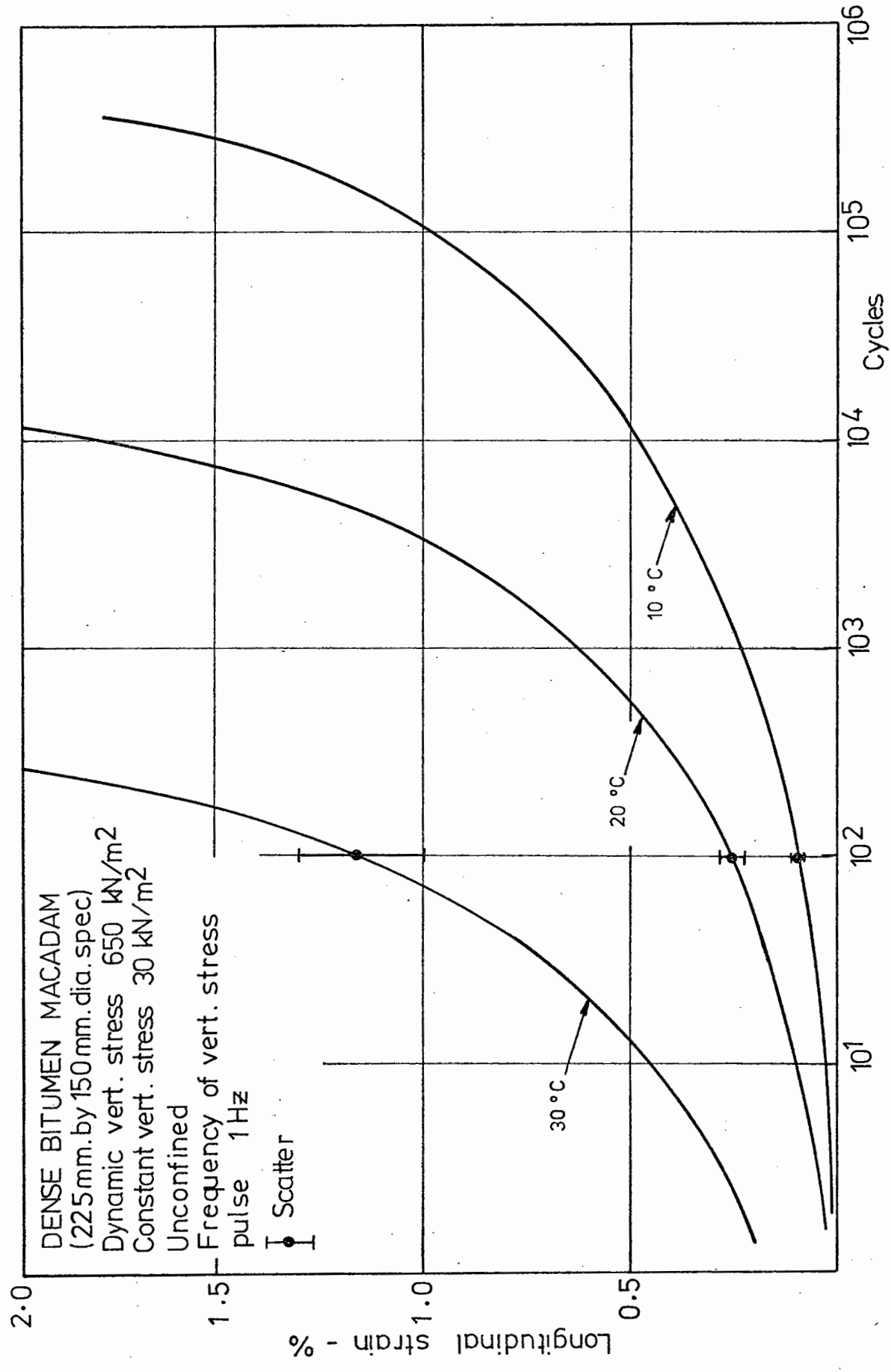

INFLUENCE OF TEMPERATURE ON PERMANENT LONGITUDINAL STRAIN.

Fig. 7.6

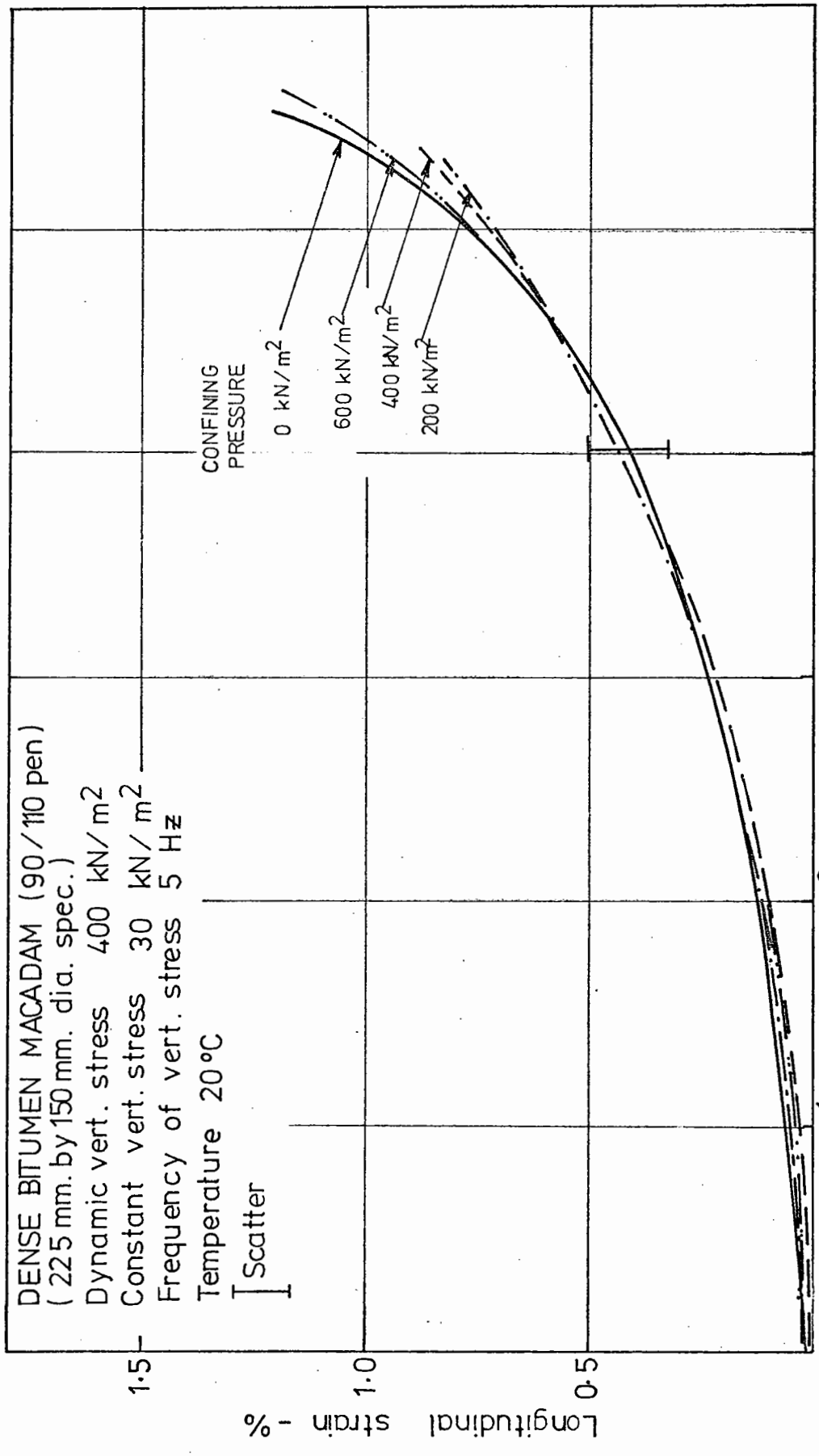

THE APPARENT INFLUENCE OF CONFINING PRESSURE ON PERMANENT LONGITUDINAL STRAIN.

(NO RUBBER MEMBRANE)

Fig. 7.7

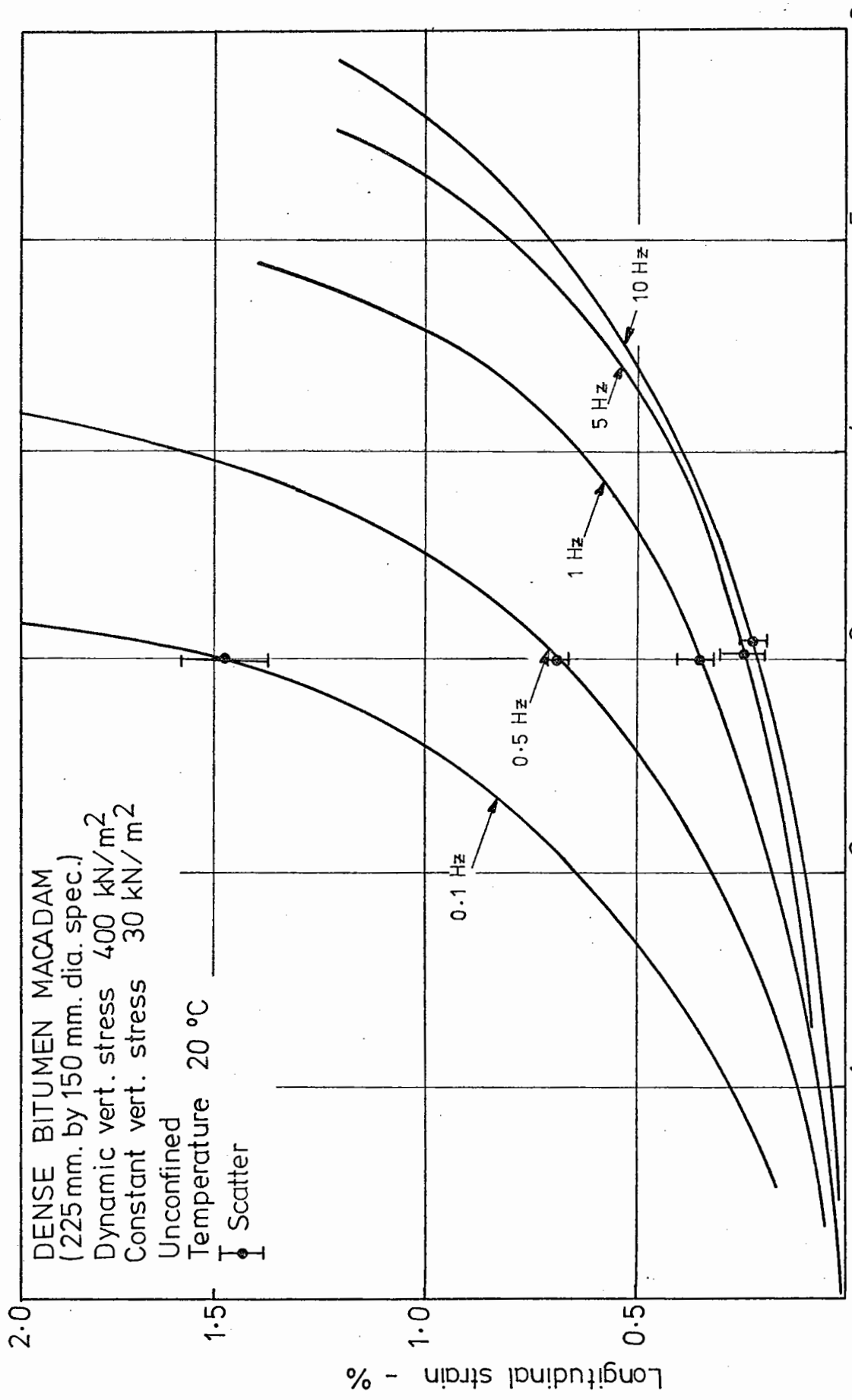

THE INFLUENCE OF THE FREQUENCY OF CYCLING OF THE VERTICAL STRESS PULSE ON THE PERMANENT LONGITUDINAL STRAIN.

Fig. 7.8

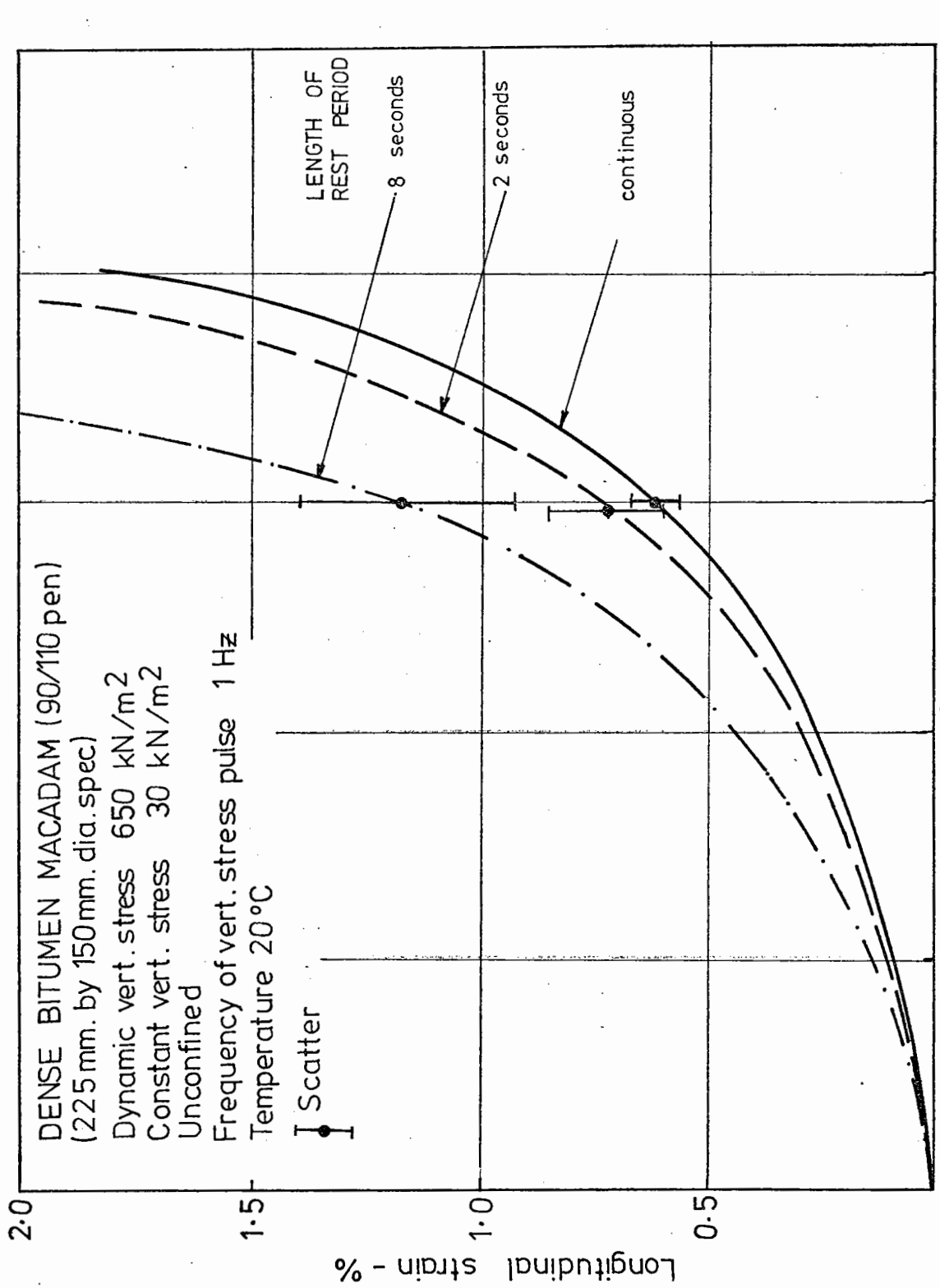

THE INFLUENCE OF REST PERIODS ON PERMANENT LONGITUDINAL STRAIN AT A FREQUENCY OF 1 Hz

Fig. 7.9

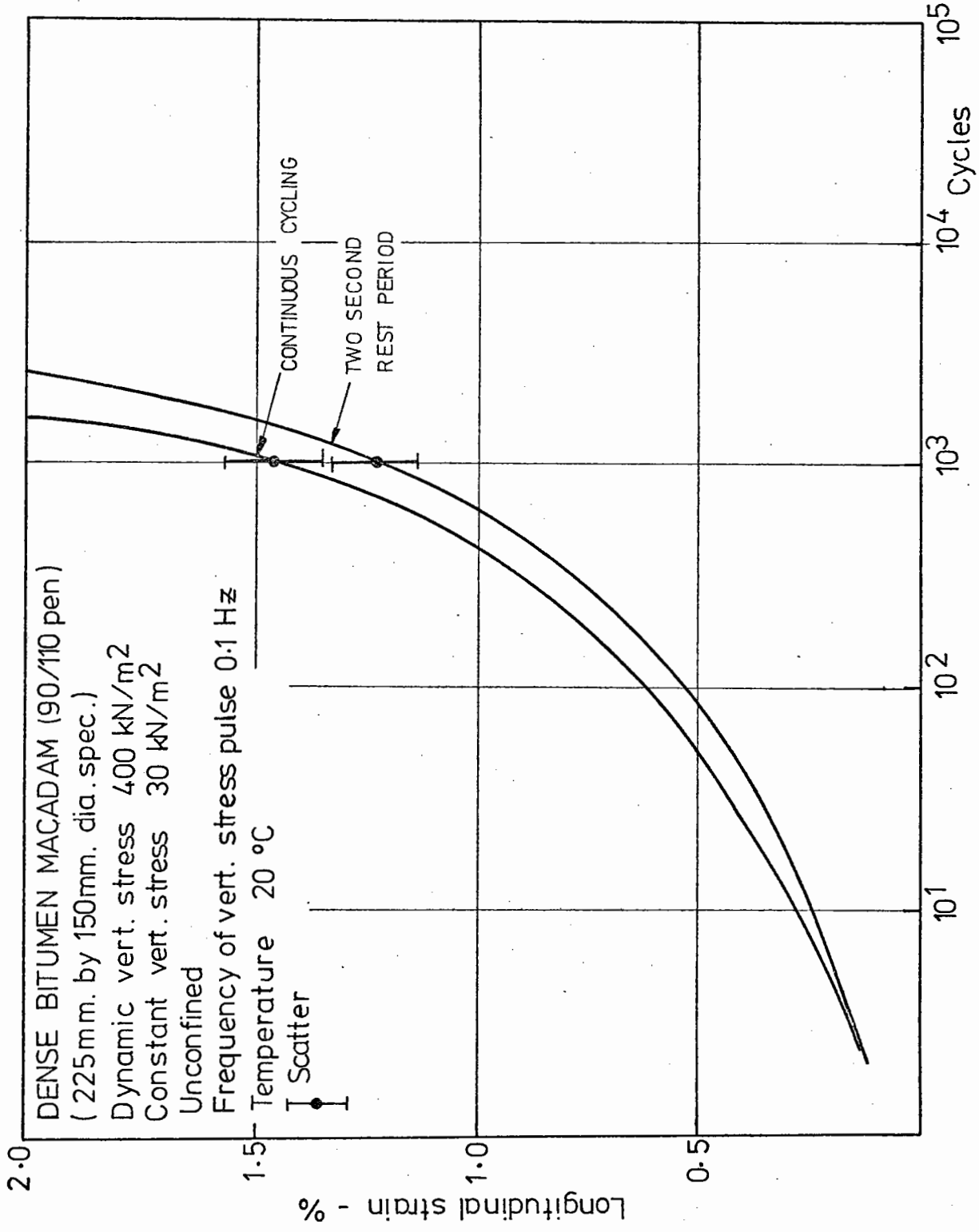

THE INFLUENCE OF REST PERIODS ON PERMANENT LONGITUDINAL STRAIN AT A SLOW RATE OF LOADING.

Fig. 7.10

DENSE BITUMEN MACADAM (90/110 pen)
(225 mm. by 150 mm. dia. spec.)
Dynamic vert. stress 650 kN/m^2
Constant vert. stress 30 kN/m^2
Unconfined
Frequency of vert. stress pulse 1 Hz
Temperature indicated in °C
Mean No. of cycles to failure *

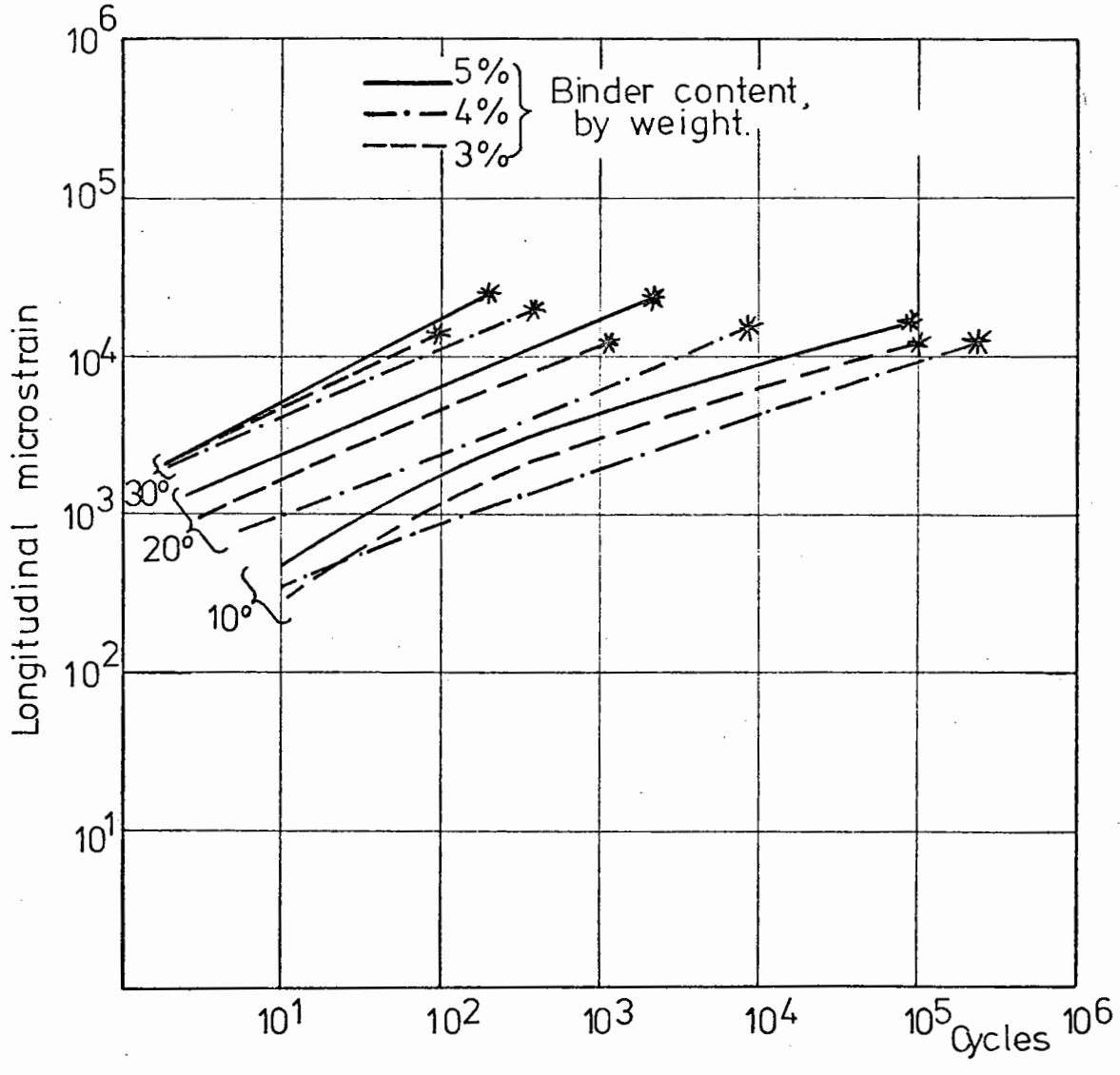

THE INFLUENCE OF BINDER CONTENT ON PERMANENT LONGITUDINAL STRAIN AT VARIOUS TEMPERATURES.

Fig. 7.11

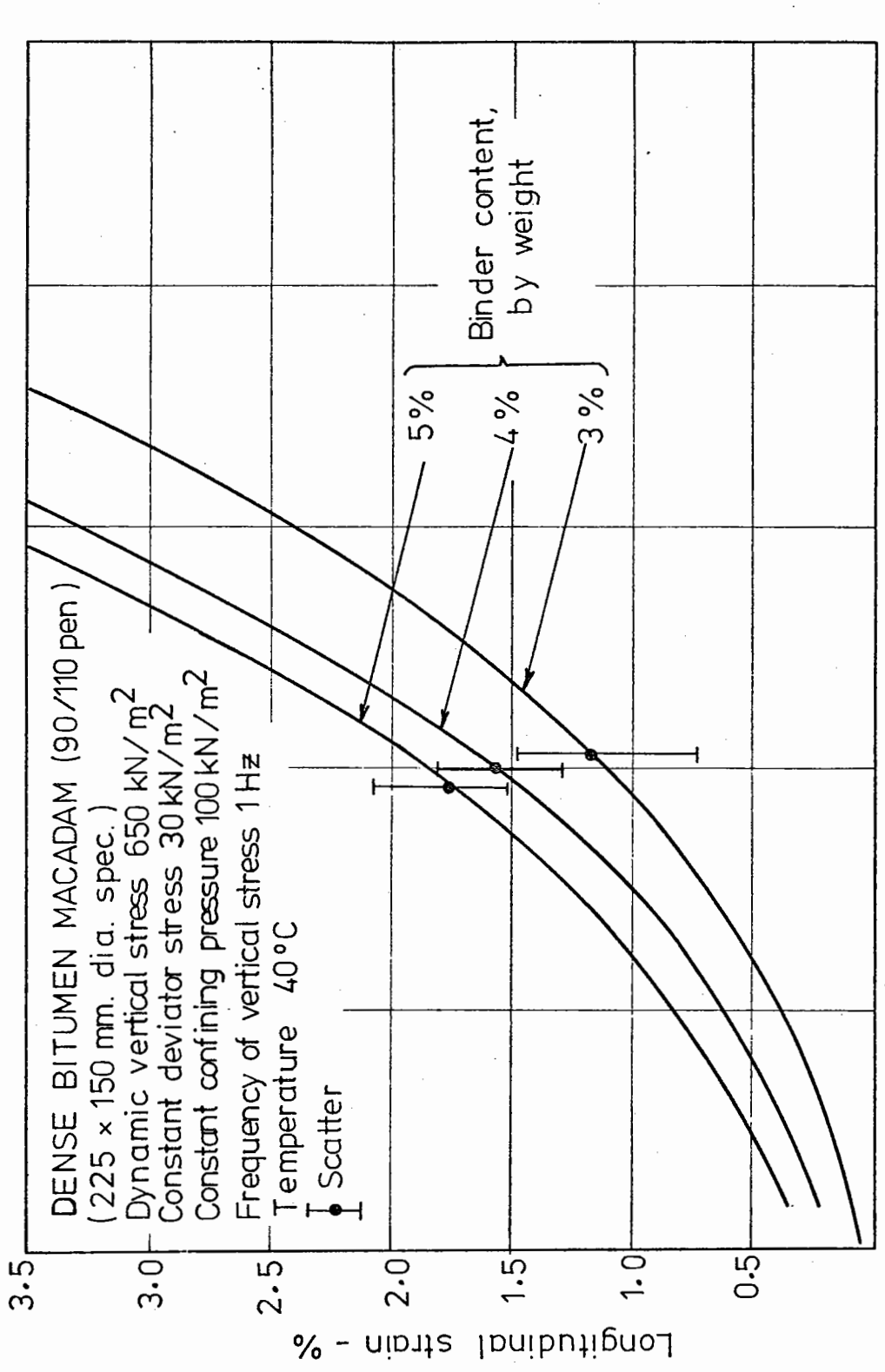

THE INFLUENCE OF BINDER CONTENT ON PERMANENT LONGITUDINAL STRAIN AT HIGH TEMPERATURE WITH A CONFINING STRESS.

Fig. 7.12

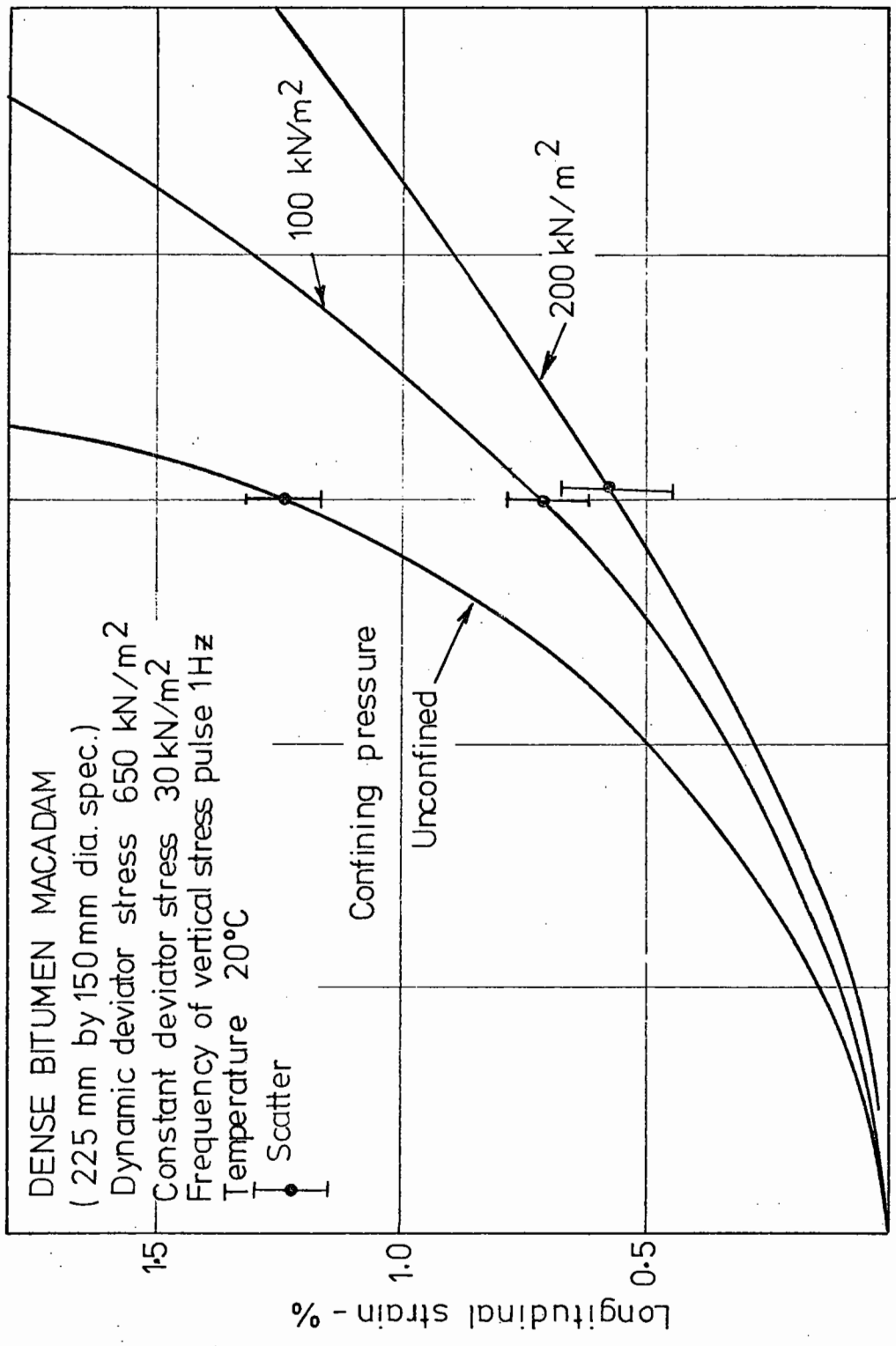

THE INFLUENCE OF CONFINING PRESSURE ON PERMANENT LONGITUDINAL STRAIN.

Fig. 7.13

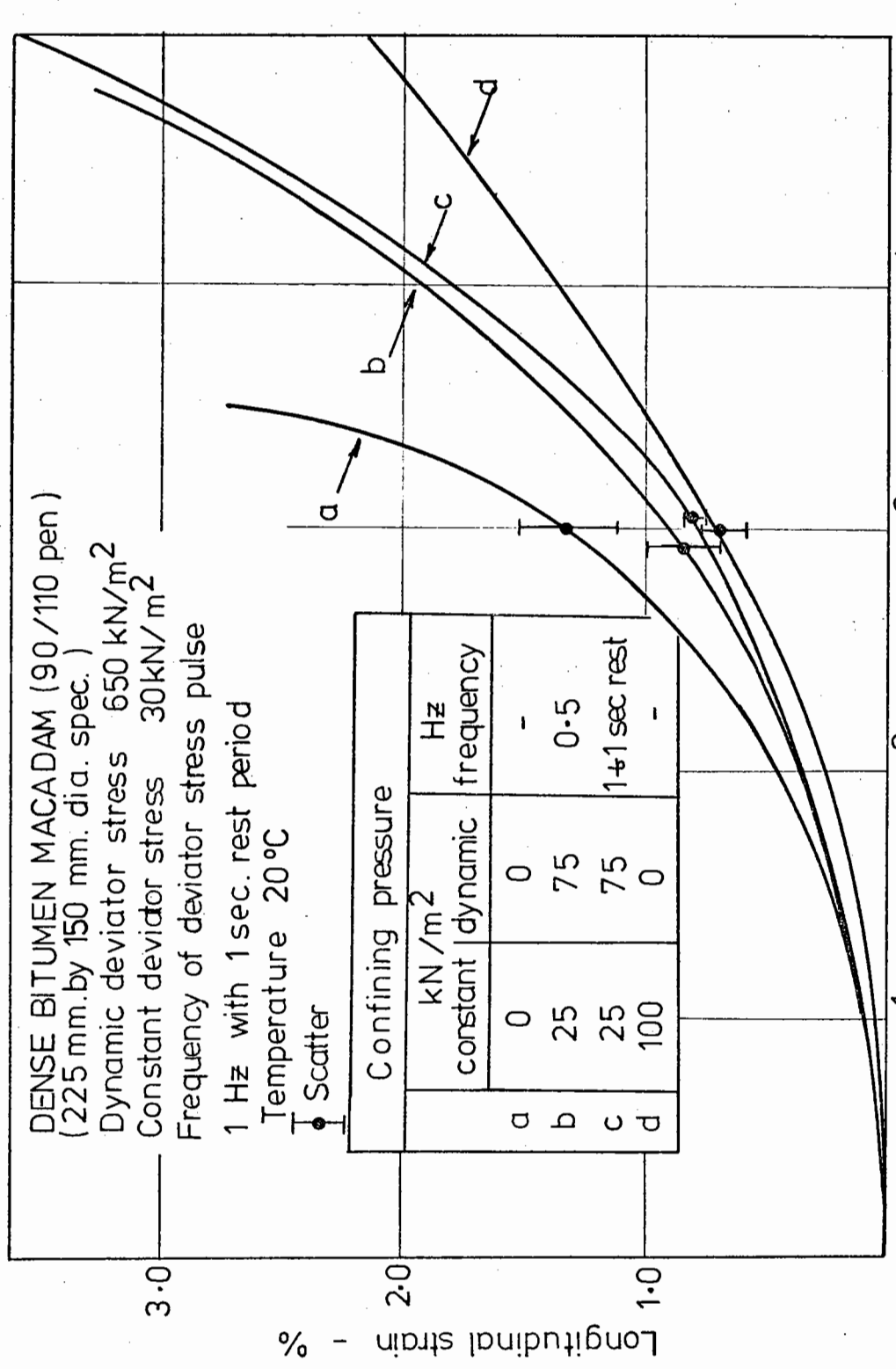

THE INFLUENCE OF THE MODE OF APPLICATION OF CONFINING PRESSURE.

Fig. 7.14

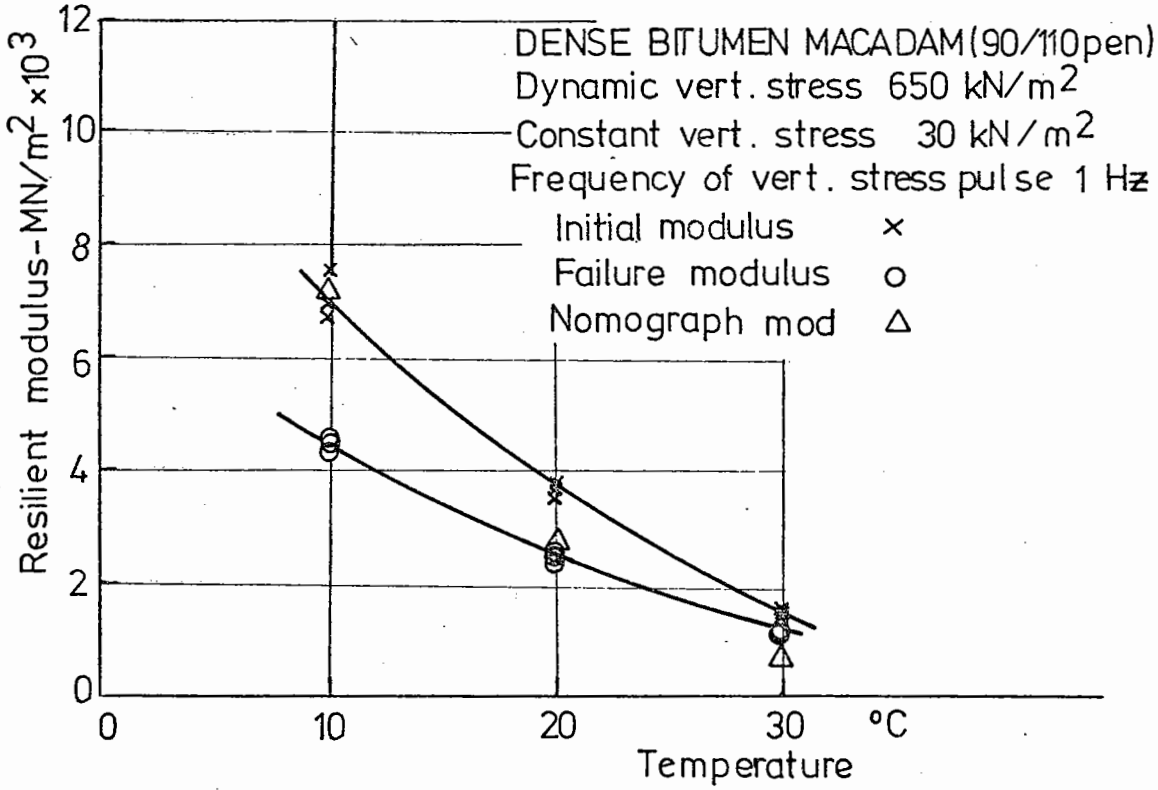

(a) RESILIENT MODULUS AS A FUNCTION OF TEMPERATURE

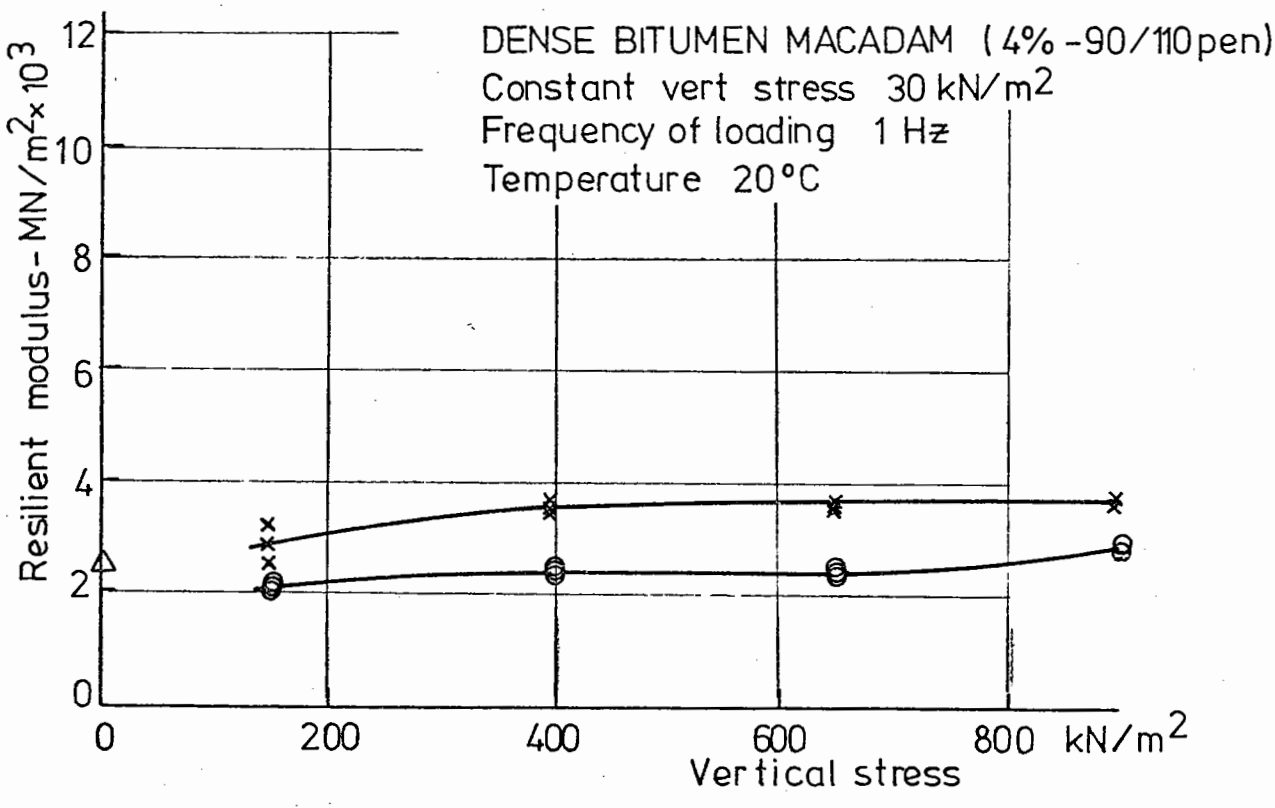

(b) RESILIENT MODULUS AS A FUNCTION OF THE APPLIED DYNAMIC VERTICAL STRESS.

Fig. 7.15

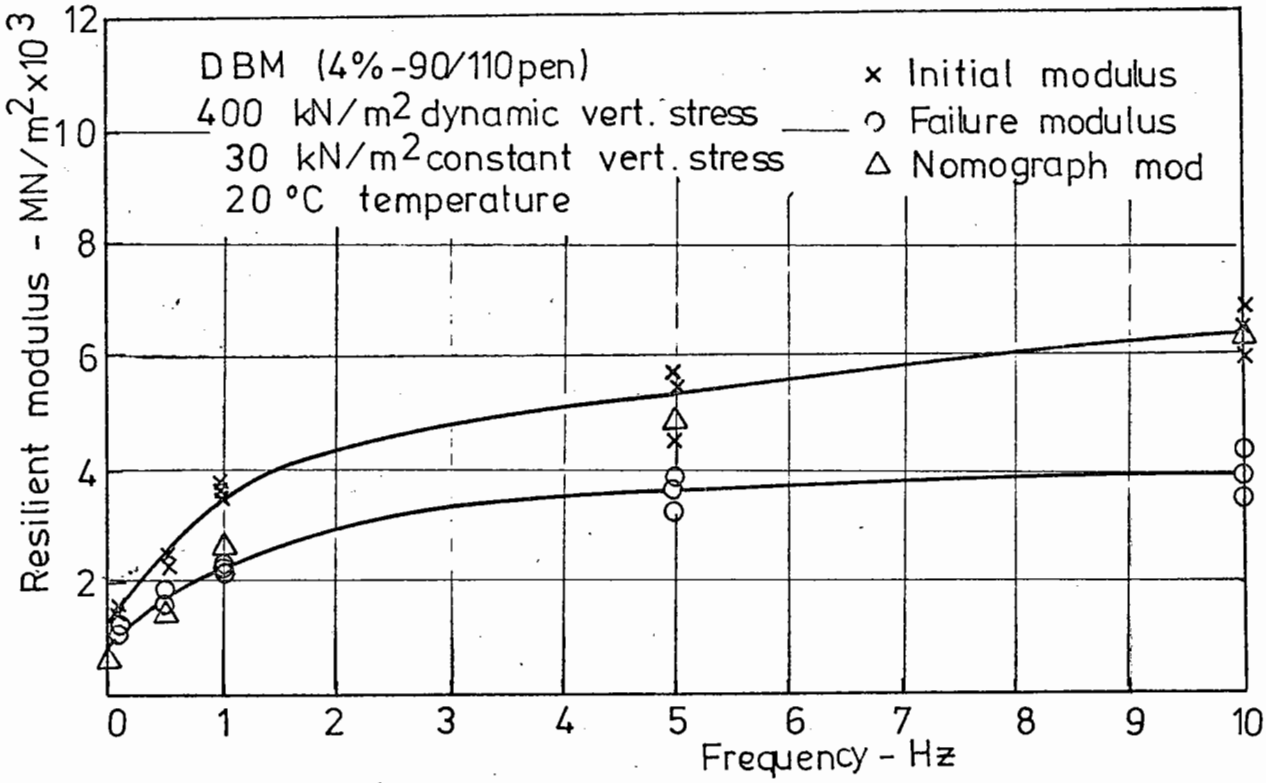

RESILIENT MODULUS AS A FUNCTION OF FREQUENCY

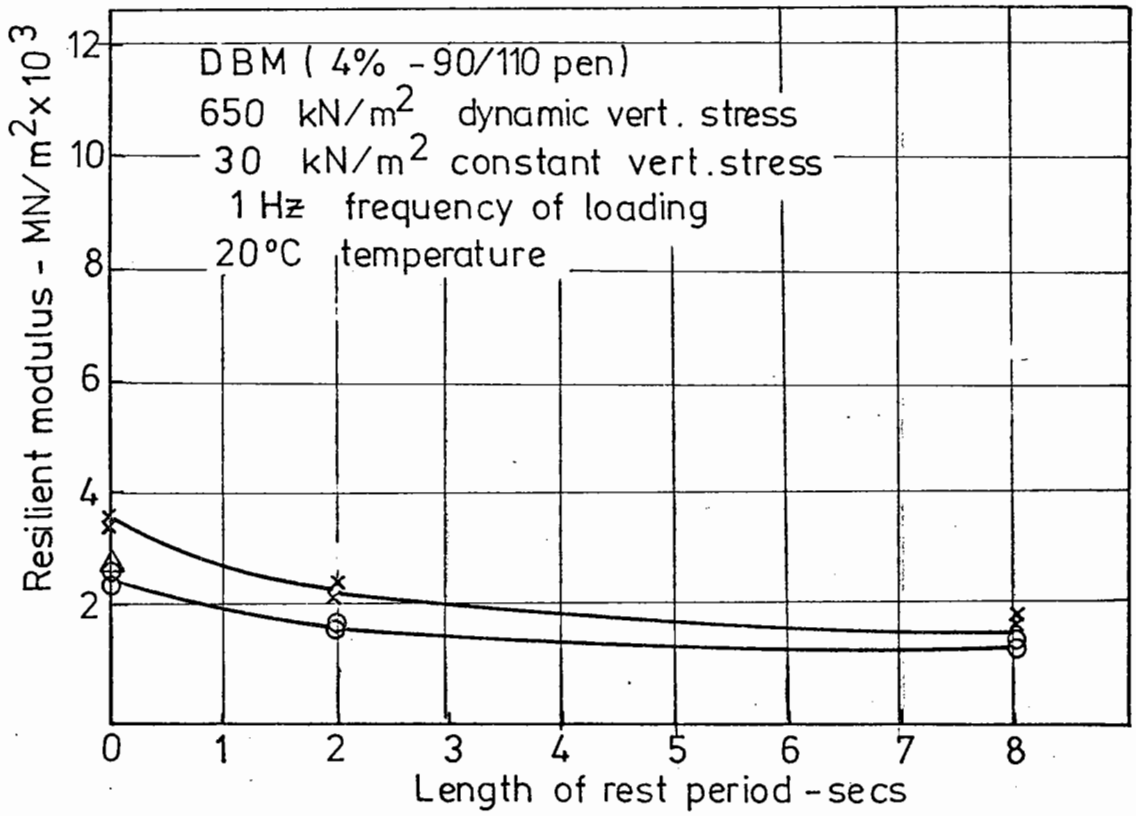

RESILIENT MODULUS AS A FUNCTION OF THE REST PERIOD BETWEEN SUCCESSIVE APPLICATIONS OF LOAD.

Fig. 7.16

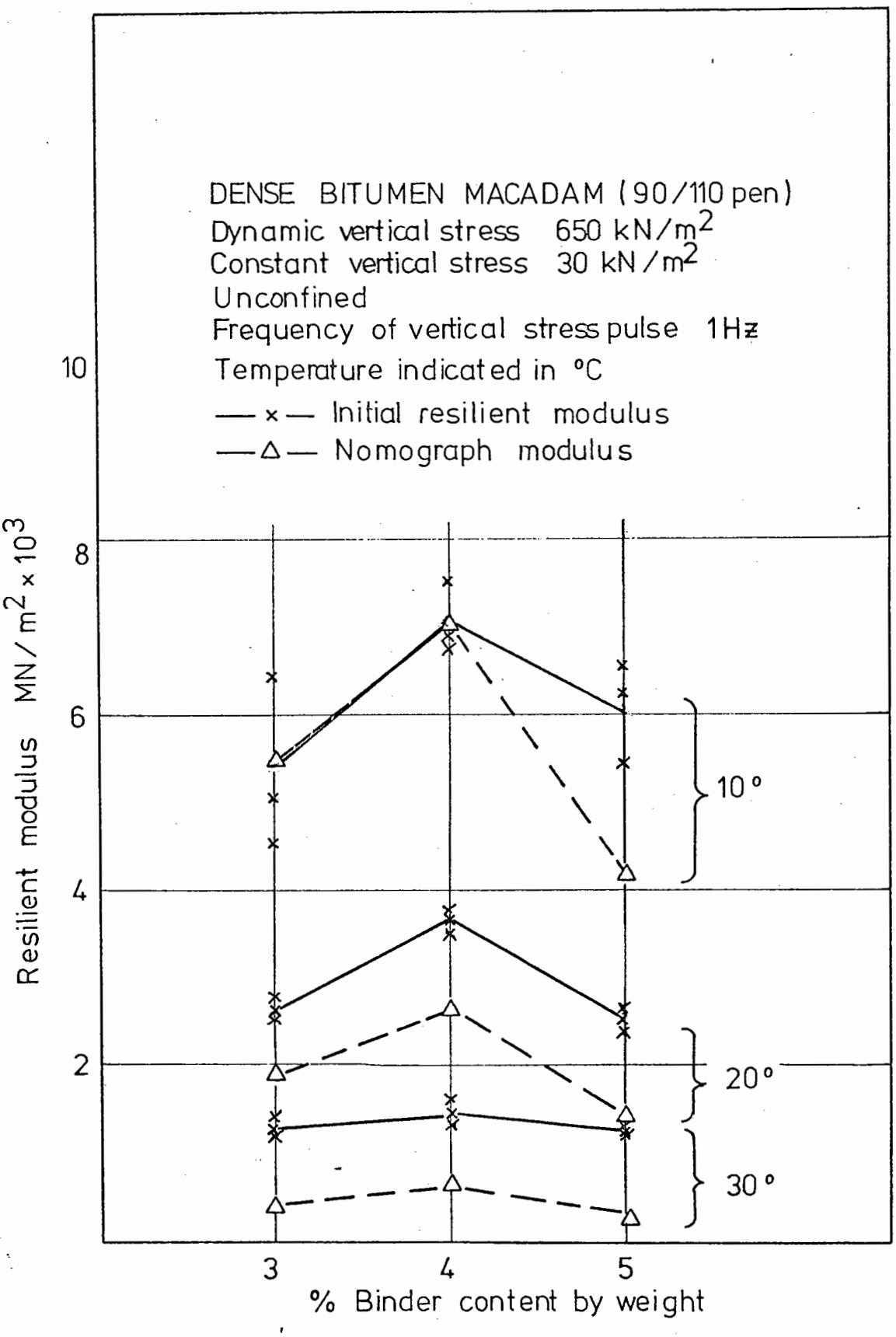

INITIAL RESILIENT MODULUS AS A FUNCTION OF BINDER CONTENTS FOR DIFFERENT TEMPERATURES.

Fig. 7.17

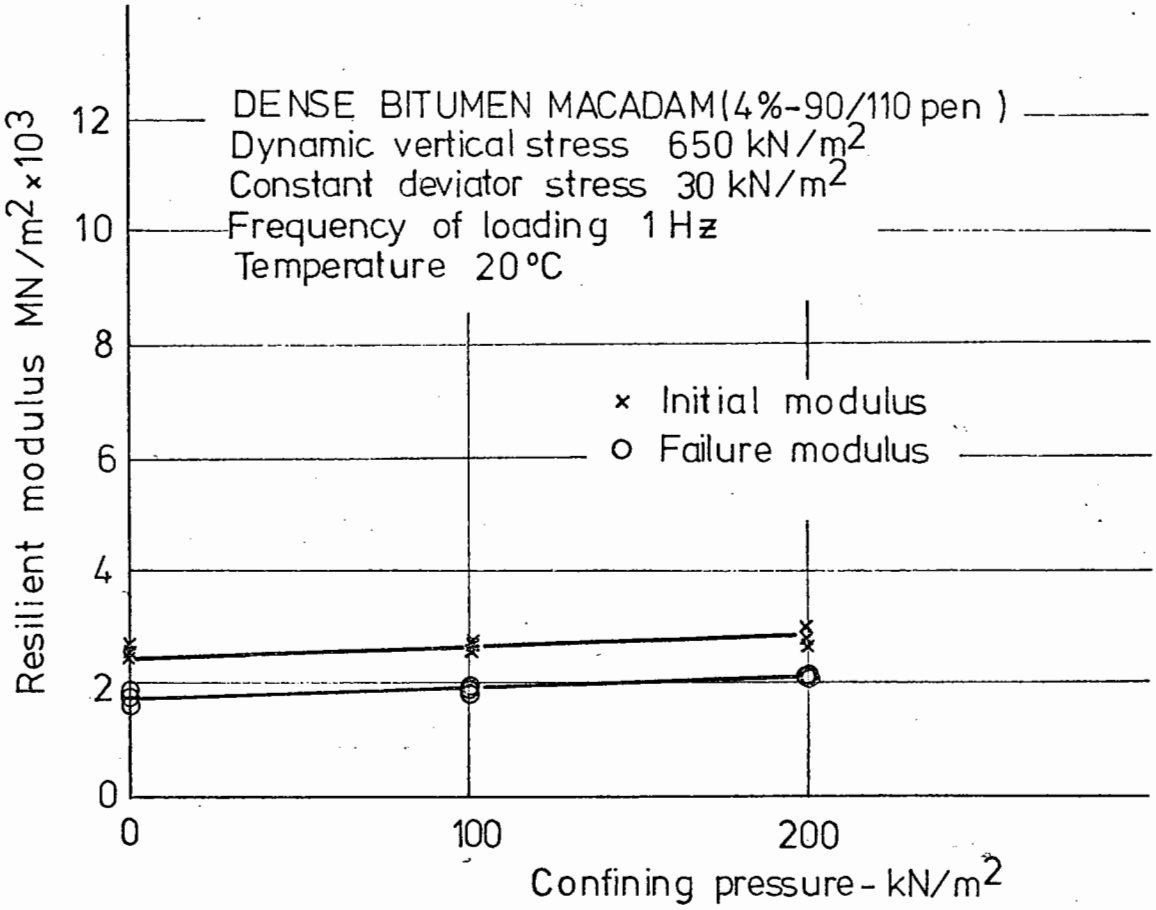

RESILIENT MODULUS AS A FUNCTION OF CONFINING PRESSURE

Fig. 7.18

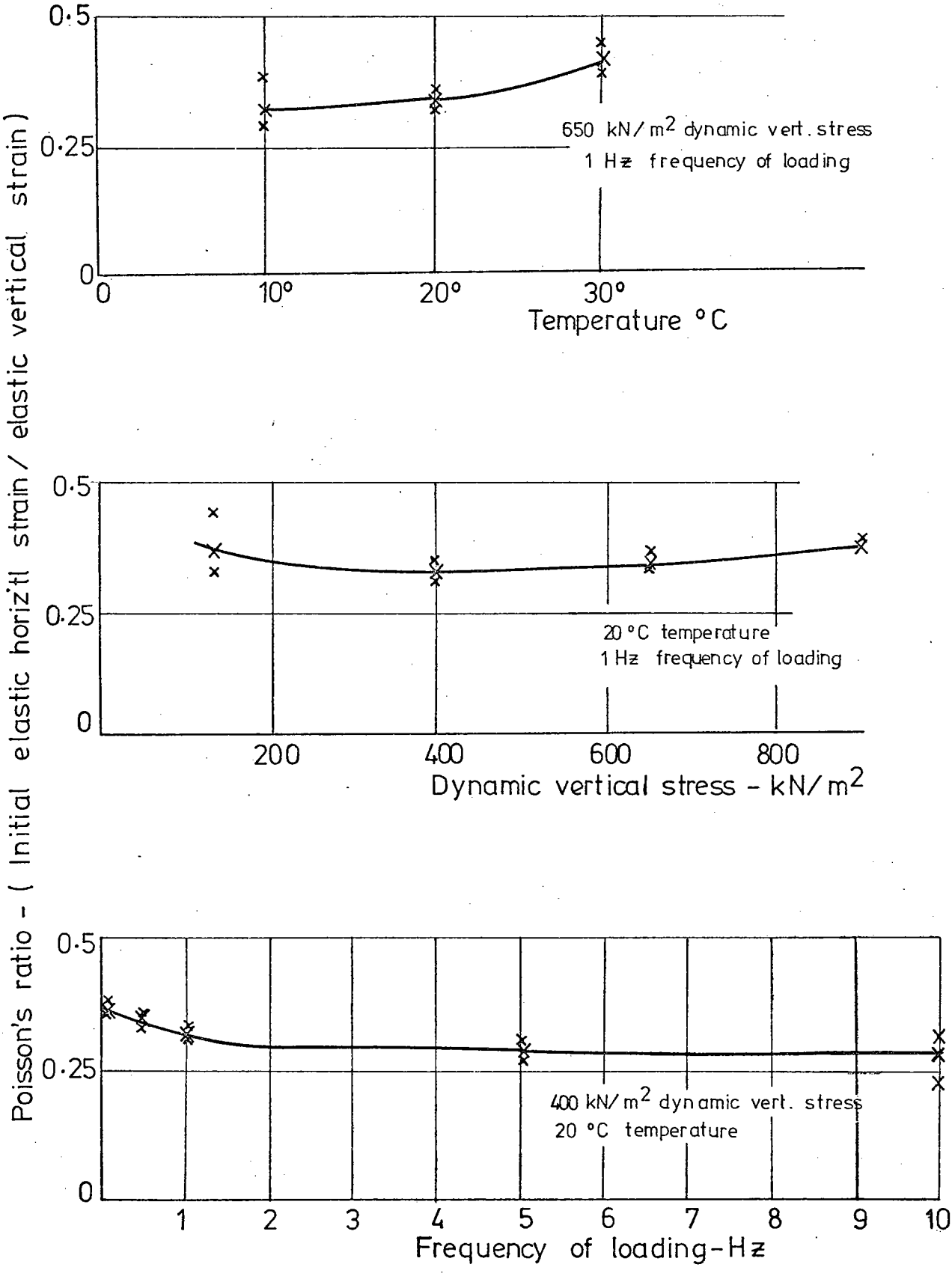

POISSON'S RATIO AS A FUNCTION OF TEMPERATURE, DYNAMIC VERTICAL STRESS AND FREQUENCY OF LOADING

(DENSE BITUMEN MACADAM, 4% -90/110 BINDER)

Fig. 7.19

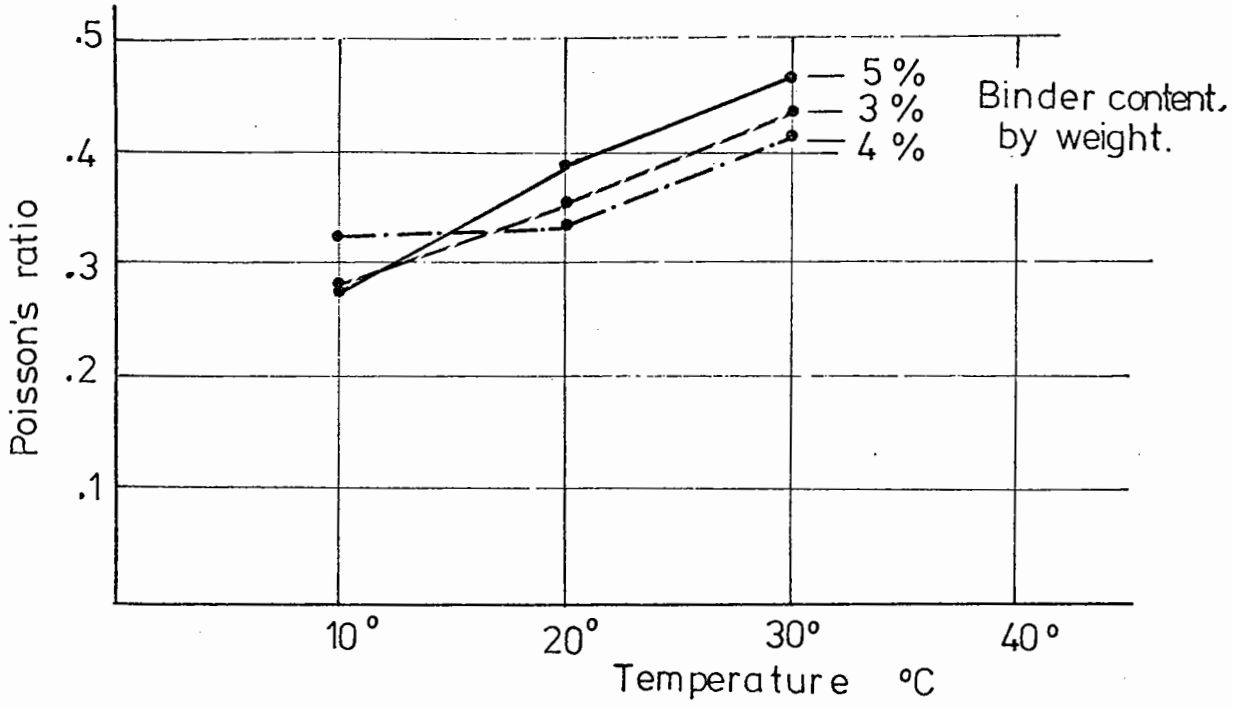

POISSON'S RATIO AS A FUNCTION OF TEMPERATURE FOR DIFFERENT BINDER CONTENTS.

Fig. 7.20

DENSE BITUMEN MACADAM (4%-90/110 pen)
Dynamic vertical stress 650 kN/m^2
Constant deviator stress 30 kN/m^2
Frequency of loading 1 Hz
Temperature 20°C

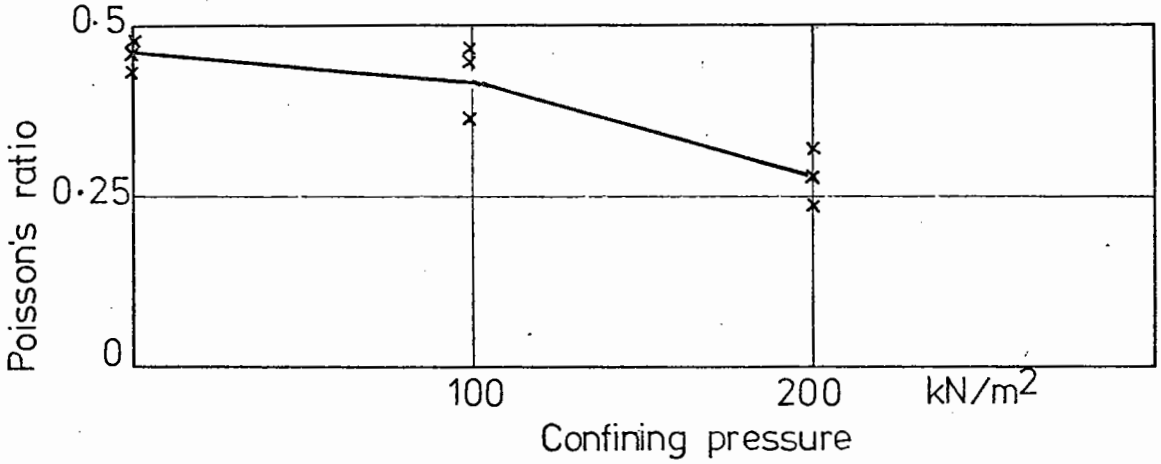

POISSONS RATIO AS A FUNCTION OF CONFINING PRESSURE.

Fig. 7.21

No constant vertical stress was applied, except for the weight of the top platen. The longitudinal permanent strain with cycles plot is shown in Fig. 7.22 and the resilient results in Table 7.7.

Programme ES was performed to investigate further the effects of frequency on the rate of permanent deformation shown in programme AS. Certain tentative conclusions had been drawn and it was necessary to check these conclusions at another specimen temperature.

The temperature selected was 25°C and the range of frequencies varied between 1 Hz and 15 Hz. The longitudinal permanent strain with cycles plot is shown in Fig. 7.23 and the resilient results in Table 7.8.

(d) Cored specimens

Due to the short length of the cores supplied and the lack of the usual three specimens per loading condition, the results shown in Table 7.9 should be treated with caution.

7.4 RESULTS FROM THE STATIC CREEP TESTING PROGRAMME

The effect of the various loading conditions onthe build up of permanent deformation with time in the 100 mm (4 in.) diameter dense bitumen macadam specimens may be seen in Figs. 7.24 and 7.25.

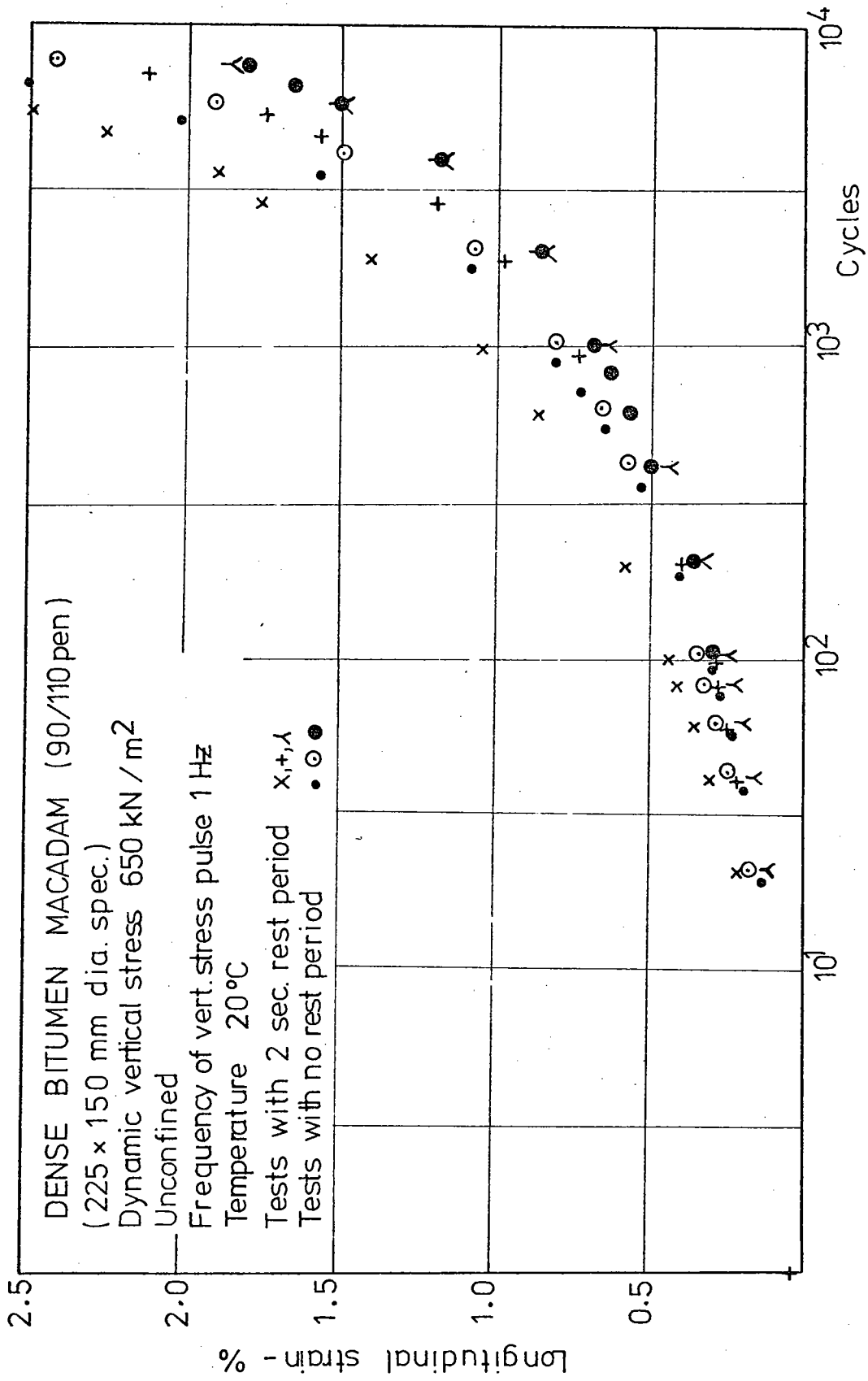

THE INFLUENCE OF REST PERIODS ON PERMANENT LONGITUDINAL STRAIN WITH NO CONSTANT VERTICAL STRESS APPLIED (Weight of platen excepted)

Fig. 7.22

Table 7.7 Results of Test Programme DS

Test No.	Dynamic vertical stress - kN/m²	Confining pressure kN/m²	Temperature - °C	Frequency of applied stress pulse - Hz	Rest period - seconds	Voids - %	Resilient Modulus MN/m²		Cycles to failure	Permanent longitudinal strain at failure - %	Initial elastic Poisson's ratio
							Initial	Final			
REST PERIOD (no constant vertical stress)											
123, 124, 127	650	0	20	1	-	5.16	3100	2100	8,050	2.278	.331
125, 126, 128	650	0	20	1	2	5.17	2040	1390	7,030	2.091	.354

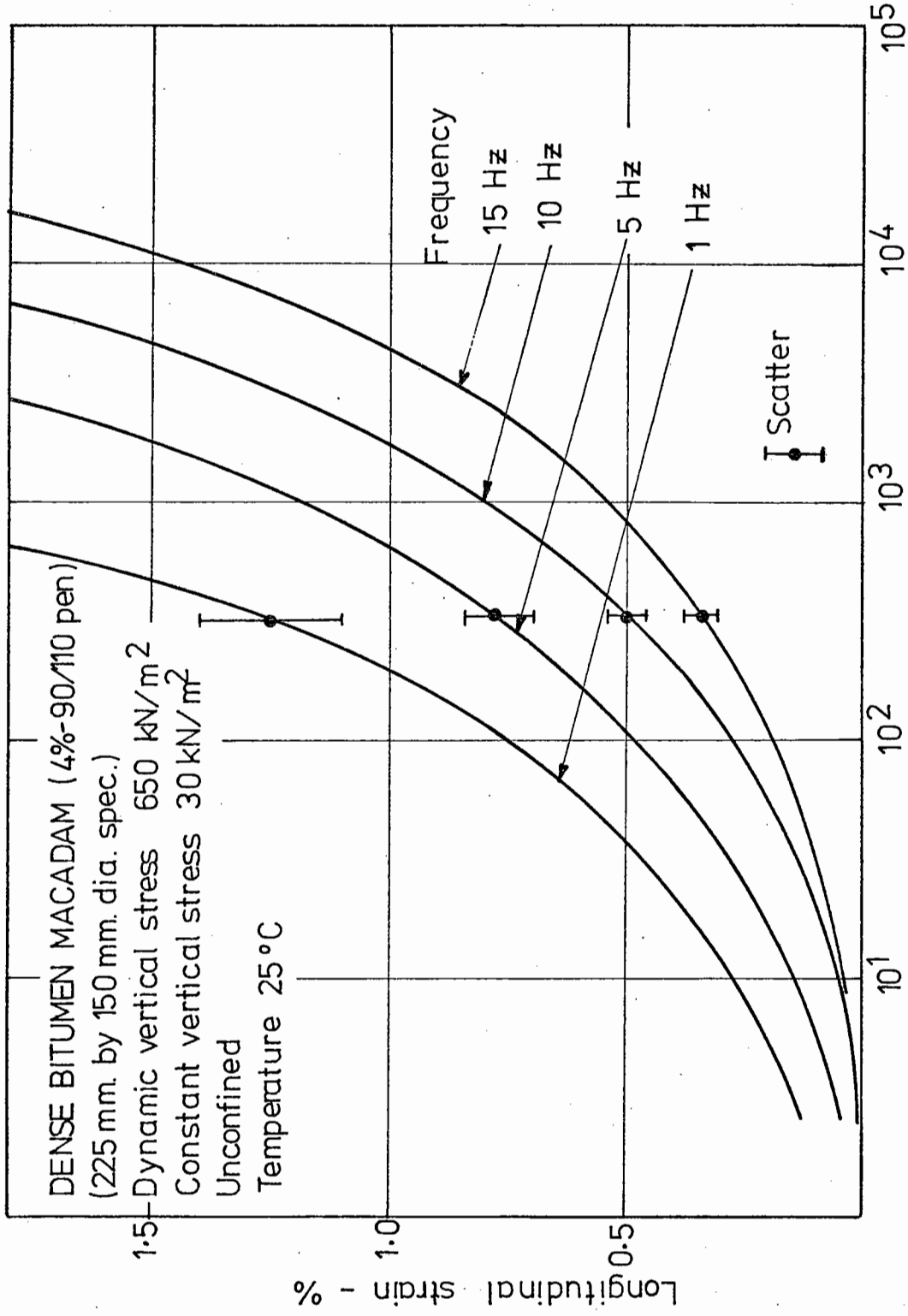

THE INFLUENCE OF THE FREQUENCY OF CYCLING OF THE VERTICAL STRESS PULSE ON THE PERMANENT LONGITUDINAL STRAIN.

Fig. 7.23

Table 7.8 Results of Test Programme ES

Test No.	Dynamic vertical stress - kN/m²	Confining pressure kN/m²	Temperature - °C	Frequency of applied stress pulse - Hz	Rest period - seconds	Voids - %	Resilient Modulus MN/m²		Cycles to failure	Permanent longitudinal strain at failure - %	Initial elastic Poisson's ratio
							Initial	Final			
VARYING FREQUENCY											
137,138,139	650	-	25	1	-	4.81	1860	1600	900	2.166	.411
129,130,131	650	-	25	5	-	4.96	2690	2140	4330	2.432	.391
132,133,134	650	-	25	10	-	5.04	3200	2410	10670	2.607	.328
135,136	650	-	25	15	-	5.00	4030	2890	14000	1.741	.292

Table 7.9 Results of Test Programme FS

All tests on 152 mm (6 in.) diameter cores at 25°C in an unconfined state

Test No.	Nominal binder content - %	Dynamic vertical stress - kN/m²	Frequency of applied stress pulse - Hz	Resilient Modulus MN/m²		Cycles to failure	Permanent longitudinal strain at failure - %
				Initial	Final		
25 PASSES OF COMPACTING ROLLER							
141	5	650	1	1,695	1,475	2,200	2.9
140	4	650	1	1,300	1,015	600	2.3
148	3	650	1	1,240	755	200	2.1
9 PASSES OF COMPACTING ROLLER							
147	5	650	1	1,060	1,105	350	3.1
142	4	650	1	1,125	-	200	2.3
145	3	650	1	940	805	100	2.4
3 PASSES OF COMPACTING ROLLER							
144	5	650	1	820	740	120	3.5
143	4	650	1	745	790	100	4.2
146	3	650	1	690	760	50	2.9

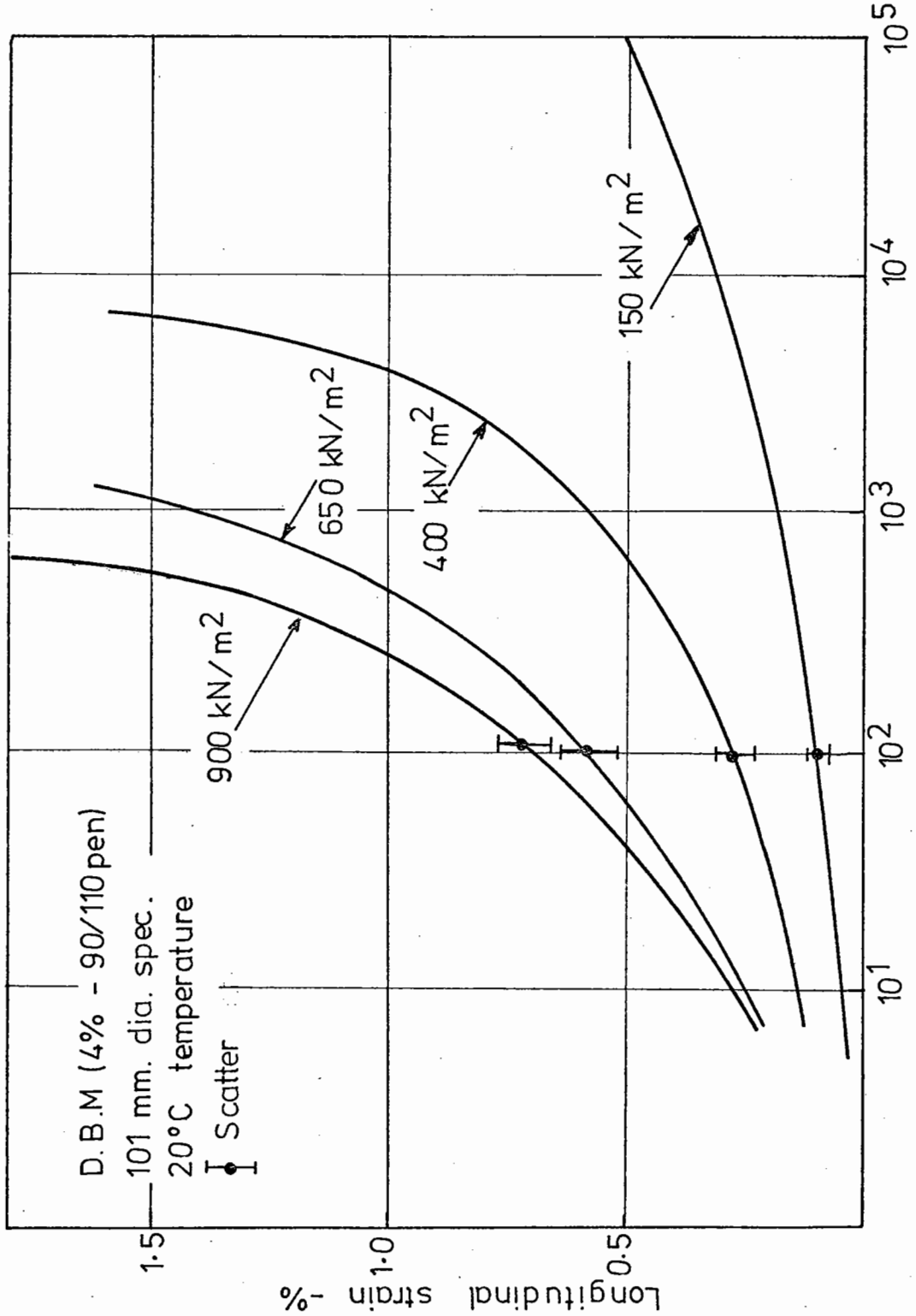

CONSTANT STRESS TESTS ON DENSE BITUMEN MACADAM (EFFECT OF STRESS LEVEL)

Fig. 7.24

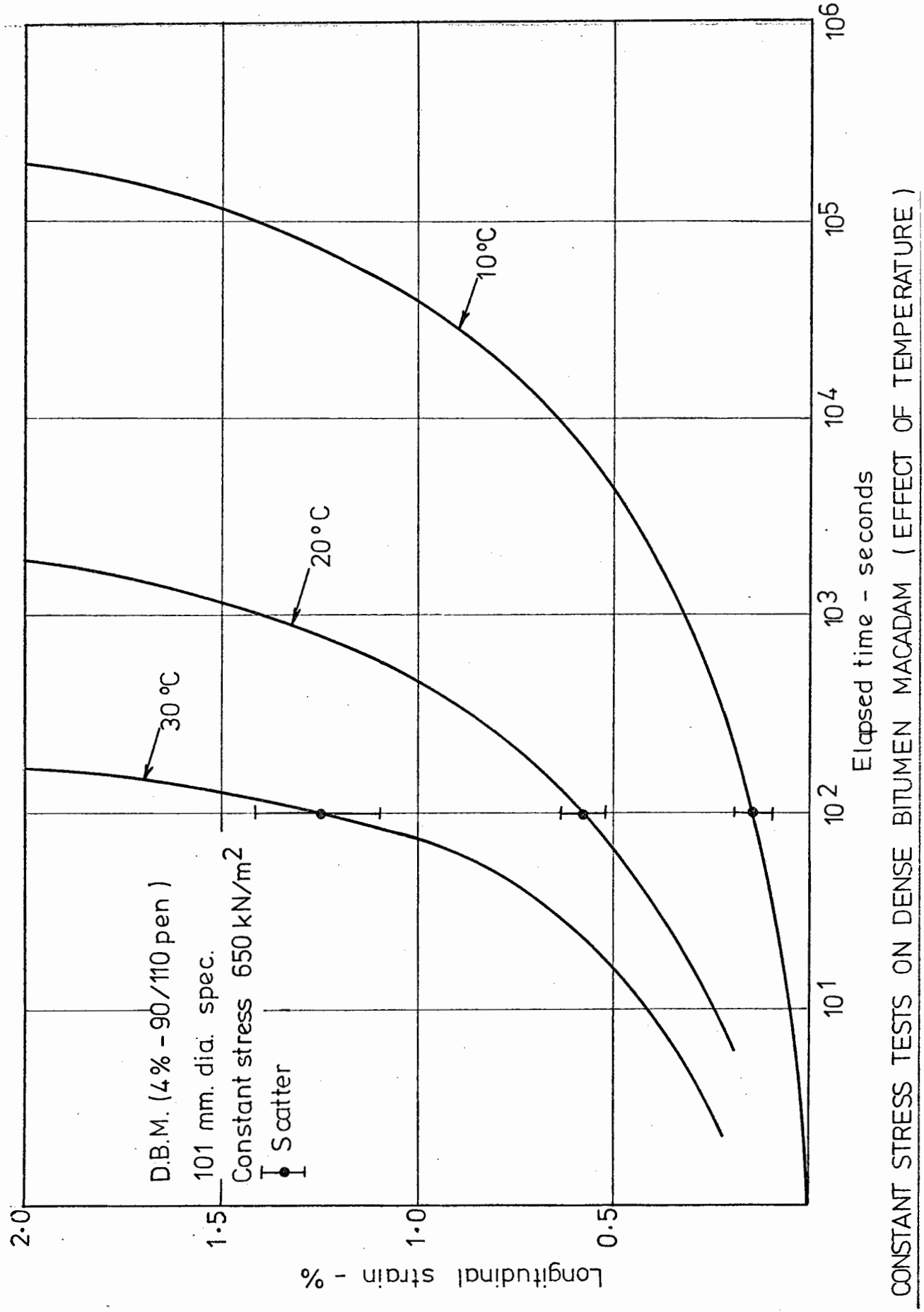
CONSTANT STRESS TESTS ON DENSE BITUMEN MACADAM (EFFECT OF TEMPERATURE)
Longitudinal strain - %
2·0
1·5
1·0
0·5
Elapsed time - seconds
10¹
10²
10³
10⁴
10⁵
10⁶
10°C
20°C
30°C
D.B.M. (4% - 90/110 pen)
101 mm. dia. spec.
Constant stress 650 kN/m²
Scatter

Fig. 7.25

CHAPTER EIGHT

DISCUSSION OF RESULTS

8.1 INTRODUCTION

The results of the tests carried out in the three testing machines are presented in Chapter 7. The discussion of these results will be divided into six parts. The first will consider the results of the "Instron" tests. The next three sections will discuss the behaviour of the material in the servo-hydraulic machine. Whilst it is realised that permanent and resilient deformation characteristics and the time to failure are related, they have been placed into these three separate sections, for ease of presentation. Section 8.6 concerns the creep behaviour of specimens observed under static loading. Section 8.7 presents a method for the prediction of the permanent deformation of a specimen undergoing a dynamic test, and the last section suggests that a relationship exists between the permanent deformation behaviour of the material under dynamic and static loading.

It should be reiterated that the ranges of the loading variables investigated were chosen to cover the in situ conditions of the material (Chapter 2).

8.2 INSTRON TEST PROGRAMME AND THE TRANSITION TESTS

As stated in Section 5.1, the principal purpose of the dynamic "Instron" tests was to provide data for the design of the servo-hydraulic machine. The results obtained were superseded by those from the new machine and therefore comment is not made on them.

Twenty years ago there was considerable interest shown in the determination of the cohesion (c) and the angle of shearing resistance (φ) of bituminous bound materials. Unfortunately, there is no simple method of relating these parameters to road pavement design.

Such tests as the Marshall test are more simple to operate and have resulted in the production of roads in North America that have performed satisfactorily. However, in 1955, Hveem (10) drew attention to the incidence of fatigue failure of flexible road pavements. This resulted in research being channelled into fatigue investigations to the detriment of research concerned with the stability of bituminous mixtures employing triaxial modes of testing. As little work has been done in this field since then, a limited number of constant rate of strain triaxial tests were performed to obtain values of c and φ for different temperatures, rates of loading, and void contents in the specimens. Fig. 7.2 shows that the cohesion drops with increasing temperature and Fig. 7.3 shows that it increases with an increased rate of strain. This latter effect had previously been reported by Goetz and Chen (53). The dependence of cohesion on temperature and rate of loading is to be expected as the binder is a viscoelastic material, and it is the binder that is responsible for the cohesion.

The angle of shearing resistance was affected by the void content of the specimens (Fig. 7.3). An increased angle of shearing resistance occurred with the lower void content due to the close packing of the aggregate in the high density specimens.

The angle of shearing resistance, which is dependent on particle interlock, does not appear to be affected by the rate of strain, which would agree with the findings of Nijboer (54) for a similar material, who explained that whilst the bitumen has a lubricating effect on the aggregate interlock, this was only small.

Transition tests were carried out to investigate the difference between testing 100 mm (4 in.) diameter specimens in the Instron machine under triangular stress pulses and testing 150 mm diameter specimens under sinusoidal stress pulses in the servo-hydraulic machine. It may be seen from Table 7.2 that the variation in resilient modulus due to these changes is of the order of 25%. The rate of longitudinal permanent deformation may be compared in Fig. 7.4 which shows that there is little difference in the permanent deformation of the three sets of tests performed. Hence, the permanent deformation behaviour obtained in this investigation may be taken as being independent of the specimen diameter and of the two vertical stress pulse shapes applied.

8.3 DYNAMIC TESTING PROGRAMME - PERMANENT DEFORMATION PROPERTIES

The General Form of the Creep Curve

The increase in the permanent strain with the number of load cycles for various different loading conditions is shown in Figs. 7.5 to 7.14, and it is apparent that all exhibit the same form of creep curve. It may be observed that in all the unconfined tests the rate of deformation declined continually

up to failure. When a confining pressure was applied to a specimen the rate of deformation did approach a constant value which made the determination of the failure point more difficult.

It was found that if the results of the dynamic tests were plotted on a log strain versus log cycles basis a linear relationship was obtained. An example of this may be seen in Fig. 8.1. The first plotted point is not on the line, but this may be corrected, if required, in the manner suggested by Onaran and Findley (55). They found that it was possible to describe creep for a non-linear viscoelastic material in the following manner:

$$\epsilon_t = \epsilon_o + mt^n \qquad 8.1$$

where ϵ_o and m are functions of the stress, n is a constant and ϵ_t is the strain at any time t.

From 8.1:

$$\epsilon_t - \epsilon_o = mt^n \qquad 8.2$$

Hence

$$\text{Log}(\epsilon_t - \epsilon_o) = n \log t + \text{Constant} \qquad 8.3$$

and hence, if a suitable value of ϵ_o is chosen, the plot of $\log(\epsilon_t - \epsilon_o)$ against log t is a straight line. Some of the results of the testing programmes were plotted in this manner, and may be seen in Fig. 7.11 and Figs. 8.2 - 8.8.

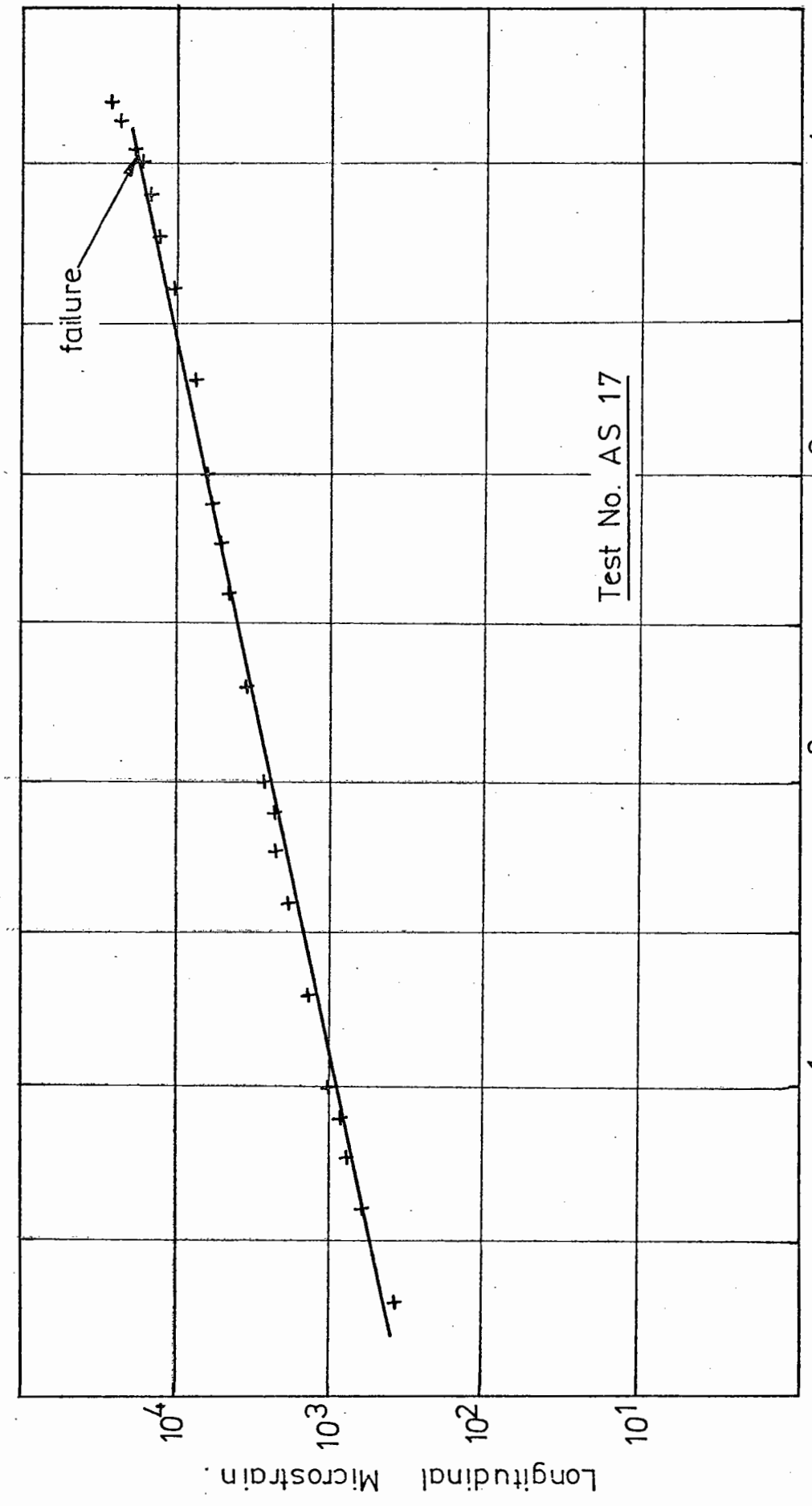

TYPICAL LOG, PERMANENT VERTICAL DEFORMATION , vs. LOG CYCLES PLOT.

Fig. 8.1

DENSE BITUMEN MACADAM (90/110 pen)
(225 mm. by 150 mm. dia. spec.)
Constant vert. stress 30 kN/m^2
Unconfined
Frequency of vert. stress pulse 1 Hz
Temperature 20 °C
Mean no. of cycles to failure *

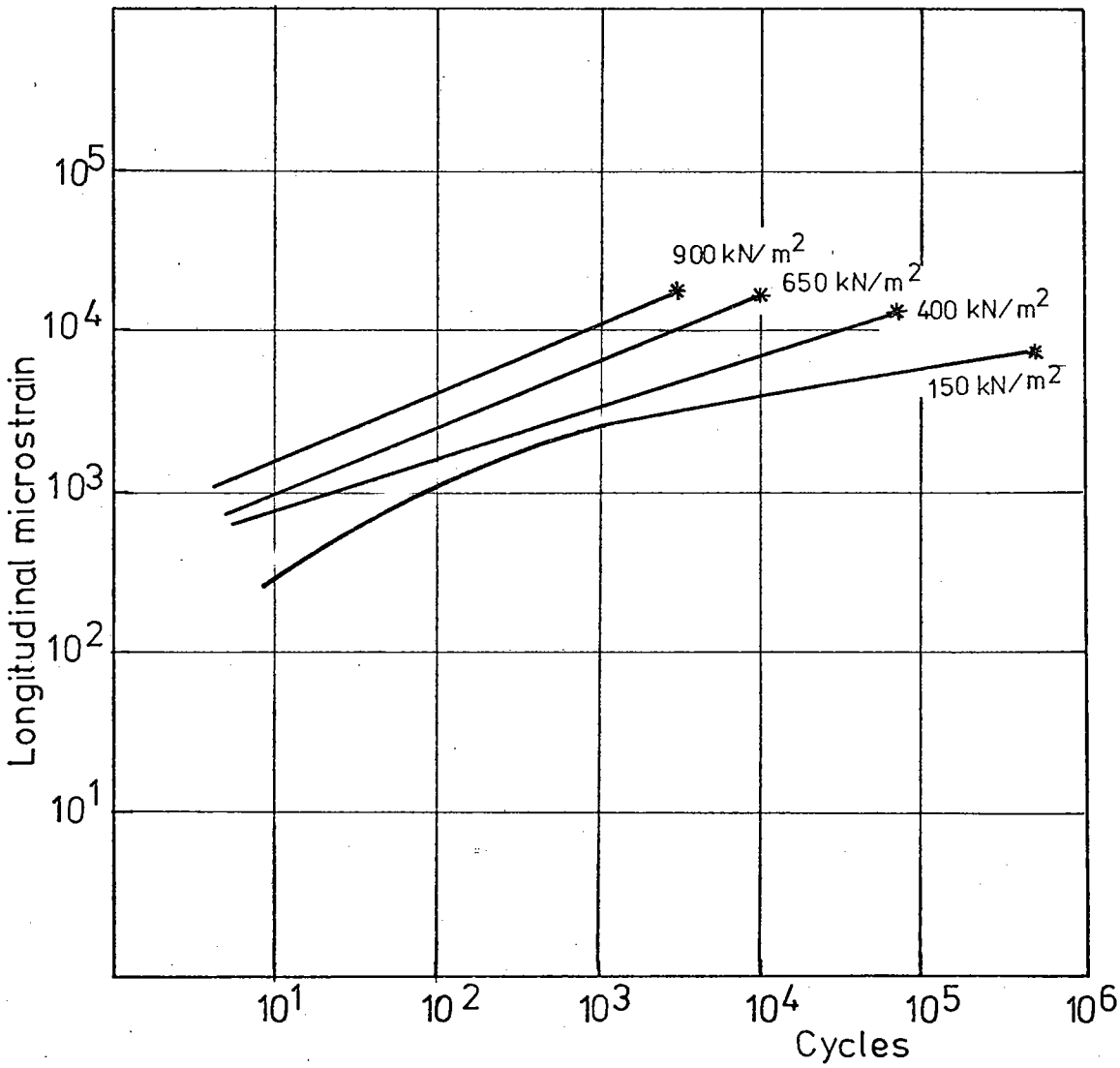

THE INFLUENCE OF THE MAGNITUDE OF THE VERTICAL STRESS PULSE ON PERMANENT LONGITUDINAL STRAIN.

Fig. 8.2

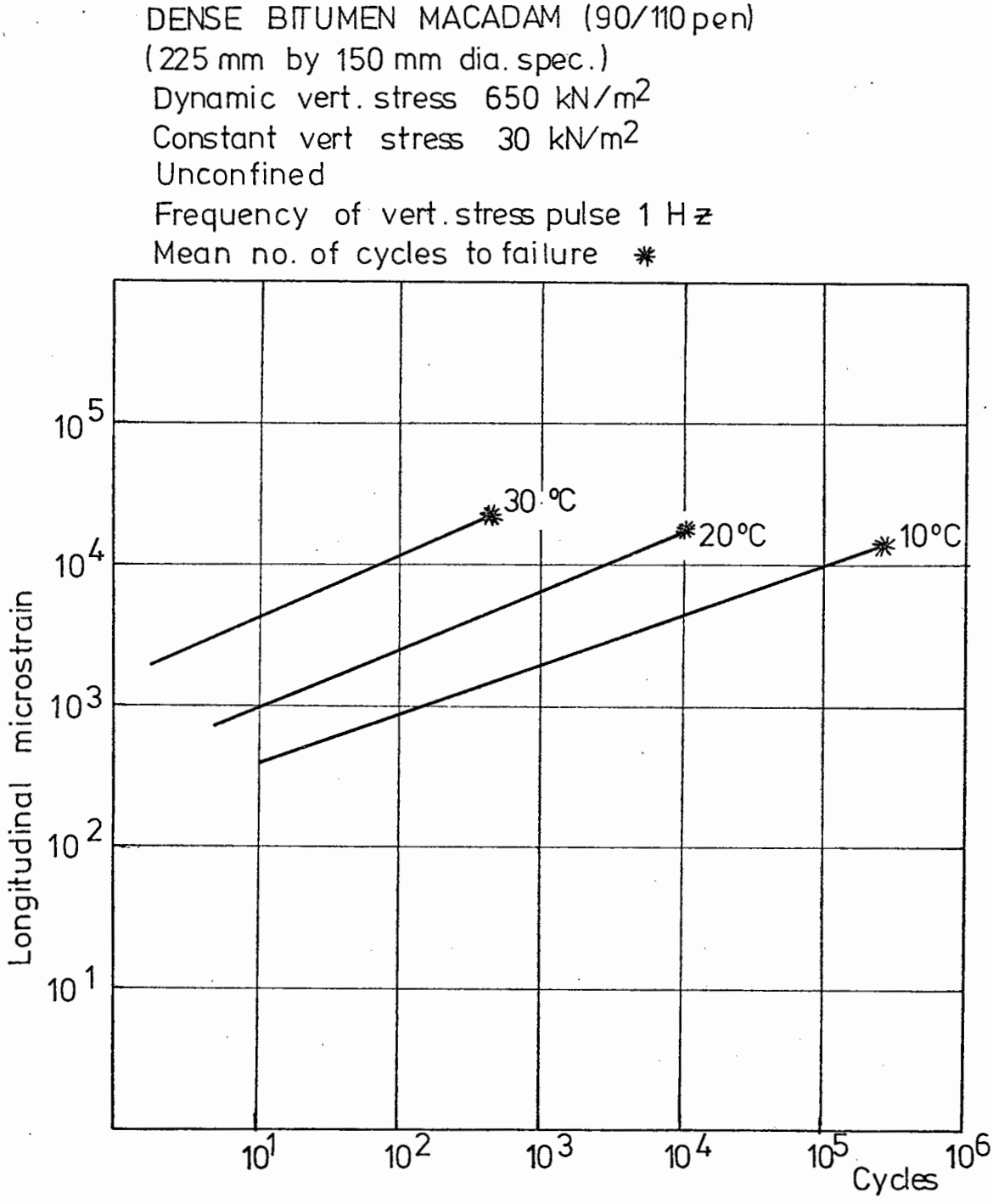

THE INFLUENCE OF TEMPERATURE ON PERMANENT LONGITUDINAL STRAIN.

Fig. 8.3

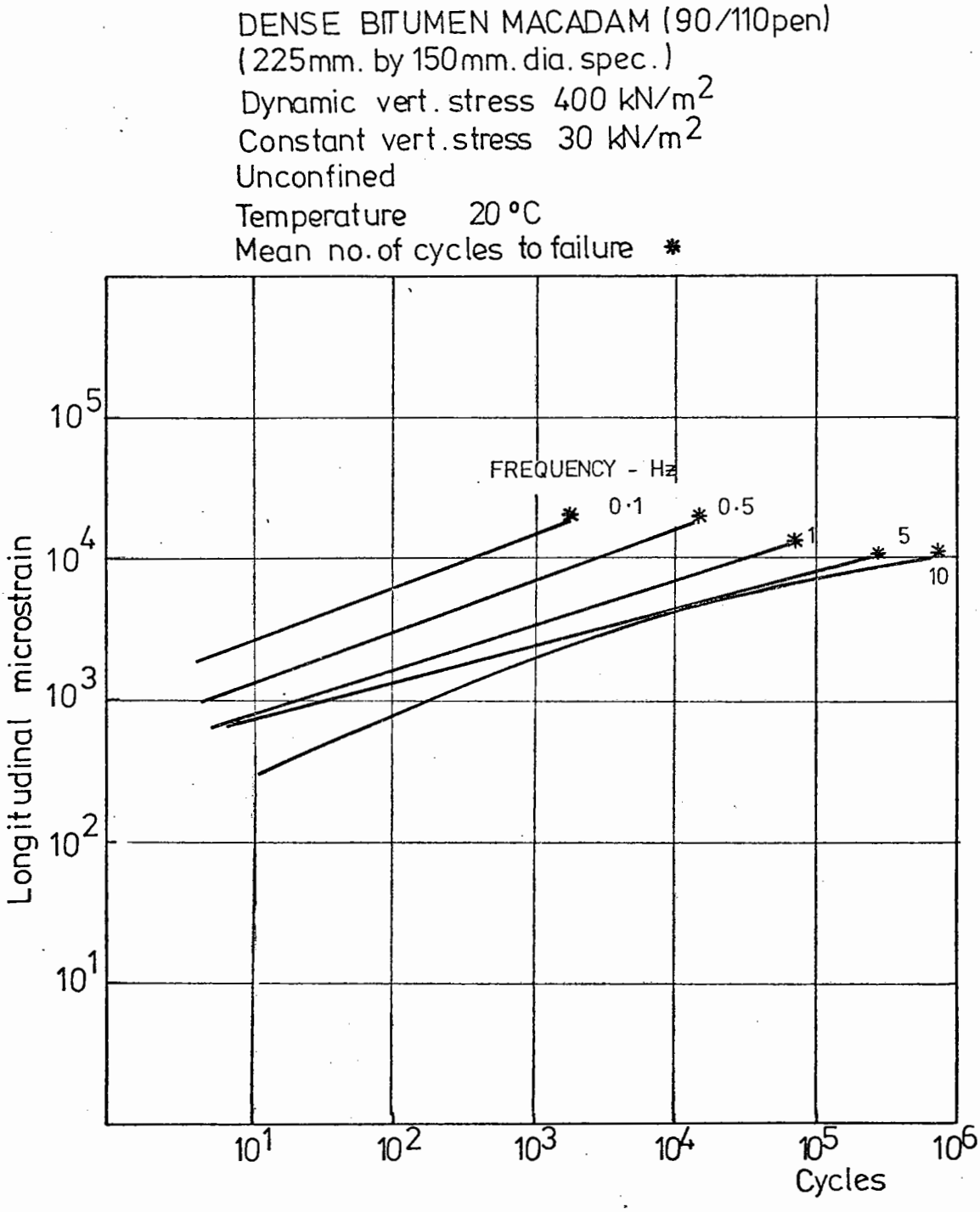

THE INFLUENCE OF THE FREQUENCY OF CYCLING OF THE VERTICAL STRESS PULSE.

Fig. 8.4

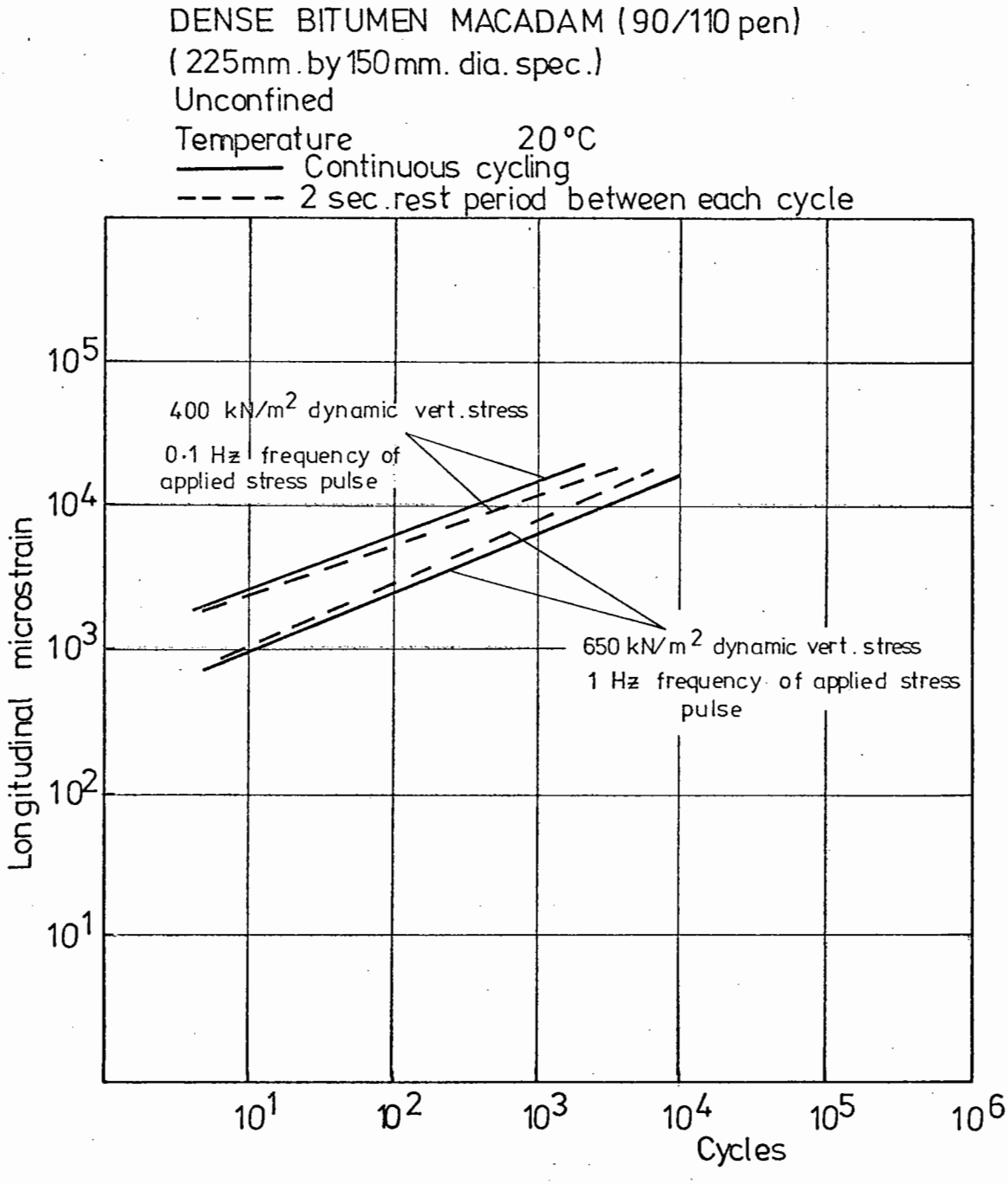

THE INFLUENCE OF REST PERIODS ON PERMANENT LONGITUDINAL STRAIN

Fig. 8.5

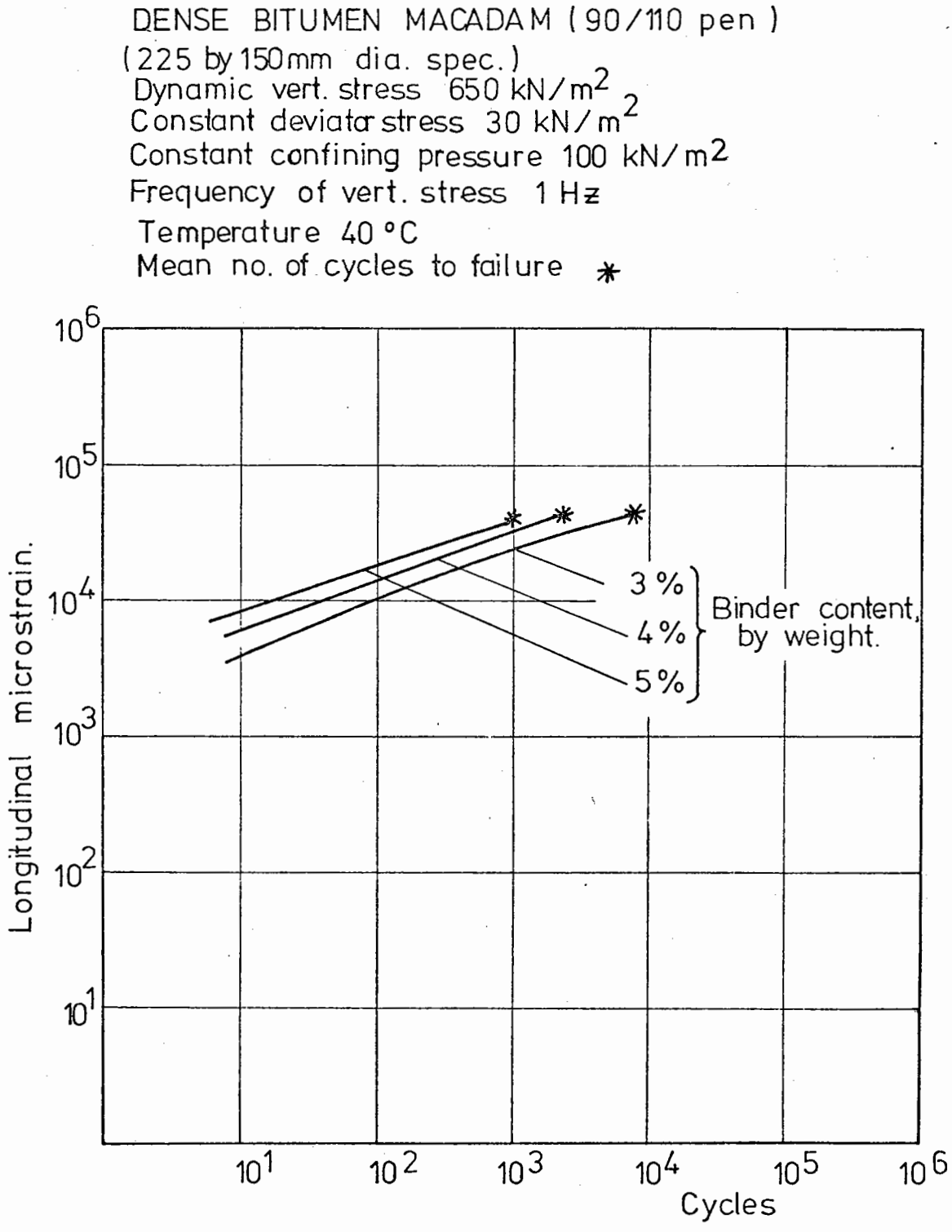

THE INFLUENCE OF BINDER CONTENT ON PERMANENT LONGITUDINAL STRAIN AT HIGH TEMPERATURE WITH A CONFINING STRESS.

Fig. 8.6

DENSE BITUMEN MACADAM (90/110 pen)
(225 mm. by 150 mm. dia. spec.)
Dynamic vert. stress 650 kN/m^2
Constant vert. stress 30 kN/m^2
Frequency of vert. stress pulse 1 Hz
Temperature 20°C

Mean no. of cycles to failure *

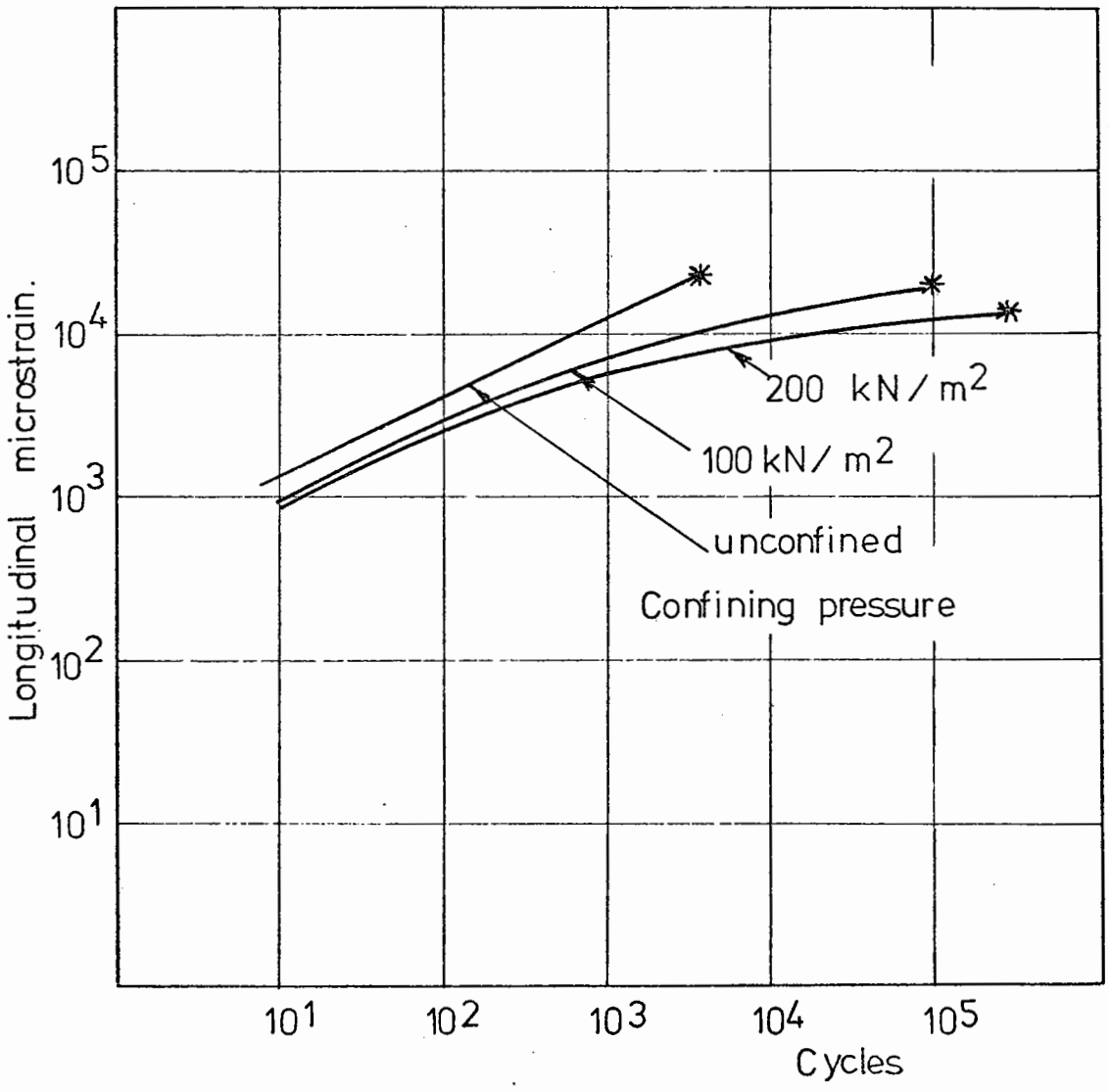

THE INFLUENCE OF CONFINING PRESSURE ON PERMANENT LONGITUDINAL STRAIN.

Fig. 8.7

DENSE BITUMEN MACADAM (90/110 pen)
(225mm by 150 mm dia. spec.)
Dynamic deviator stress 650 kN/m^2
Constant deviator stress 30 kN/m^2
Frequency of deviator stress pulse
1 Hz with 1 sec. rest period
Temperature 20 °C

	Confining pressure kN/m^2 constant	dynamic	Hz frequency
a	0	0	-
b	25	75	0·5
c	25	75	1 & 1 sec. rest
d	100	0	-

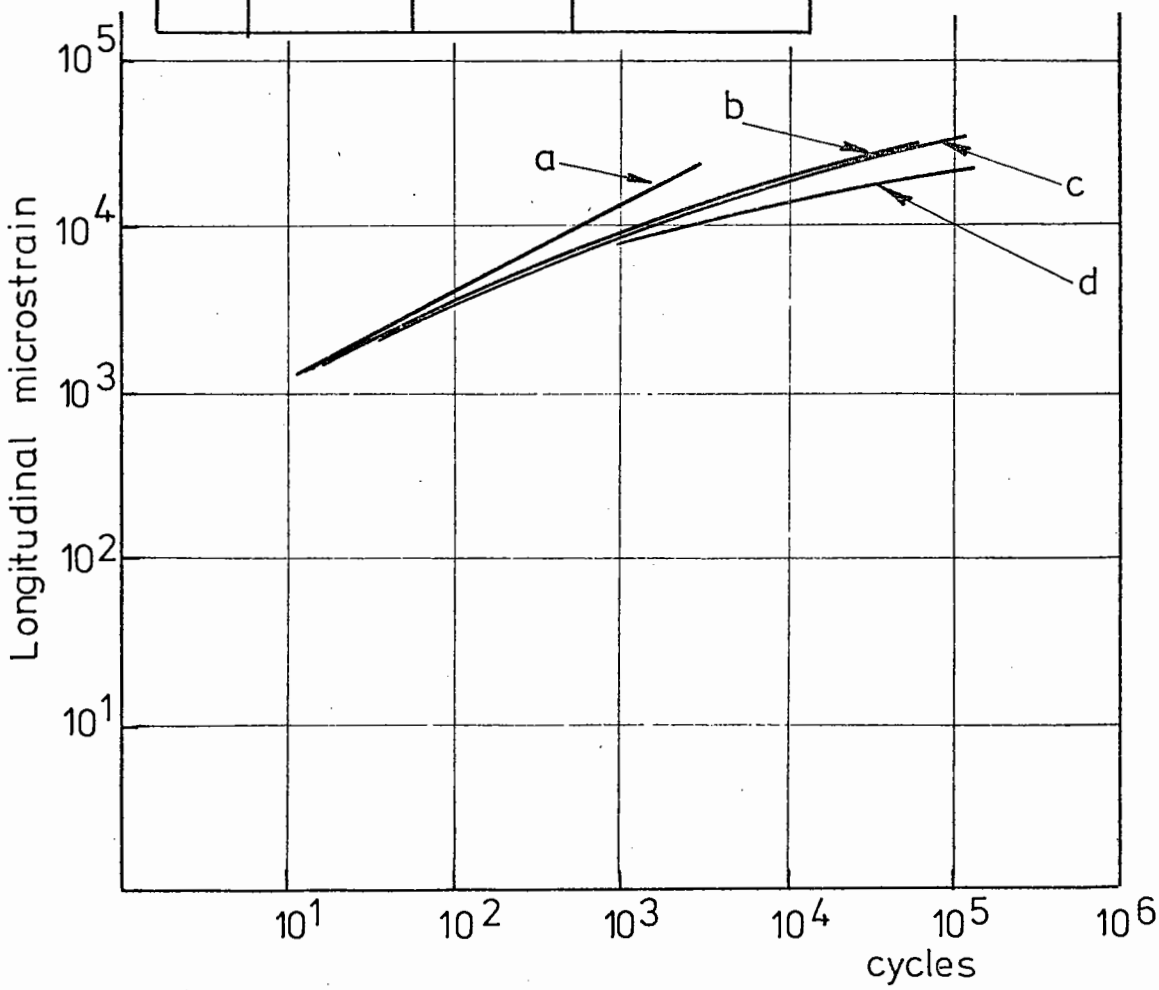

THE INFLUENCE OF THE MODE OF APPLICATION OF CONFINING PRESSURE.

Fig. 8.8

The Effect of the Dynamic Vertical Stress Level

The influence of the magnitude of the vertical stress pulse on the longitudinal permanent strain at any stage in a test may be seen in Fig. 7.5. It is apparent from this figure that, as expected from the work of other investigators (14,56,57), an increase in the stress level accelerates the rate of permanent deformation substantially.

It would simplify the prediction of permanent deformation of the material if it exhibited linear viscoelasticity. The results of the AS programme are shown in Fig. 8.9 plotted to show creep compliance at a fixed number of cycles - the creep compliance is defined as the longitudinal permanent strain divided by the magnitude of the dynamic vertical stress. For linear viscoelasticity the creep compliance must be a constant for the various stresses at a particular number of cycles. It is clear from the figure that this is not so for the range of stresses and cycles illustrated.

The Effect of Temperature

The influence of specimen temperature on the rate of increase in permanent strain may be seen in Fig. 7.6. It is clear from the figure that temperature is a dominant factor in the creep behaviour of the dense bitumen macadam. This is not unexpected as the properties of the bitumen binder are highly sensitive to temperature. It is noticeable that the modest range of temperatures used, of 10^{o} to $30^{o}C$, produced greater changes in the permanent deformation rates than the wide range of dynamic stresses applied.

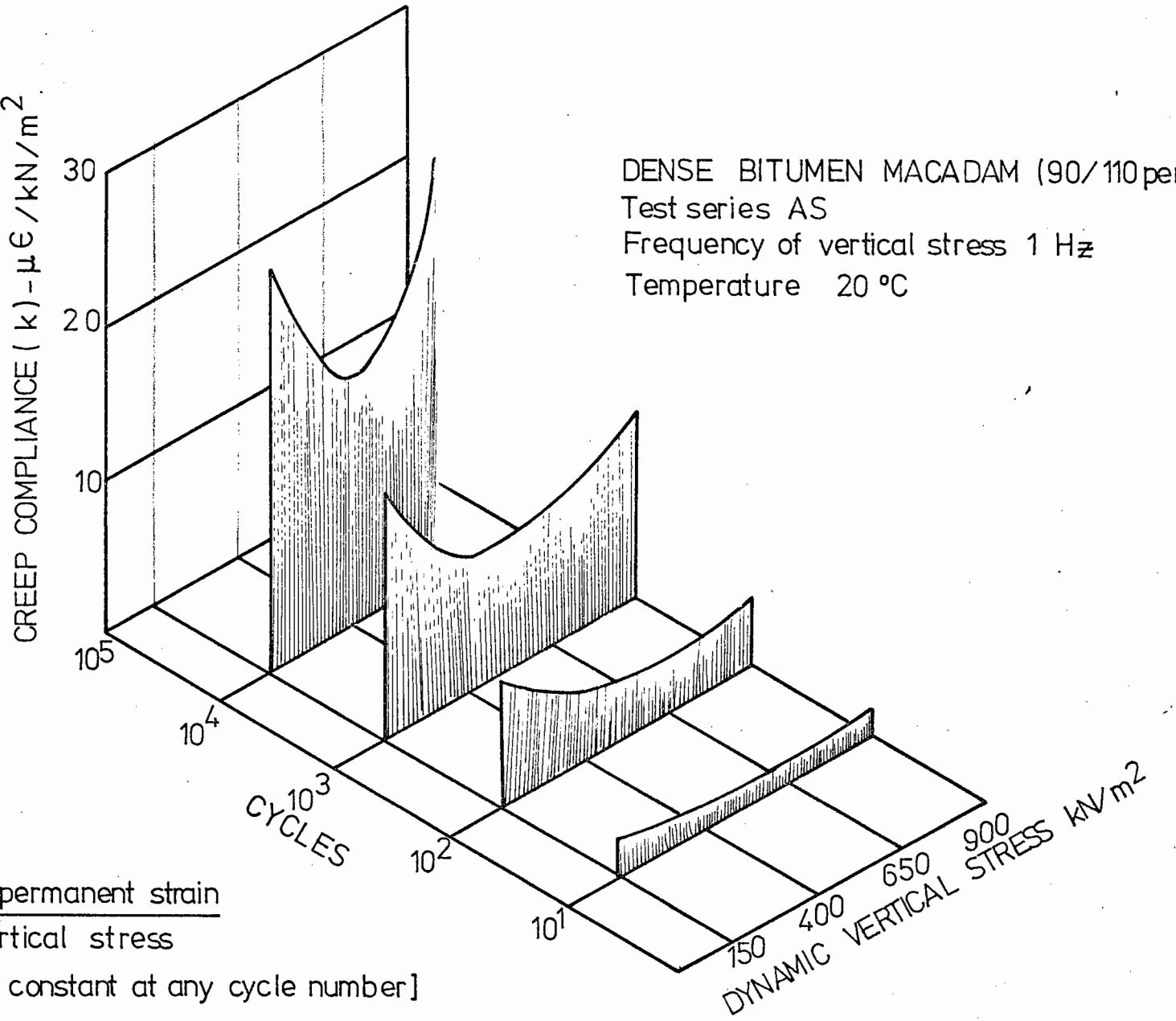

$$k = \frac{\text{Longitudinal permanent strain}}{\text{Dynamic vertical stress}}$$

[For linearity k = constant at any cycle number]

Fig. 8.9

DIAGRAM SHOWING THE NON LINEAR VISCOELASTIC BEHAVIOUR OF DENSE BITUMEN MACADAM UNDER DYNAMIC LOADING.
(CONSIDERED OVER THE RANGE OF STRESSES FOUND IN A PAVEMENT)

The Effect of Confining Pressure

The influence of the confining pressure in programme AS would appear to be negligible from Fig. 7.7. These tests were conducted using air as the confining medium, with the specimen unprotected from the ingress of air. It would be normal for materials with an angle of shearing resistance (φ) to be affected by the confining pressure and Goetz (58) has shown that this parameter does indeed affect flow in bituminous materials. It was therefore thought possible that the confining medium was permeating the specimen and nullifying the effect of this confining pressure. To see if this was the case, a simple test was performed. A specimen was protected against the ingress of the confining medium by a neoprene sheath. 10,000 deviator stress pulses were applied to the specimen with a constant confining pressure of 400 kN/m^2. The test was halted, the confining pressure removed and the test continued. Fig. 8.10 shows the deformation behaviour of the specimen. It may be seen that there was a distinct change in the rate of increase of permanent deformation from the moment the confining pressure was removed, thus demonstrating that confining pressure does have a significant effect on the rate of deformation.

In the light of this, specimens protected from the ingress of the confining medium were subjected to dynamic loading at three different levels of constant confining pressure during programme CS. The log strain versus log cycles relationship in these tests may be seen in Fig. 8.7. The rate of deformation appears to be slowed by relatively

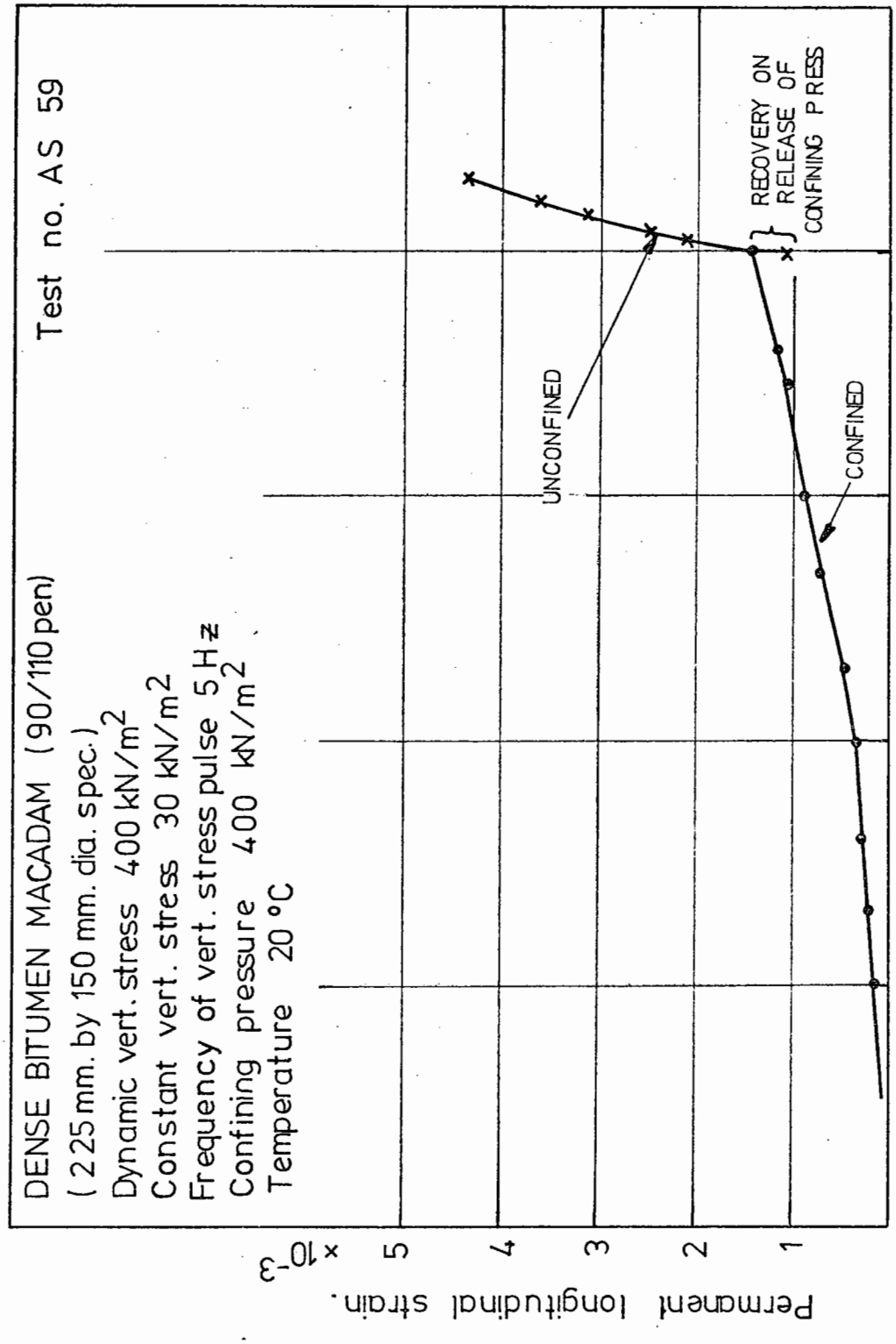

TEST DEMONSTRATING TRUE EFFECT OF A CONFINING PRESSURE.

Fig. 8.10

small confining pressures thus prolonging the life of the specimen. It will be noted that the linear log strain-log cycles relationship observed in the unconfined tests is not present.

As in situ horizontal stresses are transient, the CS programme contained tests to investigate the deformation of specimens subjected to various confining stress regimes. The results are shown in Figs. 7.14 and 8.8. Single dynamic deviator stress pulses were applied at a frequency of 1 Hz with a gap of 1 second between each pulse. The constant confining pressure (curve d) gave the maximum support to the specimen leading to the slowest deformation rate, whilst the unconfined tests (curve a) showed the greatest rates of deformation. The effect of pulsing the confining pressure was to produce a rate of deformation between these two extremes, which is to be expected as the support applied to the specimen is also between the two extremes. The difference between applying the confining pressure as a pulse of the same length as the deviator stress pulse (curve c) or as a longer pulse (curve b) is not significant and therefore this variable could be excluded from future test investigations.

If Figs. 7.13 and 7.14 are compared, it may be seen that the effect of pulsing a 75 kN/m^2 confining pressure on top of a 25 kN/m^2 constant confining pressure is approximately the same as might be expected for a 70 kN/m^2 constant confining pressure, which is a little over the mean level of the pulsed pressure.

The Effect of the Frequency of the Dynamic Vertical Stress Pulse

It is obvious from Fig. 7.8 that the effect of increasing the frequency is to decrease the rate of deformation, which is consistent with the viscoelastic nature of the binder. However, if the results of these tests are plotted on a time basis (Fig. 8.11) rather than against the number of cycles, then the deformation at 20°C is clearly time dependent at frequencies above 1 Hz. If this break in behaviour at this frequency is due to the viscoelastic condition of the binder at 1 Hz, then this state could be repeated at 25°C at a frequency of 5 Hz due to the interchangeability of the time of loading and temperature (59). Tests were, therefore, carried out in programme ES at 1 Hz, 5 Hz, 10 Hz and 15 Hz, at a temperature of 25°C. The deformation, shown as longitudinal strain, is plotted against log cycles in Fig. 7.23 and against log time in Fig. 8.12. It may be seen from the latter that the deformation approaches a time dependent behaviour. Furthermore, there appears to be no evidence of a change in behaviour below 5 Hz and therefore the change noted at 20°C and 1 Hz is attributed to the time of action of the 30 kN/m² constant stress rather than the viscoelastic behaviour of the binder.

The Effect of Rest Periods between Vertical Load Pulses

The results of programme AS appear to show that a rest period of any length between loading pulses is of no beneficial effect (Fig. 7.9). Indeed, rather than a reduced rate of deformation when rest periods were present, the reverse has occurred. Any small beneficial effect due to

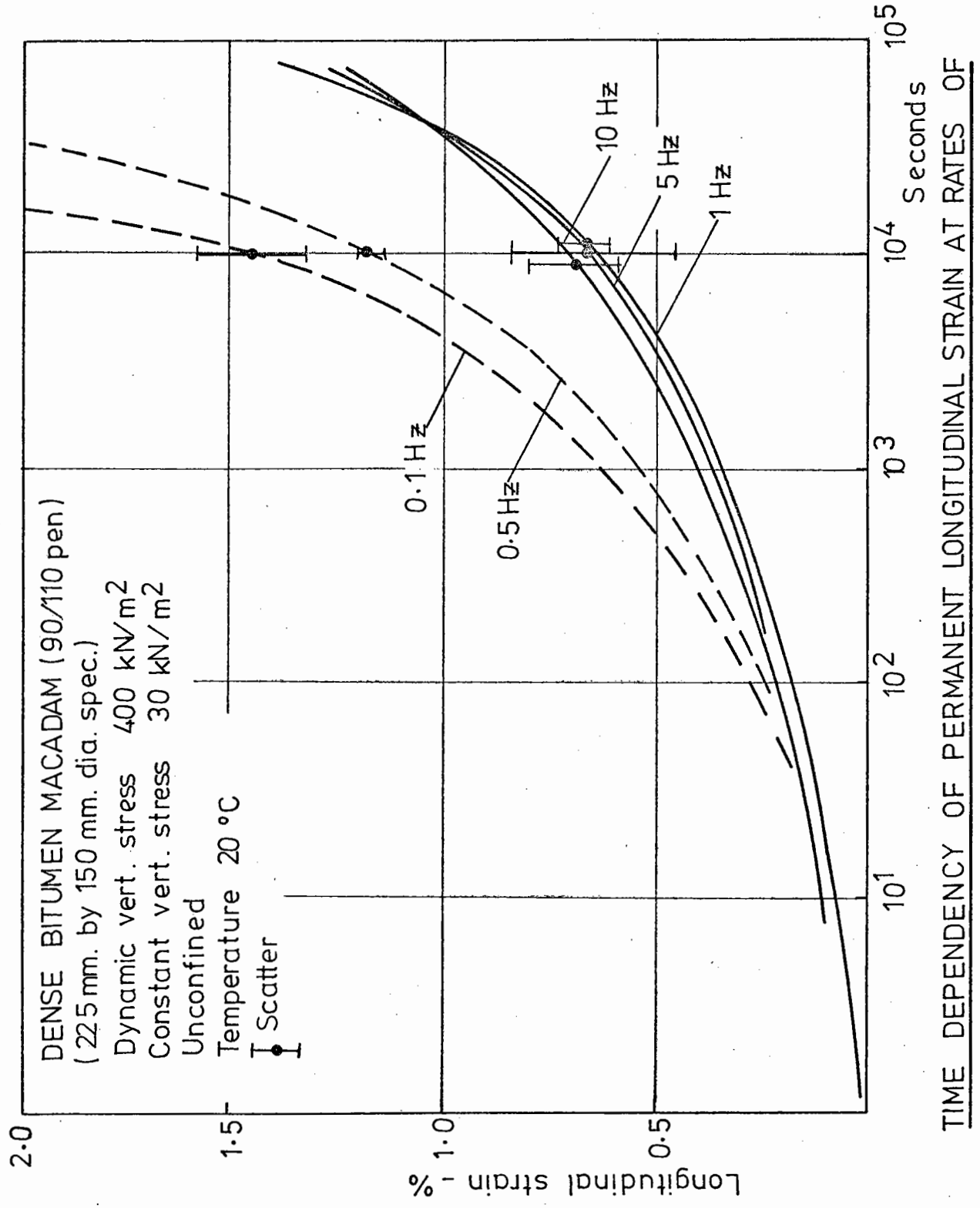

TIME DEPENDENCY OF PERMANENT LONGITUDINAL STRAIN AT RATES OF CYCLING ABOVE 1 Hz

Fig. 8.11

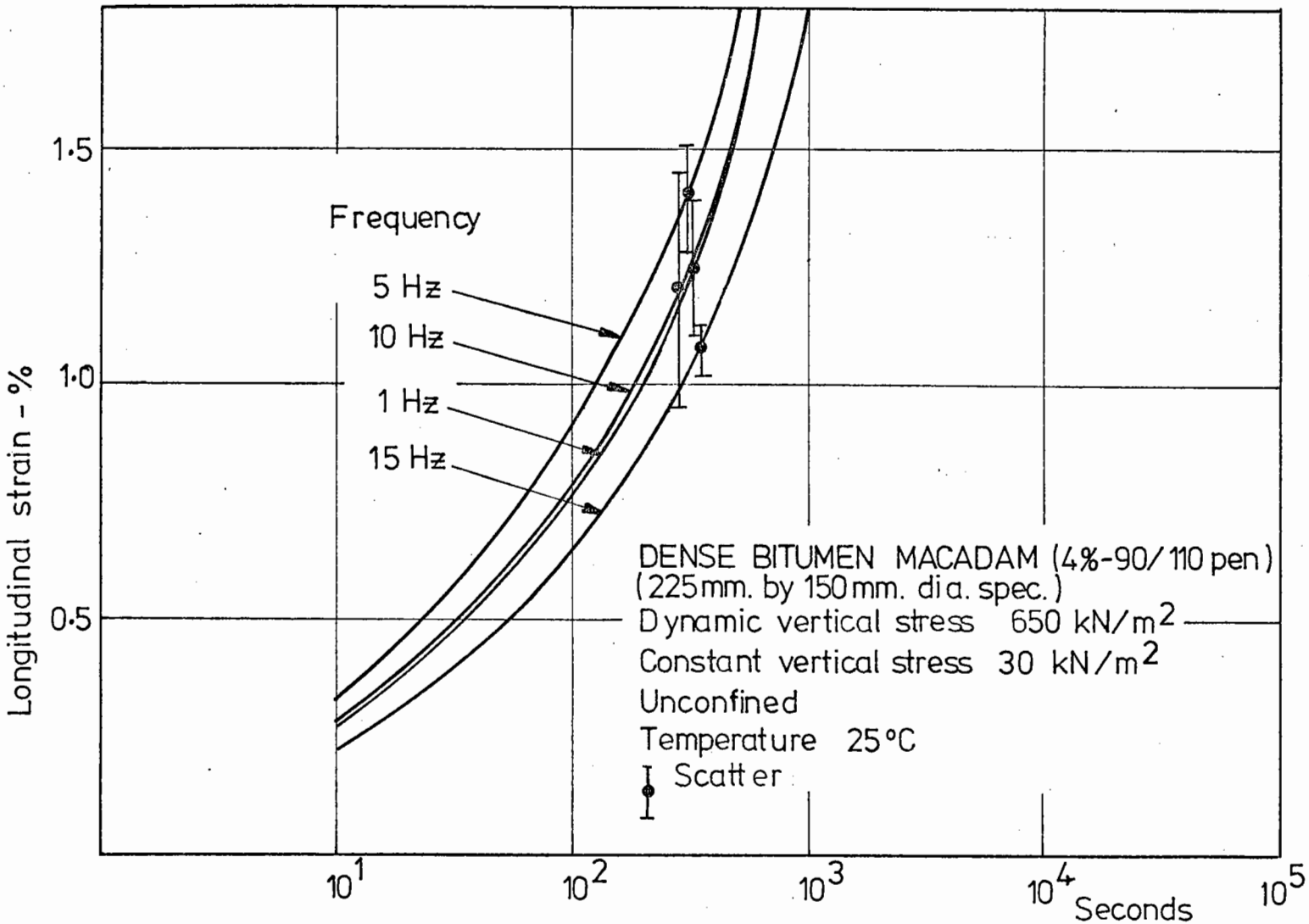

INVESTIGATION INTO THE TIME DEPENDENCY OF PERMANENT LONGITUDINAL STRAIN.

Fig. 8.12

the rest period has been negated by the constant stress of 30 kN/m² acting on the specimen. This is because, as the rest period increases, so also does the time of action of the constant stress between each load pulse, and therefore the rate of deformation increases.

Tests were also performed at a frequency of 0.1 Hz (Fig. 7.10). When a two second rest period was used a small reduction in deformation rate was obtained, which appeared to indicate that there was a small beneficial effect, which was not lost due to the action of the constant stress. If the tests with a two second rest period are considered, the increase of the constant stress loading time per cycle is only 20% at 0.1 Hz whereas at 1 Hz the increase in loading time is 200%.

Programme DS sought to clear this point by testing specimens at a frequency of 1 Hz, with no constant vertical stress. The deformations recorded for the individual tests are shown in Fig. 7.22. It may be seen from this that there is no definite effect due to a rest period between stress pulses, though the top platen weight is bearing onto the specimen and further tests are required to clarify this point.

Effect of Variations in Binder Content

Programme BS investigated the deformation behaviour of dense bitumen macadam with three levels of binder content, under dynamic loading at three different temperatures. The deformation behaviour was presented in Fig. 7.11. It is

obvious from this figure that at 10°, 20° and 30°C, the resistance to deformation of the 4% binder content dense bitumen macadam is greater than that with either 3% or 5% binder content. It is evident that within this temperature range an "optimum" binder content exists for the resistance of the material to permanent deformation. As might be expected, the higher binder content specimens, with greater interaggregate lubrication, have a faster rate of deformation. The low binder content specimens appear to have insufficient binder to hold the specimens together.

The latter part of programme BS sought to test this at 40°C. At this temperature it was realised that rapid failure would occur in an unconfined test. A confining pressure of 100 kN/m² was applied to increase the life of the test specimens. Fig. 8.6 shows that as at lower temperatures, the 4% binder content specimens are more resistant to the acquisition of permanent deformation than the 5% binder content specimens. The deformation rate of the specimens with 3% binder content is, however, slower than the "optimum" 4%. This may be due to the confining pressure mobilising the particle interlock characteristics of the material.

General Discussion of Permanent Deformation Properties

At the present time there is little relevant information available from other sources that can contribute to a better understanding of the permanent deformation behaviour of dense bitumen macadam. It is felt, however, that there is sufficient data from other work that may be related to that

reported in this thesis in the cases of the general form of the creep curve, and the effect of vertical stress level and rest periods on the rate of permanent deformation.

It has been stated that in unconfined tests the rate of deformation declined up to failure. Hofstra and Klomp (12) show a similar behaviour with the results of a test track investigation in which the asphalt vertical strain rate per wheel pass declined steadily throughout the test. Goetz et al (13), when performing similar tests to those reported herein, also found this. Indeed, when the permanent deformation results of their tests were plotted on a log strain versus log cycles basis, they showed that a linear relationship, similar to that observed by the author, existed.

Francken (56), however, has reported, in a preliminary presentation of his work, that there was a stage in a test when the rate of acquisition of deformation was constant. This behaviour was found, by the author, only when a confining pressure was applied and then the rate of deformation did approach a constant value.

It has been shown that the results of this investigation indicate that the permanent deformation behaviour of this material is not of a linear viscoelastic nature. Yet Pagen (47) has shown apparent linear viscoelastic creep behaviour of a bituminous material. However, the test results reported in support of this claim are apparently for small ranges of

applied stress, time and hence permanent deformation. To be a useful concept the linearity must extend over the spectrum of loading variables likely to be found in pavement structures. When this was done for the results of programme AS the behaviour was seen not to be linearly viscoelastic (Fig. 8.9). However, from Fig. 8.9 it may be visualised that if only the early part of the test and a very small range of stresses are considered, then the apparent change in creep compliance at any cycle number would seem to be negligible, indicating erroneously that the material exhibited a linear viscoelastic behaviour. If the results obtained by Chomton and Valayer (14) from dynamic triaxial tests on a bituminous mix at 20°C are analysed to show the creep compliance after 15,000 cycles a non-linear behaviour is again found.

In Section 8.5 it is shown that there does appear to be a connection between fatigue cracking under flexure and the dynamic compression tests reported herein. Hence, use may be made of the conclusions arrived at by investigators observing the fatigue of bituminous materials.

McElvaney (52) has stated that:

"The fatigue process involves the progressive localised permanent structural change of a material subjected to fluctuating stress (strain) amplitudes ..."

and also that:

"The introduction of a rest period between pulses does not, of course, permit the recovery of the permanent damage incurred in the cycle immediately preceding it as this is considered irreversible. However, as it permits strain

recovery it creates the physical conditions whereby the level of damage sustained in the subsequent load pulse is less than that which would occur in continuous loading."

McElvaney's concept of the action of a rest period on the behaviour of a specimen would appear to suit that observed and reported by the author, and is in no way contradicted by the observations of previous research workers.

If suitable conditions are provided, bituminous bonds that have been broken may "heal" with time. These conditions were investigated by Bazin and Saunier (38). After rupturing parallelepipedic specimens in tension, the two parts were put in contact and stood upright. The self weight of one part bearing on the point of rupture meant that a stress of about 2 kN/m^2 was forcing the two broken surfaces together. Specimens were left to heal in this manner for various lengths of time and levels of temperature. These tests indicated that the higher the temperature, the more rapid the healing. It was found that the ruptured surfaces must be held together to obtain any definite effect. Furthermore, the recovery of the tensile strength required a reasonable period of time. For instance, in order to obtain a 90% recovery of the original strength, three days at 25^{o}C was required.

Raithby and Sterling (37) carried out dynamic tension-compression tests on a hot rolled asphalt to determine the effect of a rest period between individual cycles of loading. Between each pulse the specimen was allowed to rest with no external stress applied. Various rest periods were investigated and it was observed that an increase in the fatigue

life of the specimen resulted. They found, however, that:

"Where full strain recovery did not take place (between pulses), the life was still longer than for continuous cycling but not so long as when full recovery occurred."

It would seem, therefore, that to obtain a reasonable increase in life by "healing" in the binder, any residual strain due to a stress pulse must have been dissipated before the next pulse is applied.

McElvaney has described the influence of rest periods on the fatigue life of specimens tested in a rotating-bending fatigue machine (52). A block loading sequence of high stress followed by a period of low stress (approximating a rest period) was applied to specimens. In this form of testing the strain dissipation stipulated by Raithby and Sterling would not have occurred and therefore the small increase in life over similar tests with no rest periods would be in agreement with the findings of Raithby and Sterling (37).

The dynamic loading tests in the servo-hydraulic machine were all in compression. Section 8.5 shows that specimens underwent a radial dilation under compression loading. Furthermore, this led to longitudinal tension cracks at the surface that were visible at failure (Figure 3.8). This meant that ruptured surfaces were at no time forced into contact to promote "healing". Hence, even with rest periods between stress pulses, favourable conditions for strain recovery, or "healing", in the binder were not present and therefore an increased resistance to deformation was not

expected. It may be concluded therefore, that when considering the behaviour of bituminous materials in dynamic compression triaxial tests, rest periods do not have any significant effect.

8.4 DYNAMIC TESTING PROGRAMME - RESILIENT PROPERTIES

Observed Behaviour of Resilient Modulus during a Test

Fig. 6.3 illustrates the typical variation of resilient modulus during a test. There is a slight increase in modulus at the start, which is attributed to an initial compaction of the specimen. Apart from this, the decline in modulus is similar to that shown by Hanson (25), McElvaney (52) and Raithby and Sterling (37). Because of the compression mode of testing, the steep drop in modulus, just prior to failure, reported by McElvaney (52) and Raithby and Sterling (37), was not observed.

Figs. 7.15 and 7.16 show the variations in resilient modulus observed in programme AS for changes in dynamic vertical stress magnitude, temperature, frequency of loading and length of rest period between individual load pulses. As stated in Chapter 6 the individual test results are plotted on these figures and it may be seen that there is little scatter in the results.

The Effect of the Dynamic Vertical Stress Level

The results shown in Fig. 7.15b imply that the material response is linear elastic as the resilient modulus is practically

independent of the magnitude of the applied dynamic stress level for the specified loading conditions. The Poisson's ratio also appears, within the ranges tested, to be independent of the dynamic vertical stress (Fig. 7.19).

The Effect of Temperature

As with the permanent deformation behaviour, temperature is the most critical loading variable. The decrease in modulus with increasing temperature shown in Fig. 7.15a is considerably larger than any change in modulus caused by any of the other loading variables. With Poisson's ratio also, temperature has a considerable effect. Figs. 7.19 and 7.20 indicate that there is a marked increase in Poisson's ratio with temperature throughout the range of loading conditions and variations of binder content used in the manufacture of the specimens.

The Effect of Confining Pressure

Earlier in this chapter it was stated that the dense bitumen macadam under investigation did exhibit an angle of shearing resistance, which would indicate that there is a dependence of the resilient modulus on the level of confining pressure. The results of programme CS tests presented in Fig. 7.18 support this view. The rise in modulus with increasing confining pressure is not great but the trend is none the less apparent. The effect of confining pressure on the Poisson's ratio is the reverse as may be seen in Fig. 7.21, i.e. an increase in confining pressure leads to a considerable reduction in the ratio.

The Effect of the Frequency of the Dynamic Vertical Stress Pulse

The results of the programme AS investigation into the frequency effect on the deformation properties of dense bitumen macadam are seen in Fig. 7.16a. The results show that the modulus is highly dependent on the frequency, with increasing frequency resulting in an increase of the resilient modulus.

Poisson's ratio is seen, in Fig. 7.19, to become practically independent ofthe frequency above 1 Hz.

The Effect of Rest Periods between Vertical Load Pulses

The effect of a rest period between successive load pulses on resilient modulus is shown in Fig. 7.16b. There is a reduction in modulus for rest periods of up to two seconds, but longer rest periods do not produce a very significant further decrease. The decrease is due to the definition of resilient strain used for resilient modulus determination (Chapter 2).

Table 7.3 shows the values of Poisson's ratio obtained under the standard set of loading conditions with varying lengths of rest period between the stress pulses. It may be seen from this that the values of the ratio obtained by varying from no rest period to an 8 second rest period are contained within a 0.05 scatter and therefore Poisson's ratio may be considered as constant for varying lengths of rest period.

The Effect of Variations in Binder Content

The effect on the resilient modulus of various binder contents and temperatures may be seen in Fig. 7.17. It was reported in Section 8.3 that the "optimum" binder content for resisting permanent deformation was 4% at 10°, 20° and 30°C. It was therefore not surprising that specimens with 4% binder content gave higher resilient moduli than specimens with 3% or 5% binder content at these same temperatures. It should be noted that the confined tests at 40°C of programme BS, did not show the 4% binder content to be an optimum. Rather the resilient modulus increased with decreasing binder content (Table 7.4) as did the resistance to permanent deformation (Section 8.3).

The behaviour trends of Poisson's ratio with binder content, at different temperatures, shown in Fig. 7.20, may be seen to be inconclusive.

General Discussion of Resilient Properties

On Figs. 7.15 to 7.17 the values of stiffness, derived from what is generally known as Van der Poel's nomograph are given. Van der Poel (60) showed that the stiffness of a particular bitumen could be described by one variable that was a function of the loading time, Penetration Index (P.I.) and the difference of the temperature of the bitumen from its Ring and Ball temperature. From this work he produced a nomograph. From this, using only two standard measurements, the Ring and Ball temperature and the P.I., it is possible to determine the stiffness of a bitumen for various conditions

of temperature and frequency (or time) of loading, to within a factor of two. He extended this work (61) to dense graded bitumen-aggregate mixtures and showed that the stiffness of the mix could be related to the stiffness of the bitumen through the volume concentration of the aggregate (C_v) where:

$$C_v = \frac{\text{Volume of compacted aggregate}}{\text{Volume of aggregate and bitumen}}$$

Van der Poel's relationship has been extended by Heukelom and Klomp (62) to give the following expression for mixture stiffness:

$$S_{mixture} = S_{bitumen} \left[1 + \frac{2.5}{n} \times \frac{C_v}{1-C_v}\right]^n$$

where $n = 0.83 \log\left(\frac{4 \times 10^4}{S_{bitumen}}\right)$

and $S_{bitumen}$ is the nomograph stiffness of the bitumen in MN/m^2.

More recently, Van Draat and Sommer (63) have proposed a correction to C_v for mixes having greater than 3% void content:

$$C_v' = C_v / [1 + (V_v - 0.03)]$$

where V_v = volume concentration of voids.

The values of "nomograph stiffness" calculated by the author for the dense bitumen macadam used in this investigation were worked out using the bitumen properties stated in Section 4.6, and were corrected in the manner suggested above.

In general, the nomograph stiffnesses shown are in reasonable agreement with those measured. Fig. 7.17 shows that the value of the optimum binder content obtained from

the dynamic tests could have been predicted from the nomograph. It may therefore be unnecessary to test specimens at all to obtain the resilient properties if a batch is made so that the void content may be obtained to give the appropriate correction factors. The nomograph value will be a reasonable assessment both of the resilient modulus and the "optimum" binder content for a particular material.

Unlike the results from the plastic behaviour investigation, there is sufficient data from other dynamic investigations of resilient behaviour to allow comparison with these reported herein.

Fig. 8.13 shows the author's values of initial resilient modulus against dynamic vertical stress with those obtained by Pagen (57) and Cragg and Pell (26). The three sets of results all show the same order of magnitude for the resilient modulus. Furthermore, neither Pagen nor Cragg and Pell show any marked deviation from the linear elastic behaviour shown by the author.

The decrease of the modulus with increasing temperature has been widely reported by other investigators. Fig. 8.14 shows the author's results together with those of Kallas (64) and Cragg and Pell (26), whose results show similar magnitudes and trends to the author's. Research data on Poisson's ratio from other sources is not as readily available, but the effect of temperature has been investigated by Monismith

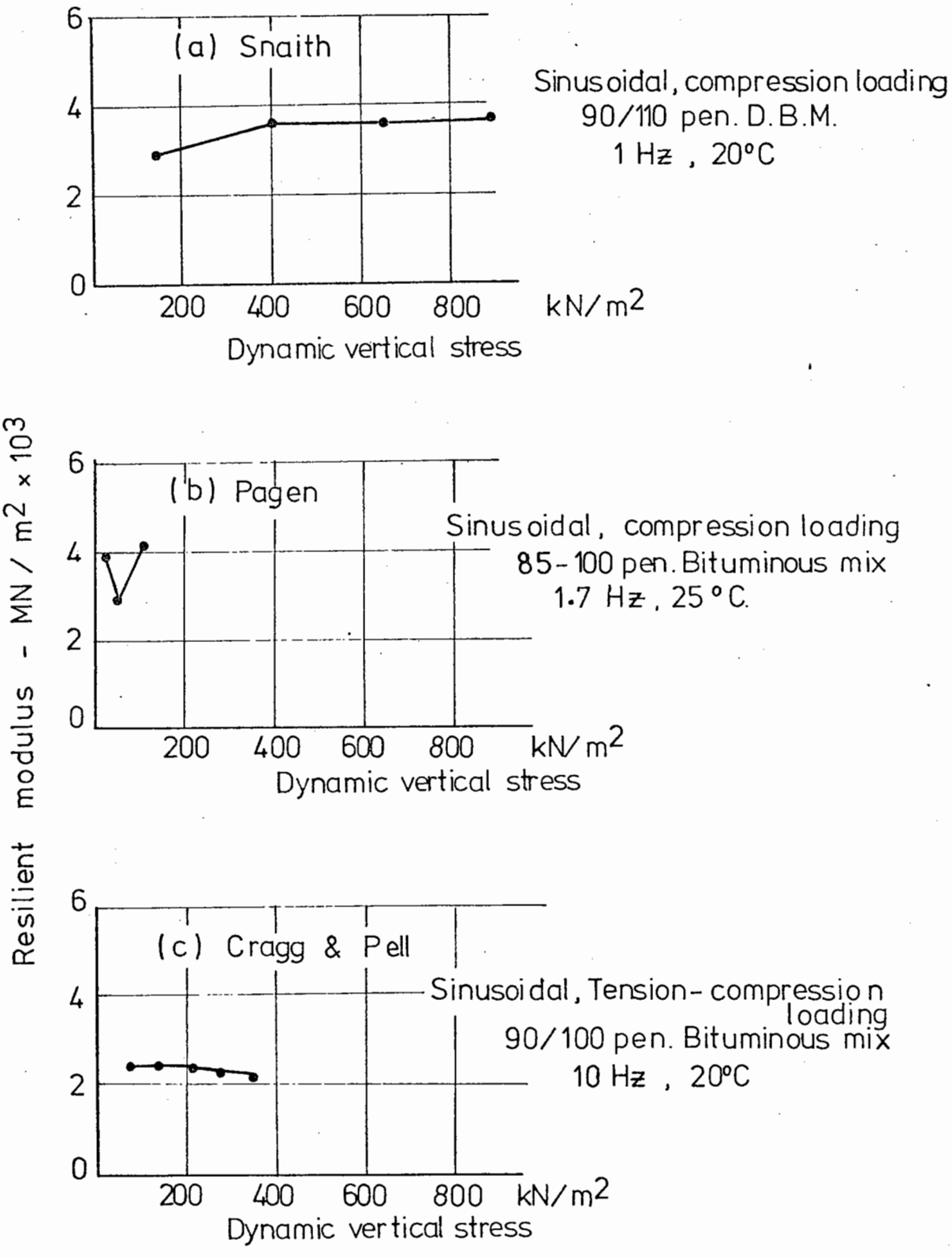

COMPARISON OF RESILIENT MODULI OBTAINED AS A FUNCTION OF APPLIED VERTICAL STRESS.

Fig. 8.13

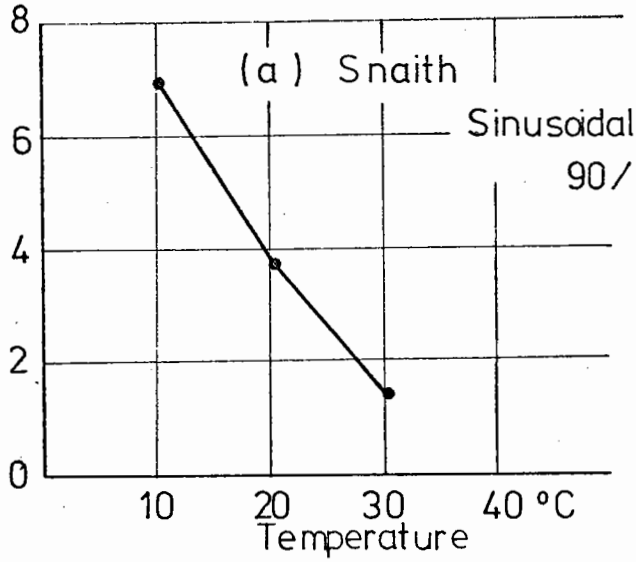

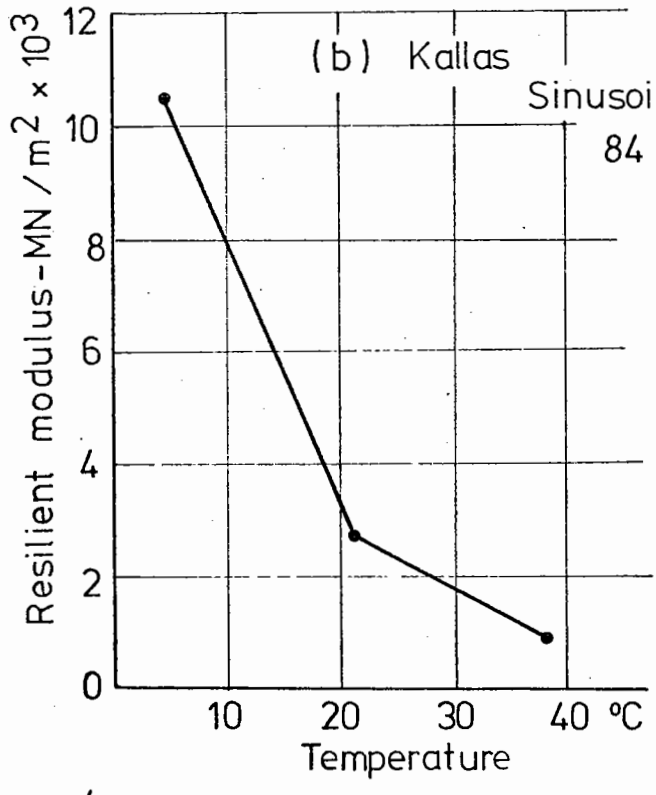

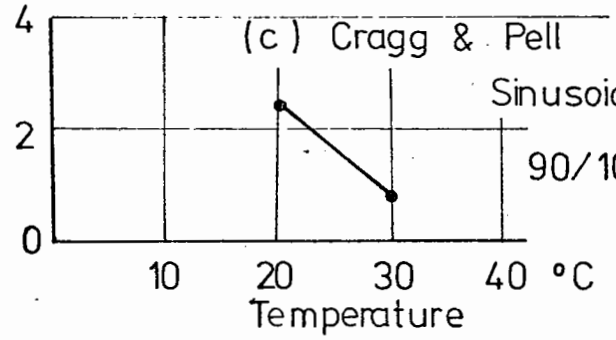

COMPARISON OF RESILIENT MODULI OBTAINED AS A FUNCTION OF TEMPERATURE.

Fig. 8.14

and Secor (65), Fossberg et al (66) and Cragg and Pell (26). The results of the latter two investigations are shown together with the author's in Fig. 8.15. Although the absolute values from the three investigations are different, the increase in the ratio for a given temperature rise is similar.

The influence of a constant confining pressure on the resilient modulus has not been extensively investigated elsewhere due to the lack of suitable equipment. However, the results of programme CS may be seen plotted together with those of Terrel (67) and Awad (30) for comparison in Fig. 8.16. Terrel's results would appear to be very close to the author's. In the cases shown, an increase in the confining pressure has led to a small increase in the resilient modulus. This increase, however, is small enough to allow a constant value of resilient modulus to be used for varying horizontal stresses in the elastic analysis of proposed road pavements. Indeed, the author would agree with Root et al (31) who have stated that:

"The resilient modulus is generally independent of vertical and lateral stresses on the specimen."

The effect of frequency as seen in the results of programme AS was similar to that obtained, under comparable conditions, by Kallas (64) and Sayegh (68). Similarly, the appearance of an "optimum" level of binder content observed in programme BS and predictable from Van der Poel's nomograph, was observed by other investigators (30,64, Fig. 8.17).

From the discussion in this section of the resilient

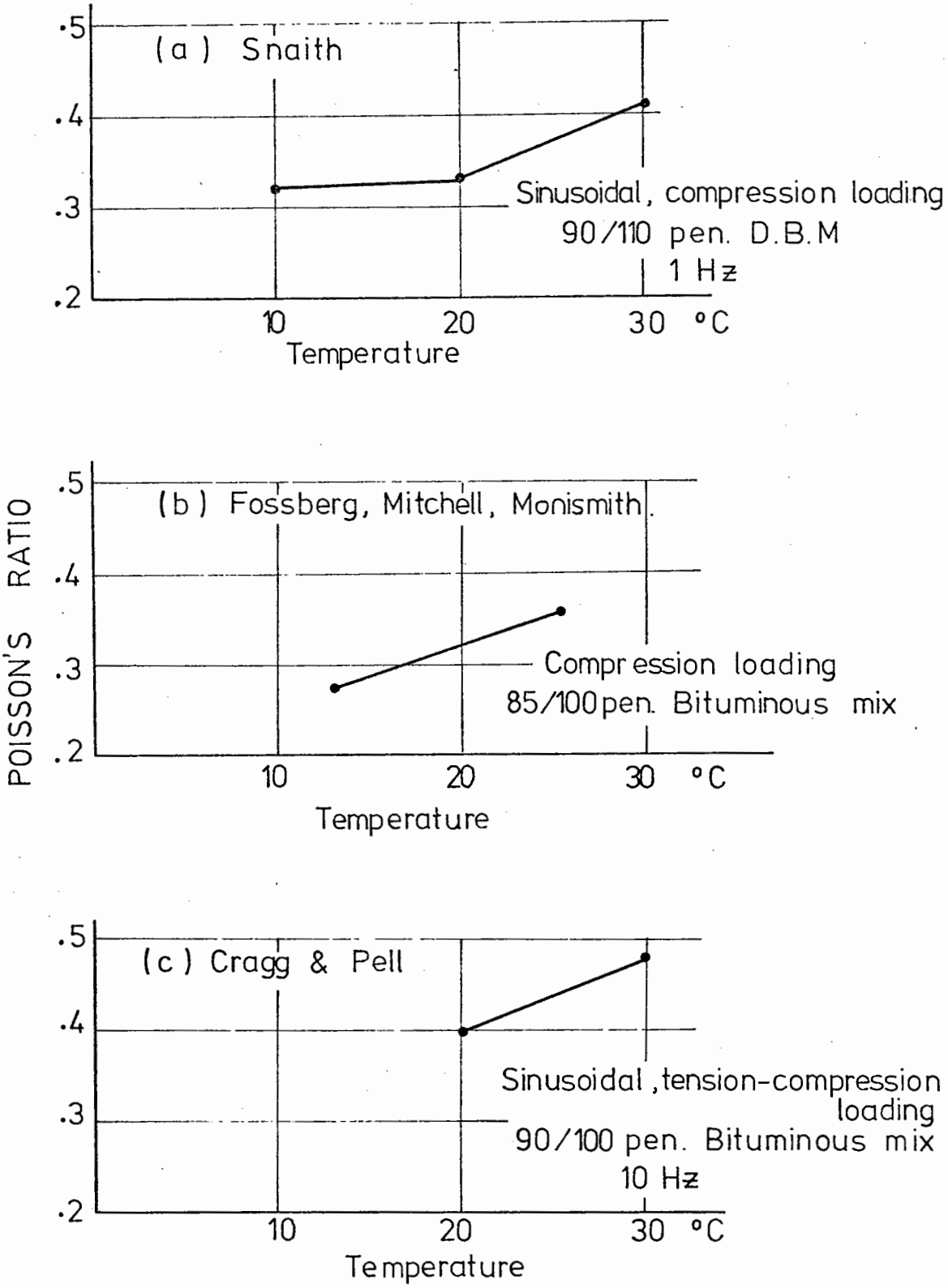

COMPARISON OF POISSON'S RATIO OBTAINED AS A FUNCTION OF TEMPERATURE.

Fig. 8.15

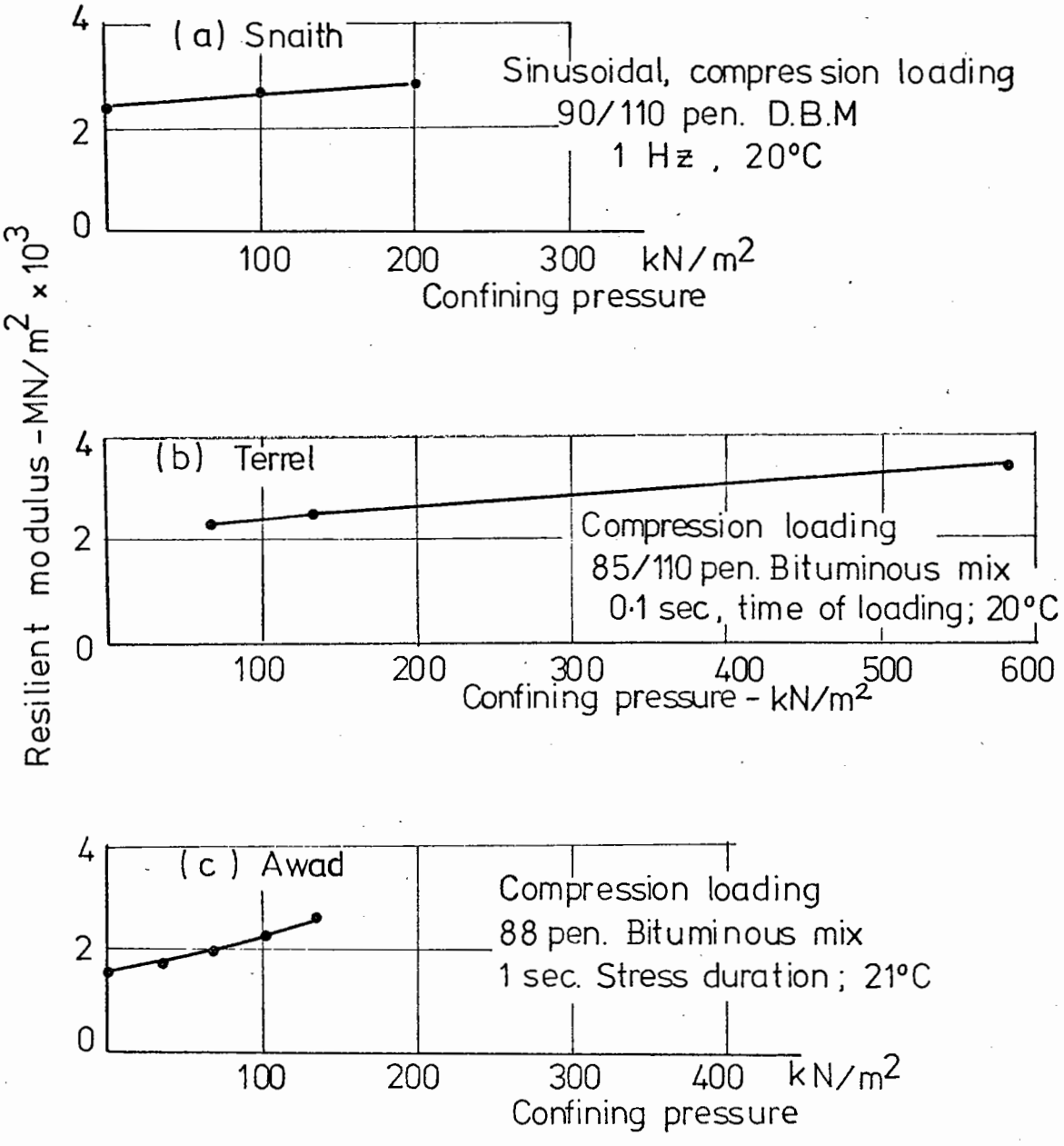

COMPARISON OF RESILIENT MODULI OBTAINED AS A FUNCTION OF A CONSTANT CONFINING PRESSURE.

Fig. 8.16

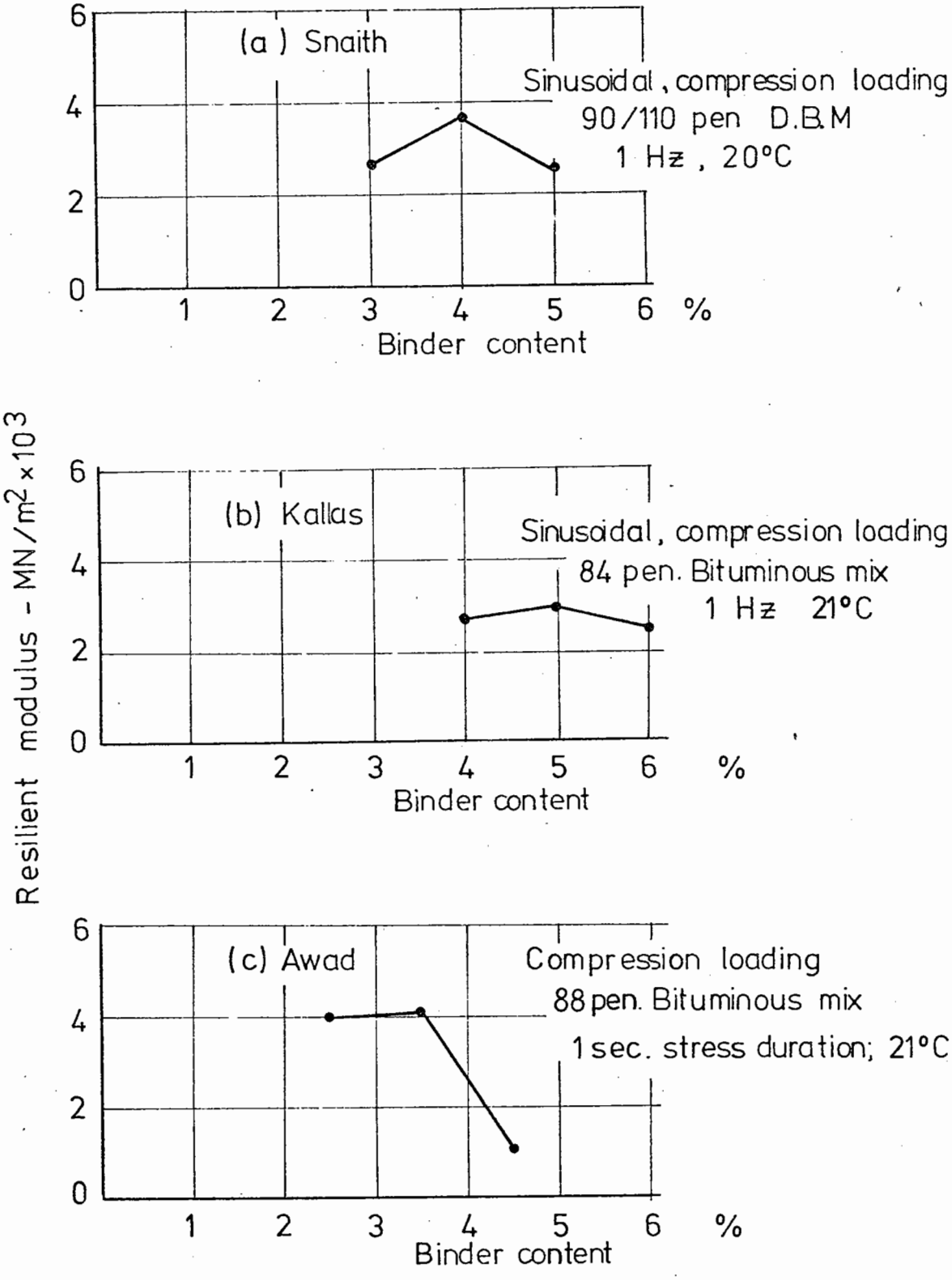

COMPARISON OF RESILIENT MODULI OBTAINED AS A FUNCTION OF BINDER CONTENT.

Fig. 8.17

properties of bituminous materials it may be seen that the results of this investigation were in good agreement with those of other investigators where corroboration was available. It may be concluded, therefore, that the dynamic triaxial test is well able to obtain the resilient parameters of modulus and Poisson's ratio required for the elastic analysis of flexible pavement systems.

8.5 DYNAMIC TESTING PROGRAMME - OBSERVATIONS OF SPECIMEN FAILURE

In this investigation, specimen failure has been defined in terms of the rate of increase in the longitudinal permanent deformation (Section 6.3). The visual appearance of a specimen at failure is shown in Fig. 3.8. Longitudinal cracks are visible on the surface. Similar cracks were observed to exist at failure both by Heukelom (69) and Barksdale (70). This cracking, which occurs in the mortar, is perhaps better seen in Fig. 8.18, where the end of a failed specimen is shown. (The discolouration at the centre is due to silicone grease contamination.) Fig. 3.8 gives little evidence of bulging and the sectioned view of a failed specimen indicates that dilation has occurred. A typical plot of the plastic strain ratio is given in Fig. 8.19. It is evident from this also that dilation has occurred since the plastic strain ratio has exceeded 0.5 at an early stage of the specimen's life.

When the results from programmeAS were plotted to show permanent longitudinal strain at failure against the number

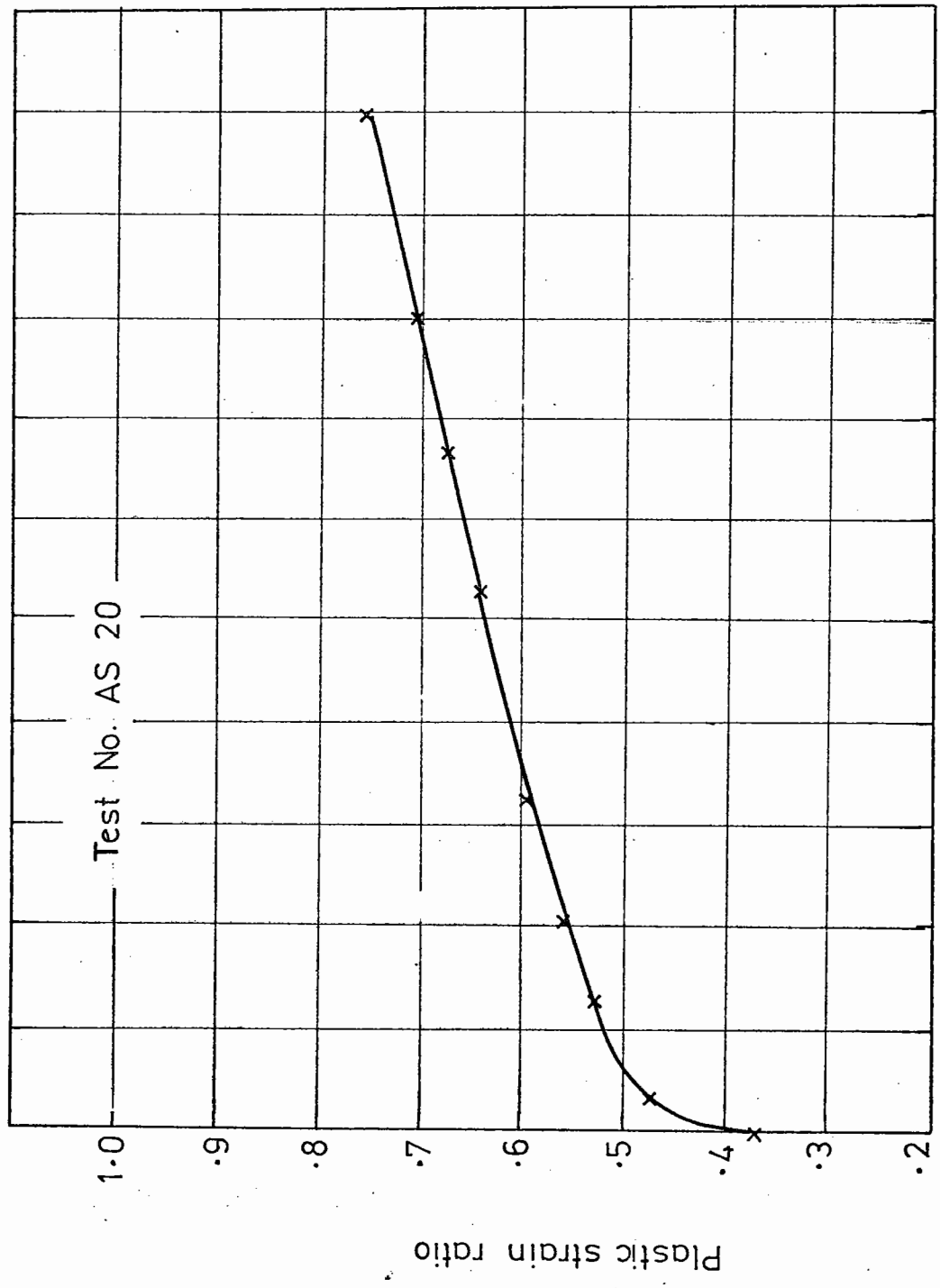

TYPICAL PLASTIC STRAIN RATIO BEHAVIOUR THROUGH A TEST.

Fig. 8.19

of cycles to failure (Fig. 8.20) a trend of decreasing strain with increasing cycles was seen. This indicated that the ability of the specimen to deform plastically to failure was dependent on the number of cycles of load applied, which indicated that damage to the material was occurring similar to that in fatigue tests.

Saal and Pell (71) have stated that the dominant factor affecting the fatigue life of a particular bitumen aggregate mixture is strain. As it appeared that the author's dynamic tests were also a fatigue type of test, the results of all tests in programmes AS and BS were plotted in a similar manner to Saal and Pell in Fig. 8.21. The initial hoop tensile elastic strain is the resilient hoop strain of the specimen (which is numerically equal to the radial strain).

It may be seen from the figure that not only is the specimen life apparently independent of temperature, magnitude of load and frequency as found by Saal and Pell (71), but also of the binder content. The fatigue line from tests on a similar mix, reported by Cooper and Pell (72), is shown in the figure for comparison. Although the test conditions are not directly comparable it would seem that there is a prima facie connection between fatigue cracking under flexure and the tests reported herein.

8.6 STATIC TESTING PROGRAMME - DISCUSSION OF RESULTS

Figs. 7.24 and 7.25 show the longitudinal permanent deformation (creep) behaviour of the specimens tested under constant stress conditions. A linear log strain against

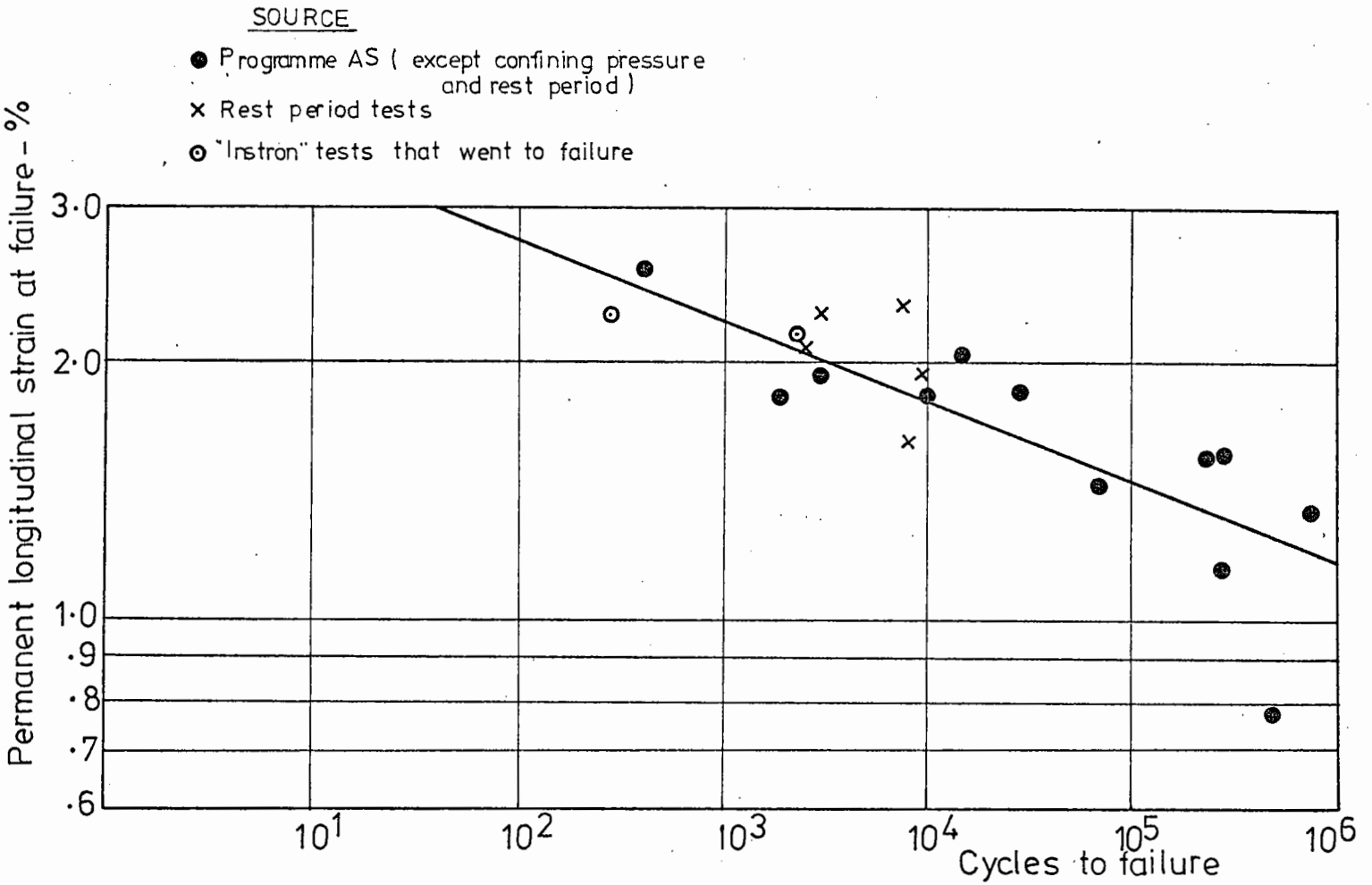

RELATIONSHIP OF LONGITUDINAL PERMANENT STRAIN AT FAILURE TO THE NUMBER OF CYCLES TO FAILURE.

Fig. 8.20

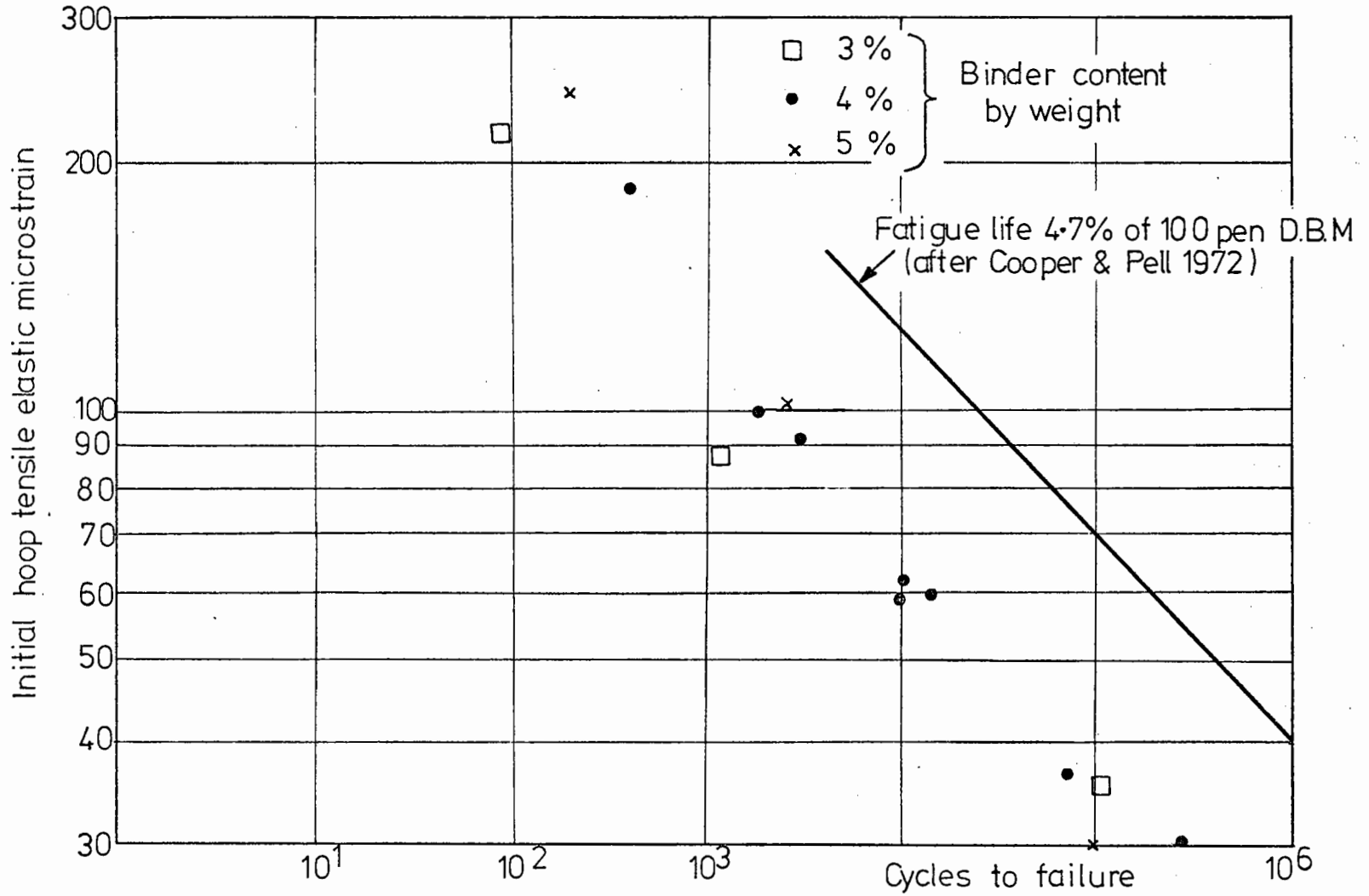

RELATIONSHIP OF INITIAL RADIAL TENSILE ELASTIC MICROSTRAIN TO THE NO. OF CYCLES TO FAILURE

(All tests plotted of series AS and BS except those with confining pressure and rest periods)

Fig. 8.21

log time relationship was observed as may be seen in Figs. 8.22 and 8.23. Correction to the readings to obtain these plots was performed as described in Section 8.3. For these tests it was found that the correction factor ε_o in the relationship:

$$\log(\varepsilon_t - \varepsilon_o) = n \log t + \text{constant} \qquad 8.3$$

was equal to the creep induced in the specimens due to the weight of the loading yoke.

It is noticeable that although the dynamic and static longitudinal permanent deformation plots have the same form, the effect of the magnitude of the load is different. In Section 8.3 it was shown that the permanent deformation behaviour of the specimens subjected to dynamic loading was not linearly viscoelastic (Fig. 8.9). In view of the observed difference in behaviour of the specimens under static and dynamic loading a plot was made to investigate the viscoelastic behaviour of the specimens in the constant stress testing machine. Fig. 8.24 shows that, whilst the material behaviour is not linear viscoelastic, the material does appear to behave in a manner which indicates that the errors induced by an assumption of linearity would not be great for static tests.

It is unfortunate that the time to failure was not obtained from these tests. This was due to the method of specimen loading with a loading yoke acted on by a lever system. If the specimen showed any tendency to buckle, there was no correcting force. Indeed, as the point of loading

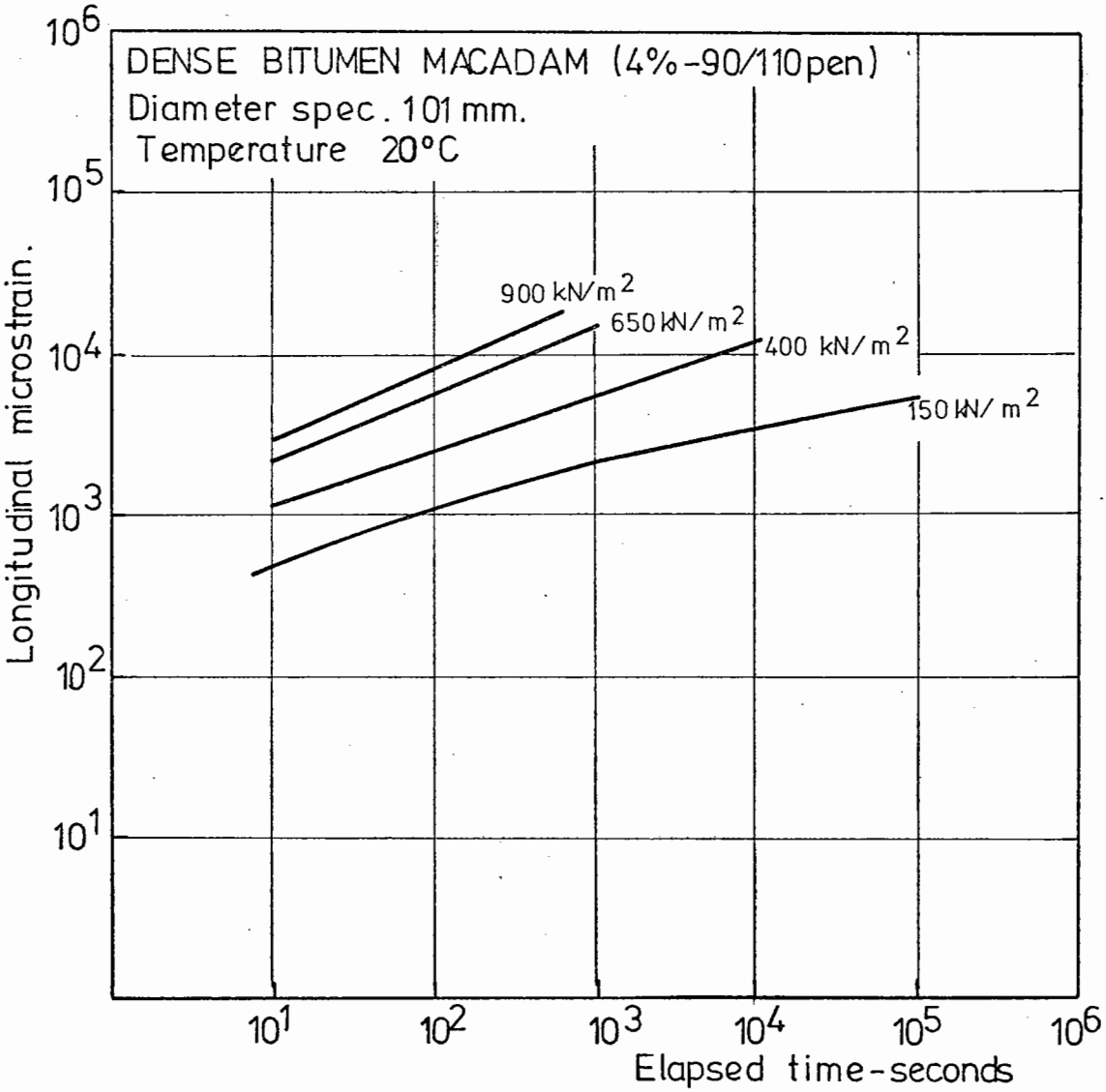

CONSTANT STRESS TESTS ON DENSE BITUMEN MACADAM

(EFFECT OF STRESS LEVEL)

Fig. 8.22

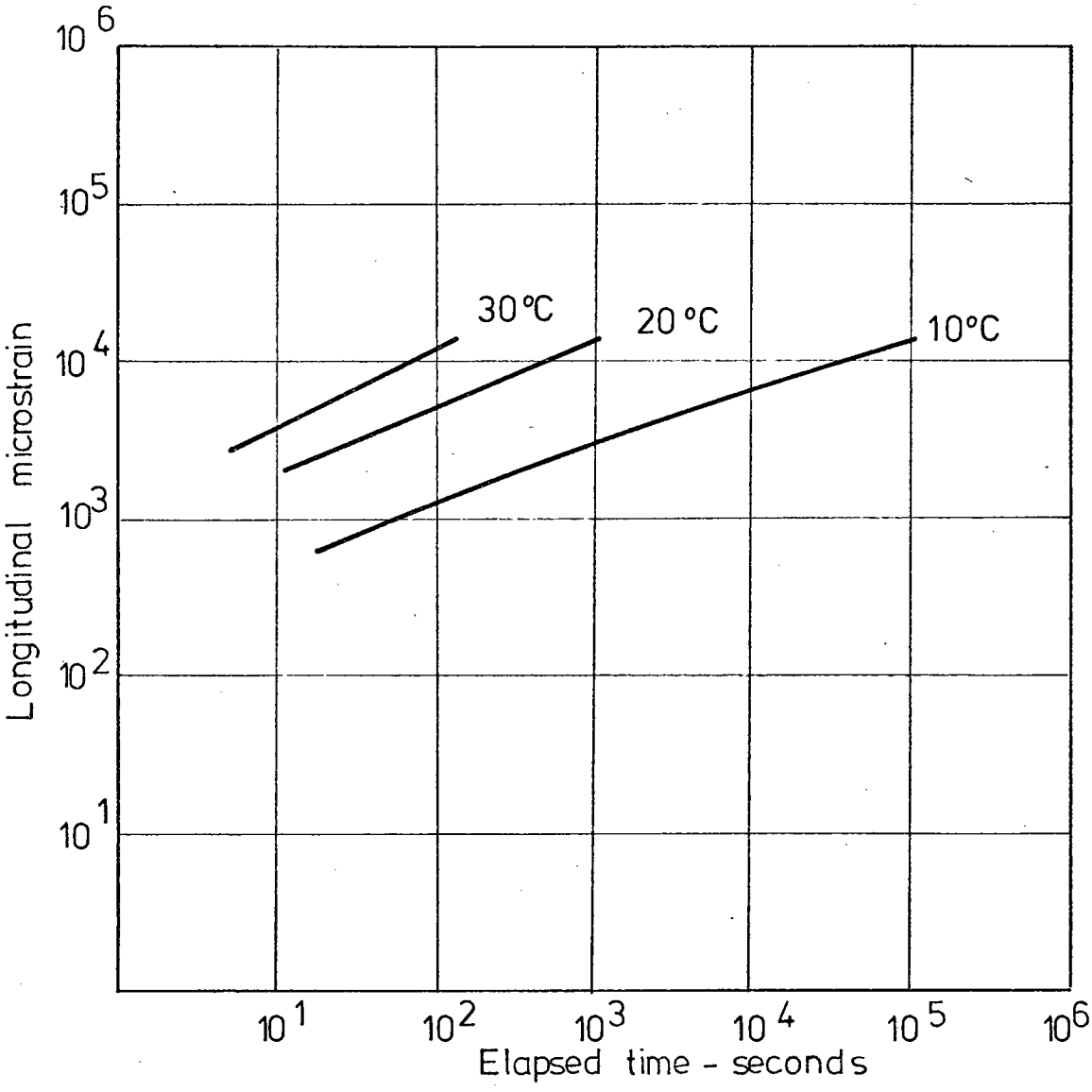

CONSTANT STRESS TESTS ON DENSE BITUMEN MACADAM.
(EFFECT OF TEMPERATURE)

Fig. 8.23

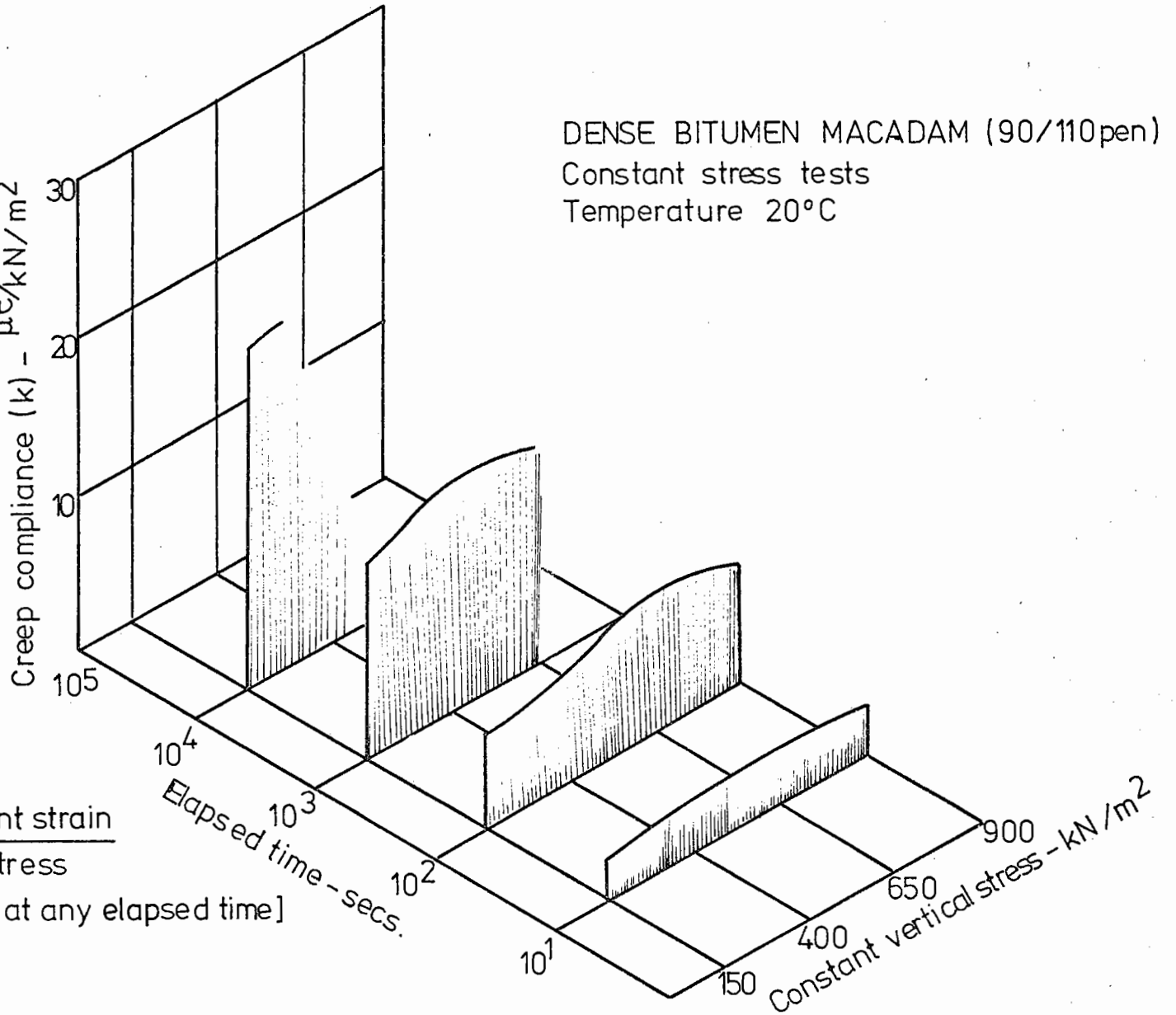

$$k = \frac{\text{Longitudinal permanent strain}}{\text{Dynamic vertical stress}}$$

[For linearity k = constant at any elapsed time]

DIAGRAM SHOWING THE NON LINEAR VISCO-ELASTIC BEHAVIOUR OF DENSE BITUMEN MACADAM IN CONSTANT STRESS CREEP TESTS.

(Considered over the range of stresses found in a pavement)

Fig. 8.24

was fixed to the top of the specimen with a spigot the line of action of the load would move to an eccentric position and accelerate the buckling.

8.7 A METHOD OF SPECIMEN CREEP PREDICTION

In Sections 8.3 and 8.6 it was shown that a linear log strain - log cycles (or time) relationship exists for dense bitumen macadam under both dynamic and static loading conditions.

In Section 8.3 it was stated that the creep curve for a non-linear viscoelastic material could be described by the equation:

$$\epsilon_t = \epsilon_o + mt^n \qquad 8.1$$

where ϵ_o and m are functions of the stress, n is a constant and ϵ_t is the strain at any time t. The term ϵ_o is small and therefore may be ignored. Hence, the equation becomes:

$$\epsilon_t = mt^n \qquad 8.4$$

hence $$\log \epsilon_t = n \log t + \log m \qquad 8.5$$

and $$\log \epsilon_t = \text{constant} + n \log t \qquad 8.6$$

This is the log strain - log cycles relationship shown in Figs. 7.11 and Figs. 8.2 to 8.8 and Figs. 8.22 and 8.23. A representation of these figures is shown in Fig. 8.25. The equation of the strain line is:

$$y = a + bx \qquad 8.7$$

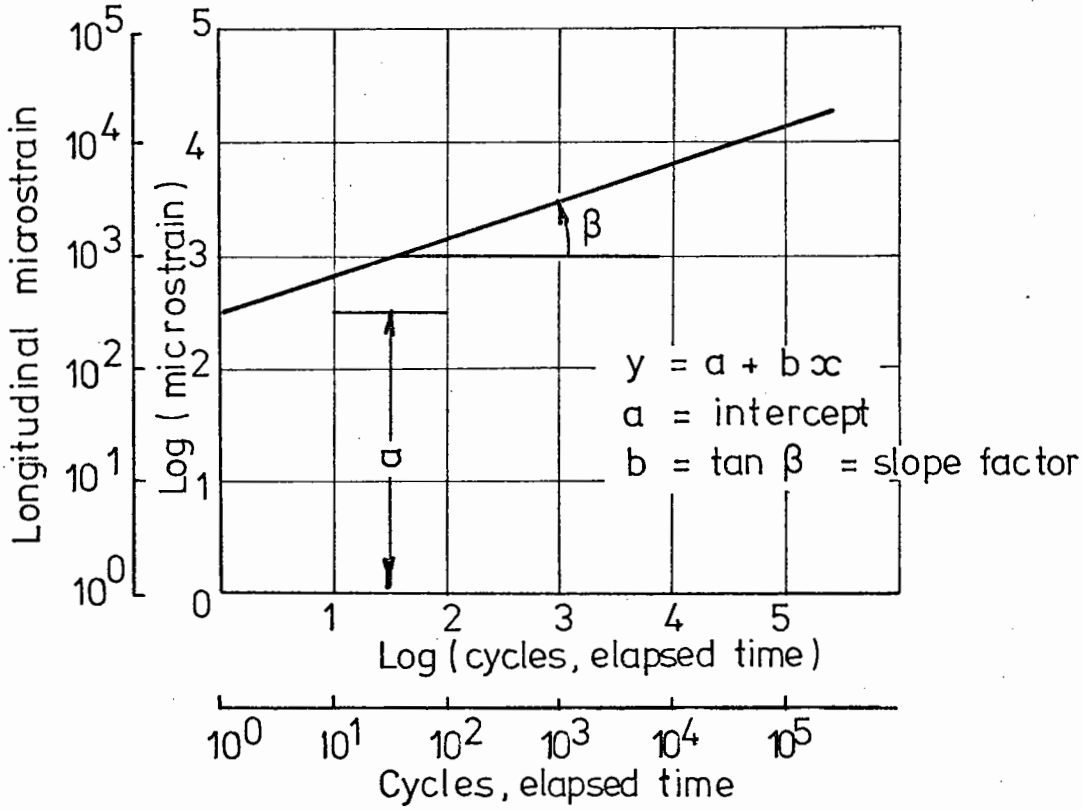

EXAMPLE OF OBTAINING COEFFICIENT 'a' and 'b'.

Fig. 8.25

Comparison with equation 8.6 shows that:

$$y = \log \varepsilon_t$$

$$x = \log t$$

and $$b = n$$

From Fig. 8.25 it is seen that "a" is the intercept value with the log strain axis and "b" is the slope of the line.

If the log strain - log cycles (or time) figures of Section 8.3 and 8.6 are studied, it may be seen that a straight line may be drawn, by eye, to approximate to the longitudinal permanent strain path followed by specimens under each particular set of conditions. At the lower stresses and temperatures, the experimentally derived curves are not linear and therefore the straight lines are placed to coincide with the curves at a thousand cycles and at failure. This approximation was used as it is more important to know the level of permanent deformation of a specimen as it approaches failure than in the early stages of a test. The idealised strain plots constructed in this manner may be seen in Figs. 8.26 to 8.28 for the dynamic tests and Figs. 8.29 and 8.30 for the static tests.

From these figures it is possible to determine the intercept value "a" and the slope factor "b" under any set of loading conditions. These two parameters may be seen plotted for specimens in an unconfined state as functions of dynamic vertical stress and temperature (Figs. 8.31 and 8.32). The relationship of "a" and "b" to the stress level at 20°C (shown in the figures) is taken as the standard for calculation

DENSE BITUMEN MACADAM (90/110 pen)
(225 mm by 150 mm dia. spec.)
Constant vertical stress 30 kN/m^2
Unconfined
Frequency of vertical stress pulse 1 Hz
Temperature 20 °C
Mean no. of cycles to failure *

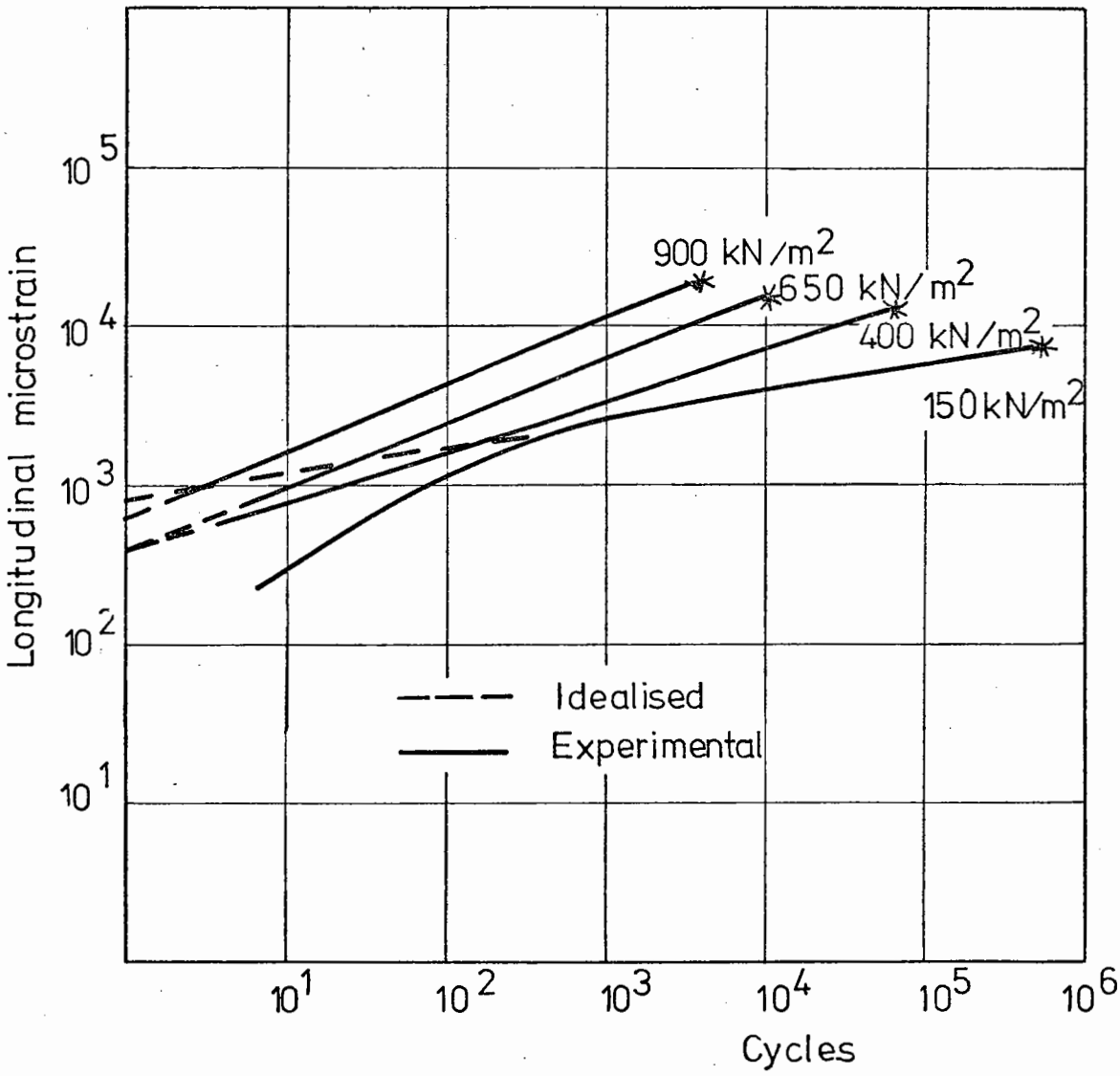

THE IDEALISED RELATIONSHIP OF PERMANENT LONGITUDINAL STRAIN TO NUMBER OF STRESS APPLICATIONS FOR A RANGE OF DYNAMIC VERTICAL STRESSES.

Fig. 8.26

DENSE BITUMEN MACADAM (90/110 pen)
(225 mm by 150 mm dia. spec.)
Dynamic vertical stress 650 kN/m^2
Constant vertical stress 30 kN/m^2
Unconfined
Frequency of vertical stress pulse 1Hz
Mean no. of cycles to failure *

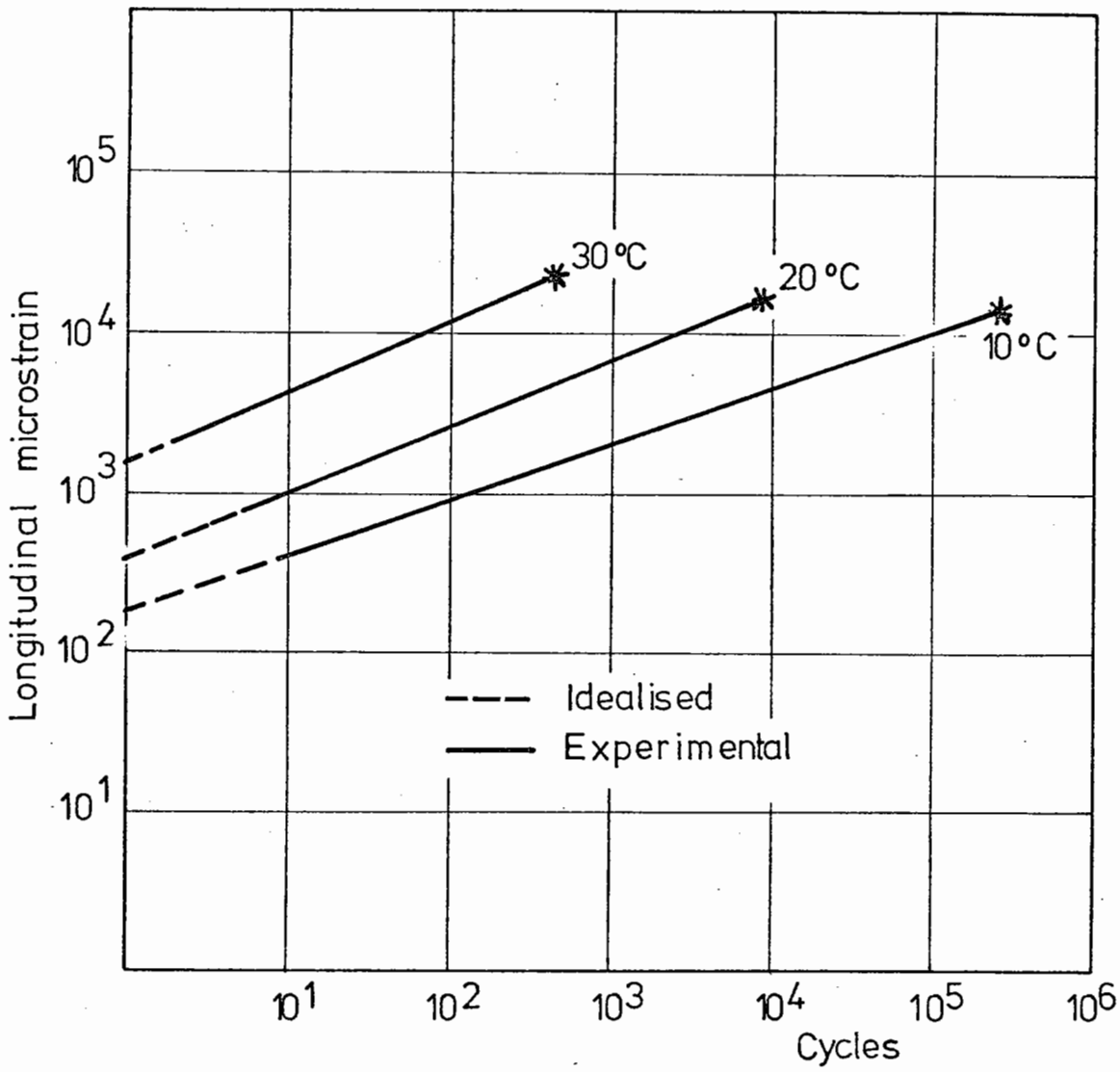

THE IDEALISED RELATIONSHIP OF PERMANENT LONGITUDINAL STRAIN TO NUMBER OF STRESS APPLICATIONS FOR A RANGE OF TEMPERATURE CONDITIONS.

(Test series-AS)

Fig. 8.27

DENSE BITUMEN MACADAM (90/110 pen)
(225 mm by 150 mm dia. spec.)
Dynamic vertical stress 650 kN/m^2
Constant deviator stress 30 kN/m^2
Frequency of vertical stress pulse 1 Hz
Temperature 20°C
Mean no. of cycles to failure *

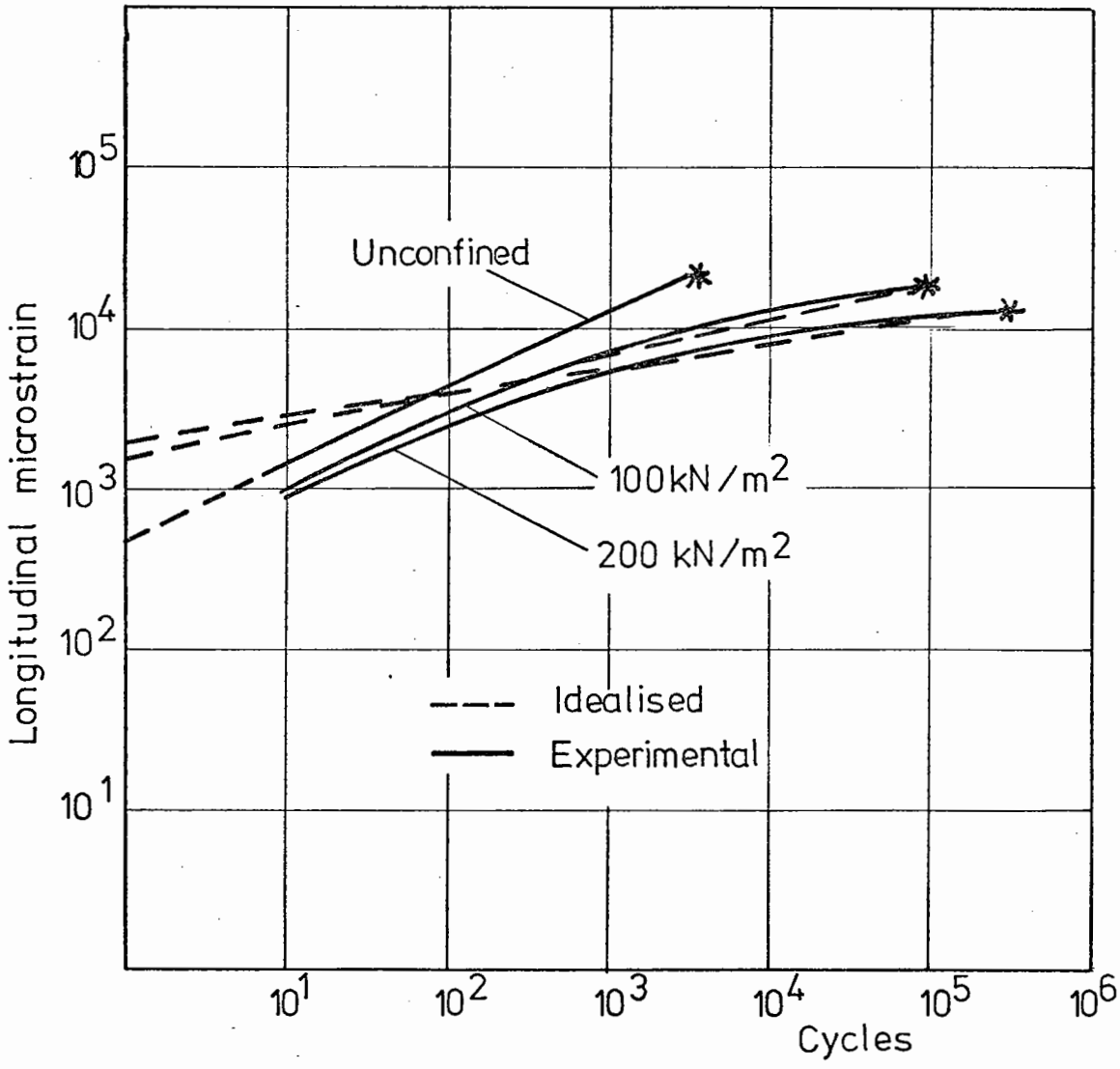

THE IDEALISED RELATIONSHIP OF PERMANENT LONGITUDINAL STRAIN TO NUMBER OF STRESS APPLICATIONS FOR A RANGE OF CONFINING PRESSURES.

(Test series - CS)

Fig. 8.28

DENSE BITUMEN MACADAM (4%-90/110 pen)
Diameter spec. 101 mm.
Temperature 20 °C

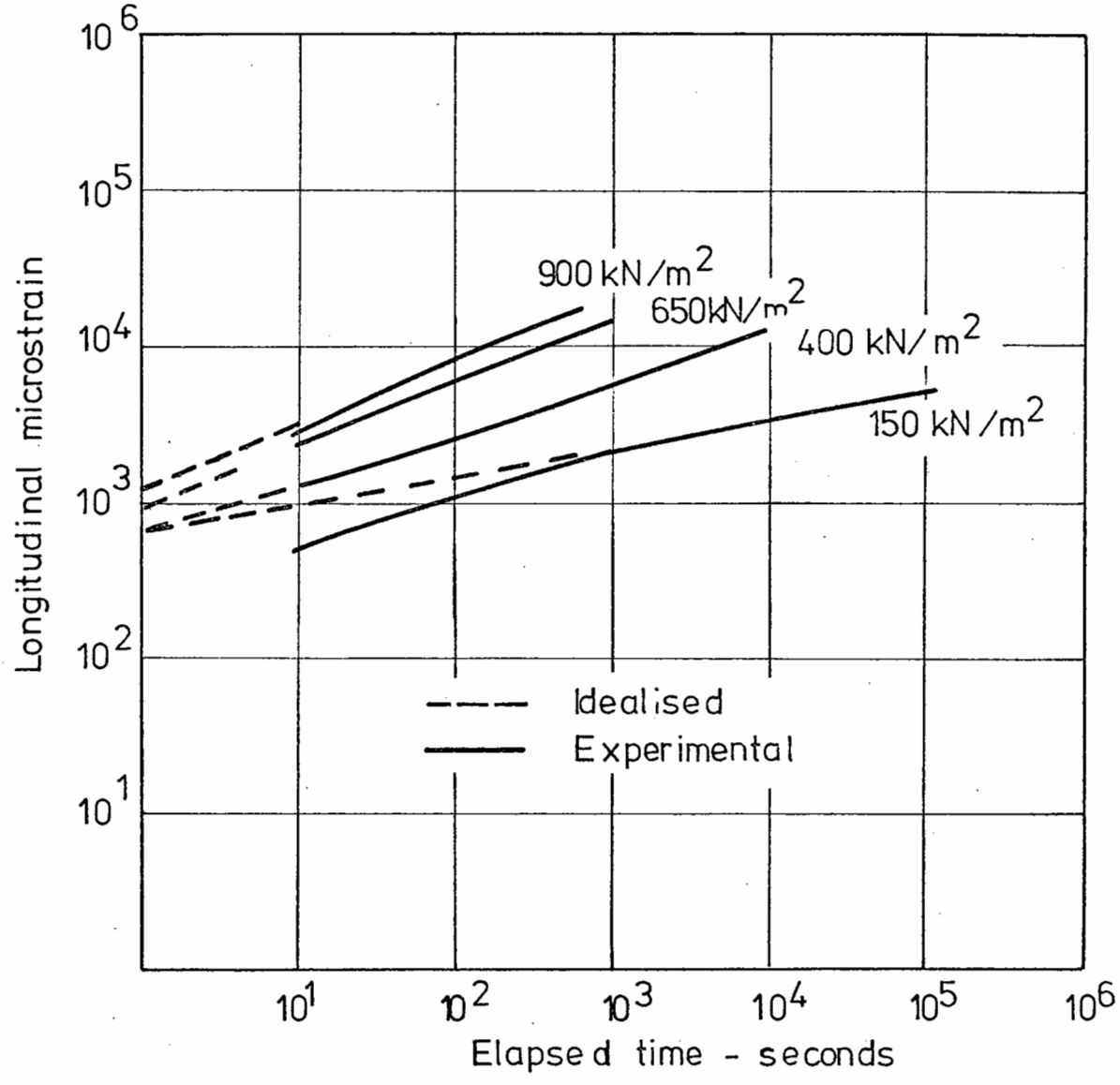

THE IDEALISED RELATIONSHIP OF PERMANENT LONGITUDINAL STRAIN TO ELAPSED TIME FOR A RANGE OF CONSTANT VERTICAL STRESSES (CONSTANT STRESS SERIES)

Fig. 8.29

DENSE BITUMEN MACADAM (4%-90/110 pen)
Diameter of spec. 101 mm.
Constant vertical stress 650 kN/m^2

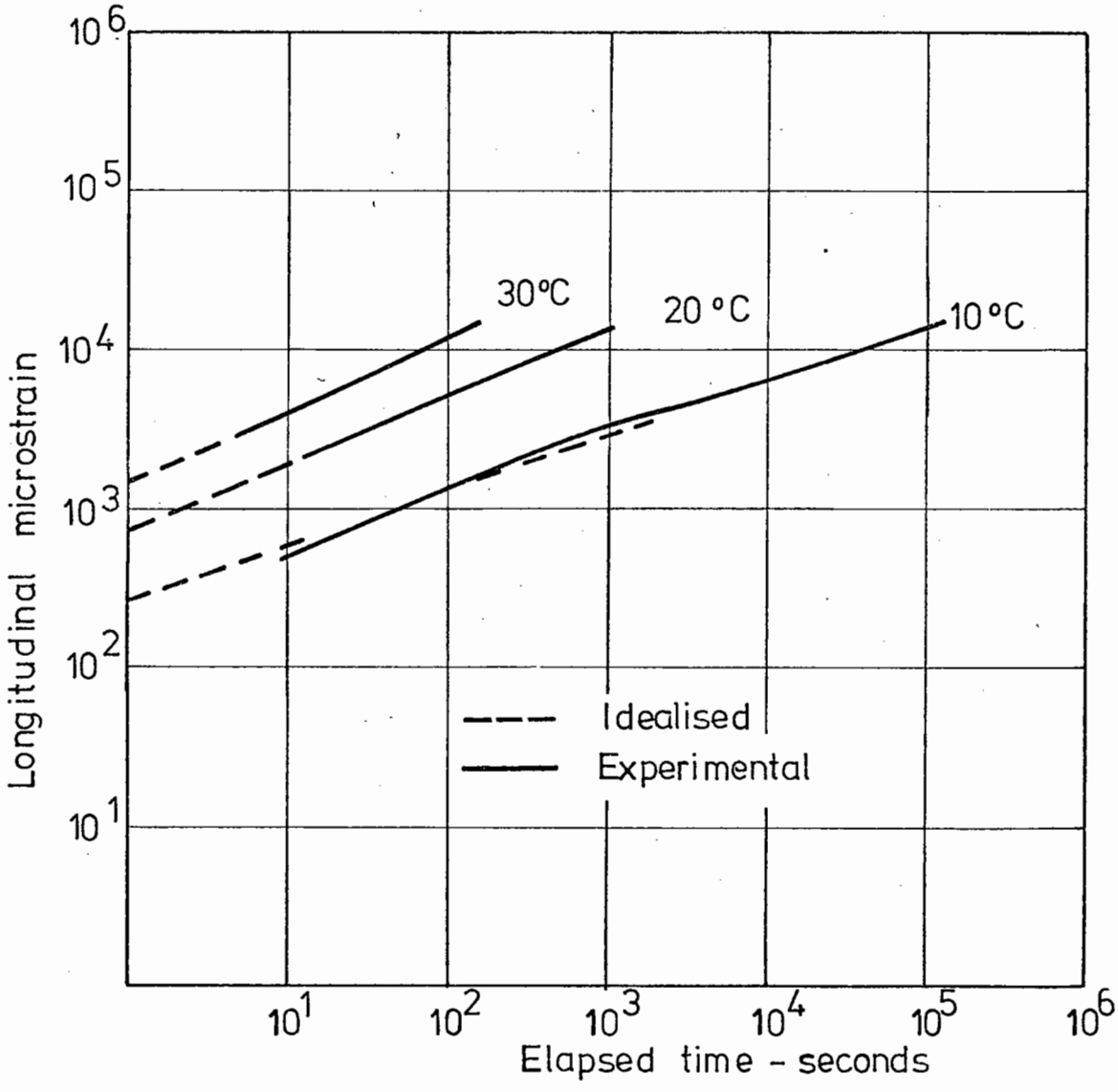

THE IDEALISED RELATIONSHIP OF PERMANENT LONGITUDINAL STRAIN TO ELAPSED TIME FOR A RANGE OF TEMPERATURES (CONSTANT STRESS SERIES)

Fig. 8.30

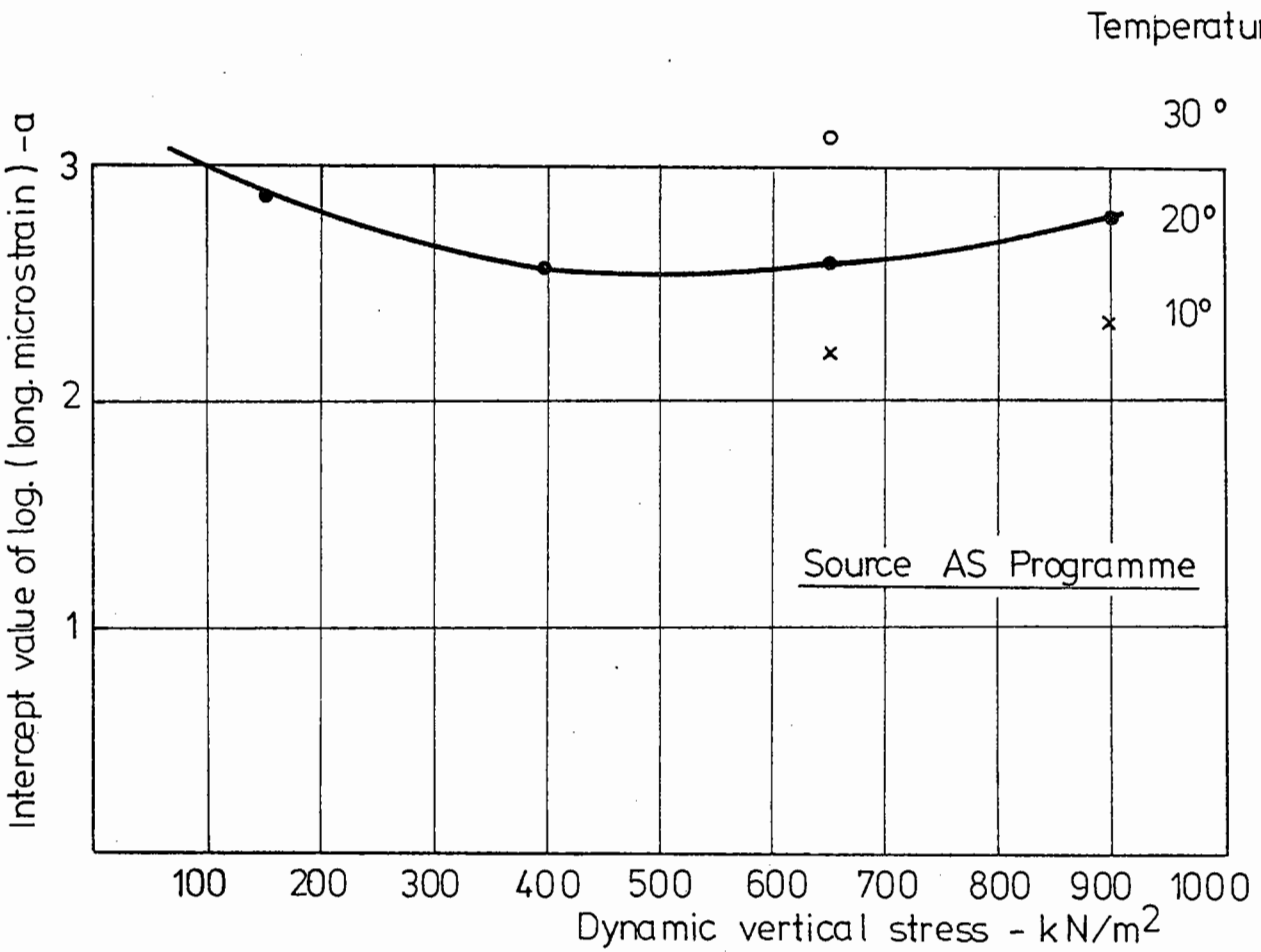

Fig. 8.31

INTERCEPT VALUE "a" FOR DEFORMATION PREDICTION TECHNIQUE (Unconfined)

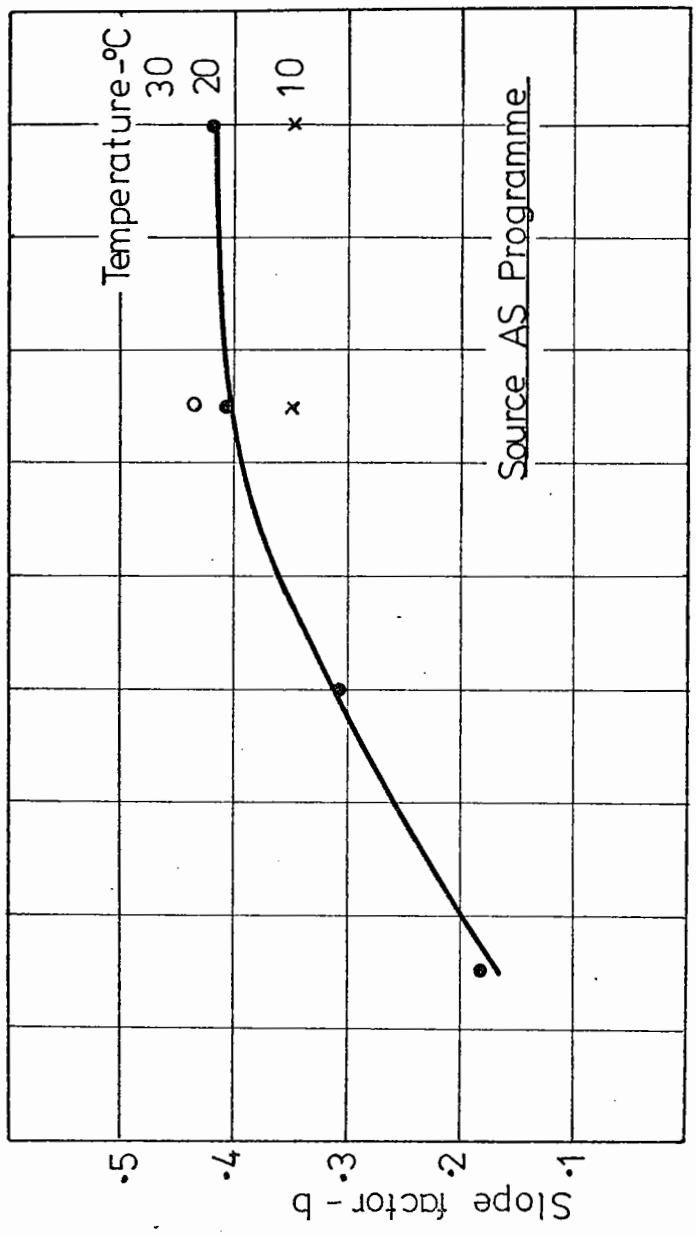

SLOPE FACTOR "b" FOR DEFORMATION PREDICTION TECHNIQUES (Unconfined)

Fig. 8.32

purposes. Furthermore, the percentage variation of "a" or "b" from the standard due to different temperature levels is assumed to be equal to the percentage change on the standard level measured at 650 kN/m^2. A similar assumption is made to cater for changes in confining pressure. Using these assumptions the equations giving "a" and "b" were formulated with the aid of a computer.

The equations thus produced were:

$$a = \{3.183 - 2.22\times10^{-3}s + 2\times10^{-6}s^2\}\{0.75 + 6.7\times10^{-3}t + 2.9\times10^{-4}t^2\}\{1 + 2.26\times10^{-3}c - 5.5\times10^{-6}c^2\} \qquad 8.8$$

and

$$b = \{0.063 + 8.32\times10^{-4}s - 4.8\times10^{-7}s^2\}\{0.623 + 2.73\times10^{-2}t - 4.2\times10^{-4}t^2\}\{1 - 7.5\times10^{-3}c + 2\times10^{-5}c^2\} \qquad 8.9$$

where s is the dynamic vertical stress in kN/m^2

t is the temperature in ^{o}C

c is the confining pressure in kN/m^2

The solid lines on Figs. 8.31 and 8.32 show the values of "a" and "b" given at 20^{o}C using the above equations. With this information it is possible to predict the permanent strain of a specimen at any stage in a test subjected to any loading conditions within the ranges explored in the laboratory. Given the magnitude of the dynamic vertical stress, temperature, and confining pressure, the intercept value "a" and the slope factor "b" may be obtained. With these two values the predicted log strain - log cycles curve may be constructed,

which allows the permanent longitudinal strain to be found after any number of cycles.

This work was all carried out at a frequency of testing of 1 Hz so that "number of cycles" and "time" in seconds are interchangeable. It was shown in Section 8.3 that the permanent deformation behaviour of a specimen was close to being time dependent. It is suggested, therefore, that, for tests at frequencies of 1 Hz and above, the deformation be considered on a time basis.

Using the above prediction methods the actual and predicted deformations at 10,000 cycles and failure are shown in Fig. 8.33 for specimens tested in programme AS. It may be seen that the predicted results are less than the actual strains occurring but in no case give less than 60% of the true value.

The implementation of the above procedure has been simplified by the use of a computer programme that will give the permanent deformation at any cycle number if the stresses, temperature and frequency are known. (Details of this may be seen in the Appendix.)

8.8 THE RELATIONSHIP BETWEEN DYNAMIC AND STATIC CREEP BEHAVIOUR

The previous section has shown how each log strain - log cycle (or time) curve may be replotted to yield an idealised strain behaviour.

It was noticed that the slope factor "b" of the tests in the dynamic and static tests was the same for similar

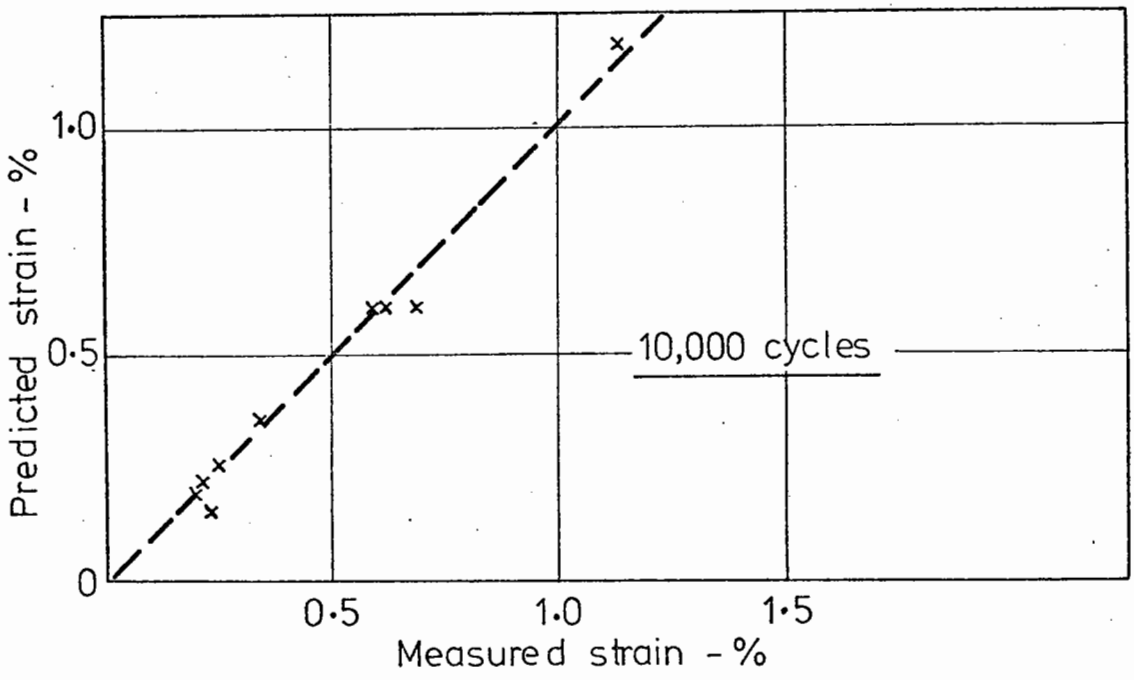

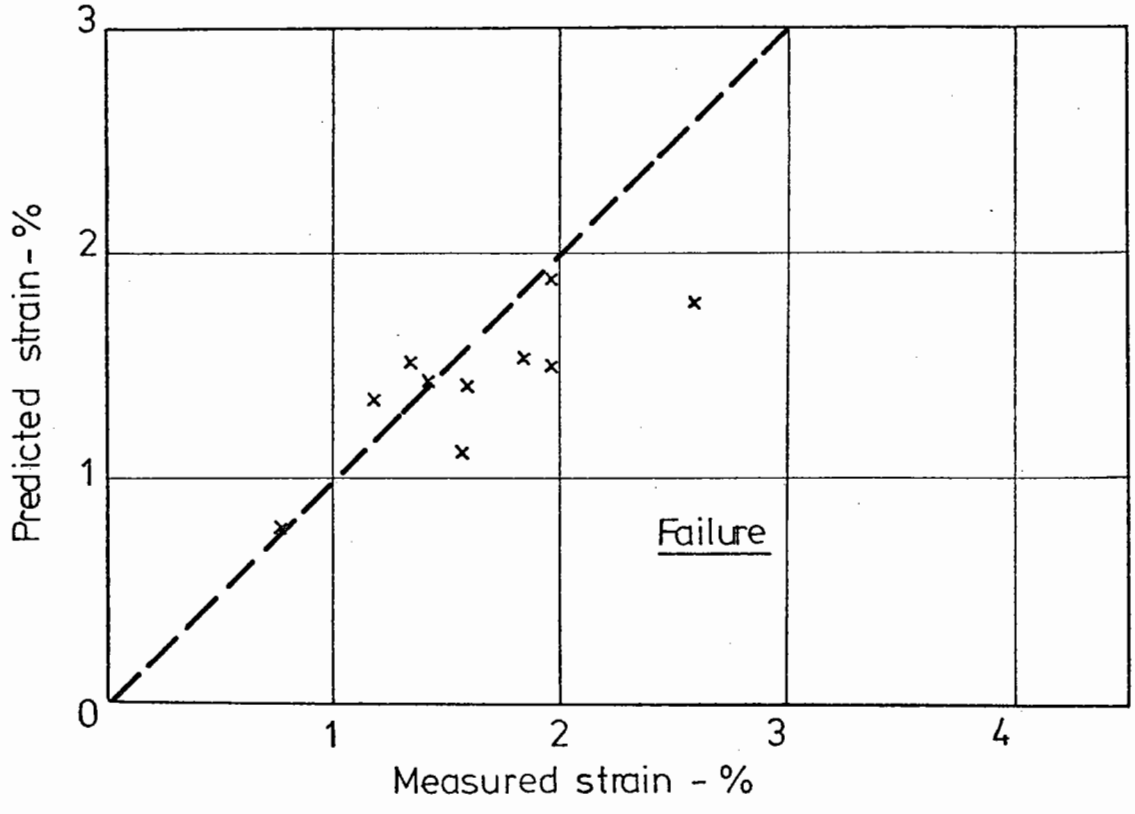

COMPARISON OF OBSERVED AND CALCULATED PERMANENT LONGITUDINAL STRAIN (PROGRAMME AS)

Fig. 8.33

conditions. Therefore, any difference in the strain behaviour due to the manner of loading would be shown in the intercept value alone.

The intercept values (a) for the dynamic tests are plotted against the intercept values (a_s) for the equivalent loading conditions in the static tests in Fig. 8.34. This figure shows that a relationship may exist between dynamic and static tests within the bounds of the six loading combinations investigated. The equation linking the two intercept values is:

$$a = 1 - 0.087a_s + 0.229a_s^2 \qquad 8.10$$

It is suggested that further combinations of stress and temperature are required to verify this relationship between dynamic and static tests.

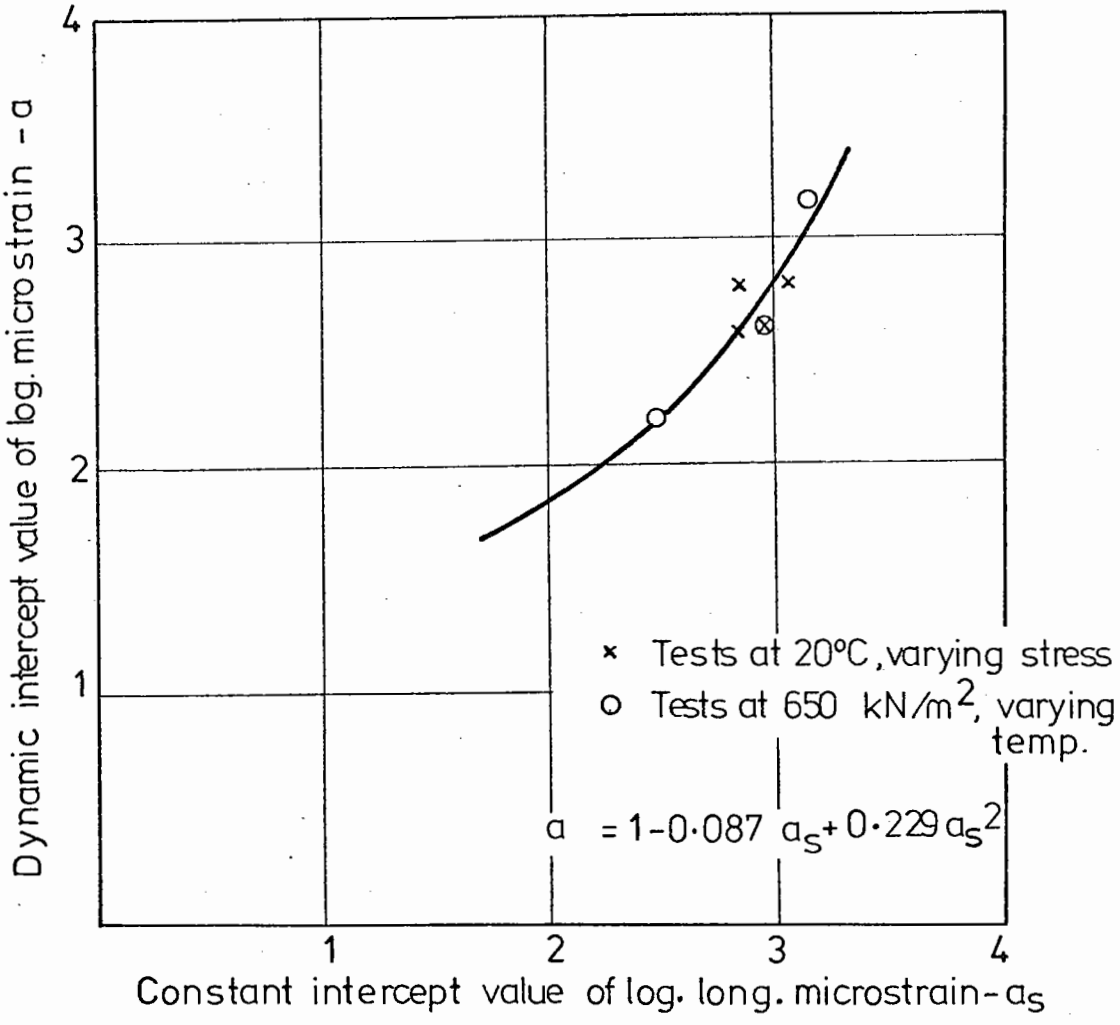

RELATIONSHIP BETWEEN CONSTANT AND DYNAMIC LOADING TESTS.

Fig. 8.34

CHAPTER NINE

APPLICATION OF THE RESULTS TO FLEXIBLE PAVEMENT DESIGN

9.1 INTRODUCTION

The previous chapter has discussed the permanent and resilient deformation properties of the dense bitumen macadam under investigation. This discussion, however, is more valuable if the facts gained on the behaviour of the material can be used. The resilient modulus and Poisson's ratio values may be employed to provide more accurate elastic analysis of pavement systems using existing techniques and computer programmes. The permanent deformation behaviour has, on the other hand, no direct application to any generally accepted method for the prediction of rutting in flexible pavements. This chapter attempts to show that the permanent deformation behaviour of the dense bitumen macadam discussed in Chapter 8, may be successfully applied to the problem of pavement design.

9.2 COMPARISON OF LABORATORY SPECIMEN AND IN SITU PERMANENT DEFORMATION BEHAVIOUR

It was stated in Chapter 2 that it is not possible to reproduce in the laboratory the exact stress pattern occurring in a pavement beneath a rolling wheel load. Pell and Brown (17) have observed that as the triaxial test cannot apply shear stresses directly to a specimen, then the simulated in situ pavement element must be subjected only to normal principal stresses and hence "rotate" as the wheel passes,

and this should be remembered when direct comparison is made between laboratory and in situ behaviour. None the less, it will be shown in this section that there is, in certain important facets of the behaviour of the material, a degree of similarity. Those discussed are:

The behaviour of the material subjected to dynamic loading.

Cracking of the material.

and The general form of the acquisition of permanent strain with time.

The Behaviour of the Material Subjected to Dynamic Loading

The laboratory specimens were seen to dilate during a test as deformation accrued (Section 8.5). Compaction occurred only at the start of a test and thereafter a steadily increasing plastic strain ratio, exceeding 0.5 (Fig. 8.19), was indicative of the increasing voids in the specimen. This does bear a resemblance to in situ material behaviour. Nijboer (73) has shown that there may be an increase in voids under trafficking in the bituminous layers. Furthermore, Hofstra and Klomp (12) and Goetz et al (13) have stated that there is no indication that densification causes rutting but rather that the evidence indicated a lateral flow from the area of the rut. Although observations of the AASHO road test (74) pavements indicated that densification may have contributed to 20% of the change in the thickness of the bituminous layers, it would appear that a lateral movement of the material associated with an increase in voids does generally occur and this behaviour is similar to that of the material under the laboratory loading conditions.

Cracking of the Material

Ramsamooj et al (75) and Coffman et al (76) have observed cracks around the point of loading in asphaltic concrete pavements. The latter have stated that:

"Theoretical calculations suggested that pavement cracking originated on the bottom of the asphaltic concrete at the load plate center and propagated radially and vertically as dynamic loads were applied."

In the U.K. cracking is not a major feature of pavement failure (Chapter 1), and rarely is anything but longitudinal surface cracking observed. However, it is very possible that the vertical cracks, analogous to those observed in laboratory specimens at failure, are present beneath the surface of the pavement and have merely not propagated through to the top of the bituminous layer.

General Form of the Acquisition of Permanent Strain with Time

The permanent deformation behaviour of a bituminous bound material in a laboratory test track has already been noted as similar to that of the author's specimens with a steadily declining rate of increase in permanent deformation (Section 8.3).

The three facets of in situ and laboratory tested material behaviour discussed do give an indication that the laboratory specimen does behave in a similar manner to the in situ pavement material. If this is so, a phenomenological

prediction of permanent deformation of the bituminous layers of a road pavement should be possible from the results of the laboratory tests.

In order to use the phenomenological approach care must be exercised in any extension of the results beyond those conditions at which specimens were tested. It was shown in Section 8.3 that, in the laboratory, a linear log permanent strain - log cycles relationship existed to failure. Failure was defined as the point at which the rate of permanent deformation increased, not the point at which the load bearing capacity of the specimen disappeared. Hofstra and Klomp (12) have reported changes in thickness of 15% in the bound layers of a pavement without its disintegration, whilst it was shown in Section 8.5 that the laboratory specimen tended to "fail" at about 2% permanent strain. It is felt that in the wheel tracks the ability of the in situ bituminous material to withstand high deformations may well be due to the passive support provided by the surrounding bituminous material. This will not markedly change the mode of deformation but will, together with the continuity of the material in the pavement carpet, prevent the total disintegration of the material that occurs in the laboratory specimen due to excessive hoop strain, even when confining pressures are applied.

9.3 METHODS OF PREDICTION OF PERMANENT DEFORMATION IN THE BITUMINOUS BOUND LAYER

The question confronting the author was, which of the existing methods should be used for the prediction of strain,

and hence deformation, in the bound layers? There appeared to be four main proposals which are discussed here.

A linear viscoelastic approach was suggested by Pagen (47). If a material was viscoelastic, it would be relatively simple to obtain the permanent strain at various levels merely by referring to a master creep curve. Unfortunately, as Romain (16) stated, several road materials do not exhibit the required linearity, and the dense bitumen macadam, investigated by the author, is one of these (Section 8.3).

The plastic strain may be determined by the "yield strain" of a material where yield strain is defined as the constant elastic strain value beyond which the strain is permanent. This concept, which was proposed by Heukelom and Klomp (77), is simple to use. The initial elastic strain under a standard wheel load is calculated and the yield strain subtracted from this to give that portion of the strain that is irrecoverable. It is felt that this method would be effective if a yield strain, that would remain constant throughout the life of a pavement, could be defined experimentally.

Rheological models of the behaviour of the material under dynamic loading would appear to be the most attractive means of describing the experimental behaviour of the material under investigation. Barksdale and Leonards (78) found that this approach gave a "realistic first approximation to the actual behaviour of a bituminous pavement system". A

more recent attempt by the Asphalt Institute (79) to obtain realistic results with this method was less encouraging. They reported that "the predicted values of rut depth were approximately 5 to 10 per cent of the measured values".

Direct interpolation from laboratory strain behaviour has been suggested by Barksdale (15), and the author has followed this approach. It is felt that if a method of prediction is to be employed by road engineers, then a reasonably simple technique is necessary that does not require a knowledge of rheological models.

Barksdale proposed that each layer should be divided into a number of sublayers. The major principal stress and the average confining pressure could be calculated at the centre of each sublayer beneath the wheel load. The plastic strain at the centre of each sublayer could then be calculated using direct interpolation from the plastic stress-strain curves of the laboratory. The total rut depth could then be obtained by summing the deformation of each sublayer assuming that the central strain was representative of the whole sublayer.

This method envisaged sublayers within each layer. Unfortunately, the confining pressure beneath the point of loading in the bottom half of a bituminous bound layer is likely to be negative, and no experimental work was carried out, in this investigation, to observe specimen behaviour under negative confining pressures. To overcome this difficulty it is suggested that the bituminous layer is considered as a whole and that the stresses are calculated

at the centre of this layer. In order to use this simplification, it must be established that the vertical plastic strains throughout such a layer are in fact similar.

The relative magnitudes of vertical and horizontal stress pulses, at a point beneath a moving wheel load, will change with depth. As the depth increases, the vertical stress declines tending therefore to reduce the rate of deformation. Conversely, the associated decrease in the horizontal stresses observed with depth will tend to increase the rate of deformation. Furthermore, the "contact time" of the vertical stress pulse is also a controlling factor (Section 8.7). This will increase with depth (Chapter 2) further counteracting the effects of the diminishing magnitude of the vertical stress pulse with depth.

Hofstra and Klomp (12) observed that a 100 mm thick bituminous layer deformed in a uniform manner when subjected to wheel passes in a circular test track. Indeed, observations on a 200 mm thick layer showed that the strain in the lower half was only 20% lower than in the top half after 200,000 wheel passes. It was found that the author's method of deformation prediction (shown in the following section) corroborated these findings. It was assumed for the purposes of the prediction that the 200 mm layer of the test track was made up in three sublayers of a material with the properties of the dense bitumen macadam reported in this thesis. It was possible to determine the strain in the central and top thirds of the pavement and it was found that they differed by only 14%. It may be seen that both practice and proposed

theory indicate that the bituminous layer may be considered as a whole.

In Section 8.7 it was shown that the deformation parameters of a specimen could be predicted from two equations (Eqns. 8.8 and 8.9) for any reasonable temperature or stress condition. The method of the prediction of in situ permanent deformation is exactly the same as for a specimen. The stresses and temperature at the centre of the bituminous layer are found and the permanent strain at this point is calculated on a time basis as if for a laboratory test. The strain is then multiplied by the thickness of the layer to produce the rut contribution of the bound layer.

The elastic analysis of the pavement system necessary to give the vertical and horizontal stresses for the plastic strain calculation were calculated with the BISTRO computer programme using a modulus appropriate to the chosen temperature. Kasianchuk (80) has performed a thorough investigation into the method of stress analysis of the pavement system to take account of the effect of different wheel loads on pavements at different temperature conditions. He proposed a modified modulus that would combine the effects of temperature and load. This he called "traffic weighted mean stiffness". Kasianchuk has stated that the effect of a wheel load is dependent on the temperature at any particular point in the pavement. In order to investigate the necessity of using this parameter an analysis of the pavement was carried out by the author to ascertain the changes in vertical and horizontal stresses due to temperature variations.

The diurnal and annual temperature variations considered are taken from tests on a bituminous slab, at the T.R.R.L., reported by Forsgate (81) and used by Taylor (40). Fig. 9.1 shows the T.R.R.L. slab details together with the layered system used in the elastic analysis with the BISTRO programme. The bituminous layer was divided into three sub-layers for the purpose of the analysis, with a 40 kN load applied as shown. The indicated temperatures in the slab are for three times of the day on 7th July, 1970. Assuming that the material was the dense bitumen macadam investigated by the author, values of modulus were assigned to the various positions in the slab at the three different times of the day, as shown.

The modulus values at the centres of each sublayer of the elastic system were taken as representative of the modulus in each sublayer. The vertical and horizontal stresses directly beneath the wheel load were then computed for the three times of the day. Fig. 9.2 shows the variation in the vertical and horizontal stress associated with the temperature changes in the pavement. In addition to the diurnal variations, the difference between typical summer (24^{o}C) and winter (6.5^{o}C) conditions was investigated, again using the modulus appropriate to the conditions observed at the T.R.R.L. Fig. 9.2 also shows the seasonal variation in the stresses that might be expected. From the two analyses, it would appear that variation in the temperature of a pavement, in the U.K., does not influence the stresses of a flexible pavement to a sufficient degree to require detailed attention.

Although changes in the temperature of a pavement do

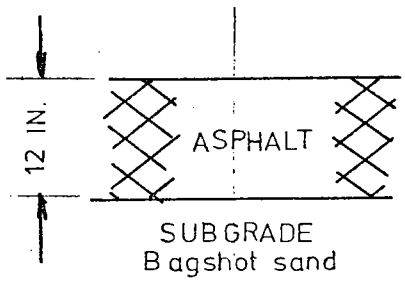

T.R.R.L. Temperature slab

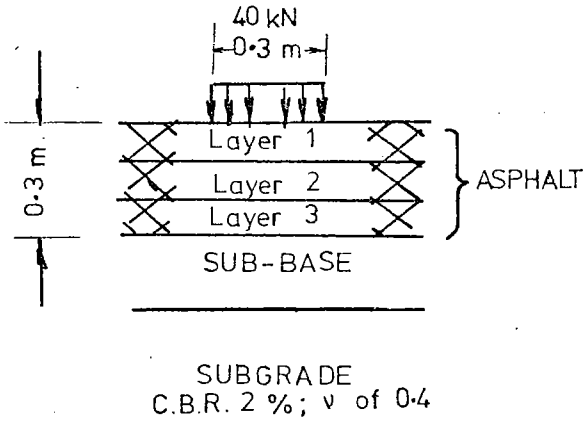

Layered system used in elastic analysis.

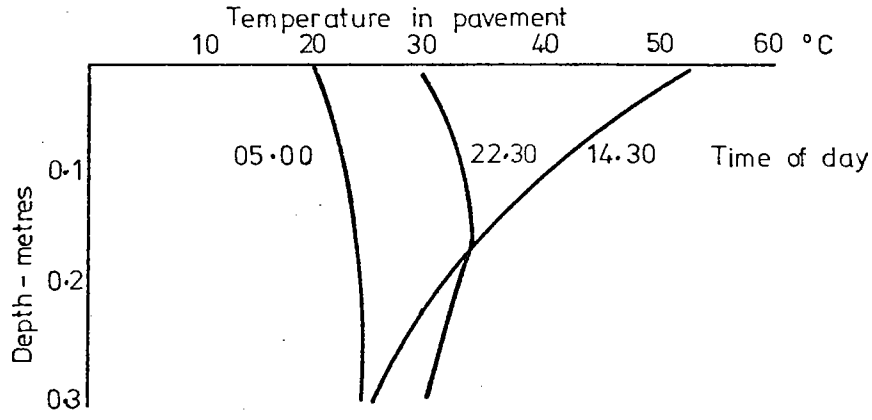

ASPHALT TEMPERATURE OF T.R.R.L. SLAB, 7th July 1970.

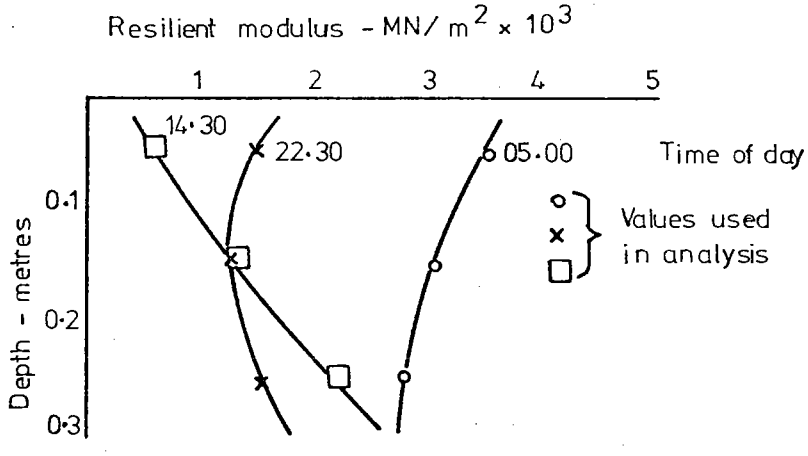

RESILIENT MODULI ASSOCIATED WITH TEMPERATURE OF SLAB
(obtained from test series AS on D.B.M.)

TEMPERATURE TO RESILIENT MODULUS CONVERSION FOR THE ELASTIC ANALYSIS OF A PAVEMENT.

Fig. 9.1

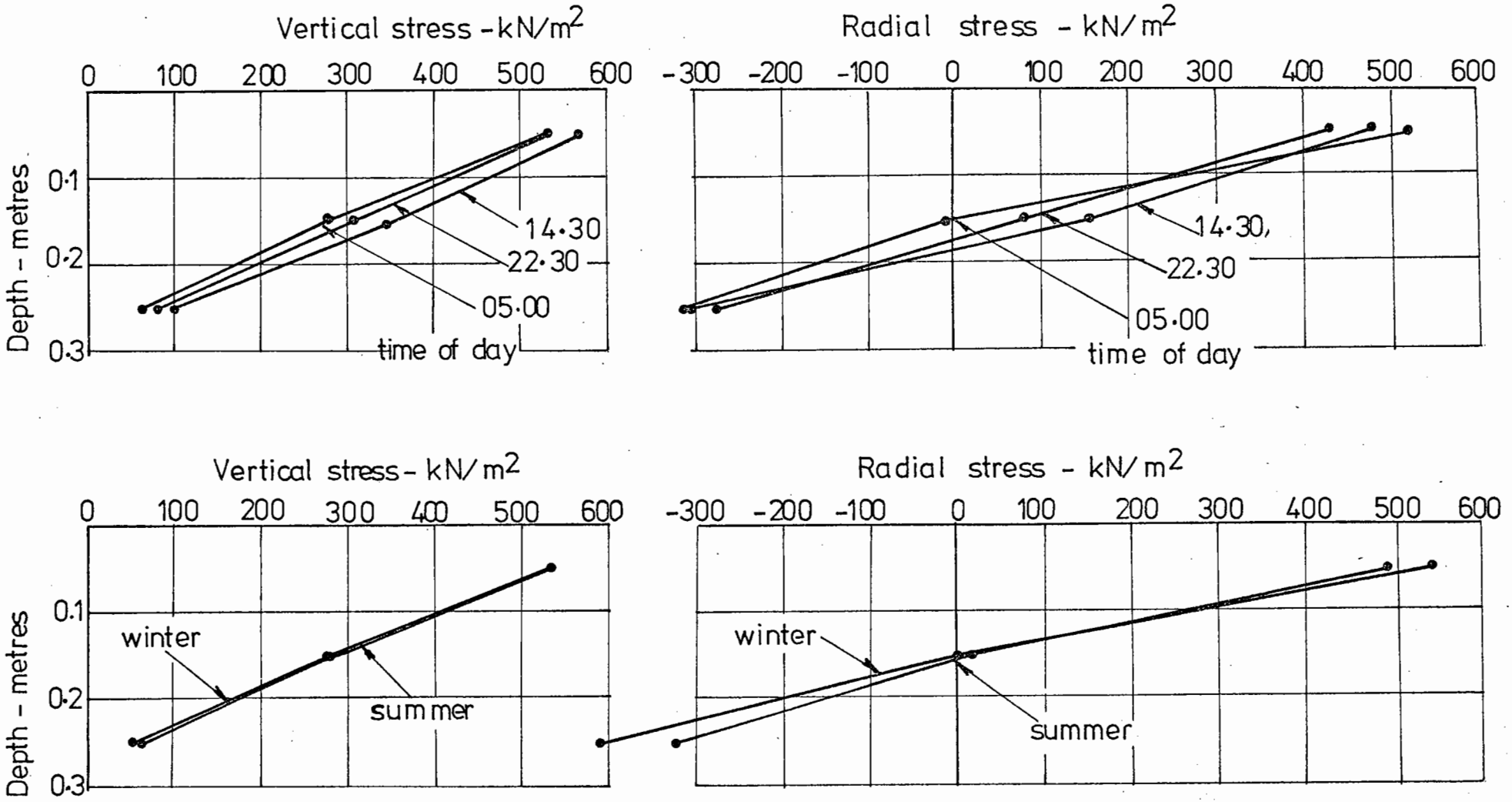

Fig. 9.2

THE VARIATION OF THE DIRECT STRESSES BENEATH A WHEEL LOAD DUE TO DAILY AND SEASONAL VARIATIONS IN TEMPERATURE OF THE ROAD PAVEMENT.

not markedly affect the stress distribution in the bound layers, the rate of permanent deformation is susceptible to a change of temperature. However, with the lack of laboratory data available for the plastic strain behaviour of a specimen under changing temperature conditions, it is felt that it is advisable to choose the average temperature of the pavement, in order to obtain the permanent strain factors "a" and "b" (Section 9.5).

The method of obtaining the "contact time" of a moving wheel load is to determine the time of action of a vertical stress pulse at the centre of the bituminous layer either as described in Chapter 2 or from Barksdale's curves (29). From this the relationship between continuous contact time and the number of wheel passes may be obtained, enabling the "permanent strain-time" prediction to be reduced to a "permanent strain-number of wheel passes" prediction.

9.4 AN EXAMPLE OF PERMANENT DEFORMATION PREDICTION IN THE STRUCTURAL DESIGN OF A FLEXIBLE PAVEMENT

In order to demonstrate the permanent deformation prediction method together with its applicability to the structural design of flexible pavements, an example of the design procedure of Brown and Pell (5) is shown, together with a prediction of the deformation of that pavement at the end of its service life. Brown and Pell stated that excessive permanent deformation was the normal failure condition of roads in the U.K. and therefore it is the logical step to extend their procedure to include a permanent deformation check.

It should be noted that in this example only the deformation of the bound layers is considered as the permanent deformation behaviour of the other layers is outside the scope of this investigation.

The procedure of Brown and Pell is only outlined as the details are available elsewhere (5).

Step 1 Analysis of the traffic loading to be expected in the design life. — 19×10^6 equivalent 80 kN axle loads

Step 2 Estimate of materials and layer thickness required. — See table

Layer	Material	Modulus of elasticity (MN/m^2)	Poisson's ratio	Thickness (mm)
Surfacing	Rolled asphalt	7,000	0.4	100
Base	Dense bitumen macadam	5,500	0.4	320
Sub-base	Crushed stone	75	0.3	150
Subgrade	Cohesive soil	30	0.4	-

Step 3 Analysis of the structure to determine critical stresses, strains and deflections. This requires a knowledge of the stress-strain characteristics of the materials and the use of an appropriate theoretical model. — BISTRO computer programme

Step 4 Comparison of these critical values with the maximum allowable. — See table

Stress or strain	Computed value	Design value
Asphalt strain ϵ_r	-38×10^{-6}	-40×10^{-6}
Subgrade strain ϵ_z	116×10^{-6}	370×10^{-6}
Sub-base stress σ_r	-2.7 kN/m^2	-7.3 kN/m^2

Step 5 If satisfactory, continue with permanent deformation check, if not return to step 2.

The base layer of the pavement is a dense bitumen macadam which for this calculation is taken to be at 20°C. Furthermore, the surfacing material is considered to be dense bitumen macadam, thus forming a continuous bituminous layer, 0.42 m thick, on the sub-base. The speed of the passing vehicles is taken as 50 km/h.

The steps in the permanent deformation calculation are shown below.

Step 1	Determine the traffic loading in equivalent 80 kN standard axles (as above)	19×10^6
Step 2	Determine the wavelength of the vertical stress pulse at the centre of the bituminous layer (Section 2.5)	2.8 m
Step 3	Determine the time of action of the vertical stress pulse at the centre of the bituminous layer	0.2 seconds
Step 4	Hence the number of stress pulses per second continuous contact time.	5
Step 5	Determine the maximum vertical stress at the centre of the bituminous layer. (Assume zero horizontal stress.)	192 kN/m^2
Step 6	Determine "a" value from Eqn. 8.8 for 192 kN/m^2 at 20°C.	2.83
Step 7	Determine "b" value from Eqn. 8.9 for 192 kN/m^2 at 20°C.	0.205
Step 8	Calculate micro-strain (ϵ_t) at a contact time (t) from ϵ_t = Antilog {a+b log t}.	
Step 9	Construct a graph of deformation against axle passes (1 sec = 5 axle passes) or calculate the deformation at end of design life.	Fig. 9.3 6.4 mm

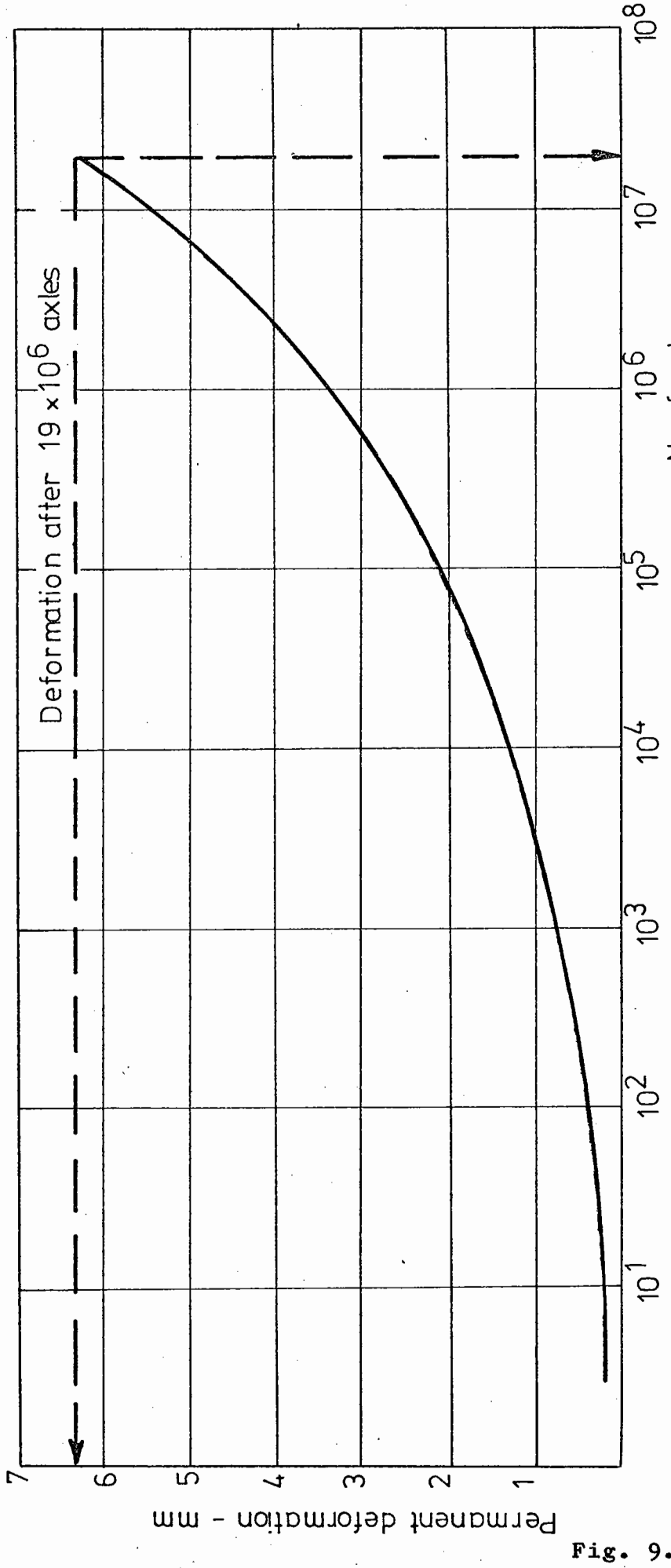

PERMANENT DEFORMATION IN THE BITUMINOUS BOUND LAYER OF A PAVEMENT DESIGNED USING THE STRUCTURAL DESIGN PROCEDURE.

Fig. 9.3

It may be seen that the pavement design is within the elastic design criteria of a limiting horizontal strain at the bottom of the asphalt surfacing, a limiting horizontal stress at the bottom of the unbound base and a limiting vertical strain on the subgrade. The permanent deformation at the end of the service life, 6.4 mm, which has been contributed solely by the dense bitumen macadam is also reasonable, as this would indicate that there is anything between a 6.4 mm and 16 mm overall change in the surface level of the pavement. The upper limit is derived from the observations of Lister, on the A.1 trunk road, which indicated that the bound layers contributed to 40% of the total rut depth (11). If the evidence of Hofstra and Klomp (12) is valid then the lower figure is the more reliable as they suggest that with thick bituminous layers all the deformation occurs in these layers. However, the comparison of predicted and observed values seen in Section 8.7 suggests that the 6.4 mm deformation could be an underestimate, though this will only be ascertained by in situ trials.

It would appear that the permanent deformation level is within the permanent deformation failure limit of 25 mm observed by Croney (9) and therefore the pavement design may be considered as satisfactory both from the elastic stress and strain criteria and from the permanent deformation criterion of failure. It is apparent that the limiting fatigue criterion is the most critical in this example. However, in the U.K. it is accepted that excessive permanent deformation is the more usual mode of failure and therefore

a tentative conclusion is that either the fatigue criterion is too severe or the predicted values of deformation are too small.

For comparison purposes the deformation contribution from the bound layer of a road pavement, designed using Road Note No. 29 (1) recommendations, was calculated. The road was designed to meet the same traffic and subgrade conditions as that designed by the structural design procedure of Brown and Pell (5). At the end of the service life the surface deformation due to a bound layer of 280 mm of dense bitumen macadam was predicted to be just over 5 mm. This is less than that in the structurally designed pavement but with less bituminous cover to the lower layers it is probable that the overall rut depth would be greater.

9.5 CONCLUDING DISCUSSION

The preceding section has attempted to show that a structural design approach, together with a permanent deformation check, may be used to facilitate the design of road pavements in the U.K. The method shown in this chapter for the prediction of permanent deformation in the bound layers of a bituminous pavement must still be considered as tentative. However, if the following suggestions are followed, it is thought that it may be suitable for adoption by the road designer.

The acquisition of experimental data should be continued so that the "a" and "b" parameters are found for all the materials likely to be encountered in the bound layers of a

road pavement. However, two more fundamental points also need attention. Firstly, there is no experimental data available for the permanent deformation behaviour of dense bitumen macadam for variations of either the load or the temperature during a test. At the moment, the actual axle loads are converted to 80 kN standard axles (1) to normalise the stress; and the constant temperature is selected to be representative of the diurnal and annual variations of temperature in the pavement, but it is possible that these values are not the most appropriate approximations to use for the prediction of permanent deformation.

Secondly, it will have been noticed that considerable reference has been made to the work of Hofstra and Klomp (12). This is because, in order to use laboratory results in the design of road pavements, it is first necessary to compare laboratory with in situ behaviour. Unfortunately, field results of sufficient detail are not available and the only laboratory test track which is reported in sufficient detail for comparison is that of Hofstra and Klomp. It is expected that information will become available from a full scale experiment at Grangemouth being conducted by the T.R.R.L.

CHAPTER TEN

CONCLUSIONS

In order to study the deformation behaviour of dense bitumen macadam it was necessary to develop three major items of equipment: an electro-hydraulic servo-controlled testing machine for the application of both static and dynamic forces to triaxial specimens of the material, a constant stress testing machine for the application of static forces to unconfined triaxial specimens and the design of an "on-sample" method of measuring the longitudinal and radial deformations of a specimen used in conjunction with an automatic recording system. Satisfactory operation of these systems together with the use of "frictionless" end platens have allowed an accurate picture of the permanent and resilient behaviour characteristics of the dense bitumen macadam to be constructed.

A summary of the more important facts to emerge from the investigation are listed below under three headings.

Principal Conclusions Concerning Permanent Deformation

(a) The permanent deformation behaviour of dense bitumen macadam may not be considered as linear viscoelastic.

(b) An increase in the magnitude of the applied static or dynamic vertical stress caused an increase in the rate of permanent deformation.

(c) An increase in the temperature of the material caused a marked increase in the rate of permanent deformation.

(d) An increase in the level of the confining pressure caused a decrease in the rate of permanent deformation.

(e) The retarding effect, on the increase in permanent deformation, due to a cycled confining pressure when pulsed to a specified level was less than that due to a static confining pressure at that level.

(f) Above a frequency of loading of 1 Hz, the rate of increase of permanent deformation was time dependent at 20°C.

(g) The effect of the introduction of rest periods between successive load cycles was insignificant.

(h) An optimum binder content of 4% existed for the resistance to permanent deformation of the dense bitumen macadam at 10°, 20° and 30°C.

(i) A method of predicting the magnitude of the permanent deformation of a specimen during a test is presented.

Principal Conclusions Concerning Resilient Deformation

(a) The resilient modulus was found to be linear elastic within the loading conditions investigated.

(b) The resilient modulus decreased with an increase in the temperature of the material.

(c) The resilient modulus increased with an increase in the frequency of the dynamic vertical stress.

(d) The resilient modulus increased slightly with an increase in the confining pressure.

(e) An optimum binder content of 4% existed to give a maximum resilient modulus at 10°, 20° and 30°C.

(f) Poisson's ratio was little affected by the magnitude of the dynamic stress level, the frequency or the binder content of the material.

(g) Poisson's ratio was decreased by an increase in the confining pressure.

(h) Poisson's ratio was increased by an increase in the temperature of the material.

Conclusions Drawn from Computer Aided Analyses

(a) The apparent pulse length (or loading time) of the vertical stress, due to a passing wheel load, was found to increase linearly with depth, in any one layer of a pavement.

(b) The vertical and horizontal stresses induced in the bound layers of a pavement due to a passing wheel load were not significantly affected by the annual or diurnal variations of atmospheric temperature in the U.K.

(c) Stress controlled testing was found to be more suitable for the dynamic testing of a bituminous bound roadbase material than strain controlled testing.

(d) A computer programme has been written to facilitate the prediction of the magnitude of the permanent deformation of the bituminous layer of a road pavement during its service life.

REFERENCES

1. "A guide to the structural design of pavements for new roads", Road Note No. 29, Dept. of the Environment, RRL, 3rd Edit., HMSO, 1970.
2. Millard, R.S., "The Third International Conference on the Structural Design of Asphalt Pavements - London, September 1972", Bitumen, Vol. 6, 1972, pp. 154-159.
3. "Specification for road and bridge works", Ministry of Transport, HMSO, London, 1969.
4. "Shell 1963 design charts for flexible pavements", Shell Int. Pet. Co. Ltd., London, 1963.
5. Brown, S.F. and Pell, P.S., "A fundamental structural design procedure for flexible pavements", Proc. 3rd Int. Conf. on the Struct. Design of Asphalt Pavements, London, 1972, pp. 369-381.
6. Dormon, G.M. and Metcalf, C.T., "Design curves for flexible pavements based on layered system theory", Highway Research Board, HRR No. 71, 1965, pp. 65-84.
7. Heukelom, W. and Klomp, A.J.G., "Dynamic testing as a means of controlling pavements during and after construction", Proc. Int. Conf. on the Struct. Design of Asphalt Pavements, Ann Arbor, 1962, pp. 667-679.
8. Finn, F.N., "Observation of distress in full-scale pavements", Highway Research Board Special Report No. 126, 1971, pp. 86-90.
9. Croney, D., "Failure criteria for flexible pavements", Proc. 3rd Int. Conf. on the Struct. Design of Asphalt Pavements, London, 1972, pp. 608-612.

10. Hveem, F.N., "Pavement deflections and fatigue failures", Highway Research Board, Bull. No. 14, 1955, pp. 43-73.

11. Lister, N.W., "The transient and long term performance of pavements in relation to temperature", Proc. 3rd Int. Conf. on the Struct. Design of Asphalt Pavements, London, 1972, pp. 94-100.

12. Ibid Hofstra, A. and Klomp, A.J.G., "Permanent deformation of flexible pavements under simulated road traffic conditions", pp. 613-621.

13. Goetz, W.H., McLaughlin, J.F. and Wood, L.E., "Load deformation characteristics of bituminous mixtures under various conditions of loading", Proc. AAPT, Vol. 26, 1957, pp. 237-292.

14. Chomton, G. and Valayer, P.J., "Etude de l'ornierage en laboratoire: L'essai de fluage dynamique", Revue Generale des Routes et des Aerodromes, No. 458, October 1970, pp. 95-104.

15. Barksdale, R.D., "Laboratory evaluation of rutting in base course materials", Proc. 3rd Int. Conf. on the Struct. Design of Asphalt Pavements, London, 1972, pp. 161-174.

16. Ibid Romain, J.E., "Rut depth prediction in asphalt pavements", pp. 705-710.

17. Ibid Pell, P.S. and Brown, S.F., "The characteristics of materials for the design of flexible pavement structures", pp. 326-342.

18. Lashine, A.K.F., "Some aspects of the behaviour of Keuper marl under repeated loading", Ph.D. thesis, Univ. of Nottingham, 1971.

19. Seed, H.B., Chan, C.K. and Lee, C.F., "Resilience characteristics of subgrade soils and their relation to fatigue failures in asphalt pavements", Proc. Int. Conf. on the Struct. Design of Asphalt Pavements, Ann Arbor, 1962, pp. 611-636.

20. Glynn, T.E., "Deformation characteristics of boulder clay subjected to repeated stress applications", Ph.D. thesis, Univ. of Dublin, 1969.

21. Chomton, G. and Valayer, P.J., "Applied rheology of asphalt mixes practical application", Proc. 3rd Int. Conf. on the Struct. Design of Asphalt Pavements, London, 1972, pp. 214-225.

22. Pell, P.S., "Fatigue of asphalt pavement mixes", Proc. 2nd Int. Conf. on the Struct. Design of Asphalt Pavements, Ann Arbor, 1967, pp. 577-593.

23. Kingham, R.I. and Kallas, B.F., "Laboratory fatigue and its relationship to pavement performance", Proc. 3rd Int. Conf. on the Struct. Design of Asphalt Pavements, London, 1972, pp. 849-865.

24. Monismith, C.L. and Deacon, J.A., "Fatigue of asphalt paving mixtures", ASCE TE2, May 1969, pp. 317-346.

25. Hanson, J.M., "The behaviour of roadbase materials under repeated loading", Ph.D. thesis, Univ. of Nottingham, 1971.

26. Cragg, R. and Pell, P.S., "The dynamic stiffness of bituminous road materials", Proc. AAPT, Vol. 40, 1971, pp. 126-147.

27. Dehlen, G.L., "The effect of non-linear material response on the behaviour of pavements subjected to traffic loads", Ph.D. thesis, Univ. of California, 1969.

28. van Dijk, W., Moreaud, H., Quedeville, A. and Uge, P., "The fatigue of bitumen and bituminous mixes", Proc. 3rd Int. Conf. on the Struct. Design of Asphalt Pavements, London, 1972, pp. 354-366.

29. Barksdale, R.D., "Compressive stress pulse times in flexible pavements for use in dynamic testing", Highway Research Board, HRR No. 345, 1971, pp. 32-44.

30. Awad, I.S., "Characterization of the stress-strain relationship of asphalt treated base material", Graduate Report, Univ. of Washington, 1972.

31. Root, R.E., Skok, E.L. and Jones, D.L., "Structural and mixture design of low volume roads using the elastic theory", Proc. 3rd Int. Conf. on the Struct. Design of Asphalt Pavements, London, 1972, pp. 1074-1083.

32. Gregg, J.S., Dehlen, G.L. and Rigden, P.J., "On the properties, behaviour and design of bituminous stabilized sand bases", Proc. 2nd Int. Conf. on the Struct. Design of Asphalt Pavements, Ann Arbor, 1967, pp. 863-882.

33. Thrower, E.N., Lister, N.W. and Potter, J.F., "Experimental and theoretical studies of pavement behaviour under vehicular loading in relation to elastic theory", Proc. 3rd Int. Conf. on the Struct. Design of Asphalt Pavements, London, 1972, pp. 521-535.

34. Snaith, M.S., Brown, S.F. and Pell, P.S., "Permanent deformation of flexible paving materials", Internal Report, Univ. of Nottingham, 1971.

35. Brown, S.F., "Determination of Young's modulus for bituminous materials in pavement design", to be published by the Highway Research Board, 1973.

36. Klomp, A.J.G. and Niesman, Th.W., "Observed and calculated strains at various depths in asphalt pavements", Proc. 2nd Int. Conf. on the Struct. Design of Asphalt Pavements, Ann Arbor, 1967, pp. 671-688.

37. Raithby, K.D. and Sterling, A.B., "The effect of rest periods on the fatigue performance of a hot rolled asphalt under reversed axial loading", Proc. AAPT, Vol. 39, 1970, pp. 134-152.

38. Bazin, P. and Saunier, J.B., "Deformability, fatigue and healing properties of asphalt mixes", Proc. 2nd Int. Conf. on the Struct. Design of Asphalt Pavements, Ann Arbor, 1967, pp. 553-569.

39. Rowe, P.W. and Barden, L., "The importance of free ends in triaxial testing", ASCE, SM1, Vol. 90, 1964, pp. 1-27.

40. Taylor, K.L., "Finite element analysis of layered road pavements", Ph.D. thesis, Univ. of Nottingham, 1971.

41. Ko, H-K, Masson, R.M. and Nymoen, L., "Effects of end constraints and multiaxial testing of soils", Proc. RILEM Symposium on the Deformation and Rupture of Solids Subjected to Multiaxial Stresses, Vol. 2, Cannes, 1972, pp. 71-86.

42. Bishop, A.W. and Henkel, D.J., "The measurement of soil properties in the triaxial test", Edward Arnold Ltd., London, 1957, pp. 70-74.

43. Snaith, M.S. and Brown, S.F., "Electro-hydraulic servo-controlled equipment for the dynamic testing of bituminous materials", Proc. RILEM Symposium on the Deformation and Rupture of Solids Subjected to Multiaxial Stresses, Vol. 3, Cannes, 1972, pp. 139-154.

44. Vallerga, B.A., "Recent laboratory compaction studies of bituminous mixtures", Proc. AAPT, Vol. 20, 1951, pp. 117-152.

45. Nevitt, H.G., "Compaction Fundamentals", Proc. AAPT, Vol. 26, 1957, pp. 201-206.

46. Shackel, B., "The compaction of uniform, replicate, soil specimens", Australian Road Research, Vol. 4, No. 5, Sept. 1970, pp. 12-31.

47. Pagen, C.A., "Dynamic structural properties of asphalt pavement mixtures", Proc. 3rd Int. Conf. on the Struct. Design of Asphalt Pavements, London, 1972, pp. 290-315.

48. Hughes, B.P. and Bahramiam, B., "Cube tests and the uniaxial compressive strength of concrete", Magazine of Concrete Research, Vol. 17, No. 53, Dec. 1965, pp. 177-182.

49. Valayer, P.J., "Research on mechanical phenomena in roads and asphalt mixes", Roads and Road Construction, Vol. 48, No. 566, Feb. 1970, pp. 53-58.

50. Pell, P.S., "Fatigue characteristics of bitumen and bituminous mixes", Proc. Int. Conf. on the Struct. Design of Asphalt Pavements, Ann Arbor, 1962, pp. 310-323.

51. Deacon, J.A., "Fatigue of asphalt concrete", Ph.D. thesis, Univ. of California, 1965.

52. McElvaney, J., "Fatigue of a bituminous mixture under compound-loading", Ph.D. thesis, Univ. of Nottingham, 1972.

53. Goetz, W.H. and Chen, C.C., "Vacuum triaxial technique applied to bituminous-aggregate mixtures", Proc. AAPT, Vol. 19, 1950, pp. 55-81.

54. Nijboer, L.W., "Plasticity as a factor in the design of dense bituminous road carpets", Elsevier, New York, 1948.

55. Onaran, K. and Findley, W.N., "Combined stress-creep experiment on a non-linear viscoelastic material to determine the kernel functions for a multiple integral representation of creep", Trans. Soc. Rheology, 9.2, 1965, pp. 299-327.

56. Francken, L., "Properties of materials", A prepared discussion at the 3rd Int. Conf. on the Struct. Design of Asphalt Pavements, London, 1972.

57. Pagen, C.A., "Rheological response of bituminous concrete", Highway Research Board, HRR No. 67, 1965, pp. 1-26.

58. Goetz, W.H., "Comparison of triaxial and Marshall test results", Proc. AAPT, Vol. 20, 1951, pp. 200-245.

59. Monismith, C.L., Alexander, R.L. and Secor, K.E., "Rheological behaviour of asphalt concrete", Proc. AAPT, Vol. 35, 1966, pp. 400-450.

60. Van der Poel, C., "A general system describing the visco-elastic properties of bitumens and its relation to routine test data", J. Appl. Chem., Vol. 4, 1954, pp. 221-236.

61. Van der Poel, C., "Time and temperature effects on the deformation of bitumen and bitumen-mineral mixtures", J. Soc. Plastics Engineers, Vol. 11, 1955, pp. 47-64.

62. Heukelom, W. and Klomp, A.J.G., "Road design and dynamic loading", Proc. AAPT, Vol. 33, 1964, pp. 92-125.

63. Van Draat, W.E.F. and Sommer, P., "Ein gerät zur bestimmung der dynamischen elastizitätsmodulu von asphalt", Strasse Autobahn 6, 1965, pp. 206-211.

64. Kallas, B.F., "Dynamic modulus of asphalt concrete in tension and tension-compression", Proc. AAPT, Vol. 39, 1970, pp. 1-20.

65. Monismith, C.L. and Secor, K.E., "Viscoelastic behaviour of asphalt concrete pavements", Proc. Int. Conf. on the Struct. Design of Asphalt Pavements, Ann Arbor, 1962, pp. 476-498.

66. Fossberg, Per E., Mitchell, J.K. and Monismith, C.L., "Load-deformation characteristics of a pavement with cement-stabilized base and asphalt concrete surfacing", Proc. 3rd Int. Conf. on the Struct. Design of Asphalt Pavements, London, 1972, pp. 795-811.

67. Terrel, R.L., "Dynamic triaxial testing for curing and strength prediction", Paper presented at the 51st Annual Meeting of the Highway Research Board, 1972.

68. Sayegh, G., "Viscoelastic properties of bituminous mixtures", Proc. 2nd Int. Conf. on the Struct. Design of Asphalt Pavements, Ann Arbor, 1967, pp. 743-755.

69. Heukelom, W., "Observations on the rheology and fracture of bituminous and asphalt mixes", Proc. AAPT, Vol. 35, 1966, pp. 358-396.

70. Barksdale, R.D., "A nonlinear theory for predicting the performance of flexible highway pavements", Highway Research Board, HRR No. 337, 1970, pp. 22-39.

71. Saal, R.N.J. and Pell, P.S., "Fatigue of bituminous road mixes", Kolloid Zeitschrift, Band 171, Heft 1, 1960, pp. 61-71.

72. Cooper, K.E. and Pell, P.S., "Fatigue properties of bituminous road materials", Internal Report, Univ. of Nottingham, 1972.

73. Nijboer, L.W., "Testing flexible pavements under normal traffic loadings by means of measuring some physical quantities related to design theories", Proc. 2nd Int. Conf. on the Struct. Design of Asphalt Pavements, Ann Arbor, 1967, pp. 689-705.

74. Benkelman, A.C., "Structural deterioration of test pavements: flexible", Highway Research Board, Special Report No. 73, 1962, pp. 173-185.

75. Ramsamooj, D.V., Majidzadeh, K. and Kauffmann, E.M., "The analysis and design of the fiexibility of pavements", Proc. 3rd Int. Conf. on the Struct. Design of Asphalt Pavements, London, 1972, pp. 692-704.

76. Ibid Coffman, B.S., Ilves, G.J. and Edwards, W.F., "The fatigue of flexible pavements", pp. 590-607.

77. Heukelom, W. and Klomp, A.J.G., "Consideration of calculated strains at various depths in connection with the stability of asphalt pavements", Proc. 2nd Int. Conf. on the Struct. Design of Asphalt Pavements, Ann Arbor, 1967, pp. 155-167.

78. Ibid Barksdale, R.D. and Leonards, G.A., "Predicting performance of bituminous surfaced pavements", pp. 321-340.

79. "R and D Progress", Vol. 1, No. 3, The Asphalt Institute, Sept. 1972.

80. Kasianchuk, D.A., "Fatigue considerations in the design of asphalt concrete pavements", Ph.D. thesis, Univ. of California, 1968.

81. Forsgate, J., "Temperature frequency distributions in flexible road pavements", TRRL Report LR 438, 1972.

APPENDIX

Two computer programmes were written for the Wang 720B computer. This computer was used rather than the large University facility as certain operational problems of the latter became apparent during the course of this investigation.

Data Processing Programme

The programme necessary to process the data enables the input data to be entered either through the keyboard or on punch tape. As stated in Chapter 6, the data for each test was normally put onto punch tape to speed analysis by the Wang computer.

The programme is stored on a magnetic tape and may be used by following the instructions listed.

(a) Load programme into computer.

(b) Verify the programme - (Correct number 9575).

(c) If the tape reader is to be used, change steps 0882 and 0883 to "GRPI" and "0000" respectively. Verify the programme - (Correct number 9549).

(d) Fill up the stores with the calibration factors.

Store Number	Calibration Factor	Units
0001	Deviator stress	kN/m^2/paper division
0002	Confining pressure	kN/m^2/paper division
0003	Longitudinal permanent deformation	mm/paper division
0004	Longitudinal resilient deformation	mm/paper division

Store Number	Calibration Factor	Units
0005	Radial permanent deformation	mm/paper division
0006	Radial resilient deformation	mm/paper division

(e) Keyboard input

Stage 1

Key "SEARCH" "1"

Key in the test number

Key in the nominal constant deviator stress reading in paper divisions

Key in the nominal constant confining pressure reading in paper divisions

Key in the nominal dynamic deviator stress reading in paper divisions

Key in the nominal dynamic confining pressure reading in paper divisions

Stage 2

Key in the cycle number

Key in the dynamic deviator stress reading in paper divisions

Key in the dynamic confining pressure reading in paper divisions

Key in the permanent longitudinal deformation reading in paper divisions

Key in the resilient longitudinal deformation reading in paper divisions

Key in the permanent radial deformation reading in paper divisions

Key in the resilient radial deformation reading in paper divisions

Stage 3

Print out will occur giving:

The cycle number and its logarithm

The permanent longitudinal strain, and its logarithm

The increase in permanent longitudinal strain per load application

The resilient longitudinal strain

The resilient modulus

The permanent radial strain

Poisson's ratio

Plastic strain ratio

The bulk modulus)
) if required
The shear modulus)

Stage 4

Repeat stage 2 until completion of the test

(f) Tape input

The tape should be prepared with the data in the same order as indicated in Stage 1 and Stage 2.

The tape should be placed in the tape reader.

Key "SEARCH" "1" will operate the programme which will process the data direct from the tape.

Prediction of Permanent Deformation in a Dense Bitumen Macadam Road Pavement Layer (or Specimen)

This programme was written to facilitate the permanent deformation prediction calculation given in Chapter 9. The dynamic vertical stress, the temperature and the dynamic horizontal stress are entered into the programme which then calculates the "a" and "b" values necessary for the prediction. These parameters are then printed out for inspection and stored for the prediction calculation. If the thickness of the

bituminous layer and number of stress pulses necessary to give one second contact time at mid-thickness are then entered into the computer the deformation after any selected number of axle passes will be printed out.

The programme is stored on magnetic tape and may be used by following the instructions listed.

(a) Load programme into computer.

(b) Verify the programme - (Correct number 3427)

(c) Stage 1

Key "SEARCH" "1"

Key in vertical stress at centre of chosen sub-layer - kN/m^2

Key in pavement temperature - ^oC

Key in horizontal stress at centre of chosen sub-layer - kN/m^2

Stage 2

Printout will occur giving:

"a" and "b", the input stresses and the input temperature

Stage 3

Key "SEARCH" "3"

Key in number of stress pulses necessary to give one second contact time at the centre of the sub-layer

Key in thickness of the sub-layer of the pavement in metres

Stage 4

Key in number of axle passes at which the deformation due to the sub-layer is required.

Stage 5

Printout will occur giving the deformation due to the sub-layer in mm and the number of axle passes.

Stage 6

Repeat stages 4 and 5 if the deformation is required at other numbers of axle passes.

AUTHOR'S NOTE

A description of the servo-hydraulic machine and the "on sample" measuring techniques was presented by the author and Dr. S.F. Brown at the "RILEM Symposium on the Deformation and Rupture of Solids Subjected to Multiaxial Stresses" held at Cannes in October 1972. The paper was entitled "Electro-hydraulic servo-controlled equipment for the dynamic testing of bituminous materials".

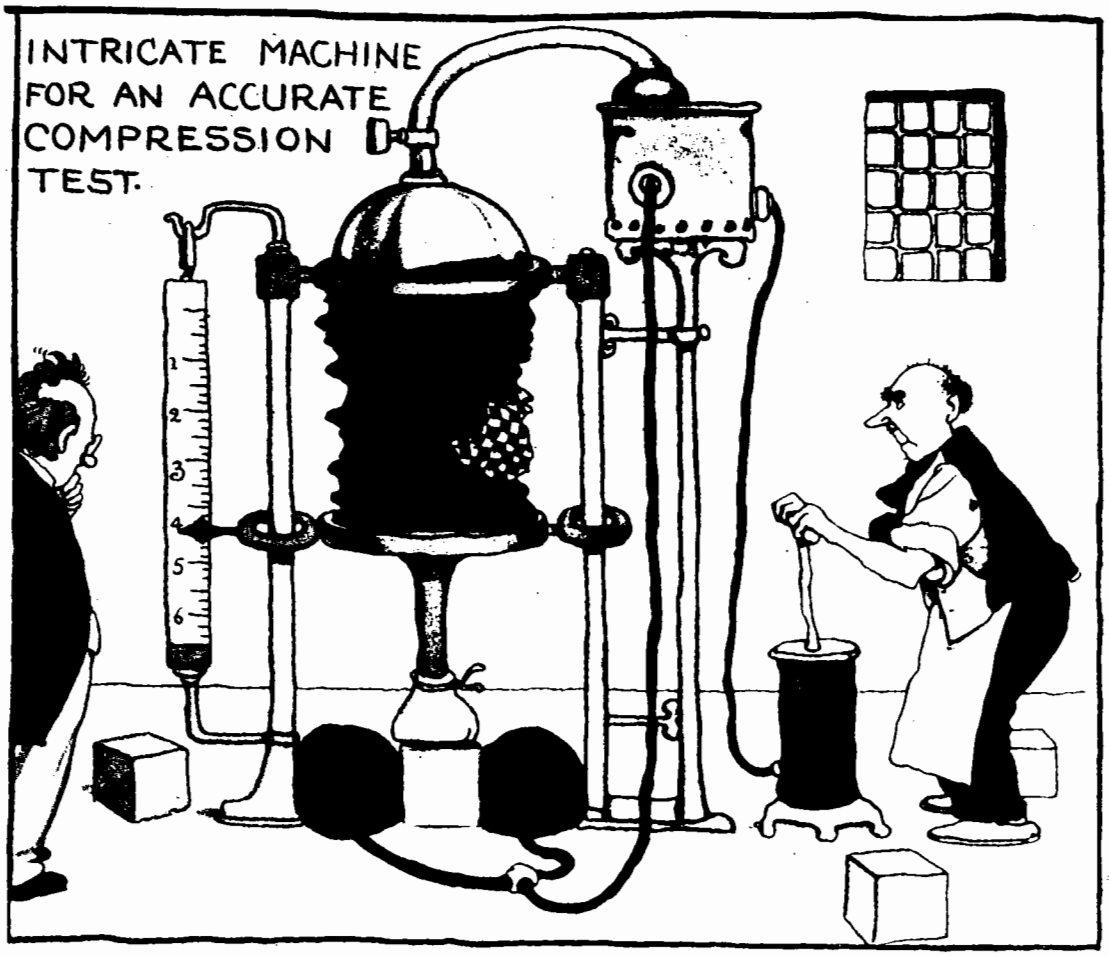

An early rival of 1928, by W. Heath-Robinson
("The Wonders of Wilmington", G. & T. Earle, 1925, Ltd.)

FIG.8.18End view of specimens before and after testing

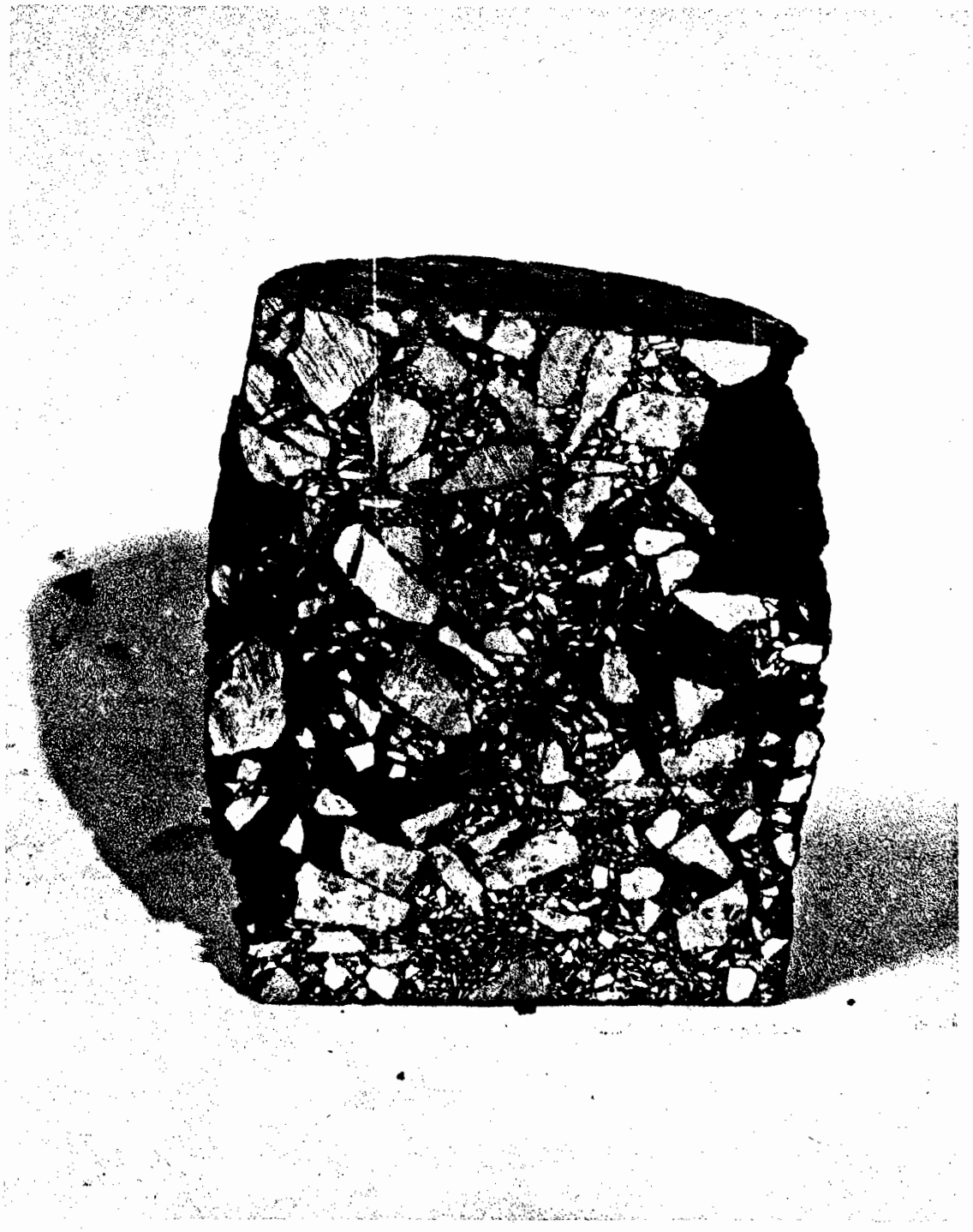

FIG.3.6 Sectioned 100 mm (4 inch) diameter specimen (showing the effect of end platen restraint on failure)

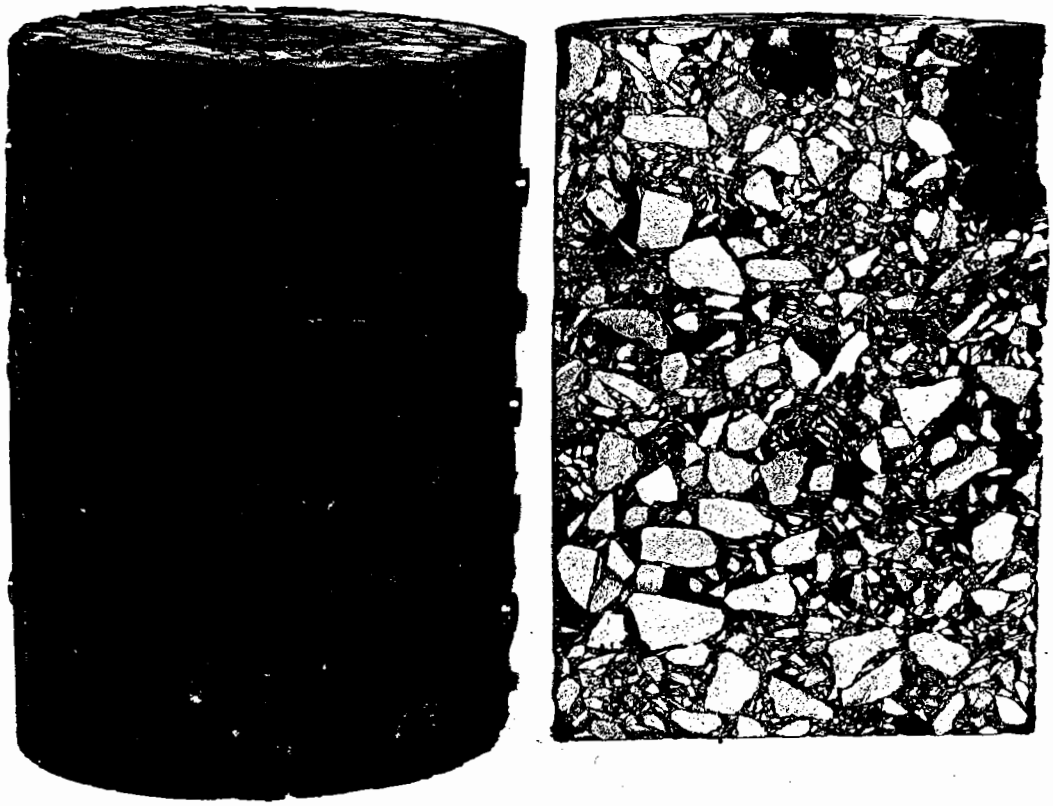

FIG.3.8 Specimens of D.B.M. after completion of a test

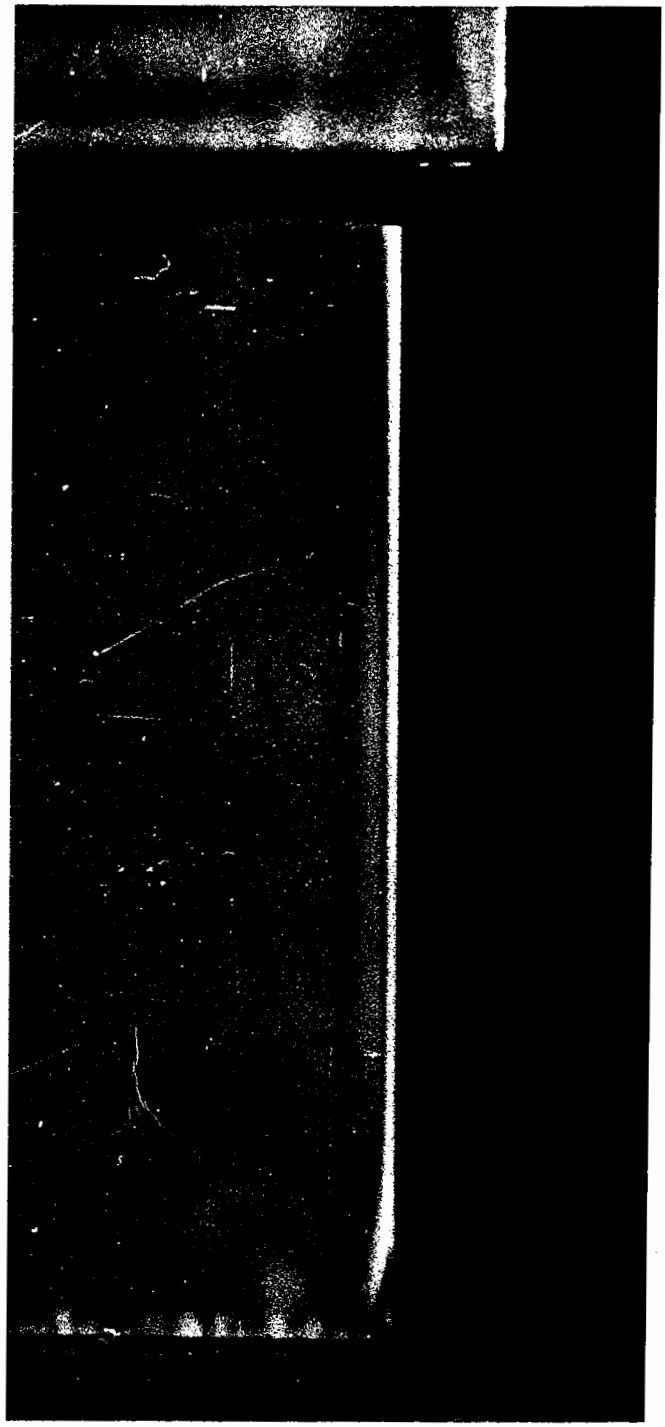

FIG.3.10 Photoelastic representation of shear zones in a triaxially tested specimen